# THE BONDING, SYNTHESIS AND ELECTROCHEMISTRY OF SOME IRON-SULPHUR-NITROSYL COMPOUNDS

Ronald J. W. Lambert

A Thesis Submitted for the Degree of PhD
at the
University of St Andrews

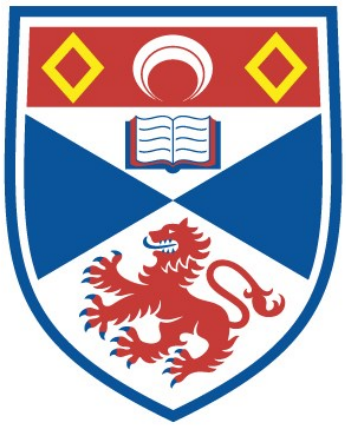

1990

# The Bonding, Synthesis and Electrochemistry of Some Iron-Sulphur-Nitrosyl Compounds

By

Ronald J. W. Lambert

A Thesis Presented to the University of St. Andrews

For the Degree of Doctor of Philosophy



ProQuest LLC.
789 East Eisenhower Parkway
P.O. Box 1346
Ann Arbor, MI 48106 – 1346

## Dedication

*To my parents, my brothers,*

*and especially to Vicky*

*( and my dog Benji)*

## Declaration

I declare that this thesis is of my own composition, that it is a record of my own work, and that none of the parts contained herein has been previously submitted in application for a higher degree.

R. J. Lambert

December 1989

## Certificate

I hereby certify that Ronald Joseph William Lambert has spent twelve terms of research under my supervision, and has fulfilled the conditions of Ordinance General No. 12 and Resolution of the University Court, 1967, No. 1, and is qualified to submit the accompanying thesis in application for the degree of Doctor of Philosophy

Dr. C. Glidewell Research Supervisor

# Acknowledgements

I would like to thank Dr. Chris Glidewell for his thoughts on this chemistry and his patience too, and the Association of International Cancer Research for financing this research.

My thanks also go to Colin Smith who gave me back my broken glassware in better condition than when I bought it; Sylvia Smith for analysing my samples; Mel Smith for my n.m.r. results and Colin Miller for all my mass-spectral data. Thanks also go to Dr. Joe Crayston for listening to my queries on electrochemistry, to Dr. Colin Vincent for loaning me the electrochemical apparatus, to Dr. Finlay MacCorquodale and Dr John Walton for their help with the e.p.r. data, and also to M. Hursthouse and M. Motevalli of the S.E.R.C. crystal service for obtaining the structures of $\{(Ph_3P)_2N\}_2[Fe_2(S_2O_3)_2(NO)_4]$ and $Me_3S[Fe_4S_3(NO)_7]$. Finally, thanks to Bill Bell and Audrey Lees for putting up with me for so long.

# Abstract

Salts of the bis(μ-thiosulphato-S)-bis(dinitrosylferrate)(2-) anion, $[Fe_2(S_2O_3)_2(NO)_4]^{2-}$ can be prepared by the reaction of iron(II)/thiosulphate mixtures with nitrite ion. The crystal structure of $\{(Ph_3P)_2N\}_2[Fe_2(S_2O_3)_2(NO)_4]$ reveals it to adopt a trans structure. $^{15}$N n.m.r. studies of this salt also show it to adopt the trans structure in solution. The anion reacts with thiolate ion, $RS^-$, to provide good yields of $Fe_2(SR)_2(NO)_4$; e.p.r. studies show the mononitrosyl $[Fe(NO)(SR)_3]^{3-}$ to be a major intermediate in this reaction.

Salts of the Black Roussin ion, $[Fe_4S_3(NO)_7]^-$ react with aryldiazonium salts, $ArN_2^+$, to produce $Fe_2(SAr)_2(NO)_4$. $^{13}$C n.m.r. studies of $Fe_2(SC_6H_4F)_2(NO)_4$ reveal it to exist in a 1:1 ratio of cis and trans isomers. Reaction of the Black anion with trialkylsulphonium or sulphoxonium salts leads to the metathesis product. The crystal structure of $Me_3S[Fe_4S_3(NO)_7]$ shows no evidence for the closure of the iron-sulphur cage by the sulphur of the $Me_3S$ cation. Reaction of the Black anion with trialkyloxonium salts provides good yields of $Fe_2(SR)_2(NO)_4$.

Electrochemical studies on $Fe_2(SR)_2(NO)_4$ by conventional cyclic voltammetry shows two chemically and electrochemically reversible one electron reductions to produce $[Fe_2(SR)_2(NO)_4]^-$ and $[Fe_2(SR)_2(NO)_4]^{2-}$. The monoanion is a paramagnetic complex with $g \approx 1.995$; coupling to four equivalent nitrogens shows the presence of a delocalised electron. The electrochemical behaviour of the dianion is dependent on the electrode material; reversible on a glassy carbon electrode but quasi-reversible on platinum. $Fe_2(SR)_2(NO)_4$ also exhibits a three electron oxidation; the anodic current of which increases in the presence of primary amines.

Electrochemical studies on the Black Roussin ion and its selenium analogue $[Fe_4Se_3(NO)_7]^-$ show similar electrochemical responses; three reversible one electron reductions and an irreversible multielectron oxidation.

Extended Hückel molecular orbital calculations on $[Fe_2S_2(NO)_4]^{2-}$ , $Fe_2(SMe)_2(NO)_4$ and $[Fe_2(S_2O_3)_2(NO)_4]^{2-}$ reveal little direct Fe-Fe interaction in these complexes. Reduction or oxidation would result in the addition or removal of electron density from orbitals of mainly Fe-S character.

An electrochemical study of $Fe(NO)(S_2CNR_2)_2$ by cyclic voltammetry shows a reversible one electron reduction and an irreversible oxidation in tetrahydrofuran and dichloromethane. In acetonitrile the reduction of the complex is coupled to a chemical step making the reduction chemically irreversible at low scan rates. The observed variation of $E^{\emptyset}$ with R is due to the inductive effect of R.

# Summary

Chapter one of this thesis is an introduction to some of the chemistry associated with iron-sulphur-nitrosyl complexes. It is by no means an exhaustive account, merely a melange of the interesting chemistry of these fascinating compounds and also of some related complexes. Chapter two deals with the molecular orbitals and bonding associated with iron dimers of the type $Fe_2B_2(NO)_4$ where B=S, SMe, $S_2O_3$. Chapter three contains a study of the synthesis, structure and chemistry of the newly characterised thiosulphato dianion, $[Fe_2(S_2O_3)_2(NO)_4]^{2-}$. This chapter also contains an examination of some of the reactions of Roussin's Black Anion, $[Fe_4S_3(NO)_7]^-$, which have a degree of relevance to the biological formation of $Fe_2(SMe)_2(NO)_4$. Chapter four contains a study of the electrochemistry of the Roussin Esters, $Fe_2(SR)_2$ $(NO)_4$ and of both Roussin's Red and Black Anions. A cursory look at the reactions of $Fe_2(SR)_2(NO)_4$ with amines is also reported. Chapter five contains a study of the electrochemistry of the mononitrosyl complexes $Fe(NO)(S_2CNR_2)_2$ and some related complexes.

# Contents

# Chapter One

## An Introduction to the Chemistry of the Roussinate Complexes

### Introduction

In 1858 an eminent French chemist by the name of Z. F. Roussin, produced the salts of two iron-sulphur-nitrosyl complexes. These were named the Black salt and the Red salt [1], the former of which was the first truly polynuclear iron-nitrosyl cluster. The actual stoichiometries of these two clusters were worked out by Pavel 24 years later; $M'[Fe_4S_3(NO)_7]$ and $M_2'[Fe_2S_2(NO)_4]$ for the Black and Red salts respectively [2]. Pavel also produced the so-called Ethyl Ester of Roussin's Red salt, $Fe_2(SEt)_2(NO)_4$, by the alkylation of the Red salt. The actual structures of the two salts were unknown. The structure of the Ethyl Ester was considered to be dimeric due to a molecular weight determination [3], and the groups were considered to be tetrahedrally arranged around the iron atoms. Application of the effective atomic number rule to this cluster required the presence of an iron-iron bond; this was used as evidence to explain the observed diamagnetism [4].

The Red salt was logically assumed to have a structure similar to $Fe_2(SEt)_2(NO)_4$. However the structure of the Black salt was more of a mystery. A core structure similar to the structure of ferrous sulphide was suggested [5], or one involving bridging nitrosyl ligands [6]. One hundred years after Roussin first prepared his complexes, the structures of $Fe_2(SEt)_2(NO)_4$ [7] and $Cs[Fe_4S_3(NO)_7]$ [8] were determined by X-ray crystallography. These structures are shown on the title page of chapter two of this thesis. In 1982, the structure of a Red salt was finally determined [9]. The assumption that the structure of $Fe_2(SEt)_2(NO)_4$ was analogous to this dianion was proven to be a valid one.

Metal nitrosyl chemistry was until recently (ca.1970) less well developed than metal carbonyl chemistry, mainly because of the latter's involvement in organic synthesis and the lack of industrial significance of the former. However because of a recent increase in the importance of metal-sulphur complexes, mainly due to the involvement of such complexes in biology (see below), but also in heterogeneous catalysis [10] and also in aspects of

superconductivity [11,12] and because of a concomitant increase in the importance of metal nitrosyl chemistry [13,14], a modicum of interest has been shown towards the Roussinate and Roussinate-like complexes [15, 16, 17, 18]. Moreover the discovery that the Methyl Ester of Roussin's Red salt, $Fe_2(SMe)_2(NO)_4$ has a possible role in the extremely high incidence of oesophageal cancer in an area of China [20], has spurred on research into this area. It has also recently come to light that the body's own hypotensive agent, known as the Endothelial Derived Relaxing Factor, is nitric oxide, NO [21]. This has led to research into the possibility of designing drugs capable of NO delivery *in vivo*.

The bioinorganic chemistry of iron-nitrosyls is not without precedent. The nitroprusside ion, $[Fe(CN)_5NO]^{2-}$ has long been recognised as a hypotensive agent [22], although the possible side-effect of cyanide poisoning has its drawbacks. Roussin's Black salt itself has been used as an effective disinfectant of drinking water [23] and acts against *Clostridium* species [23a]. The Black salt has also been shown to be an effective inhibitor of alcohol dehydrogenase [24].

## 1-1 A Note on Bioinorganic Chemistry

Bioinorganic chemistry as a discipline has only recently (within the past 25 years) reached a maturity within the scientific community at large. It is an area of science that borders on the traditional subjects of biology, chemistry and physics. As such major advances in this area are obtained through the collaboration of scientists from different fields. The two main participants in this field are the inorganic chemists and the enzyme biochemists. Until recently direct collaboration rarely existed between the two fields, and advances came about through individual groups basing work on the discoveries made in the other fields. In general the biologists attempt to understand the workings of a metalloprotein or metalloenzyme through for instance gene mapping, deletion studies and protein crystallography; the chemists attempt to understand the biology by attempting to chemically mimic the active site(s) of the enzyme. If the model works in a similar fashion to the enzyme,ie it is a true analogue, then a direct comparison to the structure of the active site of the enzyme may be made. For example, in the study of reversible dioxygen carriers, the biologists had already shown the presence of the haem group in myoglobin for instance [25], the chemists attempted to recreate the active site of the enzyme using the picket-fence models [26]. These models were never truly satisfactory, but the chemistry done in preparing them opened up new avenues of research. Another example comes from the search for analogues of the non-haem iron proteins and this

particular area of research is used here as a model study in the methods of bioinorganic chemistry.

In 1972, Lippard, Zubieta and Lewis published some work on an iron thioxanthato complex, which was proposed as a possible model for the actual site of the ferrodoxin proteins [27]. The electrochemistry of this material was similar to that of the natural enzymes. Now although Lippard's study was based on sound biological evidence [28, and references therein], it was in error; these materials were not analogues of the iron-sulphur proteins. However, the electrochemical results did have a direct relevance to the study of iron-sulphur proteins; it showed that the normal redox potential of the Fe(III)/Fe(II) couple was markedly stabilised by sulphur ligands and that groups attached to the sulphurs can alter the observed reduction potentials, as had been found with the enzymes [29]. Once the crystal structures of these proteins were solved [30], chemical research moved to produce such materials. The work of Holm and coworkers is particularly significant in this area [31]. The work done on iron-sulphur clusters has now been extended to the problems associated with the nitrogen fixing enzyme, nitrogenase.

For a substance to be an analogue of a metalloenzyme it must have similar spectroscopic and chemical properties to the actual enzyme, else it becomes another model. The iron-sulphur clusters produced as models for the enzymes have proven to be very good analogues. In the work of Holm the denatured apoprotein of a metalloenzyme was taken and mixed with a synthetic analogue of the active site [32]. On reconstituting the enzyme's structure, full activity was restored.

Once such an analogue has been prepared, the reason for its chemistry is sought; an understanding of what an analogue can achieve reflects on the enzyme itself. With iron-sulphur analogues, electrochemistry has proven to be a powerful tool in the elucidation of reactivity [33]. These iron-sulphur clusters can 'soak' up from one to four electrons and release them without undergoing fragmentation, hence the reasoning behind the idea of iron-sulphur enzymes acting as electron sinks or reservoirs. With the analogues, the effect of groups attached to the metal affects the reduction potentials observed [33]. This has helped to explain the wide range of potentials observed for the natural enzymes.

Molecular orbital calculations have attempted to explain these observations from a theoretical point of view. Although at present crude, theoretical calculations have proven useful in explaining or predicting observable phenomena. For instance using molecular orbital

calculations, Norman [34, 35, 36] has given evidence that the antiferromagnetism observed in the two iron ferrodoxins [37] is due to superexchange and not due to Fe-Fe overlap, and that the main bonding interactions are concentrated in the Fe-S bonds.

The study with which this theses was ultimately concerned with was the role of nitrosylated iron-sulphur clusters in the formation/promotion of oesophageal cancer. As such the study of iron-sulphur proteins has a direct relevance to this study.

## 1-2 The g=2.03 complexes

In 1965 M$^{c}$Donald and coworkers [38] discovered that if NO(g) was bubbled through ferrous ion solutions containing an additional coordinating ligand, such as phosphate, molybdate, alkyl mercaptans or cysteine, then paramagnetic complexes were obtained with g values in the range 2.02 to 2.04. Hyperfine coupling to associated ligands indicated the presence of two nitrosyl ligands and two other groups, probably arranged in a tetrahedral manner around iron, ie $[Fe(NO)_2X_2]^{y-}$. It is interesting to note that the use of penicillamine gave rise to two paramagnetic species, one was identified as $[Fe(NO)_2(penicillamine)_2]^{3-}$ g=2.032, the other was apparently a mononitrosyl with g=2.04, $A^{14}N$=13.8G.

The importance and relevance of this work to the carcinogenic state was obvious when species with g≈2.03 were found in rats following the administration of specific chemical carcinogens [39, 40]. If experimental animals were maintained on a diet supplemented by sodium nitrite and ferrous sulphate only, then a species with g=2.03 was observed and tentatively identified as a $[Fe(NO)_2X_2]^{y-}$ complex. Thus iron-nitrosyl complexes were shown to have an association with the carcinogenic state.

## 1-3 Oesophageal Cancer and Iron-Nitrosyl Complexes

In 1980, the results of an epidemiological study of the geographical variation in the occurrence of various forms of cancer throughout China was published [42]. It showed, amongst other things, that a very high, but very localised, incidence of oesophageal cancer was

present in the Linxian valley of the Henan province in Northern China. The incidence of cancer was as high as one in four of the adult population.

A team of scientists investigated every aspect of life in this rural area. A variety of probable causes was arrived at; the local water supply had high levels of nitrite and nitrate, the soil had low concentrations of molybdenum and a mold which contaminated local foodstuffs was shown to be a producer of nitrosamines in the presence of nitrite. However one peculiarity of this area was the method of preserving vegetables. These were pickled in the local water for up to four weeks before consumption. An analysis of the pickled vegetables by gas chromatography/mass-spectroscopy revealed the presence of the Methyl Ester of Roussin's Red salt, $Fe_2(SMe)_2(NO)_4$ [20,43]. Never before had this cluster been found in nature. This unusual finding was followed up by an investigation of its carcinogenic properties. The complex did not by itself show mutagenic behaviour, rather it promoted the action of known carcinogens [44, 45]. It was assumed that the complex can somehow donate 'NO' in some form to secondary amines with the subsequent formation of N-nitrosamines.

N-nitrosamines are known potent carcinogens [46]. They act *in vivo* as alkylating agents. For instance dimethylnitrosoamine, $(CH_3)_2N\text{-}NO$, undergoes oxidation by cytochrome P450 to yield N-hydroxymethyl-N-methylnitrosamine. This spontaneously loses formaldehyde, generating methyldiazohydroxide. This latter compound is the primary carcinogen. It acts through the loss of dinitrogen, generating an alkylating agent. Alkylation of DNA occurs most often at the $O^6$ site of a guanine residue [46]; this causes a mismatch in a C-G base pair. On replication a C-G base pair transforms into a T-A base pair. This mutation may result in the generation of a carcinogenic state, see figure 1-1. The effect of ionising radiation is similar; the radiation produces a large amount of reactive ions capable of alkylating DNA, and replication of the damaged DNA may lead to the possibility of cancer.

Roussin's Black salt as mentioned earlier is an effective antiseptic agent against *Clostridium*. Similarly, nitrite is an inhibitor of *Clostridium* and *Salmonella* bacteria [47] and is used widely as a meat preservative. If nitrite, cysteine and ferrous sulphate are autoclaved together, Roussin's Black anion is formed [23a]. The reaction of nitrite on Roussin's Black salt produced a $g \approx 2.03$ species [48]. It has also been shown that in the presence of thiolate ions the Black salt reacts to give the paramagnetic complexes $[Fe(NO)_2(SR)_2]^-$. It is possible that this type of dinitrosyl-monoiron-paramagnetic complex may be responsible for the observed inhibition of *Clostridium*, and in view of the

association of the g=2.03 with the carcinogenic state, it is not too unreasonable to suspect that such a species is involved in the promotion of the oesophageal cancer described above.

**Figure 1-1,**

Chemical Alkylation of DNA

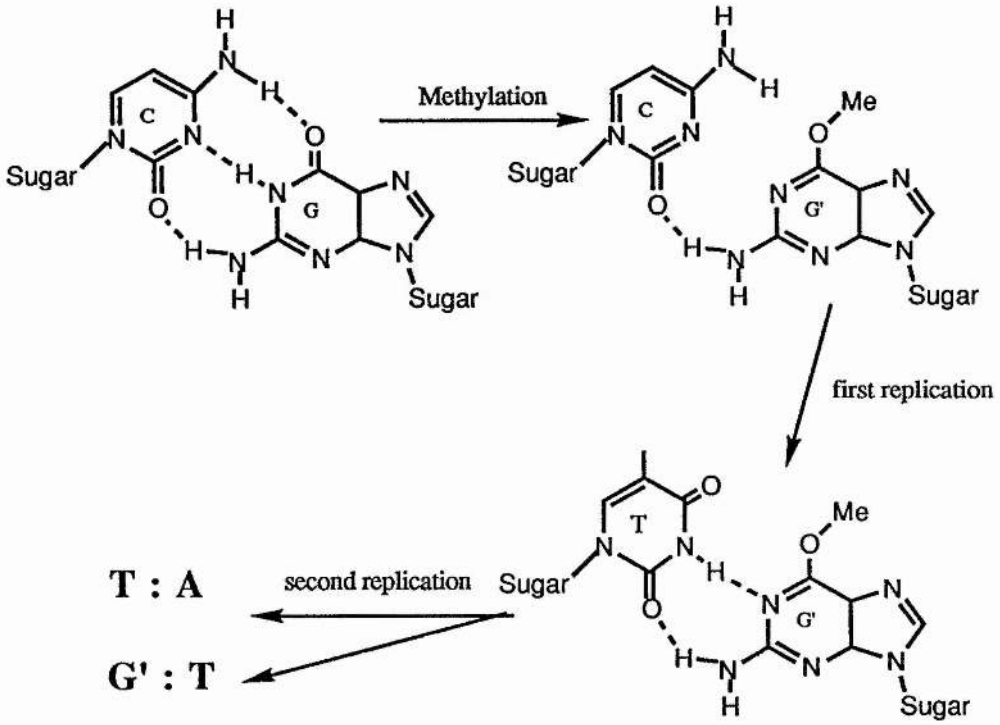


1-4 NO as a Ligand

The molecular orbital energy diagram of nitric oxide, NO, is shown in figure 2-1, page 24. A lone electron occupies a $\pi^*$ antibonding orbital. NO can function as an electron donor, forming $NO^+$; the ionisation potential for this process is low ≈ 9.5 eV $mol^{-1}$ [49]. It can also accept an electron to form $NO^-$. Attached to a metal, the nitrosyl ligand forms M-N-O bonds rather than M-O-N. The bonding modes observed for metal nitrosyls are (i), terminal linear M-NO groups, (ii) bridging NO groups and (iii) bent terminal M-NO groups. The linearity or non-linearity of terminal M-NO groups has been the subject of much debate and it was normal to consider the former as being derived from $NO^+$ and the latter from $NO^-$ [13]. The reasons

for this argument can be found from an examination of the molecular orbitals of $NO_2$. As $NO_2^+$ a linear molecule was predicted, as $NO_2^-$ a bent molecule with a lone pair on an $sp^2$-type of orbital situated on the nitrogen atom was predicted [14].

As a ligand $NO^+$ is isoelectronic with CO, $CN^-$ and $N_2$, suggesting a degree of stability. The bonding modes of $NO^+$ are very similar to CO. For instance NO is found as a terminal linear group in the complexes $Fe_2(SR)_2(NO)_4$ which has its carbonyl counterpart in $Fe_2(SR)_2(CO)_6$. As a bridging ligand $NO^+$ has been found capable of forming doubly and triply bridging systems; for instance the compound $\{[Mn(C_5H_5)]_3(\mu_2\text{-}NO)_3(\mu_3\text{-}NO)\}$ has both types present [50].

NO can be considered to be a three electron donor; one electron is donated to the metal to form $NO^+$ which then donates a lone pair. The unfilled $\pi^*$ orbitals, like those of CO, can be used in back bonding, the metal donating electron density back into the ligand. Due to this phenomenon, $NO^+$ helps to stabilise metals in low oxidation states in a similar manner to CO.

The charge on $NO^+$ can be easily observed from the change in overall charge of the following complexes; $K_2[Fe(CN)_5NO]$, $K_3[Fe(CN)_5CO]$, $K_4[Fe(CN)_5CN]$. The three electron donating capability of NO can be observed by the replacement of CO by NO in the following complexes, $Ni(CO)_4$, $Co(NO)(CO)_3$, $Fe(NO)_2(CO)_2$. All these complexes obey the 18 electron rule, the extra electron coming from the nitrosyl ligand [6].

The extent of back bonding from the metal to the NO ligand can be observed from the nitrosyl stretching frequency; for NO itself this occurs at 1840 $cm^{-1}$, for $NO^+$ salts the stretching frequency occurs between 2150 and 2400$cm^{-1}$. In the complex $[Ru(CN)_5NO]^{2-}$ the stretching frequency is at 1927$cm^{-1}$, and for $Fe(NO)(S_2CNR_2)_2 \approx$ 1693$cm^{-1}$. The back bonding is greater in the latter complex.

The bending of an M-NO group has been examined by Enemark and Feltham [14]. For instance the complex $Co(NO)(S_2CNMe_2)_2$ has been shown to have a bent M-NO group with an angle of 138° [73]. The complex $Fe(NO)(S_2CNEt_2)_2$ which has one electron fewer than the cobalt complex has a linear M-NO group. The electron in the iron-nitrosyl complex is found

primarily in a $dz^2$ metal orbital which stabilises a linear nitrosyl, whereas in the cobalt complex the electrons have been shown to be probably present in an orbital favouring the bending of the M-NO group. The reason for the bending or non-bending of the group is seen not as a consequence of $NO^+$ versus $NO^-$ but as a subtle interplay of orbital energies [14].

Quite often in dinitrosyl complexes supposedly linear M-NO groups are found to deviate markedly from $180^o$. Probable reasons for this have been put forward by Enemark [14] and Hoffmann [61], and is further examined in chapter-2 of this thesis.

## 1-5 Some Reactions of Metal-Nitrosyl Complexes

Bottomley proposed that if a metal nitrosyl had $\nu$(NO) >1886 $cm^{-1}$ then it would be susceptible to nucleophilic attack at the nitrogen by such nucleophiles as hydroxide ion, alkoxides and amines [52]. For instance nitroprusside ion, $[Fe(CN)_5NO]^{2-}$ has $\nu$ (NO)=1938 $cm^{-1}$ and is attacked by amines and thiolates. The copper(II) nitrosyl halides react with alcohols, secondary amines and ammonia to give alkylnitrites, N-nitrosamines and dinitrogen respectively [53]. In a reaction with primary amines a diazo intermediate was formulated with which the copper was intimately involved during the denitrogenation reaction.

From Bottomley's arguments complexes with a low $\nu$(NO) ought to be susceptible to attack by electrophiles. Electrophilic attack on metal nitrosyls has been considered to proceed via the prior formation of a bent M-NO group, making the nitrogen more susceptible to attack [13]. The oxygenation of $[Co(NO)(en)_2]^+$ in the presence of electron donors such as pyridine, acetonitrile or phosphites leads to complexes such as $[Co(NO_2)(en)_2(NCMe)]^{2+}$. It is often observed that oxygenation reactions produce the nitrato or nitro/nitrito species. For instance the nitrosyl dimer $[Fe(NO)_2Cl]_2$ in the presence of hexamethylphosphorictriamide (HMPA) gives an unstable complex which on oxidation by dioxygen produces the nitrato complex $Fe(NO_3)Cl_2$(HMPA).1/2HMPA [54].

The chemistry of the Roussin salts and the dimeric esters of Roussin's Red salt has been investigated mainly by the Glidewell and coworkers [55 and references therein]. A major part of the observed chemistry of these complexes involves the production of monomeric paramagnetic iron complexes such as $[Fe(NO)_2(SR)_2]^-$, ie the g=2.03 species. It was found

that in the presence of thiolates or sulphide ion the complexes $Fe_2(SR)_2(NO)_4$, $M'[Fe_4S_3(NO)_7]$, and $Fe_4S_4(NO)_4$ all fragment to produce these monomeric iron complexes [48]. Similarly the chemistry of $Fe_2I_2(NO)_4$, used by Rauchfuss and Weatherill in a preparative route to $Fe_2(SR)_2(NO)_4$ complexes [56], has been shown by Hyde to proceed through similar g=2.03 species [57]. According to Bottomley since these clusters have $\nu$(NO) lower than the threshold value given then these should not react with nucleophiles. However, the attack by thiolate is not seen as an attack at the nitrogen but rather the attack of a nucleophile on the iron.

Addition of $^{15}NO_2^-$ to a solution containing $[Fe(^{14}NO)_2(SR)_2]^-$ caused the replacement of the e.p.r. signal from the latter complex with one due to $[Fe(^{15}NO)_2(SR)_2]^-$. This suggests that the NO ligand is quite labile and the conversion was suggested to go through the 'W' intermediate shown below (figure 1-2). The fluxionality of the complex $[Fe(NO)_2(NO_2)_2]^-$ is also highly suggestive of the formation of such an intermediate [59]. The lability of the NO ligand in these complexes has relevance to the tumorigenic promoting properties of the Methyl Ester of Roussin's Red salt.

**Figure 1-2**

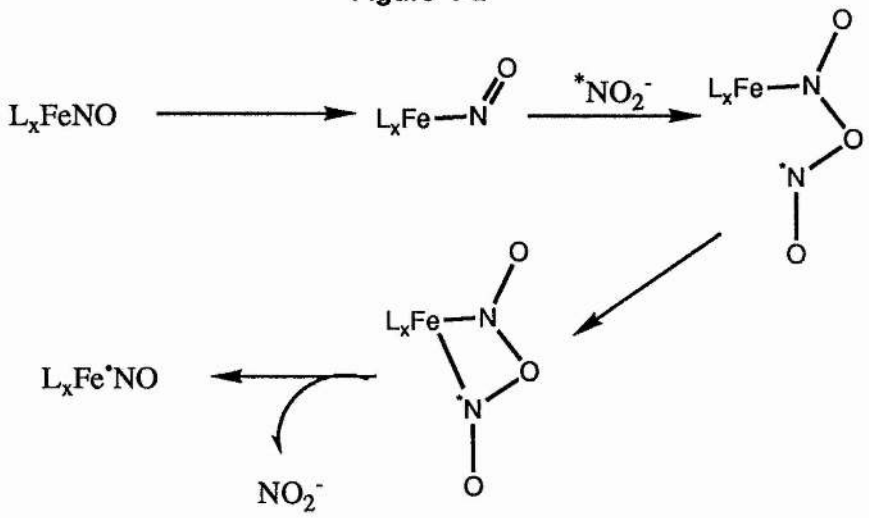


An interesting aspect of the chemistry of the iron dinitrosyl groups is the ease with which $[Fe(NO)_2]^+$ can be converted into $[Fe(NO)]^+$ ie a $d^9$ to $d^7$ conversion. This conversion proceeds readily in the presence of a chelating ligand such as the

dialkyldithiocarbamate ligands or even with the tetrathiomolybdate ion. Both these ligands produce square pyramidal complexes with the nitrosyl ligand in the apical position [61]. The reverse conversion is also quite facile. The cubic cluster $Fe_4S_4(NO)_4$ has all of its irons in the $d^7$ configuration. In the presence of thiolate ions, this cluster fragments to give the e.p.r. spectrum of $[Fe(NO)_2(SR)_2]^-$. The species $[Fe(NO)(SR)_3]^-$ has also been observed, but this decays with time producing a stronger signal from $[Fe(NO)_2(SR)_2]^-$ [48].

## 1-6 Electrochemical and Theoretical Studies of Some Iron-Sulphur Clusters

Since many of the metal-nitrosyl complexes contain $NO^+$ it would seem reasonable to suspect that the reduction of such complexes would result in the production of -NO•. Such reductions could produce complexes with labile NO ligands. This viewpoint may be valid for mononitrosyl, mononuclear complexes, but not for complexes of higher nuclearity. In these 'clusters' the HOMO/LUMO are regarded as being primarily due to metal-metal interactions and so a reduction of such a cluster would be expected to affect only the M-M interaction [63].

The reduction of $[Fe(CN)_5NO]^{2-}$ leads to the production of $[Fe(CN)_5NO]^{3-}$ described as containing Fe(II) and -NO• [13]. This complex is labile and loses a $CN^-$ ligand to give the square pyramidal complex $[Fe(CN)_4NO]^{3-}$, which has the nitrosyl ligand in the apical position. Calculations had predicted, however, a trigonal bipyramidal structure with the nitrosyl in the equatorial position [64].

The complex $[Fe(NO)(S_2CNR_2)_2]^-$ (R=CN or $CF_3$) undergoes a one electron reduction to give the dianion. The reduction potential of which is dependent on the attached sulphur ligands. Thus the LUMO is not solely associated with the nitrosyl ligand [13]. The view that the reduction of an M-$NO^+$ complex leads to an M-NO• complex is obviously a rather simplified view.

Multiple reductions of simple mononitrosyl mononuclear complexes often leads to the disruption of the complex, and in general the lower the nuclearity of a complex the more prone it is to fragmentation/loss of attached ligands on reduction or oxidation. In an impressive review of the electrochemistry of metal sulphur complexes by Zanello, this viewpoint is

borne out [62]. The cluster $Fe_3S_2(CO)_9$ (an $Fe_3S_2$ core) undergoes two well defined one electron reductions, the more negative of which is chemically irreversible. An examination of a cluster with a higher nuclearity such as $Fe_4S_4(C_5H_5)_4$ (an $Fe_4S_4$ core) reveals a plethora of redox processes, with four well defined one electron steps being recorded. It is worth noting here that the cluster $Fe_2S_2(CO)_6$ which has a similar structure to part of $Fe_3S_2(CO)_9$ (missing the $\mu_2$-$Fe(CO)_3$ ligand) shows two irreversible one electron processes [65]. However since the chemical reduction produces the known and stable complex $[Fe_2S_2(CO)_6]^{2-}$ the observed irreversibility may be due to the use of a platinum working electrode.

As described earlier in section 1-2, iron-sulphur proteins can be thought of as being electron sinks or reservoirs. The work devoted to the electrochemical examination of the $[Fe_4S_4]$ clusters is far more abundant than that devoted to any other type of metal-sulphur core. The electron changes of these analogues of the iron-sulphur proteins can be related to the oxidation/reduction potentials of the 4Fe4S ferredoxins and high potential iron proteins.

$$[Fe_4S_4(SR)_4]^{3-} \text{====} [Fe_4S_4(SR)_4]^{2} \text{====} [Fe_4S_4(SR)_4]^{1-}$$

Fd (reduced) ==== Fd (oxidised)

HPIP (reduced) ==== HPIP (oxidised)

A large amount of data is available on the structural changes that occur to the iron-sulphur cores that accompany redox changes of these clusters [62].

The observed electrochemistry of the clusters closely mimics that of the natural enzymes. However most of the electrochemical studies were done in non-aqueous systems and as a consequence most of the reduction potentials observed were too negative (about 0.5 V too low). When electrochemical studies were performed on clusters soluble in water the reduction potentials were found to be in the same range as for the enzymes. The differences between the aqueous and non-aqueous environments was seen as a consequence of hydrogen bonding and the different dielectric constants of the solvent systems. Some of the most interesting studies were done in aqueous micellar solutions. This was an attempt to recreate the biological environment of the enzyme and such studies were consistent with the results obtained for the natural complexes [62].

An examination of the electrochemistry of $Fe_4S_4(NO)_4$ by Dahl et al, revealed two well defined one electron reductions, giving the anion and dianion [66]. Relative to the reduction potentials observed for $Fe_4S_4(C_5H_5)_4$ the effect of the $NO^+$ ligand is seen as making the reduction easier to perform. Although Enemark and Feltham described M-NO chemistry as being predominantly nitrosyl centred perturbed by associated ligands [14], the electrochemistry of nitrosyl clusters of high nuclearity is seen as the effect of a metal core perturbed by all associated ligands. The electrochemistry of $Fe_4(NO)_4S_2(NCMe_3)_2$, a similar cluster to the cubic one described above has been reported to give four one electron reductions [62].

The similarities of the $[Fe_4S_4]$ cores for a variety of clusters led Dahl and coworkers to develop a qualitative molecular orbital bonding model for all clusters of this type [67]. According to the model for a cluster of type $[M_4(\mu_3S)_4X_4]^{n+}$ containing a metal of the first transition series to a first approximation the strong metal-ligand interactions can be considered separate from the weak metal-metal interactions. Thus the 3d, 4s and 4p orbitals of the four metal atoms combine to give $(a_1+2e+2t_1+3t_2)$, $(a_1+a_2)$ and $(a_1+e+t_1+t_2)$ orbitals respectively. Under $T_d$ symmetry twelve of the metal 3d orbitals give rise to six bonding $(a_1+e+t_2)$ and six antibonding orbitals $(t_1+t_2)$, the eight remaining are M-M non-bonding $(e_1+t_1+t_2)$, but these orbitals interact with the attached ligands, the nature of this interaction determines the final ordering of the orbitals. Using the crystal structures of a variety of $[Fe_4S_4]$ core containing clusters in a variety of oxidation states Dahl was able to give theoretical evidence for the structural changes that take place using this theoretical model.

Using the above model on $Fe_4S_4(NO)_4$ leads to the following electronic structure, $(e_1+t_1+t_2)^{16}$ $(a_1+e+t_2)^{12}$ $(t_1+t_2)^0$. Addition of an electron into the cluster will populate a t orbital leading to a Jahn-teller distortion. According to the model this should lead to a $D_{2d}$ distortion. The crystal structure of the mono reduced complex is indeed tetragonal $D_{2d}$ [66].

The carbonyl complex $Fe_4S_4(CO)_{12}$ a direct analogue of $Fe_4S_4(NO)_4$ has been prepared and structurally characterised [68]. The above molecular orbital scheme was

applied and led to the electronic structure $(a_1+e+t_2)^{12}$ $(t_1+t_2)^{12}$ $(e_1+t_1+t_2)$, ie all the M-M bonding and antibonding levels are filled. This is in agreement with the large Fe-Fe distances obtained from the crystal structure. The dianion $[Fe_4S_4(CO)_{12}]^{2-}$ has also been characterised, but was found to have fragmented to produce a cluster with two $Fe_2S_2$ units linked by an S-S bridge. Population of the $(e_1+t_1+t_2)$ orbitals which are predominantly M-L antibonding has fragmented the cluster.

The structure of Roussin's Black anion, $[Fe_4S_3(NO)_7]^-$ can be considered as a defective $Fe_4S_4$ core. The Dahl molecular orbital scheme can be used here with the obvious changes from Td to $C_3v$ symmetry. The Black anion has one unique iron, Fe(I) and three irons of Fe(-I), giving a total of 34 core electrons. This leads to a total of three bonding orbitals which are considered to have an electron pair shared between the apical iron and the three basal irons. Reduction of this cluster should therefore lead to an increase in the Fe-Fe distances and also to the possibility of fragmentation of the core. It has been noted that the oxidation of the complex leads to fragmentation; chemical oxidation releasing NO(g) [1]. This observation is in accordance with the loss of bonding electron density. The reduction of the analogous selenium complex $NH_4[Fe_4Se_3(NO)_7]$ has been shown to exhibit two well defined one electron reductions [69]. The structures of the monoanion [70] and the dianion [69] agree well with the ideas of adding electrons into antibonding orbitals. In chapter-4 of this thesis the electrochemistry of both $M'[Fe_4S_3(NO)_7]$ and $M'[Fe_4Se_3(NO)_7]$ are reported; the observed electrochemistry fits well with expectations from theory.

The electrochemistry of the metal dimers $Fe_2(SR)_2(NO)_4$ is investigated in chapter-4. As discussed earlier, the lower the nuclearity of a cluster the simpler its electrochemistry tends to be with the possibility of disruption of the complex. In many cases the reductive chemistry of complexes of the type $M_2(\mu_2\text{-}B)_2(Tm)_4$ or $M_2(\mu_2\text{-}B)_2(Tm)_6$ , where B=bridging ligand and Tm= terminal, has been considered to be associated with the breaking of an M-M bond. The HOMO/LUMO of such complexes has been reported to be mainly associated with the M-M interaction [63].

The reduction of $Fe_2S_2(CO)_6$ produces $[Fe_2S_2(CO)_6]^{2-}$ [71]. The reduction is seen as the breaking of an S-S bond, and it is reported that the irons are hardly affected by the reduction. This suggests that in this case the LUMO is primarily concentrated on the sulphurs.

The reduction of the complex $Fe_2(NO)_4(\mu\text{-}PPh_2)_2$ has been regarded as the loss of an Fe-Fe bond [72]. However if a hydride donor is used to achieve reduction then a terminal nitrosyl ligand is shifted into a bridging position. The nitrosyl bridging dianion, $[Fe(NO)_2(\mu\text{-}NO)(\mu\text{-}PPh_2)Fe(NO)(PPh_2)$ is thermodynamically unstable and rearranges above -70°C to $[Fe_2(NO)_4(\mu\text{-}PPh_2)]^{2-}$. This is seen as evidence that the LUMO of this cluster is not entirely Fe-Fe centered and that subtle differences to the ligands can cause a dramatic effect on orbital stabilities.

The presence of an Fe-Fe bond in a $d^9$ complex of the type $M_2(\mu\text{-}B)_2(Tm)_4$ has been the subject of an investigation by Summerville and Hoffmann [61]. However, the answer given to the question "do these clusters contain a M-M bond", was "maybe there is, but perhaps not." The examination of the $Fe_2S_2$ core structure in the 2Fe2S ferredoxins by Norman [34] concluded that there was no real Fe-Fe interaction and that the main bonding was via the Fe-S bonds. The core in the clusters $Fe_2(SR)_2(NO)_4$ is similar to the core in the 2Fe2S ferrodoxins. Calculations performed in chapter two of this theses on these nitrosyl clusters suggests a similar conclusion and that the observed diamagnetism in these clusters is also due to superexchange and not due to a direct Fe-Fe interaction.

## References


1. Roussin, Z. F., Ann. Chem. Phys., 52, 283, (1856)

2. Pavel, O., Ber. Dtsch. Chem. Ges., 15, 2600, (1882)

3. Hoffmann, Wiede, Z. Anorg. Chem., 8,318, (1895); 9, 295 (1895); Reihlen, Friedolsheim, Annalen, 71, 457, (1927)

4. Cambi, Siego, Atti. Accad. Lincei., 13, 158, (1931)

5. Seel, Z. Anorg. Chem., 249,308, (1947)

6. Addison, C.C., Lewis, J., Q. Rev. Chem. Soc., 9, 115, (1955)

7. Thomas, J. T., Robertson, J. H., Cox, E. G., Acta Cryst., 11, 599, (1958)

8. Johansson, L., Lipscomb, W. N., ibid, 11, 594, (1958)

9. Lin Xianti, Zheng An, Lin Shunhao, Huang Jingling, Lu Jiaxi, J. Struct. Chem. (Wuhan), 1, 79, (1982)

10 Müller, A., Polyhedron, 5 323, (1986)

11. Hughbanks, T., Hoffmann, R., J. Am. Chem. Soc., 105, 1150, (1983)

12. Wooley, R. G., Inorg. Chem. 24, 3519, (1985)

13. M$^{C}$Cleverty, J. J., Chemical Rev. 79, 53, (1979)

14. Enemark, J. H., Feltham, R. D., Coord. Chem. Rev., 13, 339, (1974)

15. Chu, C. T-W., Lo, F. Y-K., Rae, A. D., Dahl, L. F., J. Am. Chem. Soc., 104, 3409, (1982)

16. Chu, C. T-W., Dahl, L. F., Inorg. Chem.,16, 3245, (1977)

17. Nelson, L. L., Lo, F. Y-K., Rae, A. D., Dahl, L. F., J. Org. Met. Chem., 225, 309, (1982)

18. Gall, R. S., Chu, C. T-W., Dahl, L. F., J. Am. Chem. Soc., 96, 4019, (1974)

19. Gall, R. S., Connelly, N. G., Dahl, L. F., J. Am. Chem. Soc., 96, 4016, (1974)

20. Wang, G. H., Zhang, W. X., Chai, W. G., Acta Chim. Sin., 38, 95, (1980)

21. Gryglewski, R. J., Palmer, R. M. J., Moncada, S. E., Br. J. Pharmacol., 87, 685, (1986)

22. Johnson, C. C., Arch. Int. Pharmacodyn Ther., 35, 489, (1929)

23. Dobrey-Duclaux, A., Boyer, F., Ann. Inst. Pasteur., 71, 455, (1945); 23a. Ashworth, J., Didcock, A. G., Hargreaves, L. L., Jarvis, B, G., Walters, C, L., Larkworthy, L. F., J. Gen. Microbiol., 84, 403, (1974)

24. Dobrey-Duclaux, A., Biochim. Biophys. Acta, 39, 44, (1960)

25. Cotton, A., Wilkinson, G., "Advanced Inorganic Chemistry", 4th Edition, (1980), John Wiley (publishers)

26. Collman, J. P., Accs. Chem. Res., 16, 265, (1977)

27. Lewis, D. F., Lippard, S. J., Zubieta, J. A., J. Am. Chem. Soc., 94, 1563, (1972)

28. Jensen, L. H., Annu. Rev. Biochem., 43, 461, (1974)

29. Zubieta, J. A., Mason, R., Angew. Chem. Int. Ed., 12, 390, (1973)

30. Jensen, L. H., "Iron Sulphur Proteins", 2, 163, (1973); Spiro,T. G., "Iron sulphur proteins" , (1982) Wiley (publishers)

31. Cambray, J., Lane, R. W., Wedd, A. J., Johnson, R., Holm, R. H., Inorg. Synth., 16, 2565, (1977); Wong, G. B., Bobrik, M. A., Holm, R. H., ibid, 17, 578, (1978); Holm, R. H., Accs. Chem. Res., 10, 427, (1977)

32. Kurtz, D. M., Wong, G. B., Holm, R. H., J. Am. Chem. Soc., 100, 6777, (1978)

33. For instance, Zanello, P., Coord. Chem. Rev., 83, pages 208-230, (1988)

34. Norman, J. G., Kalbacher, B. J., Jackels, S. C., J. C. S., Chem. Comm., 1027, (1976)

35. Norman, J. G., Yang, C. Y., Johnson, K. H., Holm, R. H., J. Am. Chem. Soc., 97, 6596, (1975)

36. Norman, J. G., Jackels, S. C., J. Am. Chem. Soc., 97, 3833 (1975)

37. Sands, R. H., Dunham, W. R., Quart. Rev. Biophys., 7, 443, (1975)

38. M$^{C}$Donald, C. C., Phillips, W. D., Mower, H. F., J. Am. Chem. Soc., 87, 3319, (1965)

39. Woolum, J. C., Commoner, B., Biochim. Biophys. Acta, 201, 131 (1970)

40. Chiang, R. W., Woolum, J. C., Commoner, B., ibid 257, 452, (1972)

41. Vanin, V., Vanin, A. F., Biophysics, 28, 1125, (1983)

42. "Atlas of Cancer Maps of the Peoples Republic of China", China Map Press, Beijing, (1980)

43. Wang, M. Y., Lu, S. H., Ji, C., Wang, Y. L., Li, M. H., Cancer Res. Preven. Treat., 10, 12, (1983)

44. Cheng, S. J., Sula, M., Li, M. H., Courtois, I., Chourovlinkov, I., Carcinogenesis, 2, 315, (1981)

45. Liu, J. G., Li, M. H., Carcinogenesis, 10, 617, (1989)

46. Blackburn, G. M., Kellard, B., Chemistry and Industry. 15, 607, (1986); 15, 687, (1986); 15, 770, (1986)

47. Perigo, J. A., Roberts, J. A., J. Food Techn., 3, 91, (1968)

48. Butler, A. R., Glidewell, C., Hyde, A. R., Walton, J. C., Polyhedron, 4, 797, (1985)

49. Hogstrum, Tate., Phys. Rev., 59, 354, (1941)

50. Elder, R. C., Inorg. Chem., 13, 1037, (1974)

51. Lewis, J., Irving, R. J., Wilkinson, G., J. Inorg. Nucl. Chem., 7, 32, (1958)

52. Bottomley, F., Brooks, W. V. F., Clarkson, S. G., Tong, S-B., J. C. S., Chem . Comm., 919, (1973)

53. Doyle, M. P., Siegfried, B., Hammond, J. J., J. Am. Chem. Soc., 98, 1697, (1976) and therein.

54. Wah, K. H. L., Postel, M., Tomi, F., Inorg. Chem., 28, 233, (1989)

55. Butler, A. R., Glidewell, C., Li, M-H., Adv. Inorg. Chem., 32, 335, 1988

56. Rauchfuss, T. B., Weatherill, T. B., Iorg. Chem., 21, 827, (1982)

57. Butler, A. R., Glidewell, C., Hyde, A. R., Walton, J. C., Polyhedron, 4, 303, (1985)

58. Butler, A. R., Glidewell, C., Hyde, A. R., M$^{c}$Ginnis, J., Seymour, J. E., Polyhedron, 2, 1045, (1983)

59. Butler, A. R., Glidewell, C., Johnson, I. L., Polyhedron, 6, 2091, (1987)

60. Hoffmann. R., Summerville, R. H., J. Am. Chem. Soc., 98, 7240, (1976)

61. Butler, A. R., Glidewell, C., Johnson, I. L., Walton, J. C., Polyhedron, 6, 2085, (1983)

62. Zanello, P., Coord. Chem. Rev, 83, 199, (1988)

63. Lemoine, P., ibid, 83, 169, (1988)

64. Schmidt, J., Kuhr, H., Dorn, W., Kopf, J., Inorg. Nucl. Chem. Lett., 10, 55, (1974)

65. Lambert, R. J., unpublished work

66. Chu, C. T-W., Lo, F. Y-K., Dahl, L. F., J. Am. Chem. Soc., 104, 3409, (1982)

67. Toan, T., Teo, B. K., Ferguson, J. A., Meyer, T. J., Dahl, L. F., J. Am. Chem. Soc., 99, 408, (1977)

68. Nelson, L. L., Lo, F, Y-K., Rae, A. D., Dahl, L. F., J. Org. Met. Chem.m 225, 309, (1982)

69. Nelson, L. L., PhD thesis University of Wisconsin-Madison, 1981

70. Audrey Lees et al, University of St. Andrews, awaiting publication.

71. Weatherill, T. D., Rauchfuss, T. B., Scott, R. A., Inorg. Chem., 25, 1466, (1986)

72. Yu, Y-F., Chau, C-N., Wojcicki, A., Inorg. Chem., 25, 4098, (1986)

73. Enemark, J. H., Feltham, R. D., J. C. S., Dalton Trans., 718, (1972)

# Chapter Two

## Roussin's Black Salt

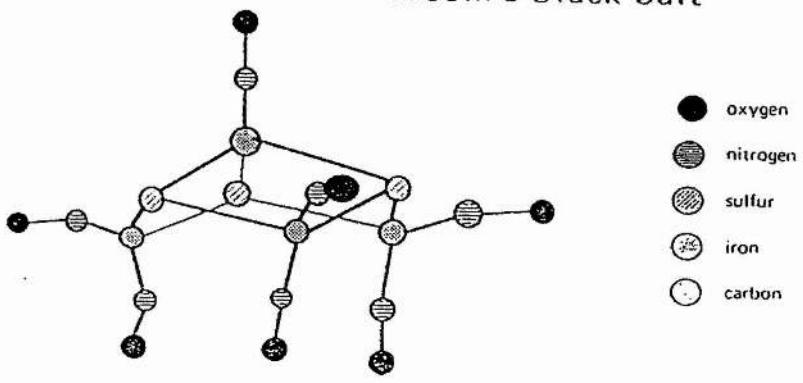


The structure of the anion $[Fe_4S_3(NO)_7]^-$ as in the $Ph_4As^+$ salt.

## Roussin's Red Salt

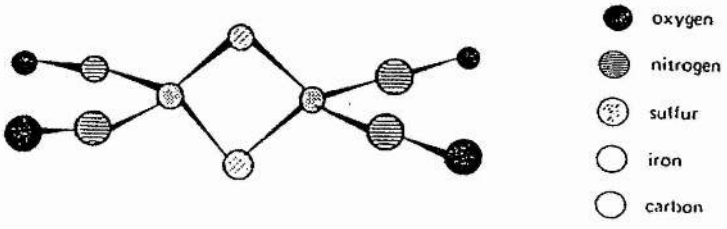


The structure of the anion $[Fe_2S_2(NO)_4]^{2-}$ as in the $Me_4N^+$ salt.

## Ethyl Ester of Roussin's Red Salt

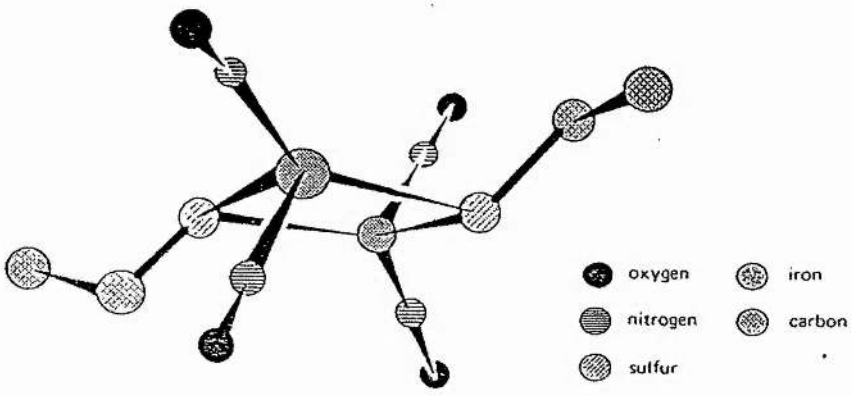


The structure of $[Fe_2(SEt)_2(NO)_4]$.

# Chapter Two

## The Extended Hückel Examination of the Bonding in Roussin's Red dianion, the Esters of Roussin's Red salt and Roussin's Black anion.

### Introduction

The alkyl esters of Roussin's Red salt, $Fe_2(SR)_2(NO)_4$, Roussin's Red salt, $[Fe_2S_2(NO)_4]^{2-}$,and the newly characterised thiosulphato complex $[Fe_2(S_2O_3)_2(NO)_4]^{2-}$ (see chapt-3), have all been shown to exhibit approximately the same electrochemical behaviour (see chapt-4). The methyl ester, $Fe_2(SMe)_2(NO)_4$ has been implicated as a possible factor in the occurrence of oesophageal cancer in the Henan province of China, formed most probably by the action of nitrite on natural iron-sulphur enzymes. Knowledge of how these iron-sulphur-nitrosyl clusters act under redox conditions is of great interest since it is presently thought that the methyl ester is oxidised to an iron-nitrosyl species which acts as a nitrosyl donor towards amines with the subsequent formation of N-nitrosamines; known potent carcinogens.

Molecular Orbital calculations used as part of an overall examination of the chemistry of a compound can lead to explanations of observed phenomena and can also be used predictively. Such calculations are, however, prone to many approximations making the data obtained of a qualitative nature, especially when used for heavy atoms such as iron and other metals. When used by itself, with no back up from other experimental observations, then criticism of the technique may be just, but used as part of an overall examination then molecular orbital calculations become as much a tool to the chemist as is n.m.r. or I.R. spectroscopy.

In this chapter the molecular orbitals of the iron sulphur dimers, $[Fe_2S_2(NO)_4]^{2-}$, $Fe_2(SMe)_2(NO)_4$, and $[Fe_2(S_2O_3)_2(NO)_4]^{2-}$ were examined using the Extended Hückel method [4,5]. The tetrameric cluster $[Fe_4S_3(NO)_7]^-$ was also examined by the same technique. Although such calculations have been performed on the Red dianion and

$Fe_2(SH)_2(NO)_4$ [1], the HOMO and LUMO were described as being Fe-Fe bonding and antibonding respectively. An examination of the calculation revealed that there was very little interaction between the two iron atoms, because of this the orbitals of these clusters were examined more closely using the method outlined in the experimental section.

## Experimental

Bonding in Roussin's Red Salt

The methodology used in determining the bonding involved with Roussin's Red Salt was a sort of synthon-disconection approach, that is to say the bonding of parts of the whole are examined in order to understand that whole. The geometry used was obtained from the X-ray structure of $Fe_2(SCH_2CH_3)_2(NO)_4$ [2] by the removal of the alkyl groups and standardising the bond angles and lengths such that $D_{2h}$ symmetry was obtained. The complex was split into the following fragments; $NO^+$, $[Fe(NO)_2]^+$, $[Fe_2]^{2-}$, $[S_2]^{4-}$, $[Fe_2(NO)_4]^{2+}$, $[Fe_2S_2]^{6-}$, (with and without sulphur d-orbital participation). The bonding involved in each fragment was determined and its relationship to the other fragments as the cluster was 'rebuilt' examined. Finally the bonding in $[Fe_2S_2(NO)_4]^{2-}$ was examined on the basis of the previous calculations.

Bonding in $Fe_2(SMe)_2(NO)_4$

Again the X-ray structure of $Fe_2(SCH_2CH_3)_2(NO)_4$ [2] was used in the calculation of the molecular orbitals of this cluster. The end methyl groups were removed and a hydrogen placed on the C-C vector at an appropriate distance for a C-H bond. The geometry manipulations which were carried out were done by moving the methyl group at an angle (+/-)Ø to the plane of the $Fe_2S_2$ core while leaving all other bond angles and lengths untouched,(ie, a constrained geometry optimisation). The coordinate positions of the atoms of the methyl groups were calculated using the normal methods of linear algebra.

Bonding in $[Fe_2(S_2O_3)_2(NO)_4]^{2-}$

The X-ray structure of $(PNP)_2$ $[Fe_2(S_2O_3)_2(NO)_4]$ was obtained from crystals grown in this laboratory. The atomic coordinates obtained for the dianion were used without

alteration in this study of the molecular orbitals. The geometry manipulations carried out on this cluster were done by moving the sulphite groups relative to the $Fe_2S_2$ plane as done for $Fe_2(SMe)_2(NO)_4$. The effect of bridge geometry was examined by constraining the geometry such that the angles and distances of the $Fe(NO)_2$ fragments were untouched and that the Fe-S distances were unchanged; the calculations were solely based on the effect of changing the Fe-Fe distance and therefore the S-Fe-S angle.

Bonding in $[Fe_4S_3(NO)_7]^-$

The molecular orbitals of Roussin's Black anion were examined using the data from the X-ray of Chu and Dahl [3]. No changes were made to the original structure, and bond lengths and angles are as for the crystal structure.

Calculations

Extended Hückel Molecular Orbital Calculations (EHT) [4,5] based on the above geometries, used atomic parameters available from the literature [6,7,8]. The calculations were performed on a VAX 11/785 computer.

## Results and Discussion

2 - 1

Bonding in Nitric Oxide, NO

Nitric oxide as a ligand has been described at length in chapter one and apart from a brief description of its molecular orbitals little is added here. The molecular orbital energy diagram for NO is given in figure 2-1. The $\sigma_3$ and $\sigma_4$ orbitals of NO are low lying occurring at -35.5 and -22 ev respectively. The degenerate $\pi_1$ orbitals and the $\sigma_5$ orbital lie at -16 and -14.7ev respectively. The degenerate $\pi^*$ orbitals occur at -11.2 ev and contain a single electron; giving the molecule its observed paramagnetism. In $NO^+$ the $\sigma_5$ orbital will be the HOMO. This $\pi$ acceptor ligand operates as such a ligand because of these empty $\pi^*$ orbitals, orbitals which are of comparable energy to many metal d-orbitals, hence its success as a ligand for metals in low oxidation states.

**Figure 2-1**

Molecular orbital Energy Diagram of NO

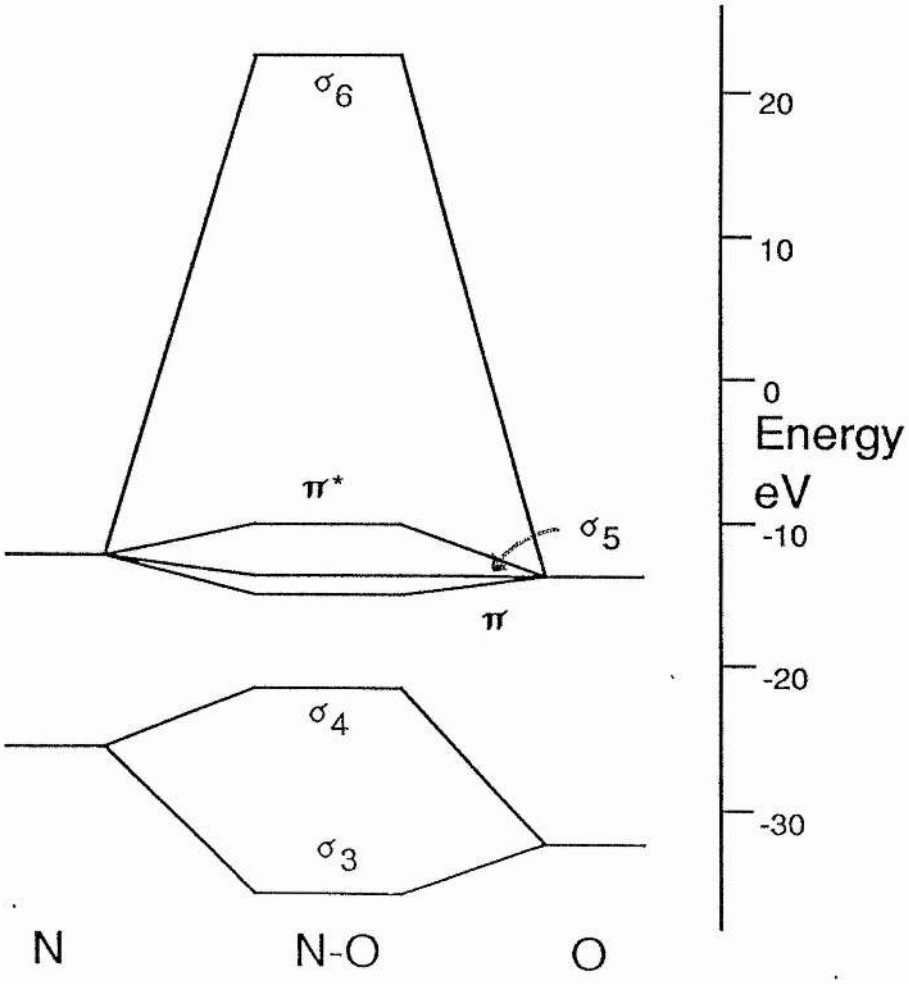

2 - 2

Bonding in dinitrosyliron(-I), $[Fe(NO)_2]^+$

The fragment $[Fe(NO)_2]^+$ derived from Roussin's Red Salt was examined by EHT using the same coordinate system as that used for the parent complex. The molecular orbital energy diagram, figure 2-2, graphically portrays the results of the calculations. The lowest levels, $\sigma_3$, are unchanged from those of NO. The $\sigma_4$ levels have been stabilised by an average of 0.53 ev relative to NO. This is a direct consequence of metal d-orbitals of the correct symmetry mixing, in a bonding arrangement, with the $\sigma_4$ orbitals of NO of a similar symmetry, figure 2-3a. The a, b, g or u notation used to label the orbitals is explained in Appendix-1.

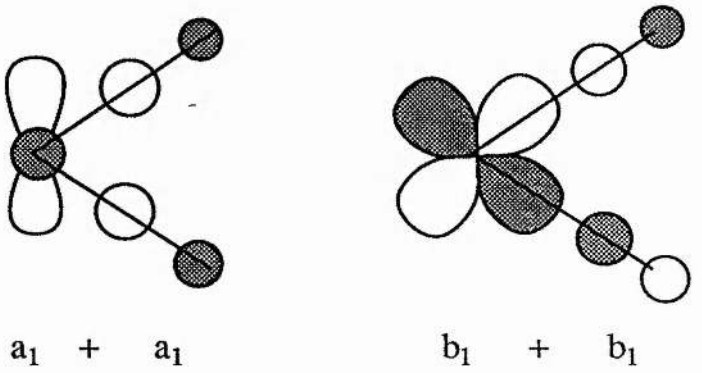


**Figure 2-3a**
**$\sigma_4$ Orbitals**

The $\pi_1$ levels lie lower in energy than the $\sigma_5$. However there is no significant stabilisation of these levels compared to the equivalent orbitals found with NO, although slight mixing with the d-orbitals has occurred (fig 2-3b). Orbital $1a_1$ is of interest. It is a mix of $dx^2$-$y^2$ and $dz^2$ resulting in an increased amount of electron density in the Z and Y direction but lower in the X. This results in a "round the corner" bonding arrangement. This form of hybridisation we have termed Fe $dx^2$-$y^2$/$dz^2$-(Y). The slight stabilisation involved in these orbitals can be correlated with a d-orbital involvement of between 2 and 8%. Since the Z axis-Fe-NO angle is $58^o$ and not $45^o$, dyz becomes bonding (orbital $1b_1$). At the latter angle the d orbital would lie in the node of the $\pi$ orbital of NO.

## Figure 2-2

Molecular Orbital Energy diagram of $[Fe(NO)_2]^+$

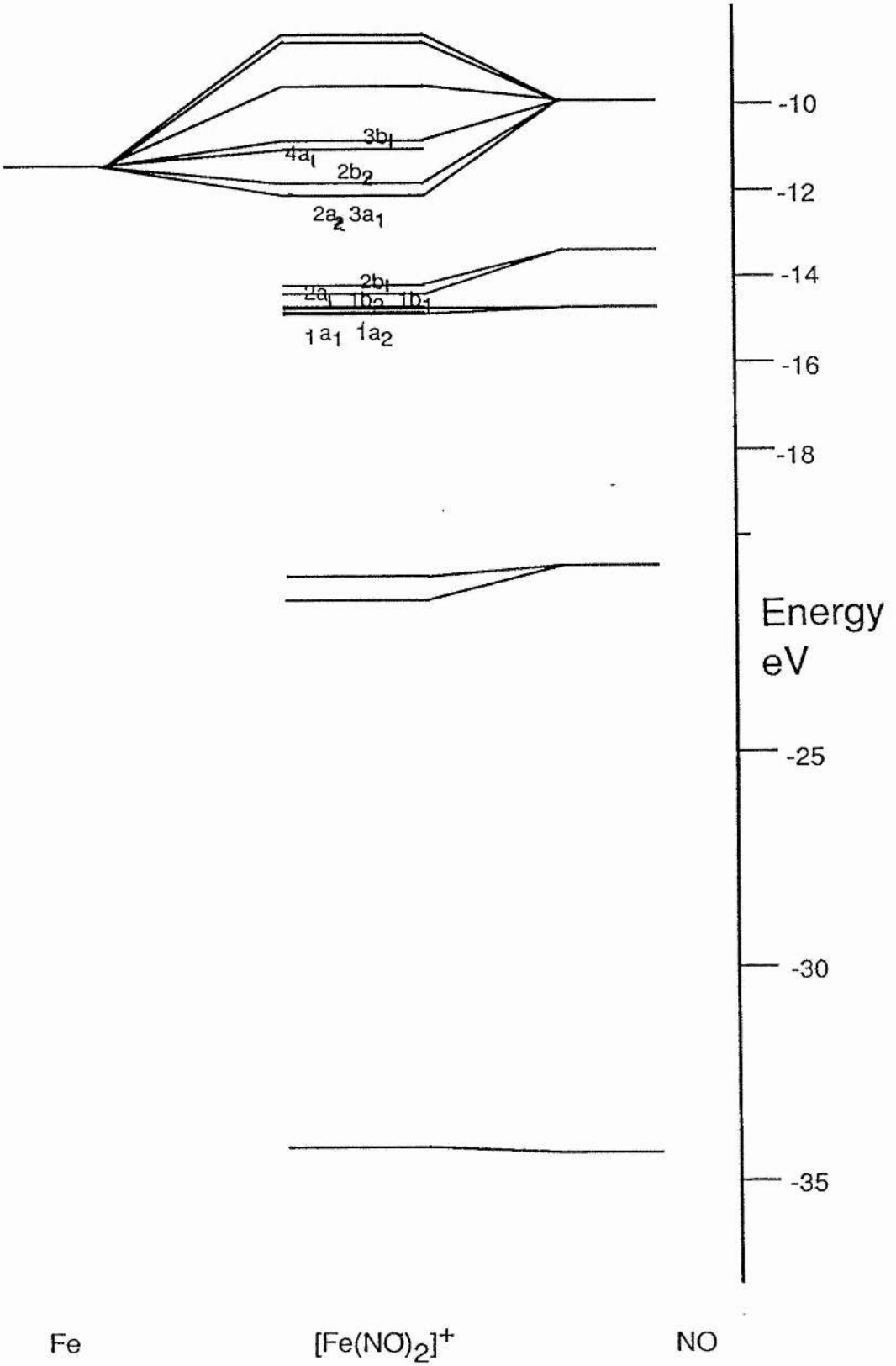

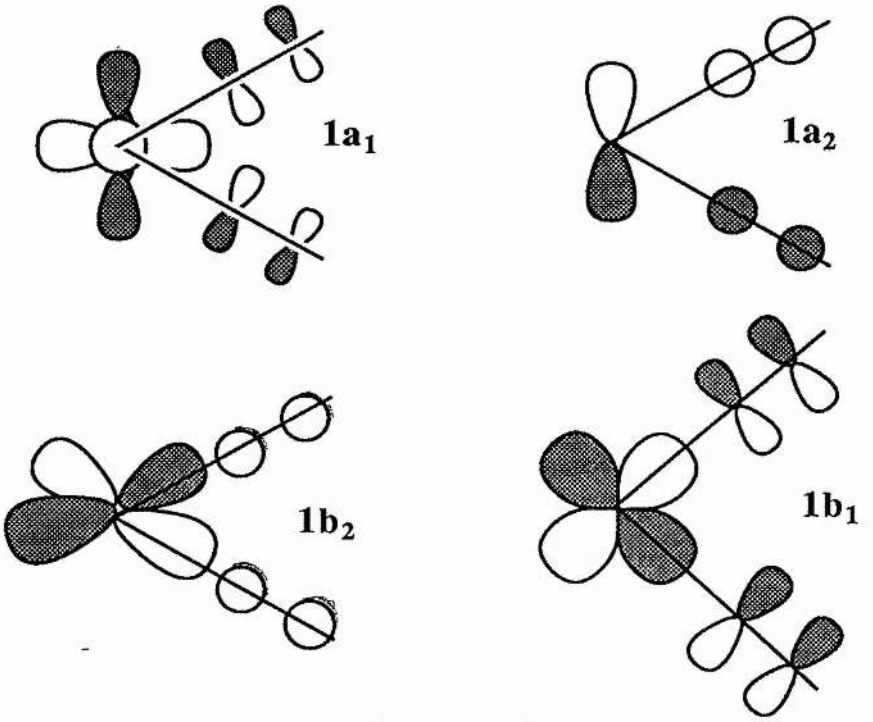


**Figure 2-3b**
**$\pi_1$ levels**

The $\sigma_5$ levels have become more stable than the corresponding level in NO by an average of 0.9 ev (fig 2-3c). There is an average of 12% electron density on the iron for each level. Although with orbital $2a_1$, the p-orbital of the nitrogen points towards the node of the metal orbital and as such we would expect no net bonding, a mixing of metal s-orbital character into the metal d-orbital results in the net bonding overlap.

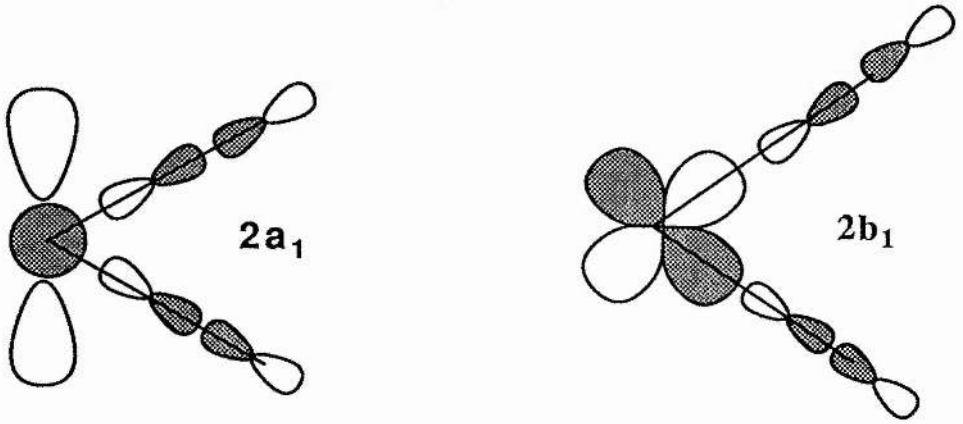


**Figure 2-3c**
**$\sigma_5$ levels**

Mixing of the metal d-orbitals with the empty $\pi^*$ orbitals of NO results in a stabilisation of energy ranging from 2.1 to 0.9 ev. There are four NO $\pi^*$ group orbitals but five metal d-orbitals, hence one level is non bonding. Of the four bonding metal orbitals, three have been stabilised relative to a parameterised value of -12.700 ev,(fig 2-3d). The lone electron is localised in the $3b_1$ (Fe dyz-NO $\pi^*$) orbital. Orbital $3a_1$ is similar to that already observed in the "round the corner" bonding arrangement (orbital $1a_1$). The non-bonding level, $4a_1$, is also a $dx^2\text{-}y^2/dz^2$ hybrid, however in this case there is increased electron density along the X-axis where no ligand lies, this level we have termed Fe $dx^2\text{-}y^2/dz^2\text{-}(X)$. The HOMO, orbital $3b_1$, contains 35% of available electron density situated on the iron, the LUMO which is the antibonding orbital of orbital $2b_2$ contains 33% of available electron density on iron, the non-bonding orbital 95%.

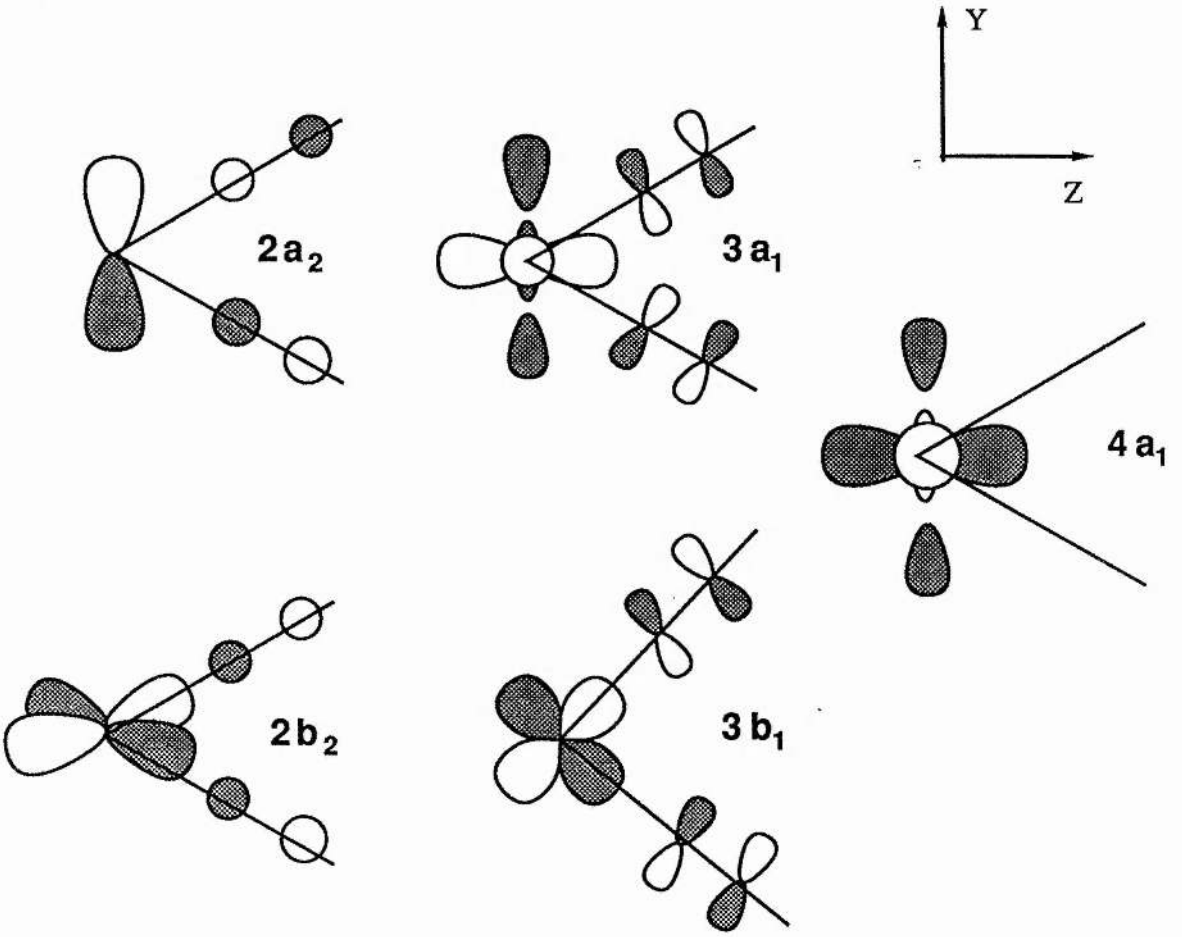


**Figure 2-3d**
**Fe-$\pi^*$NO orbitals**

The simplest polynitrosyl species is $M(NO)_2$. In a linear geometry it has the symmetry $D_{\infty}h$, in a bent geometry it has $C_2v$ symmetry. The correlation diagram given by Enemark and Feltham [9] fits very well with the results of these calculations. The ordering of the orbitals found here fits well with that predicted by these workers.The one electron orbital scheme put forward by Enemark and Feltham predicts a $C_2v$ symmetry for the $\{M(NO)_2\}^8$ species, however in the $\{M(NO)\}^{10}$ species the electrons would be placed in a non-bonding orbital (of $b_1$ symmetry) with respect to the metal, and antibonding with respect to N and O. They predict that the N-M-N angle should increase from the $90^o$ value. The $[Fe(NO)_2]^+$ fragment from Roussin's Red dianion is an $\{M(NO)_2\}^9$ species and the N-M-N angle is $116^o$, this is in accordance with the above prediction. As the angle increases from $90^o$ the non-bonding orbital will become bonding as the nitrosyl ligands achieve a net bonding interaction with the metal as shown in figure 2-3d,(orbital $3b_1$). Thus further addition of electrons to this orbital will cause the N-M-N angle to increase more. However these workers also predict that the oxygens of the nitrosyls should bend away from each other as the angle widens, but the crystal structure [10] of the Red dianion shows the nitrosyls bending towards each other .

The bending of supposedly linear M-N-O in an $M(NO)_2$ fragment has been examined in detail by Enemark [9] and also by Hoffmann[11]. According to Enemark if the electrons populate an $a_1$ or $b_2$ orbital then the bending of the oxygens towards each other will stabilise the orbital; in an $a_2$ or $b_1$ orbital a decrease in stability is proposed if the nitrosyls bend towards each other. Examination of the relevent orbitals in figure 2-3d show this idea. The polymeric complex $\{Co(NO)_2I\}_n$ , for example, has a N-Co-N angle of $118^o$ and a Co-N-O angle of $170^o$ bending towards each other [12], in the complex $[(Ph_3P)_2Rh(NO)_2]^+$ a Rh-N-O angle of $159^o$ bending away from each other is observed [13]. The actual structure of $[Fe_2S_2(NO)_4]^{2-}$ shows an N-Fe-N angle of $113^o$ and an Fe-N-O angle of $165^o$ bending towards each other[10].

Hoffmann puts forward the view that the N-M-N angle is a consequence of the number of electrons on the metal and the $\pi$ accepting properties of the ligand. However the explanation put forward by Hoffmann to explain the M-N-O bending contradicts that of Enemark. From Hoffmann's work an orbital of $b_1$ symmetry will be *stabilised* if the nitrosyls bend *towards* each other, and an $a_1$ orbital will be *stabilised* if the nitrosyls bend *away* from one another. This explanation is based on the overlap of a lone pair on the nitrogen increasing or decreasing

the antibonding overlap with the central metal atom. From his calculations which way the nitrosyls will bend is strongly dependent on the N-M-N angle.

The structure of $[Fe_2(S_2O_3)_2(NO)_4]^{2-}$ shows that the Fe-N-O fragments bend towards each other, the Fe-N-O angle is $170^o$, with a N-Fe-N angle of $118^o$ (see chapter-3). Calculations on $[CoH_2(NO)_2]^-$ at a N-M-N angle of $120^o$ predict an M-N-O angle of $174^o$ bending towards each other[11]. At greater N-M-N angles the nitrosyls begin to bend away from each other. The similarity of the geometry of the M-NO for $[Fe_2(S_2O_3)_2(NO)_4]^{2-}$ to the geometry predicted by Hoffmann for a similar N-M-N angle suggests the validity of Hoffmann's ideas, however since in this case the fragments are very different it would be difficult to separate the effect predicted by Hoffmann to that of Enemark.

The real effect may be a mix of the two ideas. At a low N-M-N angle there is greater possibility of overlap between the nitrosyls and a stabilisation of the $a_1$ and $b_2$ orbitals would occur, destabilising $a_2$ and $b_1$. At large N-M-N angles there will be little overlap between the nitrosyls and the effect of the lone pair on nitrogen would be the dominant effect again stabilising the $a_1$ and $b_2$ orbitals. This does suggest that the $a_2$ and $b_1$ orbitals will only be at greatest stability at intermediate N-M-N angles.

2 - 3

Bonding in di-iron(-I), $[Fe_2]^{2-}$

The Fe-Fe distance of the parent complex is 2.72Å. When two irons each with a negative charge are brought together at this distance the d-orbitals are split from their parameterised value of -12.700 eV, and range from -13.3 to -12.2 eV, (fig 2-4). From an examination of the overlap only 0.18 of an electron is shared between the two irons. $[Fe_2]^{2-}$ is however more stable than two isolated iron anions by 108 $KJmol^{-1}$. An Fe-Fe bond strength of 156+/- 25 $KJmol^{-1}$ is reported for the neutral [14]. The $dz^2$ orbitals interact the most via a direct (if somewhat weak) $\sigma$ bond (orbital $1a'_{1g}$) followed by the dxz and dyz which are involved in a $\pi$ bonding arrangement (orbitals $1b'_{1u}$ and $1b'_{2u}$ respectively). The $dx^2$-$y^2$ and the dxy are $\partial$ bonded (orbitals $2a'_{1g}$ and $1a'_{2g}$ respectively), but these 'interactions' are insignificant and best regarded as non-bonding.

This calculation leads to a <u>formal</u> bond order of one (one antibonding orbital is left

unfilled), and a weak bond is shown to exist by virtue of a $dz^2$ $\sigma$-bond. The theoretical reduction of this system would lead to the loss of iron-iron bonding, by populating the last unfilled orbital, leading to the instability of the couple. In the same vein it can be appreciated that oxidation would increase the bond order and stabilise the molecule. The HOMO/LUMO gap is so small that if the species was ever produced it would probably exist as a triplet. From this simple examination of the interaction between the two irons at this distance it appears that there is little significant overlap between the two.

**Figure 2-4**

Molecular Orbital Energy Diagram of $[Fe_2]^{2-}$

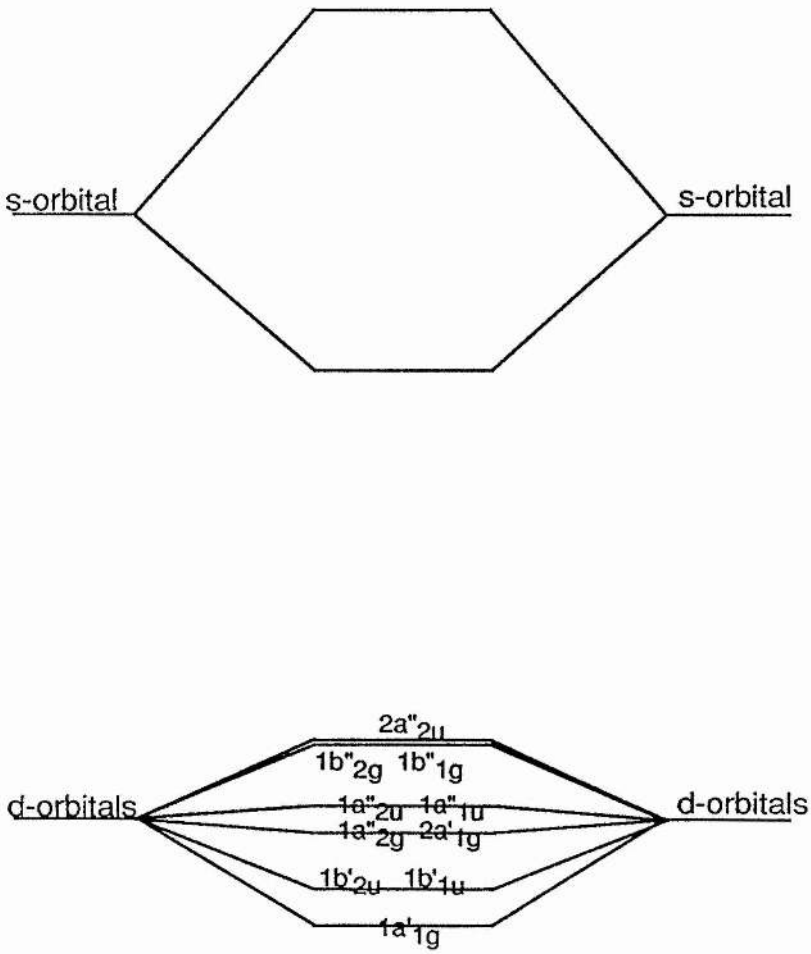


Fe $[Fe\text{-}Fe]^{2-}$ Fe

2 - 4

Bonding in Bis(dinitrosyliron(-I)), $[Fe_2(NO)_4]^{2+}$

Removal of two sulphurs from the parent complex leaves the iron-nitrosyl frame, $[Fe_2(NO)_4]^{2+}$. The bonding in this fragment was examined by an EHT calculation. The results were examined from the point of view of bringing up two $[Fe(NO)_2]^+$ units to an Fe-Fe distance of 2.72Å, as found in the parent complex. Figure 2-5, gives the orbital energy diagram for the uppermost levels of this fragment.

As expected the lowest four orbitals (not shown in fig. 2-5) are the NO $\sigma_3$ orbitals , and no significant changes are observed relative to the same orbitals of $[Fe(NO)_2]^+$. The $\sigma_4$, $\pi_1$, and the $\sigma_5$ levels are similarly unaffected by the presence of the Fe-Fe interaction, reflecting the weakness of this interaction on these orbitals. The remaining levels up to -8 ev are the $\pi^*$NO-Fe bonding and the $\pi^*$NO-Fe antibonding orbitals. Within each of these two groupings the metals themselves are either bonding or antibonding with respect to each other. The following discussion concerns the $\pi^*$NO-Fe bonding orbitals and the antibonding/bonding arguments refer to the Fe-Fe interaction only.

The changes that are observed for $[Fe_2(NO)_4]^{2+}$ relative to the $[Fe(NO)_2]^+$ fragment are primarily due to the metal-metal interaction. Those orbitals with a Z component will be affected the most ie, the $dz^2$,dxz and the dyz. While the dxy and $dx^2-y^2$ will change little, these being more or less non-bonding in the $Fe_2^{2-}$ fragment. In fact the dxy bonding and antibonding orbitals were changed by only +/-0.04ev relative to the similar orbital in $[Fe(NO)_2]^+$. Thus these are non-bonding orbitals when considering the iron-iron interaction, although on the other hand they are important orbitals in connection with the metal bonding to NO. The $dx^2-y^2$ orbitals are more affected by the Fe-Fe interaction. In this case we have to take into account not only the effect of Fe-Fe but also the way the orbital interacts with the nitrosyls, for as we saw in the case of $[Fe(NO)_2]^+$ this orbital becomes mixed with $dz^2$ to give $dx^2-y^2/dz^2$-(X) and $dx^2-y^2/dz^2$-(Y). The $dx^2-y^2$ non-bonding orbitals, of $a'_{1g}$ symmetry interact with the $z^2$ orbitals leading to an increased interaction between the two irons than that due to $dx^2-y^2$ alone.

The most stable d-orbital in $[Fe(NO)_2]^+$ with a bonding configuration to $\pi^*$NO was the

**Figure 2-5**

Molecular Orbital Energy Diagram of $[Fe_2(NO)_4]^{2+}$

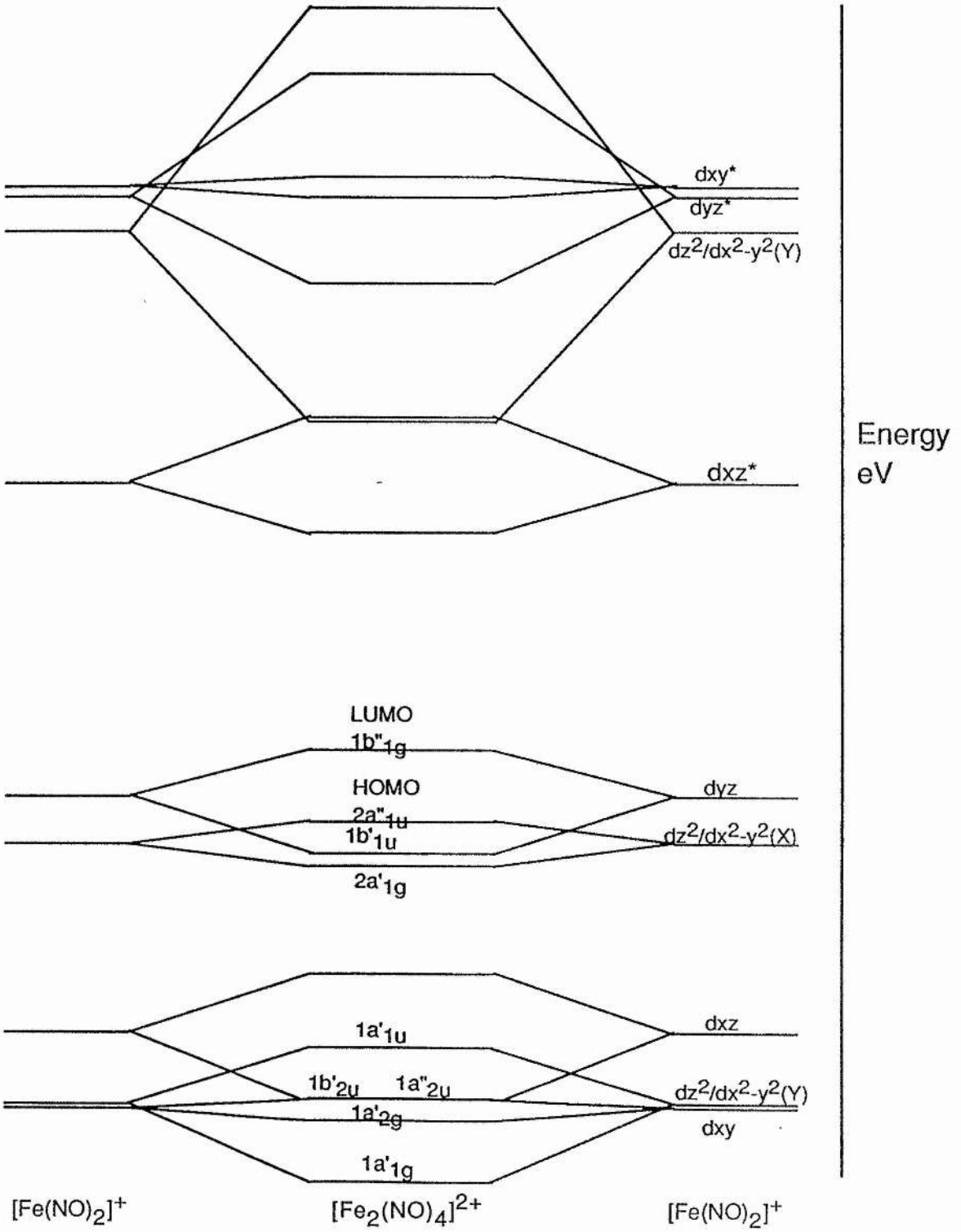

dxy (orbital $2a_2$); with $[Fe_2(NO)_4]^{2+}$ it is the hybrid orbital $dx^2\text{-}y^2/dz^2\text{-}(Y)$ (orbital $1a'_{1g}$). The effect of $dz^2$ in a bonding arrangement with the other iron has lowered the energy past the dxy,(orbital $1a'_{2g}$) conversely orbital $1a'_{1u}$ is its antibonding counterpart and is destabilised in energy relative to the dxy*(orbital $1a''_{2u}$). The $1b'_{2u}$ orbital is bonding dxz, again stabilised relative to the monoiron fragment because of a favourable Fe-Fe interaction. Orbital $1b''_{2g}$ is its destabilised antibonding counterpart.

Orbitals $2a'_{1g}$ and $2a''_{1u}$ are the non-bonding orbitals with respect to the Fe-NO interactions, but due to the presence of $dz^2$ these levels have become split from their $[Fe(NO)_2]^+$ value (as explained above). These are formally the $dx^2\text{-}y^2/dz^2\text{-}(X)$ bonding and antibonding orbitals. Orbital $2a''_{1u}$ is the HOMO and orbital $1b''_{1g}$ is the LUMO and is the dyz antibonding orbital. The next group of orbitals are the metal d-orbitals in an antibonding configuration with the NO ligands ie, the $\pi^*$NO-Fe antibonding orbitals and need not concern us.

It can be reasoned that the oxidation of this fragment would yield a more stable molecule, increasing the bond order of the hypothetical fragment. Reduction would fully populate the Fe-Fe antibonding orbitals and fragmentation would be expected. On the basis of which orbitals have their corresponding antibonding orbitals filled, we can see that the net bonding contribution is from the dyz orbitals, ie a $\pi$ Fe-Fe interaction.

Table 2-1 gives an indication of the Fe-Fe involvement in the aforementioned orbitals by comparing their energies with the energy of similar orbitals for $[Fe(NO)_2]^+$.

**Table 2-1**

| Level | Bonding(eV)(a) | Antibonding(eV)(a) |
|---|---|---|
| $dx^2\text{-}y^2/dz^2\text{-}(Y)$ | -0.32 | +0.23 |
| dxy | -0.04 | +0.04 |
| dxz | -0.27 | +0.24 |
| $dx^2\text{-}y^2/dz^2\text{-}(X)$ | -0.08 | +0.09 |
| dyz | -0.23 | +0.19 |

(a) The difference in energy between the orbital for $[Fe_2(NO)_4]^{2+}$ and the similar orbital of $[Fe(NO)_2]^+$ in electron volts.

This table follows the trends obtained from an examination of $Fe_2^{2-}$ and it also suggests that the $dx^2-y^2/dz^2$-(Y) orbital has significantly more $dz^2$ character than does $dx^2-y^2/dz^2$-(X).

2 - 5

Bonding in $S_2^{4-}$

When two $S^{2-}$ ions alone are brought together at the S-S distance (2.85 Å)observed in the complex $[Fe_2S_2(NO)_4]^{2-}$, from the E.H.T. calculation we find very little interaction between the sulphur ions. The energy of the low lying sulphur s-orbitals are unchanged from their parameterised value of -20.0 eV.Similarly the py and pz orbitals change little from their parameterised value. The px orbitals are affected slightly by this geometry; these orbitals point towards each other, giving rise to weak $\sigma$-bonding and $\sigma$-antibonding molecular orbitals. Since all available orbitals are filled a bonding order of zero is obtained, thus there is no stabilisation of this fragment relative to two isolated sulphur ions.These levels are shown on the right hand side of the molecular orbital energy diagram for $[Fe_2S_2]^{6-}$, figure 2-6.

2 - 6

Bonding in $[Fe_2S_2]^{6-}$

The core of Roussins Red Salt was examined by the EHT calculation. One calculation ignored the effect of the unfilled and high lying sulphur d-orbitals, the other took their presence into account. The low lying sulphur s-orbitals have been stabilised relative to $S_2^{4-}$by an average of 0.54 ev, mainly due to an interaction with metal 4s and metal $dx^2-y^2$ orbitals. The remaining six orbitals of the $S_2^{4-}$ group give twelve ligand orbitals for interaction with the two irons. Thus the availability of ten metal orbitals requires four non-bonding levels to be present.

The molecular orbital energy diagram for this fragment is given in figure 2-6. The diagram has been constructed by considering the effect of bringing two sulphide ions towards the $[Fe_2]^{2-}$ unit already examined, such that the geometry of the $[Fe_2S_2]^{6-}$ core of the parent complex is achieved.

The orbital with the lowest energy shown in the diagram is the $1a''_{1u}$ orbital. This

## Figure 2-6

Molecular Orbital Energy Diagram of $[Fe_2S_2]^{6-}$ (no sulphur d-orbitals)

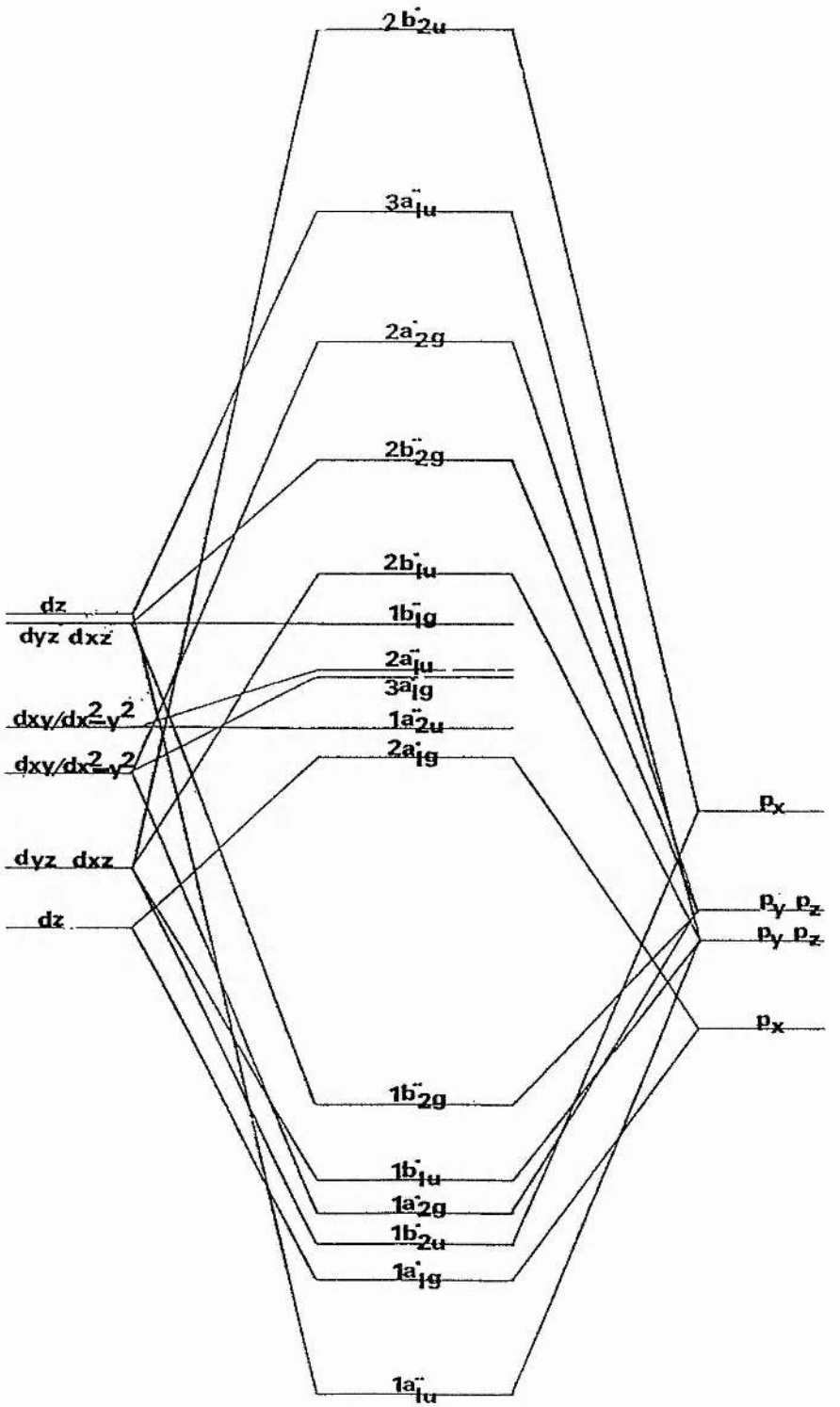


$[Fe_2]^{2-}$ $[Fe_2S_2]^{6-}$ $[S_2]^{4-}$

## Figure 2-7

Molecular Orbital Energy Diagram of $[Fe_2S_2]^{6-}$ (with sulphur d-orbitals)

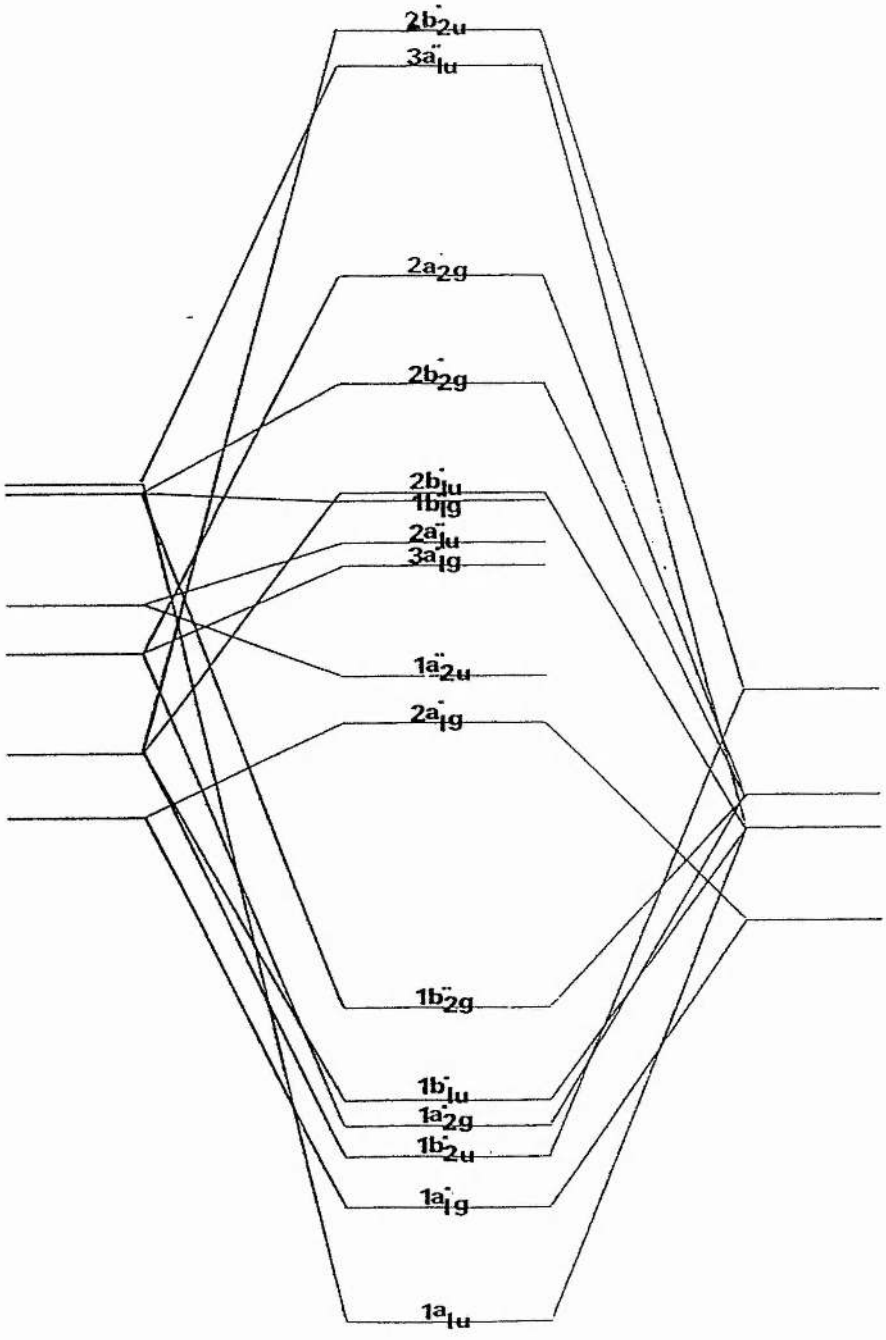


$[Fe_2]^{2-}$ $[Fe_2S_2]^{6-}$ $[S_2]^{4-}$

orbital is a hybrid of metal $dx^2-y^2$ and $dz^2$ in an antibonding configuration with respect to the irons. This orbital is similar to the non-bonding orbital encountered during the examination of $[Fe(NO)_2]^+$. The mixing involved increases the electron density along the x-axis, increasing the overlap with sulphur $p_z$ orbitals, figure 2-8a. The orbital has a 4 centred 2-electron bonding arrangement arranged in a square. The electron density is approximately equally shared between the sulphur and iron atoms.

The metal contribution of orbital $1a'_{1g}$ is mainly metal $dz^2$ character with only a little $dx^2-y^2$ mixed in. The interaction with sulphur $p_x$ is shown in figure 2-8b. Again the bonding interaction is via the sulphurs and not due to any direct Fe-Fe bond. The next few orbitals, $1b'_{2u}$ to $1b''_{2g}$ are Fe-S bonding orbitals with the weak Fe-Fe interaction either bonding or antibonding. Orbital $2a'_{1g}$ is the Fe-S antibonding orbital of $1a'_{1g}$. With this orbital the Fe-Fe interaction is bonding, but as observed in $[Fe_2]^{2-}$ this bonding is weak. The presence of the sulphur orbitals in an antibonding arrangement relative to the irons is the main bonding interaction and hence this orbitals destabilisation relative to the orbital in $[Fe_2]^{2-}$.

**Figure 2-8a**

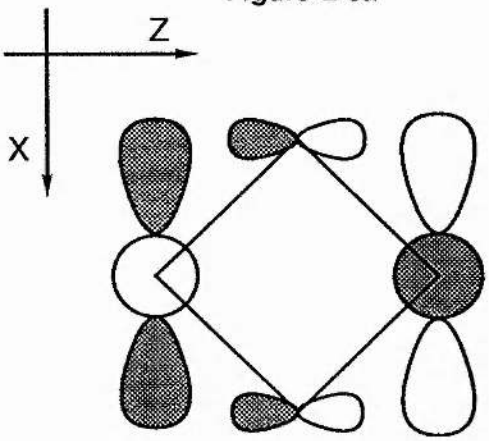


Orbital $1a''_{1u}$

**Figure 2-8b**

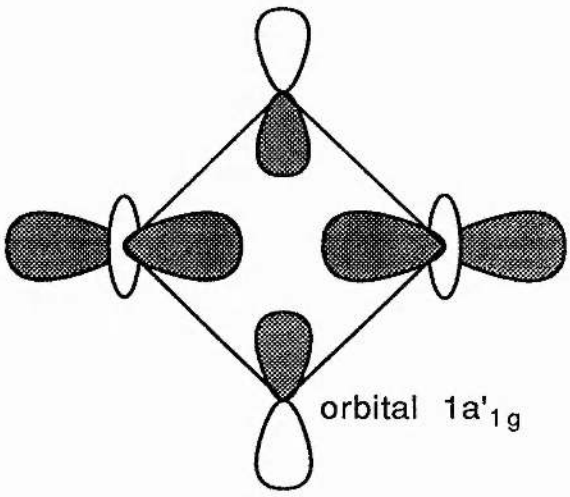

orbital $1a'_{1g}$

Orbital $1a''_{2u}$ is the first of the four non-bonding orbitals (with respect to sulphur). Examination of this orbital reveals that the sulphur p orbitals will always be non-bonding and that only a $\partial$ interaction with sulphur would lead to a bonding interaction; thus no change from the similar orbital of $[Fe_2]^{2-}$. Orbitals $3a'_{1g}$ and $2a''_{1u}$ are also non-bonding. Orbital

$3a'_{1g}$, however has a little sulphur-p mixed in, in an antibonding interaction to the irons and so has raised the energy of this orbital relative to that of $[Fe_2]^{2-}$. Orbital $2a''_{1u}$ has a metal $dz^2$ mixed in with the metal orbital in an antibonding manner and hence is also destabilised relative to $[Fe_2]^{2-}$. The other non-bonding orbital, $1b''_{1g}$ is similar to $1a''_{2u}$ in that it would require a ∂ interaction from the sulphurs to obtain a bonding arrangement. The other levels depicted in figure 2-6, $2b'_{1u}$ to $1b'_{2u}$ are the other Fe-S antibonding counterparts of the orbitals already described. The HOMO and LUMO are depicted in figure 2-9. The gap between these two orbitals is 0.6eV.

**Figure 2-9**

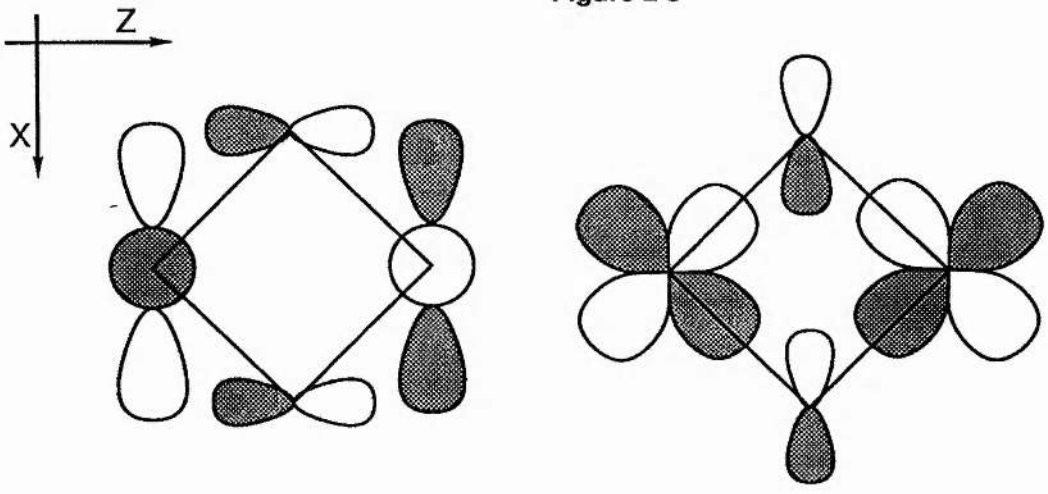


HOMO, orbital $3a''_{1u}$ LUMO, orbital $2b'_{2u}$

Oxidation of this fragment would increase the bonding order and strengthen the Fe-S bonds. Reduction would fill all the available orbitals and a net bonding order of zero would result; fragmentation of the cluster on reduction would be expected.

The important point of this calculation is that the primary bonding of the core is <u>not</u> due to Fe-Fe interactions but due to Fe-S bonds; this had been expected on the basis of the results obtained from the calculation on $[Fe_2]^{2-}$. From the charge distribution calculated for the LUMO, 69% of the charge is on iron with the rest on sulphur. The addition of an electron to this orbital would be expected to give a radical with an electron delocalised over both the irons and the sulphurs and not solely on the irons.

The Effect of Sulphur-d Orbitals on the Molecular Orbitals of $[Fe_2S_2]^{6-}$

Since the sulphur d-orbitals are unoccupied and are high lying (-8.0eV), they are not often entered into a calculation. In Summerville's work [11], the effect of the unfilled d-orbitals of the bridging ligands were ignored. However these orbitals can interact with orbitals of similar symmetry giving rise to more stable orbitals. For instance the non-bonding orbital $1a''_{2u}$ would be expected to interact with sulphur d-orbitals of an appropriate symmetry giving rise to a $\partial$ bonding interaction, and so stabilising the orbital. The molecular orbital energy diagram for this calculation is given in figure 2-7 (page 37). In all cases the orbitals have been stabilised relative to the energies of similar orbitals obtained from the previous calculation where no sulphur-d orbitals were used. The expected stabilisation of the $1a''_{2u}$ orbital was observed. The other non-bonding orbital $1b_{1g}$ is stabilised slightly by the sulphur dyz orbitals. The most interesting change is the effect that the sulphur-d orbitals have had on the HOMO and LUMO. The HOMO has been stabilised slightly by the mixing of sulphur dxz, which is bonding towards the metals. The LUMO has been significantly stabilised (by 0.55eV) and now sits 0.07eV above the HOMO. This orbital now has a large amount of sulphur $dz^2$ and $dx^2\text{-}y^2$ (in a bonding arrangement with the irons) mixed in with the sulphur $p_x$ orbitals.

From this calculation the distribution of the charge on the LUMO is 53% on the irons and 47% on the sulphurs. The calculation shows that an added electron to produce $[Fe_2S_2]^{7-}$ will be equally shared between the iron and the sulphur atoms. In many actual systems containing metal dimers, reduction is presumed to populate an orbital which is predominantly M-M antibonding. In this hypothetical case the LUMO is actually M-M bonding, and the HOMO which is supposed to be M-M bonding is actually found to be M-M antibonding in this case.

2 - 7

Molecular Orbitals of Roussin's Red Dianion, $[Fe_2S_2(NO)_4]^{2-}$

With the calculation on $[Fe(NO)_2]^+$ we observed four metal orbitals involved with M-$\pi$*NO bonding, and one non-bonding orbital. The metal orbital responsible for the latter level was the hybrid $dx^2\text{-}y^2/dz^2$-(X) (orbital $4a_1$, fig 2-2 and fig 2-3d) containing 95% of the orbital electron density on the metal. Examination of $[Fe_2(NO)_4]^{2+}$, showed the effect of the Fe-Fe interaction. The original non-bonding level was split into a

$dx^2$-$y^2$/$dz^2$-(X) bonding orbital (relative to Fe-Fe) and a $dx^2$-$y^2$/$dz^2$-(X) antibonding orbital (orbitals $2a'_{1g}$ and $2a''_{1u}$ of figure 2-5) with 92 and 97% of the orbital electron density on the irons respectively. The other hybrid $dx^2$-$y^2$/$dz^2$-(Y) was significantly altered by the Fe-Fe interaction.

When we considered $[Fe_2S_2]^{6-}$, the most stabilised orbital is an Fe-Fe antibonding orbital; the $dx^2$-$y^2$/$dz^2$-(X) (orbital $1a''_{1u}$, figure 2-6), we also found two non-bonding levels $dx^2$-$y^2$/$dz^2$-(Y) in an Fe-Fe bonding and antibonding arrangement with 91 and 99% orbital electron density on the irons respectively. On combining the $S_2^{4-}$ fragment to the bis dinitrosyldiiron fragment to obtain the geometry of the full parent complex, we should expect the most significant changes to be with these non-bonding $dx^2$-$y^2$/$dz^2$-(X) levels.

An examination of the first six orbitals of $[Fe_2S_2]^{6-}$ shown in figure 2-6 relative to the first six of $[Fe_2S_2(NO)_4]^{2-}$ shown in figure 2-10 reveals the same order of orbitals with the energies of these orbitals being only slightly changed relative to the energy of the sulphur $p_x$ orbital. All the other orbitals except one have been stabilised relative to the similar orbitals of $[Fe_2S_2]^{6-}$ due to the stabilising effect of the nitrosyl ligands. For instance the orbital $1a''_{2u}$, which is non-bonding with respect to sulphur, is more stable in $[Fe_2S_2(NO)_4]^{2-}$ with respect to $[Fe_2S_2]^{6-}$ by about 0.6eV due to its enhanced stability through the interaction with the nitrosyl ligands, cf the non-bonding orbital in $[Fe(NO)_2]^{+}$.

In the paper by Feltham and Enemark [9] they discussed the bonding of metal nitrosyls in terms of an M-NO interaction perturbed by the other attached ligands. For all but one of the orbitals shown in figure 2-10, this argument appears valid; the energies of the Fe-$\pi^*$NO orbitals of the $[Fe(NO)_2]_2^{2+}$ fragment <u>are</u> perturbed slightly by the presence of the bridging sulphurs. An examination of the relative energies for all the orbitals of $[Fe_2(NO)_4]^{2+}$, $[Fe_2S_2]^{6-}$ and $[Fe_2S_2(NO)_4]^{2-}$ reveals that the only major difference to the orbitals of the latter complex relative to similar orbitals for the two former ones occurs at the Fe-$\pi^*$NO bonding levels, all other orbitals are relatively unchanged. However the HOMO-LUMO gap observed in figure 2-5 ($[Fe_2(NO)_4]^{2+}$) and figure 2-6 ($[Fe_2S_2]^{6-}$]) is quite small. In the case of $[Fe_2S_2(NO)_4]^{2-}$ the gap between the HOMO and LUMO is large, 1.7eV. The LUMO is an Fe-$\pi^*$NO antibonding orbital. The 'missing' orbital of

## Figure 2-10

Molecular Orbital Energy Diagram of $[Fe_2S_2(NO)_4]^{2-}$ (without sulphur d-orbitals)

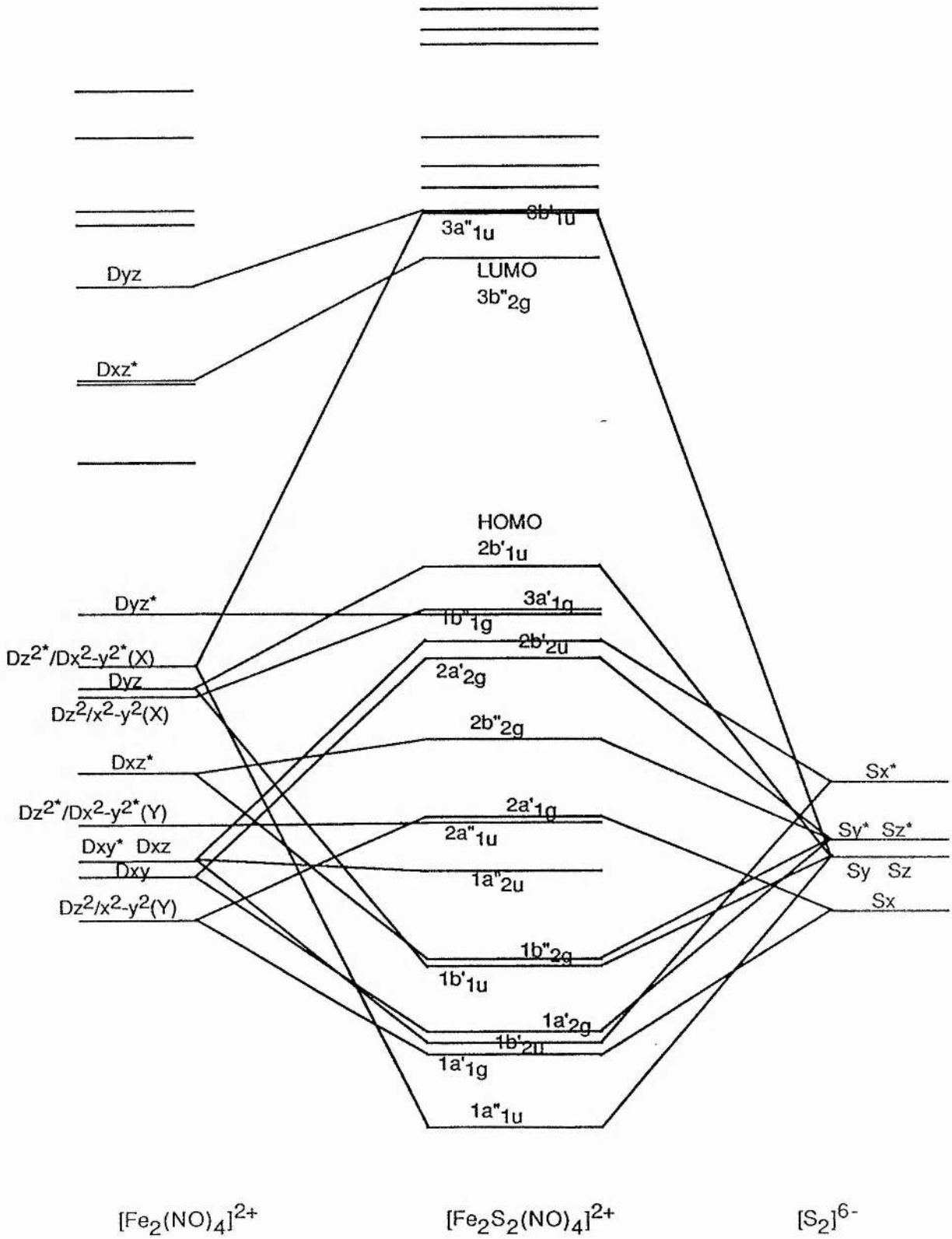

## Figure 2-11

Molecular Orbital Energy Diagram of $[Fe_2S_2(NO)_4]^{2-}$ (with sulphur d-orbitals)

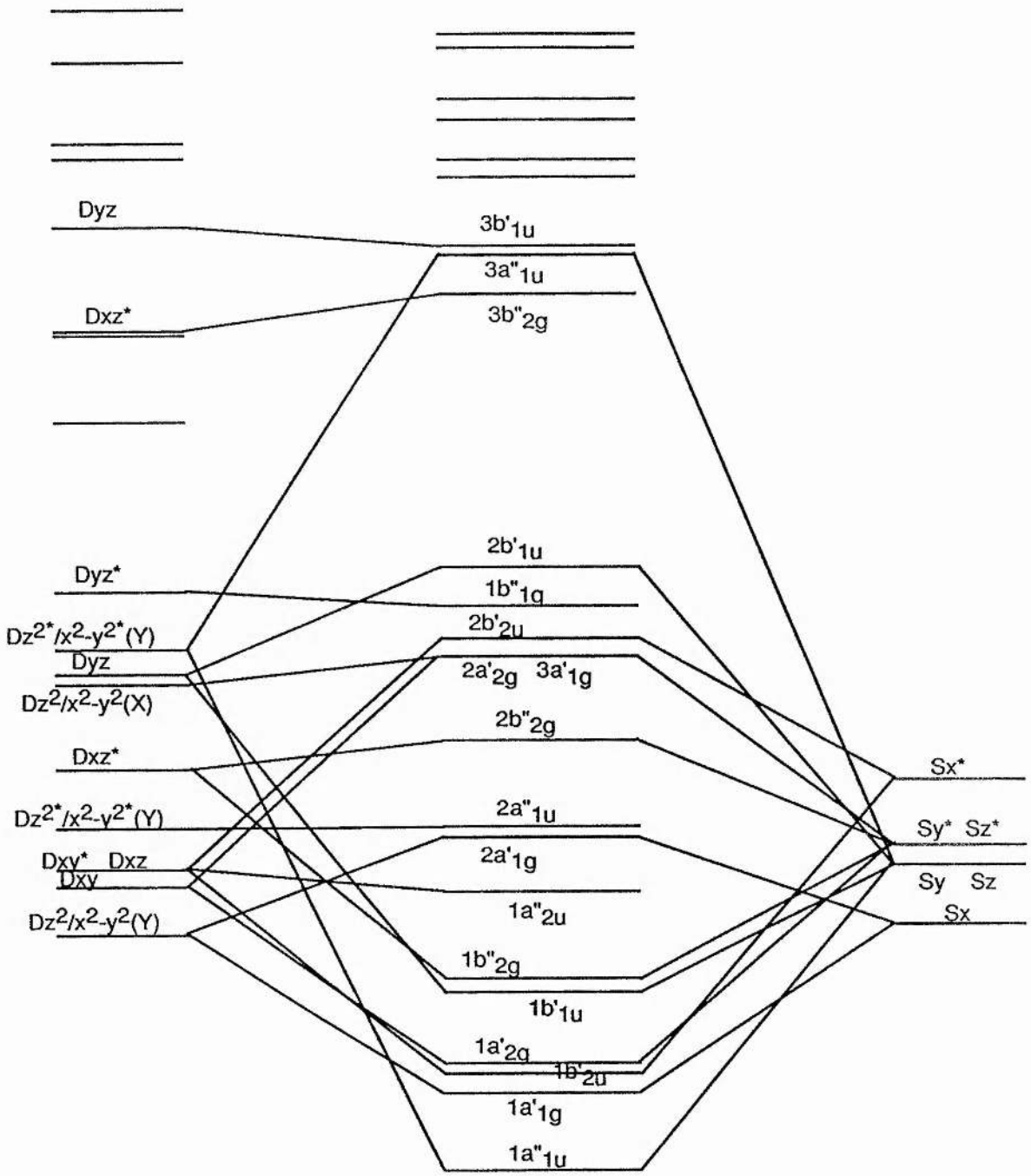

$a''_{1u}$ symmetry (orbital $3a''_{1u}$ of $[Fe_2S_2]^{6-}$) is located within the Fe-$\pi^*$NO antibonding orbitals.

The reason for the large gap is not solely because this orbital has been raised in energy (increased by +0.9eV relative to $[Fe_2S_2]^{6-}$) but also due to the filled orbitals being stabilised by favourable bonding interactions with the $\pi^*$NO orbitals. The $a''_{1u}$ orbital was observed to be formally non-bonding with respect to the nitrosyl ligands, but slight admixtures of $\pi^*$NO electron density into this orbital raised its energy relative to the parameterised -12.7eV of Fe. In $[Fe_2S_2]^{6-}$ this orbital interacted strongly with sulphur $p_z$ orbitals to give the square bonding orbital depicted in figure 2-8. With $[Fe_2S_2(NO)_4]^{2-}$, due to the slight mixing of $\pi^*$NO, the antibonding character of orbital $3a''_{1u}$ has been increased, hence the increased energy difference between the HOMO and LUMO observed.

The effect of using sulphur d-orbitals in the calculation has had the same effect found from the examination of their use on the calculation of $[Fe_2S_2]^{6-}$. The stabilisation of the orbitals is shown in figure 2-11. The HOMO-LUMO gap has also become slightly smaller (-1.4eV). Table 2-2 gives the percentage orbital electron density on the iron and sulphur atoms for the HOMO, LUMO and LUMO+1, and compares the differences between the calculation using d-orbitals and the one without.

**Table 2-2**

| Orbital | | % Electron Density No S d-orbitals used | % Electron Density S d-orbitals used |
|---|---|---|---|
| HOMO | Fe | 12 | 15 |
| | S | 19 | 31 |
| LUMO | Fe | 39 | 26 |
| | S | 11 | 28 |
| LUMO +1 | Fe | 62 | 40 |
| | S | 22 | 58 |

Table 2-2 The percentage orbital electron density on Fe and S in $[Fe_2S_2(NO)_4]^{2-}$

The interesting aspect shown in Table 2-2 is that in all three cases where sulphur d-orbitals are taken into account, there is more electron density on the sulphurs than on the

irons. The HOMO and LUMO both have a large amount of electron density on the nitrosyl ligands. The LUMO+1 orbital has, when sulphur d-orbitals are taken into account, hardly any interaction with the nitrosyl ligands.

The calculation of the molecular orbitals of $[Fe_2S_2(NO)_4]^{2-}$ explains why the complex is diamagnetic; a large difference in energy between the HOMO and LUMO. The calculation also suggests that on the addition of an electron an Fe-$\pi^*$NO antibonding orbital will be populated. Thus a bonding order of 1 will still be present and the complex will not necessarily fragment. If the electron entered this $3b''_{2g}$ orbital then it would be expected to interact with the four equivalent nitrogen atoms. If it were to enter the $3a''_{1u}$ orbital then there would be no interaction with the nitrogens. In both cases the complete delocalisation of the electron would be expected. The exchange of the electron occurring via the sulphur bridges and not via the weak Fe-Fe interaction.

The LUMO observed for this complex being an Fe-$\pi^*$NO antibonding orbital could be used as a plausible explanation of the reductive chemistry of $Fe_2(PPh_2)_2(NO)_4$ observed by Wojcicki [14]. On reduction of this complex with $LiB(Et)_3H$ a terminal nitrosyl ligand becomes bridging between the two irons. If we assume that the molecular orbitals of this cluster are similar to $[Fe_2S_2(NO)_4]^{2-}$ then reduction would populate a metal-nitrosyl antibonding orbital making it unstable with respect to the rearrangement observed. The observation that the LUMO of $[Fe_2S_2(NO)_4]^{2-}$ is an Fe-$\pi^*$NO antibonding orbital could be used to explain the observed reductive electrochemistry of this cluster; two reductions with no observable fragmentation during the time scale of the C.V. experiment (see chpt 4). An examination of the reduced $Fe_2(SR)_2(NO)_4$ by I.R. spectroscopy does not show the presence of a bridging nitrosyl, (chpt 4). The observed e.p.r. spectrum of reduced $Fe_2(SR)_2(NO)_4$ (chpt 4) is suggestive of a delocalised electron coupling to four equivalent nitrogens, an observation which would be in agreement with this calculation. Table 2-3 shows the weakness of the Fe-Fe interaction and also the strength of the Fe-S bonds. From this it can be reasoned that the main stability of the core of this cluster is due to the Fe-S interactions and not that of any direct Fe-Fe.

**Table 2-3**

| X-Y | Overlap (a) |
|---|---|
| Fe-Fe | 0.06 |
| Fe-S | 0.64 |
| Fe-N | 0.89 |
| N-O | 0.85 |

(a) given in total number of electrons shared

**Table 2-3,** total overlap between pairs of atoms in Russin's Red dianion.

2 - 8

Iron-Iron overlap

In the paper by Hoffmann and Summerville they left open the question as to whether a $d^9$ dimeric complex had an iron-iron bond or not [11]. From the simple 18 electron rule one would assume the existance of such a bond, and an examination of the electrochemistry of the alkyl esters, which show two one-electron reductions, could be interpreted as the breaking of such a bond (see chapter-4). From these calculations the total iron-iron overlap for a variety of the fragments was examined, Table 2-4. The conclusions drawn from table 2-4 are ; there is no net Fe-Fe overlap in $[Fe_2S_2]^{6-}$ and that all the net bonding interaction is via Fe-S links; in $[Fe_2(NO)_4]^{2+}$ there is a small interaction; and that in $[Fe_2S_2(NO)_4]^{2-}$ the interaction in is negligible (It can be seen from table 2-4 that the overlap of $[Fe_2(NO)_4]^{2+}$ is cancelled by the overlap of $[Fe_2S_2]^{6-}$). Thus we can say that the cluster is held together by Fe-S links and not by any net Fe-Fe bond.

**Table 2-4**

| Fragment | Overlap (a) |
|---|---|
| $[Fe_2]^{2-}$ | 0.18 |
| $[Fe_2(NO)_4]^{2+}$ | 0.16 |
| $[Fe_2S_2]^{6-}$ | -0.07 |
| " + S d-orbs. | -0.09 |
| $[Fe_2S_2(NO)_4]^{2-}$ | 0.10 |
| " + S d-orbs. | 0.06 |

(a) given in total number of electrons shared between the two iron atoms.

**Table 2-4**, the total overlap, in electrons, between the two irons of the listed fragments.

To examine further the bonding in these iron-sulphur clusters the Methyl ester of Roussin's Red salt, $Fe_2(SMe)_2(NO)_4$ was examined by E.H.T.

2 - 9

Bonding in the Methyl Ester of Roussin's Red Salt, $Fe_2(SMe)_2(NO)_4$

Using the original X-ray of $Fe_2(SEt)_2(NO)_4$ as a guide two methyl groups were added to the structure of $[Fe_2S_2(NO)_4]^{2-}$ . The two methyl groups were placed at a S-C distance of 1.82Å and at an angle of $65.8^o$ [2] relative to the plane of the $[Fe_2S_2]^{6-}$ core to achieve the trans or $C_{2h}$ configuration.

The calculation reveals that the $\sigma_3$, $\sigma_4$, $\pi_1$ and $\sigma_5$ levels of NO are as calculated for $[Fe_2S_2(NO)_4]^{2-}$, ie the presence of the methyl groups does not effect these orbitals. The sulphur s-orbitals have been affected and are found in a bonding arrangement with the methyl s-orbitals at -25.4 eV and in an antibonding arrangement at -19.4 eV. Further up at -15.9 ev, between NO $\sigma_5$ and the $\pi_1$ orbitals, the p-orbitals of the S-$CH_3$ groups are found.

The effect of the methyl groups on the energy and order of the Fe-$\pi^*$NO orbitals is shown in figure 2-12. In most cases the energies of the orbitals are changed only slightly, $^+/_-$ 0.3eV. For instance orbital $1a'_{1g}$ has been stabilised relative to the similar orbital of $[Fe_2S_2(NO)_4]^{2-}$ due to a favourable S-C interaction, whereas orbital $1a''_{1u}$ has been destabilised. The HOMO of $Fe_2(SMe)_2(NO)_4$ is the $1b''_{1g}$ non-bonding (with respect to sulphur) orbital. The orbital responsible for the HOMO in $[Fe_2S_2(NO)_4]^{2-}$ has been stabilised due to the S-C interaction. The first three unfilled orbitals have changed order relative to those found for $[Fe_2S_2(NO)_4]^{2-}$. The LUMO is now orbital $3b'_{2u}$, orbital $3a''_{1u}$ (non-bonding with respect to NO) has been destabilised further, figure 2-13 depicts these orbitals. Table 2-5 gives the percentage charge associated with the atoms for the HOMO and the latter three orbitals.

## Figure 2-12

Orbital Energies of $Fe_2(SMe)_2(NO)_4$ relative to $[Fe_2S_2(NO)_4]^{2-}$

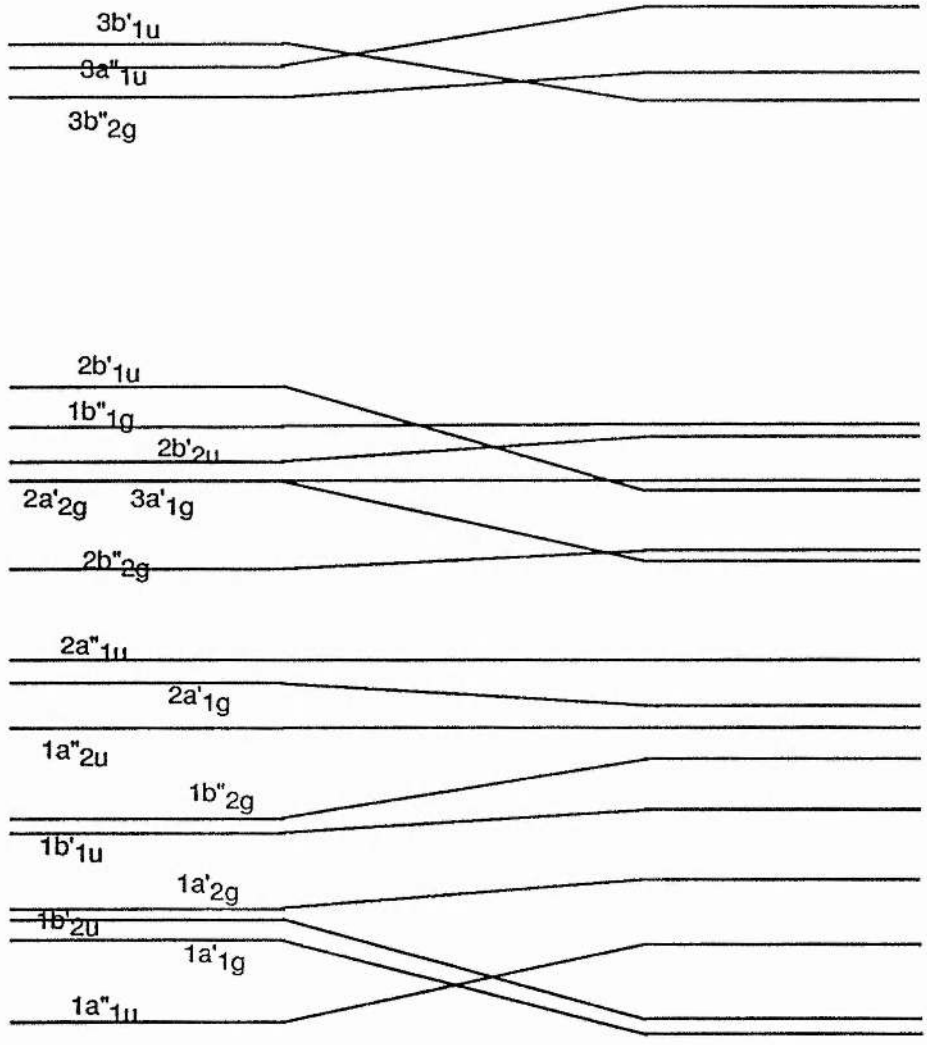


$[Fe_2S_2(NO)_4]^{2-}$ $Fe_2(SMe)_2(NO)_4$

**Figure 2-13**

Molecular Orbitals observed in $Fe_2(SMe)_2(NO)_4$

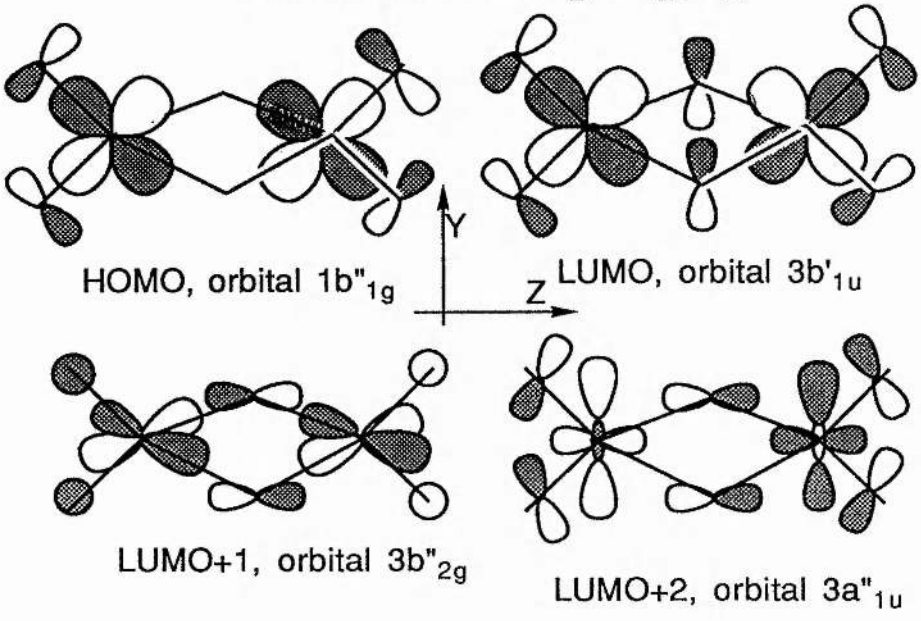


**Table 2-5**

The percentage charge calculated for the atoms of $Fe_2(SCH_3)_2(NO)_4$

| Orbital | | Fe | S | N | O | C | H | |
|---|---|---|---|---|---|---|---|---|
| HOMO | $1b"_{1g}$ | 27 | 2 | 42 | 28 | 0 | 0 | M-π*NO bonding |
| LUMO | $3b'_{1u}$ | 19 | 18 | 43 | 16 | 3 | 0 | M-π*NO antibonding |
| LUMO+1 | $3b"_{2g}$ | 27 | 28 | 32 | 11 | 0 | 0 | |
| LUMO+2 | $3a"_{1u}$ | 37 | 49 | 10 | 3 | 0 | 0 | M-π*NOnonbonding |

The HOMO is antibonding with respect to iron and non-bonding with respect to sulphur and therefore to C and H. The charge associated with the sulphur for this orbital confirms this non-bonding status.

The calculation suggests that reduction to $[Fe_2(SMe)_2(NO)_4]^-$ would place an electron in the $3b'_{1u}$ orbital. This electron would be delocalised over both irons and all four nitrogens. The presence of charge on the carbon of orbital $3b'_{1u}$ also suggests that an e.p.r. spectrum of the reduced complex may display some interaction not only with the four equivalent nitrogens but also with the two methyl groups. As was found for

$[Fe_2S_2(NO)_4]^{2-}$, reduction of the complex would not necessarily cause the fragmentation of the cluster.

The Cis-Trans conversion

From n.m.r. investigations of the alkyl and aryl esters of Roussins Red Salt it has been found [16]that the esters exist in solution in two isomeric forms; the cis and trans of $C_{2h}$ and $C_{2v}$ symmetry respectively whereas in the solid state only the trans is found [17]. The thiosulphato complex exists in the trans configuration both in solution and in the solid state; the explanation of this is given in chapter 3.

From measurements of the coalescence of the n.m.r. signals for the cis and trans in solution the energy of the activation barrier was calculated and a value of around 75KJ $mol^{-1}$ found [18]. Since the isomers are found in approximately equal abundance the total energy of both isomers is approximately equal, figure 2-14 .

**Figure 2-14**

Barrier to Cis-Trans conversion

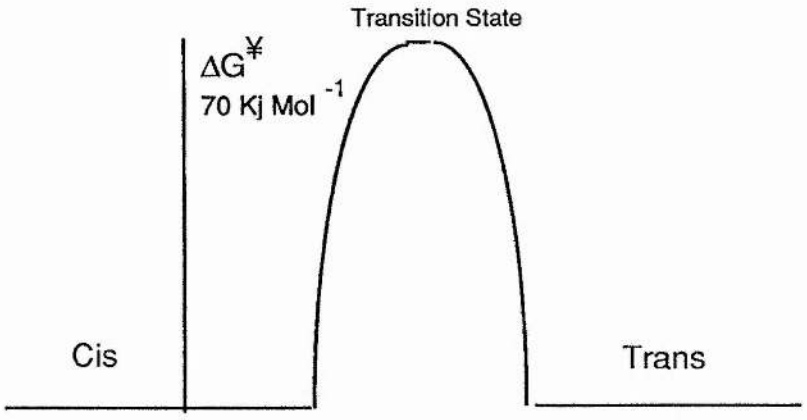


It was decided to investigate this isomerisation using the Extended Hückel method and compare the values calculated with those derived experimentally. Two possible transition states were decided upon for the calculation, these are depicted below, figure 2-15.

**Figure 2-15**

Possible Transition States in the Cis-Trans Conversion

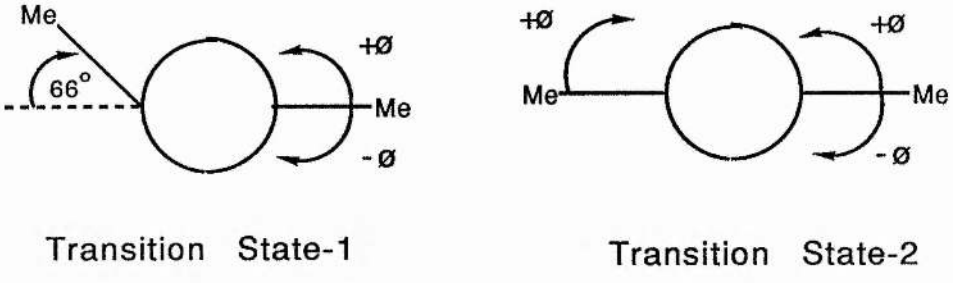


Transition State-1 Transition State-2

Calculation A; Transition state one.

One methyl was fixed at an angle of 65.8° to the plane of the $[Fe_2S_2]^{6-}$ core, (this being the value obtained from the crystal structure). The other methyl group was rotated around the sulphur normal to the Z-Y plane at the fixed S-C distance of 1.82Å. The total energy of the system was determined from the calculation. The differences in the total energy calculated from an arbitrary zero position (the differences of energies are important not the absolute) was plotted against ø. The results are given in figure 2-16 .

**Figure 2-16**

Calculation of the Barrier to Conversion Through Transition State-1

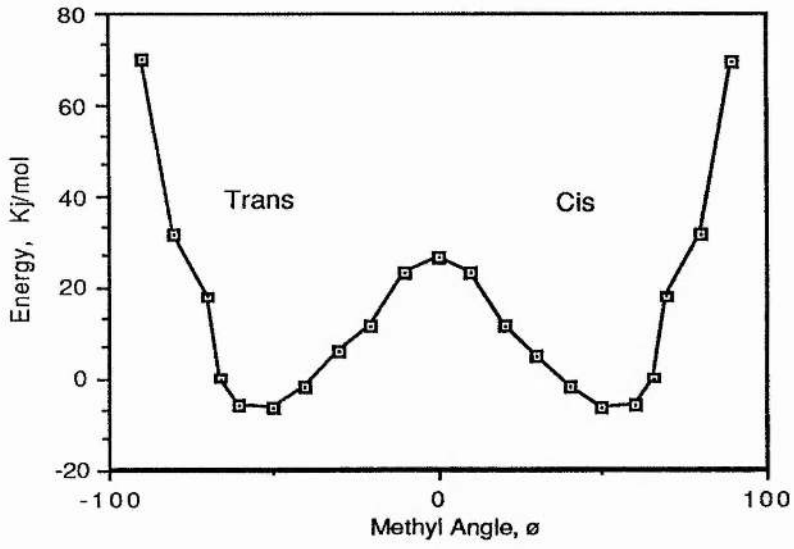


Two minima and one maximum are obtained. The maximum corresponding to the proposed transition state. The minima do not occur at the experimentally derived value of 66° but at

$55^{o}$, for both the cis and trans isomers. The energy difference between the ground state and the transition state, corresponding to the $\Delta G^{\ddagger}$, is 33 KJ $mol^{-1}$ This value is approximately half the experimental value, but at least of the correct order.

The calculation was repeated with the fixed methyl at $55^{o}$ and the other methyl group rotated as previously, although the minima are lowered in energy relative to the previous calculation but so is the maximum and a value of $\Delta G^{\ddagger}$ = 33 KJ $mol^{-1}$ is again obtained.

One interesting aspect of the calculation is the value of $55^{o}$ for the ground state. This is the value of the angle expected to be made by the methyl group between sulphur and the Z-Y-plane if the sulphur bonded in a tetrahedral manner. The reason for the difference may due to a packing phenomenon in the crystal, a constraint which is released in solution or else the calculation is not good enough.

Calculation B; Transition state two.

The above calculation was repeated. Firstly both methyl groups were placed on the plane of the $[Fe_2S_2]^{6-}$ core. Both methyls were rotated in a positive ß direction. This allowed a minimum energy to be calculated for the $C_{2v}$ isomer. Secondly, one methyl was rotated +Ø the other -Ø; allowing the minimum of the $C_{2h}$ isomer to be found. A similar plot to the above was made, figure 2-17. Again two minima and one maximum, corresponding to the transition state, were obtained. The minima correspond to an angle of $55^{o}$ to the plane of the core; the activation barrier was calculated to be 65 KJ $mol^{-1}$, which is closer to the experimental value than that previously calculated.

These calculations suggest that the conversion of cis methyl ester to the trans methyl ester will proceed through the movement of one methyl group through the plane of the $[Fe_2S_2]^{6-}$ core with a transition state similar to transition state-1. This has the lowest barrier to the conversion. The other calculation done on transition state-2 suggests that both methyls move to Ø=0 and they then either both go back up or both go down, ie no interconversion, or that one goes up and the other goes down, ie interconversion. The calculation suggests this method to be unlikely.

**Figure 2-17**

Calculation of Energy Barrier for the Cis-Trans conversion Through Transition State-2

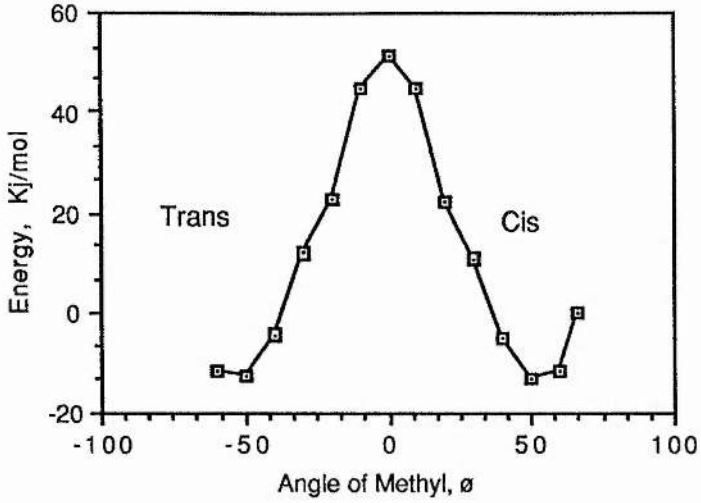


An interesting aspect of the calculation was the changes in the charges associated with the iron and sulphur atoms and the changes in energy of the HOMO as the methyl group was rotated. Figure 2-18a a shows the the charges of the Fe and S atoms as a function of the methyl angle. As the iron gains in negative charge so does the sulphur, at an approximately equal rate. A minimum is obtained for the iron at $50^{o}$ and one for sulphur at $60^{o}$. Figure 2-18b gives a plot of the energy of the HOMO and the total energy of the cluster as a function of methyl angle. The discontinuity at $45^{o}$ and at $80^{o}$ for the HOMO plot suggests that a different orbital, which is unaffected by changes in the methyl angle, becomes the HOMO between these two angles. This was found to be the $3a'_{1g}$ orbital. The increase in energy of the HOMO at the extreme angles is apparently due to the overlap of the methyl group with the $dx^2\text{-}y^2$ of the metals.

Although many factors are involved in setting the geometry of a complex, the charge associated with the metals is certainly one factor. According to Pauling's theory of electroneutrality, a metal will try and remove as much charge from it as possible to achieve electroneutrality. The minimum charge on the iron at $50^{o}$ is perhaps a consequence of this rule.

**Figure 2-18a**

Effect of methyl angle on the charge of the iron and sulphur atoms

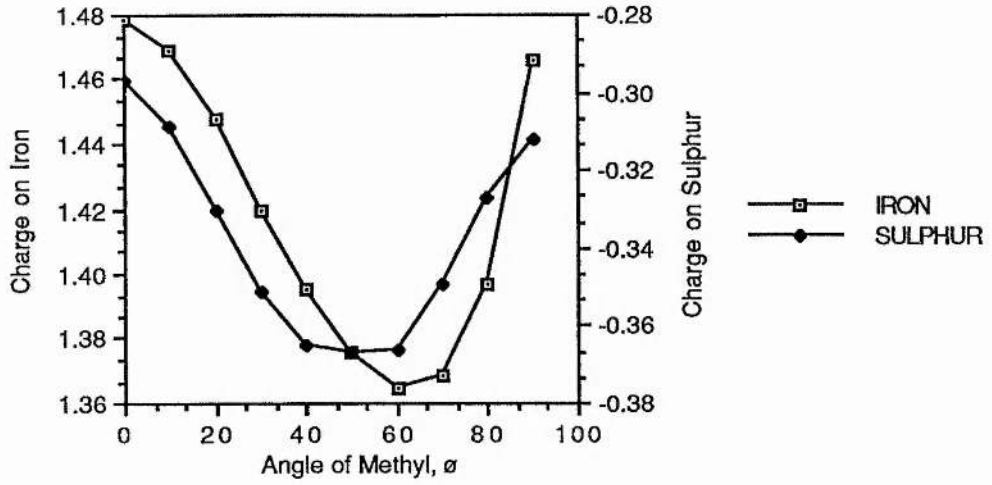


**Figure 2-18b**

Effect of methyl angle on the energies of the HOMO and on the total energy of the cluster

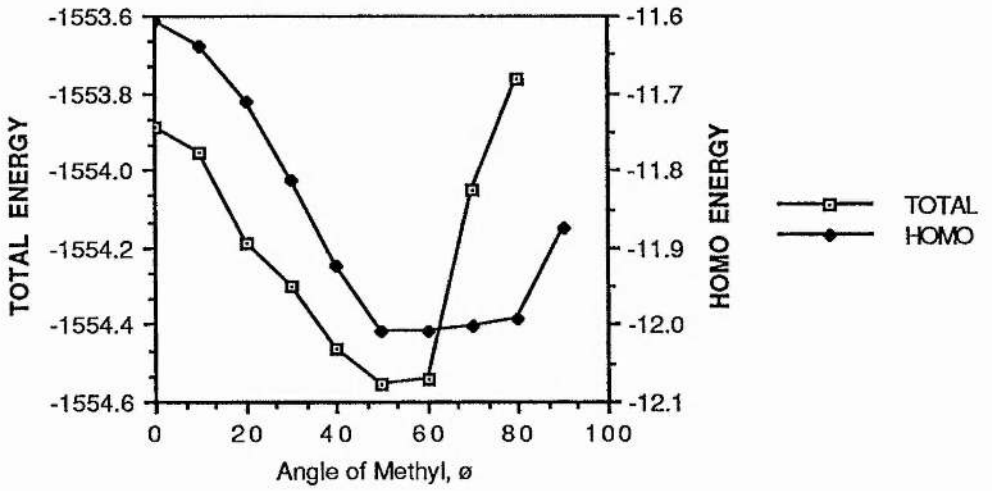


2-10

Bonding in the Thiosulphato Complex, $[Fe_2(S_2O_3)_2(NO)_4]^{2-}$

The crystal structure of $(PNP)_2[Fe_2(\mu_2\text{-}S_2O_3)_2(NO)_4]$ was determined (see chpt-3) and the atomic coordinates were used to examine the orbitals of the cluster by the extended Hückel method. The examination was done to reveal differences, if any, with the calculation

on the methyl ester, and also to see if a geometry manipulation would give an insight into the observed electrochemistry of this cluster and the others of type $Fe_2(SR)_2(NO)_4$.

In brief, the $\sigma_3$, $\sigma_4$, $\pi_1$ and $\sigma_5$ orbitals of NO are at the same energies as found for Roussin's Red Salt and Roussin's Methyl Ester. The $SO_3$ $\sigma$ orbitals are observed at -33.5 ev and -16.5 ev; the $SO_3$ $\pi$ orbital interactions occurring at -14.5 ev. The $dx^2\text{-}y^{2*}/dz^{2*}$-(X) (orbital $1a'_{1g}$) lies amongst the $SO_3$ $\pi$ orbitals, and has been stabilised slightly over the same orbital in $Fe_2(SMe)_2(NO)_4$. Apart from this level all other orbitals up to and including the HOMO are the same as found for $Fe_2(SMe)_2(NO)_4$. The first three unoccupied levels, however, have changed order relative to $Fe_2(SMe)_2(NO)_4$; the $3b''_{2g}$ occupying the LUMO, with $dx^2\text{-}y^{2*}/dz^{2*}$-(X)(orbital$3a''_{1u}$) being the LUMO+1 and the dyz (orbital $3b'_{1u}$) the level above that.

From this calculation there is little difference between $Fe_2(SMe)_2(NO)_4$ and $[Fe_2(S_2O_3)_2(NO)_4]^{2-}$

Effect of Bridge Geometry on the Orbitals in $[Fe_2(S_2O_3)_2(NO)_4]^{2-}$

The effect of changing the geometry of the bridge on the energies of the calculated orbitals was investigated. This work was similar to that of Hoffmann and Summerville [11], but in this case the symmetry is lower ( $D_{2h}$ -> $C_{2v}$), and the empty d-orbitals of the bridging ligand were taken into account.

The Fe-S bond lengths were held at a distance of 2.24Å, and the terminal nitrosyl ligands were unchanged from the geometry in the crystal. The angle Ø, defined below, was changed from 60 to $100^o$ and the effect on the energies of the orbitals calculated. The results of the calculations are given in fig 2-19. At low and high values of Ø orbital $3a''_{1u}$, $dx^2\text{-}y^{2*}/dz^{2*}$-(X), is the LUMO. As Ø increases from $80^o$, the antibonding overlap decreases as the pz orbitals of the sulphur approach the node of the metal $dx^2\text{-}y^2$ and so the energy of the orbital drops. The orbital reaches a maximum energy at about $80^o$ where the total antibonding overlap with the sulphur orbitals is at a maximum. The energy decreases

## Figure 2-19

Effect of Bridge Geometry on Selected Orbitals of $[Fe_2(S_2O_3)_2(NO)_4]^{2-}$

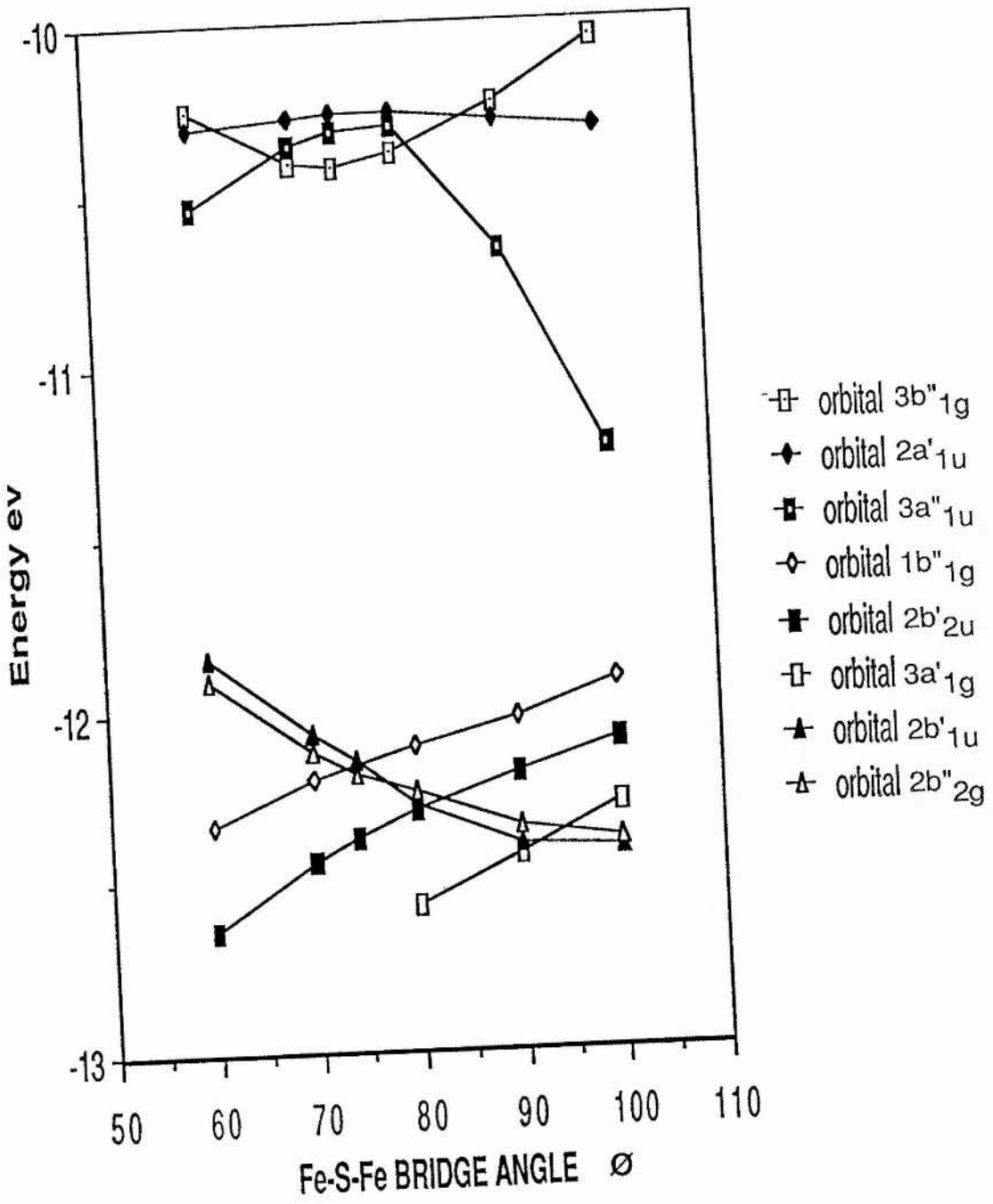

as Ø becomes less than $80^{o}$ since the sulphur orbitals move further away from the metal orbital lobes. The antibonding ∂ level of $dx^2$-$y^2$ plays little role in the energies at the distances involved.

Orbital $3b"_{1g}$, is interesting because it contains orbital character from the $SO_3$ groups. This is the LUMO at the crystal geometry. On reduction this orbital would be occupied assuming no geometry relaxation took place. However the stabilisation in energy which would occur by populating orbital $3a"_{1u}$, coupled with a geometry change to a longer Fe-Fe distance, seems more preferable. Thus reduction to the tetra-anionic complex may simply open the complex by fully populating this orbital. If this was not the case, however, and on reduction the geometry remained between 70 and $85^{o}$, then due to the closeness of the unoccupied levels a paramagnetic complex with two free electrons may be produced.

Electrochemical investigations by cyclic voltammetry of $[Fe_2(S_2O_3)_2(NO)_4]^{2-}$ show two quasi-reversible one electron reductions (see chpt 4).E.p.r. observations on the reduced $Fe_2(\mu_2\text{-}SR)_2(NO)_4$ show that the monoanion has its lone electron coupled to four equivalent nitrogens, but no hyperfine coupling to H was observed. This is suggestive of the electron populating the $dx^2$-$y^{2*}/dz^{2*}$-(X) with a concomitant increase in the Fe-Fe bond distance. Although this orbital is formally non-bonding to the nitrosyl ligands an examination of table 2-5 reveals an amount(10%) of charge on the nitrogens of this orbital; the small coupling constants obtained may reflect this small interaction with the nitrogens. Although the population of this orbital means that a formal bond order of zero between the irons exists and the fragmentation of the complex would be expected the reductions as shown by C.V. for $Fe_2(SR)_2(NO)_4$ are reversible (the reductions for salts of $[Fe_2(S_2O_3)_2(NO)_4]^{2-}$ are more complex because of the associated charge). This implies that fragmentation does not occur and that there is enough stability to prevent the collapse of the cluster on reduction at least on the C.V. time scale.

The crossing over of the filled orbitals looks complex but the essential features can be found from a detailed examination of the eigenvectors and by reference to Hoffmanns work [11]. At the crystal geometry, Ø = $74^{o}$, there are three orbitals all of similar energy. With reference to the orbitals of figure 2-19, the increase/decrease in energy can be simply correlated to the increase/decrease in bonding/antibonding overlap involved with the irons, the sulphurs or the iron-sulphur interactions.

The diagram can be used to explain the irreversible nature of the multielectron oxidation observed by cyclic voltammetry. The closeness of the first three filled levels at the crystal geometry shows that the energy required to remove one electron is approximately the same as for the other five. With the removal of one electron, orbital $1b''_{1g}$ will act as a brake, preventing the cluster from opening up. A further removal will release this constraint and Ø will increase until the effect of orbital $2b'_{1u}$ is felt. Further removal of electrons will also release this constraint and Ø will increase further.

From the calculation alone the effect of oxidation on the cluster is uncertain apart from the theory that Ø should increase. Experimentally a multielectron chemically irreversible oxidation is observed; ie the cluster falls apart. Oxidation of $(PNP)_2[Fe_2(\mu_2\text{-}S_2O_3)_2(NO)_4]$ has been shown by n.m.r. to produce $NO_2^-$, $NO_3^-$, and Roussin's Black Salt (chpt 3). It is also known from e.p.r. that the oxidation of the cluster produces $[Fe(NO)_2(NO_2)_2]^-$[19]. It appears therefore that either a cascade of electrons falls out of the complex reducing bonding overlap and leading to fragmentation or that some electrons are pulled out, the geometry restraints are released, Ø becomes larger, bonding density is lowered and fragmentation occurs.

Figure 2-20 shows the effect the change in bridge angle has on the Fe-Fe overlap. As the bridge angle increases and the irons move away from one another the overlap decreases to a slightly negative value. As expected as the angle decreases the overlap increases, but from the figure the amount of overlap is very small.

**Figure 2-20**

Effect of Bridge Geometry on the Fe-Fe Overlap

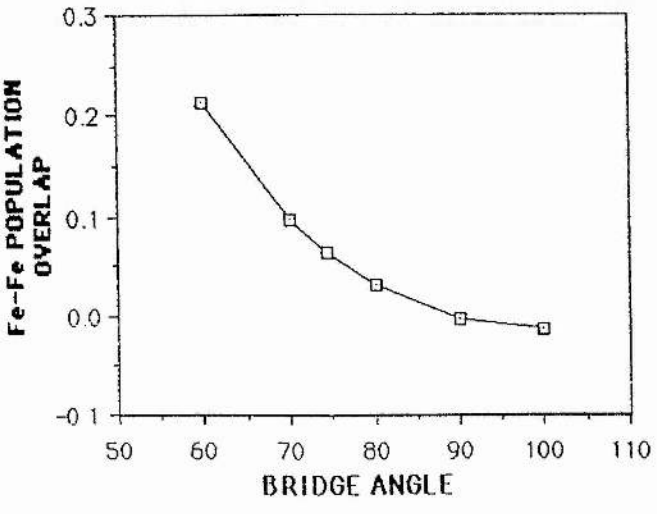

This calculation only examines the effect of the Fe-S-Fe angle and ignores any possible change in the Fe-NO angles/ bond lengths on reduction. This is a source of error, since from e.p.r. and IR examinations of the reduced esters we know that the nitrosyls are involved; the stretching frequency of the N-O bond decreases, however the calculation does provide a model for what may be occurring with the complexes during reduction or oxidation.

2-11

An Examination of the Bonding in $[Fe_4S_3(NO)_7]^-$

In a paper by Sung et al [1] the highest occupied orbitals are described as being predominantly due to Fe-Fe interactions. $[Fe_4S_3(NO)_7]^-$ can be considered a 34 valence electron cluster (one Fe $d^7$ and three Fe $d^9$). Out of a possible 20 orbitals, 17 are filled, giving a net stabilisation of three bonding levels, ($a_1$ +e). These are considered as having an electron pair shared between the apicaliron and one basal iron atom. The HOMO was described as bonding with respect to the $Fe_4$ terahedron while the LUMO was antibonding. An overlap population of 0.178 of an electron between the apical and basal irons was calculated for the anion and an overlap of 0.118 for the neutral or dianion. The bonding between iron and sulphur was described as being between -14 and -15.3 eV.

In the paper by Chu and Dahl [3], they reported that the structures of $[Fe_4S_3(NO)_7]^-$, $Fe_4S_4(NO)_4$ and $Fe_2(SEt)_2(NO)_4$ were essentially invariant in the angles and bond lengths of the Fe-Fe and $Fe_2S_2$ regions of these clusters. They intimated that as such the bonding associated with these $Fe_2S_2$ fragments must be similar. The EHT calculation on $[Fe_4S_3(NO)_7]^-$ was repeated using the atomic coordinates of Chu and Dahl.

As found for $[Fe_2S_2(NO)_4]^{2-}$ the difference between a calculation with the participation of sulphur d-orbitals to one without was manifest in the increase in stability of most orbitals when they were used; allowing more electron delocalisation to occur. For instance in this calculation the HOMO was found to be about 0.4 eV more stable than the previous calculation [1].

An examination of the net overlap between iron atoms reveals a similar picture to that of $[Fe_2S_2(NO)_4]^{2-}$, as was expected by Chu and Dahl. In the latter complex the total overlap

between the irons was calculated to be 0.06 electrons. The bonding was shown to be mainly through the Fe-S bonds and that the Fe-Fe interaction, where present, was small. For $[Fe_4S_3(NO)_7]^-$ a net overlap of 0.055 electrons was calculated to exist between the apical and basal irons. There was no bonding between the basal iron atoms themselves. An examination of the overlap between the apical iron and the three sulphurs showed an overlap of 0.67 electrons and o.65 between the basal and the two nearest sulphurs. Again, from this simple calculation, it would appear that there is little direct net bonding between the iron atoms and what there is occurs only between the apical and basal irons. the picture of a bonding terahedron of iron atoms appears to be a very simplistic model. As was found for $[Fe_2S_2(NO)_4]^{2-}$ most of the bonding in the cluster occurs via the sulphur bridges.

The following table gives the total charges associated with the iron and sulphur atoms of the cluster and also the fractional electron density on the atoms for the HOMO, LUMO and LUMO+1 orbitals.

**Table 2-6**

| | Fe(A) | Fe(B) | S |
|---|---|---|---|
| Total Charge(a) | +1.25 | +1.47 | -0.71 |
| HOMO(b) | 0.23 | 0.13 | 0.20 |
| LUMO | 0.24 | 0.12 | 0.21 |
| LUMO +1 | 0.35 | 0.10 | 0.35 |

(a)total charge calculated for Fe and S atoms in the cluster $[Fe_4S_3(NO)_7]^-$; (b) fractional electron density on the atoms for a filled orbital; for basal iron and sulphur atoms the average value is given.

The total charge associated with the apical iron and the basal irons are similar. The apical iron is formally Fe(+1) whereas the basal are formally Fe(-1). The differences in reactivity of the $[Fe(NO)]^{2+}$ group relative to the $[Fe(NO)_2]^+$ may reflect more the differences between a mononitrosyl and a dinitrosyl, as implied by Enemark [9], than that due to irons of differring oxidation states.

The HOMO and LUMO show that there is approximately an equal amount of electron density on the three sulphurs as there is on the four irons. In the work of Sung [1]the LUMO was designated an orbital of type E . In this work there was a difference of about 0.07 eV between the first two unfilled orbitals. The LUMO +1 orbital has 59% more electron density associated with the sulphurs than there is on the four irons. In both cases however, the addition of an electron to this cluster to produce the dianion, $[Fe_4S_3(NO)_7]^{2-}$ would

increase the electron density on the sulphurs. This result was the reasoning behind the investigation of the chemical reactivity of the reduced species towards the trimethylsulphonium cation, (see chapter 3).

A thorough investigation of the bonding associated with this cluster in a similar manner to that done for $[Fe_2S_2(NO)_4]^{2-}$ was undertaken, but the geometry of the cluster was such that this was very difficult and a proper investigation could really only be carried out if the computer power and programs were available.

## References


1. Sung, S-S., Glidewell, C., Butler, A. R., Hoffmann, R., Inorg. Chem., 24, 3856 (1985)

2. Thomas, T. T., Robertson, F. H., Cox, C. G., Acta Cryst., 11, 599, (1958)

3. Chu, C. T-W., Dahl, L. F., Inorg. Chem., 16, 3245, (1977)

4. Hoffmann, R., J. Chem. Phys., 39, 1397, (1963)

5. Howell, J., Rossi, A., Wallaon, D., Haruki, K., Hoffmann, R., Quantum Chemistry Exchange Program 344

6. Albright, T. A., Hoffmann, R., Hibeault, J. C.m Thorn, D. L., J. Am. Chem. Soc., 101, 3801, (1979)

7. Goldberg, K. I., Hoffmann, D.M., Hoffmann, R., Inorg. Chem., 21, 3863, (1982)

8. Hughbanks, T., Hoffmann, R., J. Am. Chem. Soc., 105, 3528, (1983)

9. Enemark, J. H., Feltham, R. D., Coord. Chem. Rev., 13, 339, (1974)

10. Lin Xianti, Zheng An, Lin Shanhao, Huang Jingling, Lu Jiaxi, J. Struct. Chem. (Wuhan), 1, 79, (1982)

11. Summerville, R. H., Hoffmann, R., J. Am. Chem. Soc., 98, 7240 (1976)

12. Dahl, L. F., Rudolfu de gal, E., Feltham, R. D., ibid, 96, 1653, (1969)

13. Kaduk, J. A., Ibers, J. A., Inorg. Chem., 14, 3070, (1975)

14. Huheey," Inorganic Chemistry, Principles of Structure and Reactivity", 2nd Edition (1976), Harper and Row (publishers)

15. Yu, Y-F., Chau C-N., Wojcicki, A., Inorg. Chem.,25, 4098, (1986)

16. a) Butler, A. R., Glidewell, C., Hyde, A. R., McGinnis, J., Seymour, J. E., Polyhedron, 2, 1045, (1983)

b) Butler, A. R., Glidewell, C., Johnson, I. L., Polyhedron, 6, 1147, (1987)

c) Butler, A. R., Glidewell, C., Hyde, A. R., McGinnis, J., Inorg. Chem., 24, 2931,

(1985)

17. For example, Ref [2]; Butler, A. R., Glidewell, C., Li, M-H., Adv. Inorg. Chem., 32, 335, (1988) and references therein; Mak, T. C. W., Book, L., Chung, C., Gallagher, M. K., Li-Cheng, S., Seyferth, D., Inorg. Chim. Acta, 73, 159, (1983); the structure of $\{N(PPh_3)_2\}[Fe_2(S_2O_3)_2(NO)_4]$ reported in chapter-3 of this thesis.

18. Glidewell, C., Hyde, A. R., Polyhedron, 4, 1155, (1985)

19. Lambert, R. J., Johnson, I., unpublished work

# Chapter Three

# Chapter Three

# An Examination of the Chemistry of the Thiosulphate Analogue of Roussin's Red Salt and the Reactions of Certain Electrophiles with Roussin's Black Salt.

## Introduction

Originally, Roussin prepared the black salt from ferrous sulphate, polysulphide and nitrite [1]. The Red salt was formed by reflux of the Black salt in sodium hydroxide solution. The composition of these two iron-sulphur-nitrosyl clusters were shown by Pavel [2] to be $M[Fe_4S_3(NO)_7]$ and $M_2[Fe_2S_2(NO)_4]$ for the Black and Red salts respectively,(M=Na,K,Tl or $NH_4$). Pavel also produced $Fe_2(SEt)_2(NO)_4$ by the alkylation of the red salt; this was the first member of a family of iron-sulphur-nitrosyl clusters known as the Esters of Roussin's Red salt. Although other methods exist for the preparation of these esters,[3,4,5,6] Pavel's original method of using an alkyl halide is one of the most versatile. This preparative method has been extended by Seyferth and Gallagher [7,8] and many new types of iron-sulphur-nitrosyl clusters have been discovered. For example the use of the dihalide $(Ph_3P)_2PtCl_2$ leads to a complex bridged across the sulphurs by the platinum atom [9]; reactions with other gem dihalides have, however, not led to bridged complexes.

The above method of reacting Roussin's Red salt with an organic halide or with a species with a labile halide cannot be applied to the formation of the aryl Esters of Roussin's Red Salt. This class of cluster can be successfully synthesised from the related carbonyl clusters, $Fe_2(SR)_2(CO)_6$[10,11]. These carbonyl clusters are easily formed from dodecacarbonyltri-iron and an organic-disulphide or from di-iron ennaeacarbonyl and the corresponding mercaptan. Nitrosylation of $Fe_2(SR)_2(CO)_6$ with nitrite or nitric oxide leads to the nitrosyl clusters in good yield [5,8].

The other main preparative route to the alkyl esters is via the dimeric iodo complex, $Fe_2I_2(NO)_4$. This reacts in THF solution with thiols in the presence of base to produce the corresponding esters [12]. This method has allowed the preparation of mixed chalcogen

esters such as $Fe_2(SCH_2Ph)(SeCH_2Ph)(NO)_4$. The pathways through which the iodo complex is changed into the esters has been worked out using e.p.r. spectroscopy [13]. The reaction has been shown to proceed via the mononuclear-dinitrosyl species $Fe(NO)_2I$ and $[Fe(NO)_2(SR)_2]^-$.

The formation of such mononuclear species is extremely important in the overall chemistry of these clusters. Addition of thiolate to solutions of $Fe_2(SR)_2(NO)_4$ causes the cluster to break open to produce the mononuclear species $[Fe(NO)_2(SR)_2]^-$ [6]. Addition of an excess of a different thiolate to such solutions followed by the addition of a solvent with a low dielectric constant, such as toluene, causes the re-dimerisation of the mononuclear species with the production of a new ester; scheme-1.

$$Fe_2(SR)_2(NO)_4 + SR^{1-} \xrightarrow[THF]{base} [Fe(SR)_2(NO)_2]^{1-} \xrightarrow{X's\ SR'^{1-}} [Fe(SR')_2(NO)_2]^{1-}$$

$$[Fe(SR')_2(NO)_2]^{1-} \xrightarrow{Toluene} Fe_2(SR')_2(NO)_4$$

Scheme-1

In a similar manner, the reaction of $Fe_4S_4(NO)_4$ or $[Fe_4S_3(NO)_7]^-$ with $MeS^-$ produces $[Fe(SMe)_2(NO)_2]^-$, from which solutions the methyl ester, $Fe_2(SMe)_2(NO)_4$, can be isolated in preparatively useful yields of 18 and 40% respectively [6].

Related to the Roussin Esters is the thiosulphato anion, $[Fe(S_2O_3)(NO)_2]^-$. This compound was first produced in 1895 [3,14] from the reaction of ferrous sulphate, thiosulphate and nitric oxide.

$$2FeSO_4.7H_2O + 4K_2S_2O_3.5H_2O + 4NO \xrightarrow{H_2O} 2K[(NO)_2FeS_2O_3.H_2O] + K_2S_4O_6 + 2K_2SO_4$$

On the basis of its I.R. spectrum, Its diamagnetism [31] and the similarity of the preparation to that of the alkyl esters of Roussin's Red salt it has been assumed to be a dimeric complex with a structure similar to that of the esters themselves. Apart from its I.R. spectrum and its diamagnetism, however, very little else was known about this complex. Part one of this chapter describes the synthesis, characterisation and reactions of this

cluster, and shows the similarity of its chemistry to that of the alkyl esters.

The methyl ester of Roussin's Red salt as described in chapter one has been implicated in the incidence of oesophageal cancer in the Linxian region of China. One possibility is that the high levels of nitrite in the local water nitrosylates natural iron-sulphur enzymes, a reaction which eventually leads to the formation of $Fe_2(SMe)_2(NO)_4$ within vegetable matter eaten by the local people.

Incubation of parsley with nitrite was shown by Johnson [15] to produce the methyl ester. Incubation of casein with nitrite produces Roussin's Black anion [16], $[Fe_4S_3(NO)_7]^{1-}$. It has further been shown by Hyde that the reaction of nitrite with analogues of iron-sulphur enzymes also produces Roussin's Black anion [17]. This work suggested that the Roussin's Black anion was a possible intermediate in the formation of the methyl ester; scheme-2.

$$Fe_4S_4(S\text{-}Cys)_4 \xrightarrow{NO_2^{1-}} [Fe_4S_3(NO)_7]^{1-} \xrightarrow{\text{"Me"}} Fe_2(SMe)_2(NO)_4$$

Scheme-2

Here "Me" denotes the *in vivo* transfer of a methyl group by means unknown, to produce the dimer from the tetramer by means unknown. Thus, reactions of Roussin's Black anion which involve the formation of an alkyl ester are relevant to the study of the *in vivo* production of $Fe_2(SMe)_2(NO)_4$. Preparations of the Roussin esters involving the production of mononuclear radicals[6] from Roussin's Black anion are low yielding reactions and for an *in vivo* mechanism would involve the participation of either $HS^-$, $S^{2-}$ or $MeS^-$ in some biological form to be a viable route to the methyl ester. Another possible pathway might involve the formation of Roussin's Red dianion, $[Fe_2S_2(NO)_4]^{2-}$ which is known to react with electrophilic carbon with ease. The laboratory preparation of Roussin's Red dianion, however involves a reflux in strong alkali whereas the conversion of the Red dianion into the Black anion is facile and can be simply done by bubbling $CO_2$ into an aqueous solution of the Red salt. It is unlikely, therefore that the methyl ester is formed from Roussin's Black anion via the Red dianion.

A paper by Jinhau[18] described the reaction of Roussin's Black salt with para-fluorobenzenediazonium salt and showed that it led to the production of the dimeric cluster $Fe_2(SC_6H_4F)_2(NO)_4$. The X-ray structure of the complex was given; figure 3-1. A

paper by Miwa and Iwasawa [19], however gave $Fe_4S_3(NO)_4N_2C_6H_4NO_2$ as the product of the reaction of the Black salt with a para-nitrobenzenediazonium salt. They gave the following as a possible mechanism;

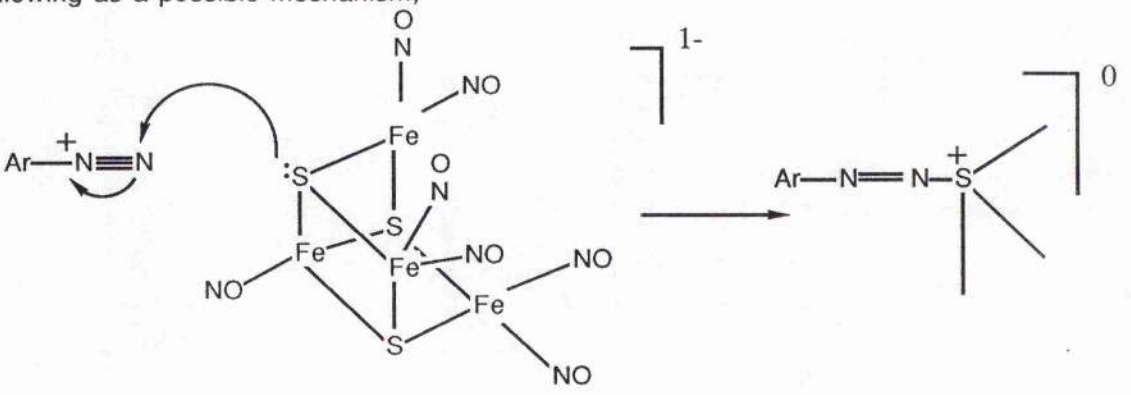


Part two of this chapter describes the reactions of Roussin's Black Salt with some electrophiles and a possible pathway for the *in vivo* production of $Fe_2(SMe)_2(NO)_4$ is given.

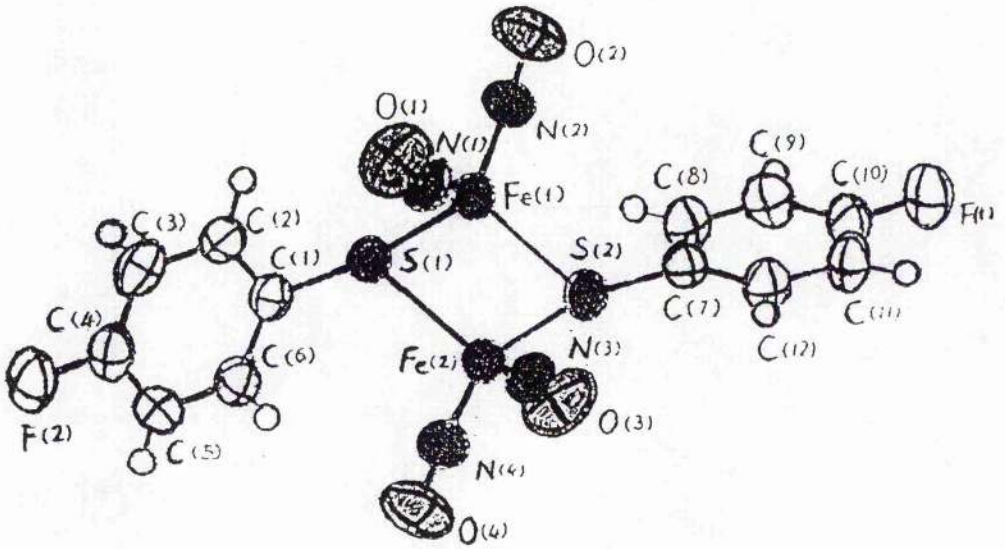


**Figure 3-1**
Structure of $Fe_2(SC_6H_4F)_2(NO)_4$
from ref. [18]

# Experimental

Instruments and materials

Elemental analyses were by the Microanalytical Laboratory of this Department. $^{15}N$,$^{19}F$, $^{13}C$ and $^{1}H$ n.m.r. were recorded using a Brüker AM-300 or a Brüker WP-80 spectrometer. $^{15}N$ chemical shifts are referred to external $CH_3{}^{15}NO$ recorded at 30.48MHz, $^{19}F$ chemical shifts are referred to internal $CCl_3F$ recorded at 75.3MHz. Infra-red spectra were recorded, either as nujol mulls or in solution using a Perkin Elmer 1330 spectrometer or a Perkin Elmer 1710 FTIR. Mass spectra were recorded using an INCOS 50 GCMS, accurate masses were obtained using an AEI MS 902. UV spectra were recorded on a Pye Unicam SP8150 UV-Vis spectrometer. E.P.R. spectra were recorded on a Bruker ER 200D spectrometer, g-values were obtained using di-t-butlynitroxide (g=2.0061) as a standard.

All preparations were carried out under nitrogen, using Shlenck techniques or a glove box where appropriate. Solvents were purified according to techniques outlined by Perrin and Perrin[21]. Light petroleum had b.p. 40-60$^{o}$C. $Na^{15}NO_2$ (99% enriched) was purchased from M.S.D. Isotopes Inc., and was used as received. $Na[Fe_4S_3(NO)_7]$ was produced using an adaptation of that outlined by Brauer[4]. $Fe_2S_2(CO)_6$ and $Li_2[Fe_2S_2(CO)_6]$ were produced from literature methods [20]. Amines were purchased from a variety of sources and purified before use. Trimethylsulphonium and sulphoxonium salts were purchased from Aldrich and used as received as were the trialkyloxonium salts, the mercaptans and disulphides used in this work. Chlorophenylmethane, chlorodiphenylmethane, iodomethane and iodoethane were used as received.

Preparation of $Na_2[Fe_2(\mu_2\text{-}S_2O_3)_2(NO)_4]$ from NO(g).

$FeSO_4.7H_2O$ (10.8 g, 39 mmol) in water (20 $cm^3$) was added under nitrogen to a stirred solution of $Na_2S_2O_3.5H_2O$ (20 g, 80mmol). Nitric oxide was bubbled through the solution for two hours. The solution darkened considerably in the first few minutes. The solution was filtered, reduced to dryness and the solid extracted with acetone (4 x 200 $cm^3$). This was reduced in volume, cooled in an ice bath and dichloromethane added slowly to

obtain a brown crystalline material. Yield of $Na_2[Fe_2(\mu_2\text{-}S_2O_3)_2(NO)_4]$ 9.0g, 17.9 mmol,90%(based on iron).

Preparation of $(PNP)_2\,[Fe_2(\mu\text{-}S_2O_3)_2(NO)_4]$.

To a nitrogen purged, stirred solution of $Na_2[Fe_2(\mu\text{-}S_2O_3)_2(NO)_4]$ (1g, 2mmol) in water (40ml) was added a hot solution of bis(triphenyl posphoranylidene) ammonium chloride (PNPCl) (2.3 g, 4mmol,20ml of $H_2O$ at $60^oc$) . The mixture was stirred for 20 minutes, filtered and washed with warm water. The solid was dissolved in $CH_2Cl_2$(3 x50ml) and dried over $MgSO_4$. The solution was reduced in volume and cooled in an ice bath. The complex crystallised as brown needles.

Microanalysis; calculated for $C_{72}H_{60}P_4N_6S_4O_{10}Fe_2$; expected C 56.4; H 3.9; N 5.5%; obtained C 56.7; H 4.1; N 5.2%. I.R.,($CH_2Cl_2$ solution); $\nu$NOasy=1787, $\nu$NOsym=1757$cm^{-1}$

Preparation of $Na_2[Fe_2(\mu_2\text{-}S_2O_3)_2(NO)_4]$ from $NaNO_2$.

To a stirred solution of $NaNO_2$ (2.84g, 41mmol) and $Na_2S_2O_3.5H_2O$ (9.9g, 40mmol) in water (40ml) was added, under nitrogen, a solution of $FeSO_4.7H_2O$ (5.52g, 19.8mmol) in water (30ml). The mixture was stirred for two hours. The solution was filtered and the water removed under reduced pressure. The solid was extracted with acetone (4 x 200ml), leaving a green residue behind. The solution was reduced in volume and the complex precipitated using a 1:5 v/v mix of $CH_2Cl_2$ and petroleum. The solid was dried under vacuum to produce a khaki coloured compound. Yield of $Na_2[Fe_2(\mu_2\text{-}S_2O_3)_2(NO)_4]$ 1.5g, 3 mmol, 30%(based on iron).

Microanalysis as the PNP salt; calculated for $C_{72}H_{60}P_4N_6S_4O_{10}Fe_2$; expected C 56.4; H 3.9; N 5.5%; obtained C 56.3; H 3.9; N 5.41%. I.R., ( $CH_2Cl_2$ solution); $\nu$NOasy=1786, $\nu$NOsym=1756 $cm^{-1}$.

The green residue was redissolved in water and $Bu_4NBr$ (8g, 25mmol) added. The green solution was extracted with $CH_2Cl_2$ until no colour remained in the aqueous layer. The organic layer was brown. The solvent was removed and the solid washed with warm water (4

x 250ml). The resulting solid was dried under vacuum and recrystallised from ethanol. Yield of $(Bu_4N)_2[Fe_2(\mu_2\text{-}S_2O_3)_2(NO)_4]$ 2g, 2 mmol. I.R.,($CH_2Cl_2$ solution); $\nu$NOasy=1787, $\nu$NOsym=1758$cm^{-1}$.

Preparation of $(PNP)_2Fe_2(\mu\text{-}S_2O_3)_2(^{15}NO)_4$ .

This followed the above method. I.R.,($CH_2Cl_2$ solution); $\nu$NOasy=1748, $\nu$NOsym = 1718$cm^{-1}$ (values expected from theory[22]).

Reaction of $Fe_2I_2(NO)_4$ with $Na_2S_2O_3.5H_2O$ in THF

$Fe_2I_2(NO)_4$ (0.5g, 0.1mmol) and $Na_2S_2O_3.5H_2O$ (1.02g, 4mmol) are stirred together in THF (30ml) overnight. The solution was black and sludge-like. The THF was removed under vacuum. The solid was washed with petrol 40/60, a red liquid was obtained and a brown solid was left. $CH_3CN$ (40ml) was added, and a green-brown solution obtained. I.R., of brown solid was identical to that of $Na_2[Fe_2(S_2O_3)_2(NO)_4]$. A green residue was left. The $CH_3CN$ was removed. I.R., of brown solid was identical to that of $Na_2[Fe_2(S_2O_3)_2(NO)_4]$. The solid was dissolved in water. $Bu_4NBr$ (4g, 12mm) was added and the water layer extracted with $CH_2Cl_2$. I.R., ($CH_2Cl_2$ solution) $\nu$NOasy=1786, $\nu$NOsym=1758$cm^{-1}$.

Preparation of Roussin's Alkyl Esters from $Na_2[Fe_2(\mu_2\text{-}S_2O_3)_2(NO)_4]$ .

1) Preparation from basic THF solutions.

Typically, to a solution of $Na_2[Fe_2(\mu_2\text{-}S_2O_3)_2(NO)_4]$(1g, 2mmol) in THF(30ml) was added triethylamine (1g, 10mmol) and RSH (5mmol equiv), R= $CH_3$, $CH_2CH(CH_3)_2$, $CH(CH_3)_2$, $(CH_2)_4CH_3$. This was stirred under nitrogen for 4 hours after which the reaction was quenched by the addition of toluene (500ml). The solvent was removed under vacuum. Petroleum (200ml) was added and a red coloured solution was obtained. This was filtered, reduced in volume and chromatographed on a silica column (15x5cm, eluted with

petrol). The solution was again reduced in volume, cooled in ice and crystallised under a stream of nitrogen. Typical yield of $Fe_2(\mu_2\text{-}SR)_2(NO)_4$ , 40-70% (based on iron). Esters were identified by Infra red spectroscopy (recorded in $CCl_4$), mass spectra, and by $^{13}C$ and $^{1}H$ n.m.r spectroscopy.

2) Preparation from basic aqueous solutions

Preparation of $Fe_2(S^tBu)_2(NO)_4$

To a stirred, deoxygenated solution of $Na_2[Fe_2(\mu_2\text{-}S_2O_3)_2(NO)_4]$ (1g,2mmol) and $Na_2S_2O_3.5H_2O$ (1g, 4mmol) in water(80ml)/ $CH_2Cl_2$ (200ml) , was added $^tBuSNa$ (3.3g,29mm) dissolved in NaOH (aq)(1g in water(30ml)) . The red, organic layer was separated from the aqueous layer, washed with water (2x200ml)and dried over $CaCl_2$; the solvent was then removed. The solid was recrystallised from hot petrol under a nitrogen atmoshere, to obtain black-red needles of $Fe_2(\mu_2\text{-}S^tBu)_2(NO)_4$. Yield 54%.

Microanalysis; calculated for $Fe_2C_8H_{18}N_4O_4S_2$ ; expected C 23.4,H 4.4, N 13.7%; obtained C 23.6, H 4.7, N 13.7%. I.R., (THF solution) $\nu$NOasym=1771, $\nu$NOsym=1745cm$^{-1}$.

Preparation of $Fe_2(S^iPr)_2(NO)_4$

To the solution of $Na_2[Fe_2(\mu_2\text{-}S_2O_3)_2(NO)_4]$ and sodium thiosulphate as described above was added a solution of $^iPrSH$ (4.1g,54mmol) in NaOH(aq) (1g,in water (100ml)). The work up followed the above procedure. On recrystallising from hot petrol under nitrogen, black-red needles of $Fe_2(\mu_2\text{-}S^iPr)_2(NO)_4$ were obtained. Yield 60%.

Microanalysis; calculated for $Fe_2C_6H_{14}N_4O_4S_2$; expected C18.9, H 3.7, N 14.7% ; obtained C 19.0, H 3.6, N14.5%. I.R., (THF solution) $\nu$NOasym=1773, $\nu$NOsym=1748cm$^{-1}$.

Preparation of $Fe_2(SMe)_2(NO)_4$

Following the procedure for $^tBuSNa$ described above, MeSNa (1.4g,20mmol) was reacted in a similar manner. On recrystallisation from petrol, black parallelepipeds of $Fe_2(\mu_2\text{-}SMe)_2(NO)_4$ were obtained. Yield 61%.

Microanalysis; calculated for $Fe_2C_2H_6N_4O_4S_2$ ; expected C 7.4, H 1.8, N 17.2% ; obtained C 7.4, H 1.3, N 17.1%. I.R., (THF solution) $\nu$NOasym=1776, $\nu$NOsym=1751$cm^{-1}$.

Preparation of $Fe_2(SCH_2CO_2CH_3)_2(NO)_4$

To a solution of $Na_2[Fe_2(\mu_2\text{-}S_2O_3)_2(NO)_4]$ (2g, 4mmol) and $Na_2S_2O_3.5H_2O$ (2g,8mmol in water(50ml)), was added a solution of methylthioglycolate(6g,56mmol) dissolved in NaOH(aq) (2.5g in water (100ml)). The product was extracted into $CH_2Cl_2$(2x150ml), and dried over $CaCl_2$. The solvent was removed and the black solid recrystallised from hot $CH_2Cl_2$ to obtain shiny black rectangular plates of $Fe_2(\mu_2\text{-}SCH_2CO_2CH_3)_2(NO)_4$. Yield 58%.

Microanalysis; calculated for $Fe_2S_2C_6H_{10}N_4O_8$; expected C 16.3, H 2.3,N 12.6%; obtained C 16.4, H 2.1, N 12.6%. Melting point $120^o$-$122^o$. Mass-spec, $M^+$ of 442 is not obtained, but the peaks at 176 and 144 are consistent with $Fe_2S_2$ and $Fe_2S$ respectively. Peaks at 208, 250,280,310,352 ,382 and 412 are consistent with the proposed structure. $^1H$ n.m.r. at RT one broad unresolved peak was observed (3.6ppm). At -$40^oC$ three peaks plus a shoulder are observed; assigned $CH_3$, 3.66, 3.72 ppm; $CH_2$, 3.7, 3.74 (shl). $^{13}C$ n.m.r.; $CH_3$, 42.6, 44.8 ppm, $CH_2$ 53.0, 53.2ppm. Using a 5 second pulse delay CO, 169.3ppm. Assignments of the $CH_2$ and $CH_3$ were confirmed using the DEPT technique. I.R., ($CH_2Cl_2$ solution) $\nu$NOasym 1788, $\nu$NOsym 1760$cm^{-1}$.

Preparation of $Fe_2(SC_2H_4OH)_2(NO)_4$

To a solution of $Na_2[Fe_2(\mu_2\text{-}S_2O_3)_2(NO)_4]$(1g, 2mmol) and $Na_2S_2O_3.5H_2O$ (1g, 4mM) in water (30ml) was added $HSC_2H_4OH$ (1.5g, 20mmol) in NaOH aq (1g in 30ml). Dichloromethane (75ml) was added and the solution stirred for ten minutes. The organic

layer was separated. To the aqueous layer was added glacial acetic acid/$H_2O$ (1:1, 100ml) and $CH_2Cl_2$ (100ml). The organic layer was separated and combined with the earlier fraction and washed with water (3x100ml). The solution was dried over $CaCl_2$ and the solvent subsequently removed to yield 0.3g of a dark brown solid. The solid was recrystallised from hot $CH_2Cl_2$ under $N_2$ to obtain 0.2g of black crystals. Yield 26%.

Microanalysis; calculated for $Fe_2S_2N_4O_6C_4H_{10}$; expected C 12.4, H 2.6, N 14.5%; obtained C 12.6, H 2.3, N 14.3%. Melting point $108^o$-$110^o$. Mass-Spec $M^+$ of 386 is not observed, but the peak at 176 is consistent with $Fe_2S_2$, and peaks at 190,220,250 296 and 326 are also consistent with the proposed structure. I.R., (THF solution) $\nu$NOasym 1780, $\nu$ NOsym 1753$cm^{-1}$. $^{13}C$ n.m.r., THF solution, $\partial\underline{C}H_2OH$-64.3ppm, $\partial\underline{C}H_2CH_2OH$-48,48.7ppm (cis and trans isomers). Signals are in approximately the ratio 2:1:1. $^1H$ n.m.r., $\partial O\underline{H}$-4.46ppm (multiplet), $\partial CH_2OH$-3.88ppm (multiplet), $\partial C\underline{H}_2CH_2OH$-3.2ppm (two overlapping triplets). Signals are in the ratio 1:2:2.

Preparation of $Fe_2(SC_4H_3N_2)_2(NO)_4$

Following the above procedure, 2-pyrimidinethiol (2.24g 20mmol) in NaOH(aq) was reacted. The aqueous layer was extracted twice with $CH_2Cl_2$ (2 x 200ml). The layers combined, dried with $CaCl_2$, and the solvent removed. Recrystallised from hot $CH_2Cl_2$ under nitrogen to obtain black crystals of $Fe_2(\mu_2\text{-}SC_4N_2H_3)_2(NO)_4$. Yield 52%.

I.R., ($CH_2Cl_2$ solution) $\nu$NOasym 1798, $\nu$NOasym 1765 $cm^{-1}$. Microanalysis; calculated for $Fe_2C_8H_6N_8O_4S_2$ ; expected C 21.2, H 1.3, N 24.7% ; obtained C 21.6, H 1.2, N 25.9%. $^1H$ n.m.r. two broad peaks at 7.1ppm and 8.6ppm. Mass-spectrum was not consistent with the proposed structure nor with an iron-sulphur cluster. The peaks observed are consistent with the degradation of the complex.

The following esters of Roussin's Red Salt were all prepared from the method outlined above; $Fe_2(SR)_2(NO)_4$ , R= $C_2H_5$, $CH_2CH(CH_3)_2$, $(CH_2)_2CH_3$, $(CH_2)_3CH_3$, $(CH_2)_4CH_3$, $CH(C_2H_5)(CH_3)$. These were all identified as being esters from their I.R. spectrum, mass-spectrum and $^1H$ n.m.r.

3) Preparation of alkyl esters from $Na_2[Fe_2(\mu_2\text{-}S_2O_3)_2(NO)_4]$ and alkyl halides

Reaction of $Na_2[Fe_2(\mu_2\text{-}S_2O_3)_2(NO)_4]$ with $Na_2S.5H_2O$

To a solution of $Na_2[Fe_2(\mu_2\text{-}S_2O_3)_2(NO)_4]$(1g, 2mmol) and $Na_2S_2O_3.5H_2O$ (1g, 4mM) in water (30ml) was added $Na_2S.5H_2O$ (6.2g, 30mmol) in water(30ml) and stirred under $N_2$ for 30 minutes. The solution changes colour from green/black to dark red on addition of the sulphide ion. The water was removed on the rotary evaporator. The resulting solid was extracted with THF (4x50ml) and reduced to dryness. IR (THF solution) shows a mixture of Roussin's Black and Red salts to be present. The solid was extracted with ether to yield 0.14g of the Black Salt (26% based on iron ). The remaining red solid was shown to be the Red Salt from I.R.,(THF solution) $\nu NO_{asym}$=1678cm$^{-1}$ , $\nu NO_{sym}$ =1655cm$^{-1}$ and shl=1737cm$^{-1}$.

Reaction of $Na_2[Fe_2(\mu_2\text{-}S_2O_3)_2(NO)_4]$ and $Na_2S.5H_2O$ with MeI

To a solution of $Na_2[Fe_2(\mu_2\text{-}S_2O_3)_2(NO)_4]$(1g, 2mmol) and $Na_2S_2O_3.5H_2O$ (1g, 4mM) in water (30ml) was added $Na_2S.5H_2O$ (4, 24mmol) in water(30ml) containing NaOH (1g, 25mmol). An equal volume of THF was added and the solution filtered. MeI (3g, 21mmol) was added and the solution stirred for 30 minutes. The solution turned bottle green in colour and the strong smell of thiol was evident. The solution was extracted into $CH_2Cl_2$(2x200ml) and the organic layer separated. The organic layer was concentrated and subjected to column chromatography ( silica, eluting with $CH_2Cl_2$). A red/brown band came off quickly and was collected. Removal of the solvent yielded 0.13g, 20% of $Fe_2(SMe)_2(NO)_4$.

Mass-spec; $M^+$ 326, sequential loss of NO, 296,266,236,206. Melting point 94-96$^oC$.

Reaction of $Na_2[Fe_2(\mu_2\text{-}S_2O_3)_2(NO)_4]$ and $Na_2S.5H_2O$ with Chlorodiphenylmethane

The above procedure was followed replacing the MeI with $(C_6H_5)_2CHCl$ (8g, 40mmol). On removal of the $CH_2Cl_2$ a red/black solid (0.19g,) which was presumed to be the cluster $Fe_2(SCH(C_6H_5)_2)_2(NO)_4$ . I.R.,($Ch_2Cl_2$ solution) $\nu NO_{asym}$=1793cm$^{-1}$, $\nu NO_{sym}$= 1761cm$^{-1}$ . Mass-spectrum was not consistent with the proposed structure but peaks at

176 and 144 correspond to $Fe_2S$ and $Fe_2S_2$ respectively.

Reactions of $Na_2[Fe_2(\mu_2\text{-}S_2O_3)_2(NO)_4]$ with chelating ligands

Preparation of $Fe(NO)(S_2CNEt_2)_2$

(a) Following the above procedure (procedure 2 page 72), sodiumdiethyldithiocarbamate trihydrate (2g, 9mmol) in NaOH(aq) was reacted. The organic layer was separated, washed with water, dried, and the solvent subsequently removed. Recrystallisation from hot ether gave green/black crystals of $Fe(NO)(S_2CNEt_2)_2$.Yield 72%.

Analysis by IR and UV spectroscopy and mass-spectrometry was identical to that of the complex obtained by the method of Cambi and Cagnasso[44].

(b) Sodium dimethyldithiocarbamate was reacted in a similar manner to obtain $Fe(NO)(S_2CNMe_2)_2$.Yield 64%.

(c) Sodium dipropyldithiocarbamate produced from the reaction of dipropylamine and carbon disulphide reacted to give $Fe(NO)(S_2CNPr_2)_2$ . Yield 68%.

A further study of these mononuclear complexes and related compounds is described in chapter 5.

Attempted preparation of $(Et_4N)[MoS_2Fe(NO)_2]$

To a solution of $Na_2[Fe_2(\mu_2\text{-}S_2O_3)_2(NO)_4]$(1g, 2mmol) and $Na_2S_2O_3.5H_2O$ (1g, 4mmol) in water (30ml) was added $MoS_4(NH_4)_2$ ( 1.1g 4.2mmol). The solution was stirred under $N_2$ for ten minutes. $CH_2Cl_2$ (100ml) was added but no coloured material extracted into the organic layer. $Et_4NCl.H_2O$ (5g, 27mmol) in water (15ml) was added and the solution was filtered to obtain a black solid. This was washed with water(2x50ml) and with $CH_2Cl_2$ (2x50ml). The washings and the mother liquor were combined and the organic layer separated. The organic layer was dried over $CaCl_2$ and the solvent removed to obtain $(Et_4N)_2[Fe_2(\mu_2\text{-}S_2O_3)_2(NO)_4]$ as identified from IR. To the aqueous layer was added

MeSNa (3g, 43mmol) in NaOH solution. On extraction into $CH_2Cl_2$ (150ml), a small amount of $Fe_2(SMe)_2(NO)_4$ was obtained ( as identified from IR and mass-spec.)

The black solid dissolves well in acetone or acetonitrile. In the solid state it was not too air sensitive but was in solution. T.L.C., a single black spot moving with the solvent front in acetone on silica gel. After ten minutes the original T.L.C. solution shows two spots, one with the solvent front and one stationary. I.R., there is very little structure observed, peaks at 1744cm$^{-1}$ and 1717cm$^{-1}$ are assigned to $\nu NO_{asym}$ and $\nu NO_{sym}$ respectively. Microanalysis of two samples of the material did not give the required proportions nor did they agree with one another. This was due to the air sensitivity of the complex formed. The latest microanalysis is closer to $(Et_4N)(NO)_2FeS_2MoS_2Fe(NO)_2$, but is still well outside the normal tolerance levels of the microanalyser. Further work is required.

Attempted preparation of $Fe_2((SCH_2)_2C_6H_4)(NO)_4$

To a solution of $Na_2[Fe_2(\mu_2\text{-}S_2O_3)_2(NO)_4]$ (1g,2mmol) and $Na_2S_2O_3.5H_2O$ (1g,4mmol) in water(50ml), was added o-xylene-dithiol (2.5g,15 mmol) in NaOH(aq). The product was extracted in to $CH_2Cl_2$. The red solution was dried over $CaCl_2$, and the solvent removed to obtain a red-black solid. Attempts to purify this material have failed.

I.R.,($CH_2Cl_2$ solution), $\nu$NOasym 1779, $\nu$NOsym1751 cm$^{-1}$. Mass-spec., $M^+$ = 400, with sequential loss of four NO ligands.

Reaction with L-Cysteine

To a solution of $Na_2[Fe_2(\mu_2\text{-}S_2O_3)_2(NO)_4]$ (1.5g, 3mmol) and $Na_2S_2O_3.5H_2O$ (1.5g,6mmol) in water (50ml) was added a solution of L-Cysteine (4g,17mmol) in NaOH(aq) (1g in water(50ml)). A reaction was obvious, but no material extracted into $CH_2Cl_2$. The water was removed, and the solid extracted with MeOH. A purple solution resulted. On standing in air the solution turned brown. I.R., of the purple or brown solutions do not show the presence of coordinated NO.

Preparation of Aryl diazo compounds

All aryl diazonium compounds used in this study were produced using the same general procedure. The preparation outlined for para-fluorobenzenediazonium tetraflouroborate can be used with the straightforward modification for all the other diazonium compounds.

Para-fluoroaniline (6.36g, 0.057mmol) and $HBF_4$ (30ml, 50% v/v) are stirred together in an ice/salt bath. $NaNO_2$ (3.96g,0.057mmol) in ice/water(10ml) was added dropwise to the solution of amine at such a rate that the temperature did not rise above -5$^oC$. After complete addition, the mixture was stirred for a few minutes and then filtered. The solid was not washed. The white solid was dissolved in $CH_3CN$ (30ml) and precipitated by the addition of a large excess of solvent ether. The white crystalline solid was filtered off and the crystallisation procedure repeated. The solid was washed with ether and dried at the water pump. Yield 75%. Structure confirmed by I.R. spectroscopy (the loss of the amine peaks and the presence of $\nu N_2$), and by $^1H$ n.m.r., in $CD_3CN$.

The yields for other diazonium compounds range from 62% for the para-acetyl benzenediazonium salt to 92% for the para-methylbenzenediazonium salt. All structures were confirmed by I.R. spectroscopy and $^1H$ n.m.r.

Preparation of the para-fluorophenyl ester of Roussin's Red Salt

A solution of $Na[Fe_4S_3(NO)_7]$ (1.18g, 2.1mmol) in $CH_3CN$ (20ml) which was cooled to 0$^oC$. p-$FC_6H_4N_2BF_4$(3g, 14mmol), freshly crystallised from $CH_3CN$/solvent ether, in ice-water(25ml) was added in one amount under nitrogen. The solution was stirred for twenty minutes. Water (200ml) was added and the solid filtered off. It was washed with water (2x50ml), dissolved in $CH_2Cl_2$ (200ml) and dried over $MgSO_4$. The solvent was reduced in volume and the material purified by column chromatography (silica 10x10, $CH_2Cl_2$). The solvent was removed and the solid recrystallised from $CH_2Cl_2$/MeOH to obtain $Fe_2(SC_6H_4F)_2(NO)_4$ . Yield 97% based on available sulphur.

Microanalysis; calculated for $Fe_2S_2C_{12}H_8F_2N_4O_4$; expected C 29.6, H 1.7, N 11.5%; obtained C 29.6, H 1.6, N 11.2%. Melting point 150$^oC$ - decomposes. I.R.,($CCl_4$ solution)

$\nu NO_{asym}$ 1789cm$^{-1}$, $\nu NO_{sym}$1763cm$^{-1}$. Mass-spectrum, $M^+$ 486, sequential loss of NO, 456,426,396,366. $^{19}F$ n.m.r., $\partial$ 112.8, 113.4 ppm (*JHa* 8.05Hz, J *Hb* 5.21Hz). $^{13}C$ n.m.r., Ca, Ca' , $\partial$ 161.67, 161.44ppm ( *JCF* 250.25, 249.95 Hz); Cb, Cb', $\partial$ 115.6 ppm (*JCCF* , 22.34Hz); Cc, Cc', $\partial$ 131.34, 131.09 ppm ( *JCCCF* , 8.30 Hz, 8.45 Hz); Cd, Cd', $\partial$, 133.66, 133.47 ppm (*JCCCCF* , 3.24, 2.94 Hz). Ratio of heights C/C' = 0.86. $^1H$ n.m.r., two complex quartets, $\partial$ 7.10, 7.07 ppm; two complex triplets, $\partial$ 6.86, 6.83 ppm.

Preparation of $Fe_2(SC_6H_5)_2(NO)_4$

The preparation of this cluster followed the method used for the p-fluorophenyl ester. Purified by column chromatography (silica, $CH_2Cl_2$). Yield 87% based on available sulphur. Melting point 150-152$^o$C. I.R., ($CH_2Cl_2$ solution) $\nu NO_{asym}$1787cm$^{-1}$, $\nu NO_{sym}$ 1762cm$^{-1}$. Mass-spec., $M^+$ 450, sequential loss of NO; 420, 390, 360, 330.

Preparation of $Fe_2(SC_6H_4Me)_2(NO)_4$

The preparation of this cluster followed the method used for the p-fluorophenyl ester. Mass spectrum, $M^+$ 478, sequential loss of NO; 448, 418, 388, 358. I.R., ($CCl_4$ solution) $\nu NO_{asym}$1783cm$^{-1}$, $\nu NO_{sym}$ 1757cm$^{-1}$. $^1H$ n.m.r., ($CS_2$, $C_6D_6$ solution, complex multiplet at $\partial$ 7.0 ppm, complex splitting at $\partial CH_3$ 2.25ppm, ratio of peaks 4:3.

Preparation of $Fe_2(SC_6H_4OMe)_2(NO)_4$

The preparation of this cluster followed the method used for the p-fluorophenyl ester. Mass spectrum, $M^+$ 510, sequential loss of NO; 480, 450, 420, 390. I.R.,( $CH_2Cl_2$ solution) $\nu NO_{asym}$1784cm$^{-1}$, $\nu NO_{sym}$ 1756cm$^{-1}$. $^1H$ n.m.r., quartet, $\partial$ 7.0 ppm; singlet, $\partial CH_3$ 3.6 ppm, ratio of peaks 4:3.

Preparation of $Fe_2(SC_6H_4COCH_3)_2(NO)_4$

The preparation of this cluster followed the method used for the p-fluorophenyl ester. Mass spectrum, $M^+$ 534, sequential loss of NO; 504, 474, 444, 414. I.R.,( $CH_2Cl_2$

solution) $\nu NO_{asym}$ 1792cm$^{-1}$, $\nu NO_{sym}$ 1765cm$^{-1}$, $\nu CO$ 1688cm$^{-1}$. $^{1}H$ n.m.r., singlet, $\partial C\underline{H}_3$ 2.59ppm; multiplets, ∂7.25, 7.38, 7.84 ppm. Ratio of peaks 2:2:3. $^{13}C$ n.m.r., $\underline{C}H_3$ 28.6ppm; $\underline{C}O$ 196.8ppm; $C_{a/b}$ 145.3,145.1 ppm; $C_{a/b}$ 136.7,136.5ppm; $C_{b/c}$ 130.8, 130.6 ppm; $C_{b/c}$ 128.7ppm.

Preparation of $Fe_2(SC_6H_4NO_2)_2(NO)_4$

The preparation of this cluster followed the method as used for the p-fluorophenyl ester. The material obtained was found to be very air sensitive and no $M^+$ peak was obtained from the mass-spectrum. The mass-spectrum, however gives fragments which are assignable to mercaptoaryl compounds. Microanalysis; calculated for $Fe_2S_2C_{12}H_8N_6O_8$; expected C 26.7, H 1.5, N 15.6%; obtained C 26.5, H 1.4, N 15.4%. I.R.,($CH_2Cl_2$ solution), $\nu$NOasym=1790, $\nu$NOsym=1760cm$^{-1}$. $^{1}H$ n.m.r., ∂H 7.4 (broad), 8.2ppm (broad), ratio of 1:1. $^{13}C$ n.m.r., no evidence of peak splitting, ∂Ca/d 148; ∂Ca/d 143; ∂Cb/c 132; ∂Cb/c 125ppm.

Preparation of $Fe_2(SC_6H_4Cl)_2(NO)_4$

The preparation of this cluster followed the method as used for the p-fluorophenyl ester. The material obtained was found to be very air sensitive and no $M^+$ peak was obtained from the mass-spectrum. I.R., ($CH_2Cl_2$ solution) $\nu NO_{asym}$1787cm$^{-1}$, $\nu NO_{sym}$ 1759cm$^{-1}$; $^{1}H$ n.m.r., ($CDCl_3$) ∂ 7.25 ppm (broad).$^{13}C$ n.m.r., poor spectrum but suggests evidence for the existance of cis/trans isomers; ∂C a/d 134.2,132.7ppm(cis/trans); ∂C a/d 133, 132.5; ∂Cb/c 131.4; ∂Cb/c three splittings 128.6 (principle peak)128.5, 128.4ppm (making the interpretation difficult).

Preparation of $Fe_2(SC_6H_4CN)_2(NO)_4$

The preparation of this cluster followed the method as used for the p-fluorophenyl ester. The material obtained was found to be very air sensitive and no $M^+$ peak was obtained from the mass-spectrum. I.R.,(THF solution) $\nu NO_{asym}$1791cm$^{-1}$, $\nu NO_{sym}$ 1763cm$^{-1}$, $\nu CN$ 2229cm$^{-1}$; $^{1}H$ n.m.r., ($CDCl_3$) ∂ 7.95 ppm (broad).

Reaction of $Fe_4S_4(NO)_4$ with p-$FC_6H_4N_2BF_4$

$Fe_4S_4(NO)_4$ (0.15g, 0.3mmol) in $CH_2Cl_2$ (30ml) was added to p-$FC_6H_4N_2BF_4$ (1.4g, 6.7mmol) in $CH_3CN$ (20ml). The mixture was stirred for eight hours, a steady evolution of gas occurred for the first twenty minutes. The solution was added to water (200ml) and the $CH_2Cl_2$ layer separated, washed with water (3x40ml), and dried over $CaCl_2$. The solution was reduced to dryness. The yield of $Fe_2(SC_6H_4F)_2(NO)_4$ was low <5% based on iron. I.R., ($CH_2Cl_2$ solution) $\nu NO_{asym}$ 1791$cm^{-1}$, $\nu NO_{sym}$ 1764$cm^{-1}$.

Reaction of $Na[Fe_4S_3(NO)_7]$ with $Me_3SI$

To a deoxygenated solution of $Na[Fe_4S_3(NO)_7]$ (0.5g, 0.9mmol) in water (50ml) was added $Me_3SI$ (1g, 4.9mmol) in water (50ml). A precipitate formed. The solution was filtered and washed with water (2x100ml). The solid obtained was dissolved in acetone (100ml) and petrol (B.Pt. 60-80$^oC$, 30ml) added to the solution. The solution was reduced in volume to produce lustrous black crystals. These were filtered off, washed with petrol (B.Pt. 40-60$^oC$, 2x50ml) and pumped dry for ten hours. Yield of $Me_3S[Fe_4S_3(NO)_7]$, 0.35g, 64%.

Microanalysis; calculated for $Fe_4S_4C_3H_9N_7O_7$; expected C 5.9, H 1.5, N 16.1%, obtained C 6.0, H 1.3, N 16.1%.

I.R., ($CH_3CN$ solution) $\nu NO$, 1800$cm^{-1}$, 1747$cm^{-1}$ and 1712$cm^{-1}$.

Refluxing the solid in $CH_3CN$ with or without added base caused no change in the I.R. spectrum nor was any change observed by T.L.C. (Silica gel, acetone or ethanol). The solid was recovered unchanged at 98% yield.

Reaction of $Na[Fe_4S_3(NO)_7]$ with $Me_3SOI$

$Na[Fe_4S_3(NO)_7]$ (1g, 1.8mm) in Methanol (20ml) had $Me_3SOI$ (0.4g,1.8mm) in methanol/water (20ml, 1:1) added to it under nitrogen. A precipitate formed which was obtained by filtration, washed with water (4x50ml) and dried over $P_2O_5$ under vacuum. Yield of $Me_3SO[Fe_4S_3(NO)_7]$ 0.79g, 70%.

Microanalysis; calculated for $Fe_4S_4C_3H_9N_7O_8$; expected C 5.8, H 1.5, N 15.7%; obtained C 6.2, H 1.3, N 15.4%. I.R., ($CH_3CN$ solution) $\nu$NO 1800cm$^{-1}$; 1747cm$^{-1}$ and 1710cm$^{-1}$.

Reflux of the solid in MeOH/water for six hours under nitrogen caused no change in the I.R. spectrum and the material was recovered unchanged.

Reaction of $Na[Fe_4S_3(NO)_7]$ with $Me_3OBF_4$

$Na[Fe_4S_3(NO)_7]$ (0.5g, 0.9mmol) and $Me_3OBF_4$ (3g,20mmol) are stirred together in water (20ml). A precipitate formed which was redissolved by the addition of methanol (10ml). $CH_2Cl_2$ (100ml) was added and the solution stirred for ten minutes. The organic layer was separated off and reduced to dryness, to obtain a red/black solid. The solid was purified by column chromatography (silica 10x10, $CH_2Cl_2$), the brown/orange band moving with the solvent front was collected. Removal of the solvent revealed a red/black crystalline material.

I.R.,($CH_2Cl_2$ solution) $\nu NO_{asym}$ 1779cm$^{-1}$, $\nu NO_{sym}$ 1752cm$^{-1}$. Mass spec., $M^+$ 326, sequential loss of NO; 296,266,236,206. $^1$H n.m.r., was consistent with $Fe_2(SMe)_2(NO)_4$.

Reaction of $Na[Fe_4S_3(NO)_7]$ with $Et_3OBF_4$

$Na[Fe_4S_3(NO)_7]$ (0.5g,0.9mmol) was added to a solution of $Et_3OBF_4$ (20ml, 1.0M in $CH_2Cl_2$). The solution was stirred overnight under nitrogen,(after 15 minutes the solution appeared reddish and some insolubles were present). Water (100ml) was added and the organic layer separated and dried over $MgSO_4$. The solvent was reduced in volume and the material purified by column chromatography (silica 10x5cm, $CH_2Cl_2$). Removal of the solvent revealed 0.12g of a red/black solid. Yield 28% of $Fe_2(SEt)_2(NO)_4$.

I.R., $\nu NO_{asym}$ 1776cm$^{-1}$, $\nu NO_{sym}$ 1750cm$^{-1}$. Mass spec., $M^+$ 354, sequential loss of NO; 324, 294, 264, 234.

Reaction of $Na[Fe_4S_3(NO)_7]$ with $Me_3OSbCl_6$

$Na[Fe_4S_3(NO)_7]$ (1.0g, 1.8mmol) dissolved in $CH_3CN$ had $Me_3OSbCl_6$ (3g,7,6mmol) added to it. On addition the extreme smell of thiol was evident. After ten minutes the I.R. spectrum showed the presence of both Roussin's Black Salt and a dinitrosyl species. After 2 hours of stirring complete decomposition had occurred. On repeating in $H_2O/CH_2Cl_2$, following the procedure for the reaction of the Black Salt with $Me_3OBF_4$, a red colour developed in the organic layer. This was identified by I.R. as being $Fe_2(SMe)_2(NO)_4$, assignment confirmed by mass-spec.

Reaction of $Na[Fe_4S_3(NO)_7]$ with 2-methyl,2-iodo propane

$Na[Fe_4S_3(NO)_7]$ (0.5g, 0.9mmol) was dissolved in methanol (30ml). A large excess of 2-methyl,2-iodo propane was added and the solution refluxed under nitrogen for 5 hours. During this period the solution turns from black to bright red. The solvent was removed under vacuum and oil pumped dry for 24 hours. A red solid identified as $Fe_2I_2(NO)_4$ was obtained, yield= 0.17g, 38%. I.R.,($CH_2Cl_2$ solution) $\nu NO_{asym}$= 1810 $cm^{-1}$, $\nu NO_{sym}$=1767 $cm^{-1}$. Mass spec., $M^+$ 486, sequential loss of NO; 456,426,396,366; other peaks correspond to iron and iodo fragments.

Reaction of $Me_3S$ $[Fe_4S_3(NO)_7]$ with sodium benzophenone

Benzophenone (0.3g, 1.6mmol) was stirred with an excess of sodium wire in ether(20ml). The solution was filtered under nitrogen into a flask containing $Me_3S$ $[Fe_4S_3(NO)_7]$ (1g, 1.65mmol). The solution was stirred for 8 hours. The solvent was removed. The solid obtained was dissolved in $CH_2Cl_2$ and purified by column chromatography (silica 10x5cm, $CH_2Cl_2$). An orange/brown band was collected. The solvent removed to obtain 0.08g of a red/black solid. Yield 23% of $Fe_2(SMe)_2(NO)_4$. Characterised by I.R. and mass-spec.

EHMO Calculations

Extended Hückel Molecular Orbital Calculations[24,25] were based on experimental geometries, and used atomic parameters available from the literature[26,27,28]. The

calculations were performed on a VAX 11/785 computer.

Molecular Graphics were obtained using the Chem-X graphics package (Oxford).

Crystal Structure Determination of $[N(PPh_3)_2][Fe_2(S_2O_3)_2(NO)_4]$

Crystals of $[N(PPh_3)_2][Fe_2(S_2O_3)_2(NO)_4]$ suitable for X-ray examination were grown from 1,2-dichloroethane.

Crystal Data; $C_{72}H_{60}Fe_2N_6O_{10}P_4S_4$, M=1533.13, triclinic, $\alpha$=10.999(5), b=12.748(4), c=14.020(7) Å, $\alpha$ =67.13(4), $\beta$ =83.31(4), $\gamma$ = 93.87(3)°, U=1785.2Å$^3$, space group $P\bar{1}$ (no.2), Z=1, $D_c$ =1.43gcm$^{-3}$, $\mu$(Mo-$K_\alpha$)= 6.17 cm$^{-1}$, $\lambda$=0.71069Å, F(000) = 790.

Data Collection [49]; CAD4 diffractometer using graphite monochromated Mo-$K_\alpha$ radiation $\omega$-2$\theta$ scan mode, $1.5 \leq \theta \leq 25^o$. 6152 Reflections measured, of which 5954 unique and 5183 with $F_o \geq 4\sigma(F_o)$.

Structure solution and refinement; Patterson method, followed by SFLS and Fourier-difference cycles. The asymmetric unit comprises one $[N(PPh_3)_2]^+$ cation and half of the anion. All non-hydrogen atoms were refined anisotropically, and all hydrogen atoms were refined with individual isotopic thermal parameters. The weighting scheme $w=1/[\sigma^2(F_o) + 0.00054F_o^2]$ gave final R and R' values of 0.034 and 0.056, with 563 refined parameters. programs and computers used, and sources of scattering factor data, were as given in reference [49].

Final refined co-ordinates for the non-hydrogen atoms are given in table 3-1. Bond lengths and angles for the anion are given in table 3-2. A perspective view of the unit cell, showing the trans conformation of the anion is given in figure 3-2, a perspective view of the anion, showing the atom-numbering scheme, is given in figure 3-3.

Crystal Structure Determination of $[Me_3S][Fe_4S_3(NO)_7]$

Crystals of $[Me_3S][Fe_4S_3(NO)_7]$ suitable for X-ray examination were grown from acetone.

Crystal Data; $C_3H_9Fe_4N_7O_7S_4$, M=606.812, triclinic, a=9.655(2), b=11.707(3), c=8.968(1) Å, $\alpha$ =106.11(2), $\beta$ =91.78(3), $\gamma$ = 84.92(2)°, U=970.04Å$^3$, space group $P\bar{1}$ , Z=2, $D_c$ =2.08gcm$^{-3}$, $\mu$(Mo-$K_\alpha$)= 6.17 cm$^{-1}$, $\lambda$=0.71069Å, F(000) = 600.

Data Collection [49]; CAD4 diffractometer using graphite monochromated Mo-$K_\alpha$ radiation $\omega$-2$\theta$ scan mode, $1.5 \leq \theta \leq 25°$. 3666 Reflections measured, of which 3406 unique and 2553 with $F_o \geq 3\sigma(F_o)$.

Structure solution and refinement; Patterson method, followed by SFLS and Fourier-difference cycles. The unit comprises of one $[Me_3S]^+$ cation and the anion. All non-hydrogen atoms were refined anisotropically, and all hydrogen atoms were refined with individual isotopic thermal parameters. The weighting scheme $w=1/[\sigma^2(F_o) + 0.00002F_o^2]$ gave final R and R' values of 0.041 and 0.042, with 244 refined parameters. programs and computers used, and sources of scattering factor data, were as given in reference [49].

Final refined co-ordinates for the non-hydrogen atoms are given in table 3-5. Bond lengths and angles for the anion are given in table 3-6. A perspective view of the unit cell, showing the atom-numbering scheme, is given in figure 3-20. A perspective view of the cation, showing its observed disorder, is given in figure 3-21.

The two crystal structure determinations were carried out by the S.E.R.C. crystal service at Queen Mary College, London.

## Results and Discussion

Part One

### 3-1 Thiosulphato Complexes

A salt described as potassium dinitrosylthiosulphatoferrate, $2K[(NO)_2FeS_2O_3].H_2O$ was first produced in 1895 by Hofmann and Weide. Unlike the Roussin esters which have been extensively studied and are known to exist as dimers both in solution and in the solid state, the thiosulphato complex was less well known. On the basis of its diamagnetism and its infra-red spectrum [31] it was assumed to have a dimeric structure similar to that of the alkyl esters of Roussin's Red Salt.

The thiosulphate ion, $S_2O_3^{2-}$ (1), closely resembles the $SO_4^{2-}$ ion in structure and can act as a monodentate (2), a bidentate bridging ligand (3), both coordinating through sulphur or as a dihapto chelating ligand (4) [30].

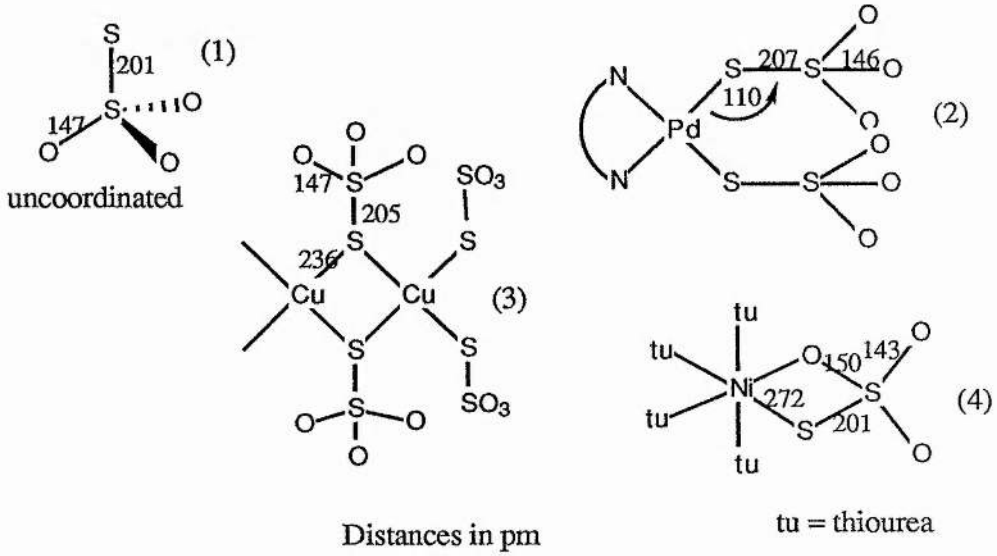


Hence it is possible that the complex could have some structure other than the dimeric one proposed. This possibility is particularly justified considering the uncertainty over the charge associated with the complex. Based on a limiting stoichiometry of $[Fe(NO)_2S_2O_3]_n^m$, values of m/n of 3 [31] and 1 [14] have been cited.

In this chapter we report the crystal structure of the thiosulphato complex, improved methods of synthesis and also some of its properties and reactions.

## 3-2 Preparation of $Na[Fe(NO)_2S_2O_3]$ from Nitric Oxide, NO

The early preparative methods used for the thiosulphato complex involved the use of $Fe_2I_2(NO)_4$. This route was found to be rather inconvenient and the resulting complex difficult to purify. $Fe_2I_2(NO)_4$ itself is difficult to prepare and purify and since its preparation involves the use of NO(g) [29], it is also an expensive route and unsuitable for $^{15}N$ labelling. The original method used by Hofmann and Weide [3] involved bubbling NO(g) through aqueous solutions of ferrous ion and thiosulphate ion. Using this method with ferrous sulphate and sodium thiosulphate, yields of around 90% were obtained of the thiosulphato complex, along with a small amount of ferric oxide. By metathesis the bis(triphenyl phosphoranylidene) salt (PNP) and the $Et_4N$ salts were produced for analytical purposes. The microanalysis of the PNP salt was consistent with a stoichiometry of $(PNP)[Fe(NO)_2S_2O_3]$ and confirmed the ratio of m/n as 1. The $Et_4N$ salt was examined for iron by atomic absorption (calculated for an aqueous solution containing a theoretical12.4ppm of Fe; obtained 9.6ppm) the result also helped to set m/n as 1. The I.R. spectrum of the PNP salt in dichloromethane solutions confirms the existence of the dinitrosyl iron fragment $Fe(NO)_2$; two absorptions can be assigned to the symmetric and asymmetric $\nu$NO stretching modes. This method of preparation is completely analogous to a method used for the preparation of the alkyl esters of Roussin's Red Salt [5,6].

## 3-3 Preparation of $Na[Fe(NO)_2S_2O_3]$ from Nitrite Ion.

Since we were interested in obtaining the structural characterisation of this material in solution as well as in the solid state, we required a method of labelling the nitrogen atoms with $^{15}N$. A method using nitrite ion which was based on the preparation from NO(g) was developed;

$$FeSO_4 + 4NaNO_2 + 4Na_2S_2O_3 \longrightarrow Na[Fe(NO)_2S_2O_3] + \text{Green Material} + \text{iron oxide}$$

Compared to the method using NO(g), this procedure gives a more modest yield (40%) and more rust was produced as a by-product suggesting that the nitrite was oxidising ferrous to ferric ion. At first this preparation was carried out in the presence of NaOH (used to stabilise the thiosulphate ion), however Fe(II) and thiosulphate in the presence of NaOH

produced black insoluble material and the yield of the thiosulphato complex was low (5-10%). Changing the reaction stoichiometry to 2:2:4 ($Fe^{2+}$: $S_2O_3^{2-}$: $NO_2^-$) with no added hydroxide, gave the salt in approximately half the normal yield although there was less green material produced, whereas a reaction stoichiometry of 4:8:4 gave an increased yield of the salt (60% based on available $NO_2^-$).

Addition of nitrite to a solution of a ferrous salt produces a brown solution which on standing will release $NO_2(g)$ with the production of ferric hydroxide. In the presence of thiosulphate ion the liberation of $NO_2$ was not observed although the production of ferric hydroxide still occurs. It is noteworthy that in the formation of Roussin's Black Salt copious quantities of $NO_2(g)$ are liberated. The reaction of ferrous sulphate and sodium nitrite with sodium thiocyanate in a similar manner to that used for the thiosulphato complex anion does not produce the expected $Fe_2(SCN)_2(NO)_4$, but on standing the solution turns blood red and a vigorous liberation of $NO_2(g)$ occurs. These observations suggest that the nitrite oxidises ferrous to ferric iron. The addition of thiocyanate to solutions of Fe(III) to produce blood-red solutions is a normal test for the presence of ferric ion. The nitrite is reduced to NO(g) which in the presence of oxygen produces $NO_2(g)$. In the presence of thiosulphate the solutions are stabilised against the release of NO(g) and suggests that the complexation of thiosulphate to the iron produces a species which is stable towards oxidation by nitrite; this does not occur with thiocyanate ion.

The preparation of the thiosulphato complex involves an extraction with acetone. It was observed that after a few extractions no further colour developed immediately in the solvent. On stirring for a few minutes the solution darkened considerably. If the acetone was decanted off and the procedure repeated a few times the ultimate yield of the salt increased to a maximum of about 40%. If however, after a few extractions with acetone, the solid remaining was dissolved in water and $Bu_4NBr$ was added to this green solution followed by extraction into $CH_2Cl_2$ , the complete decolouration of the aqueous layer and the formation of a brown solution in the organic layer occurred. The I.R. spectrum of the material obtained from the organic layer was identical to that of $Bu_4N[Fe(NO)_2S_2O_3]$. The identity of the green material is discussed in section 3-7-3.

The result of this work was to show that the material obtained through the action of nitrite ion on solutions of ferrous and thiosulphate ion was the same material obtained through the action of NO(g) on similar solutions.

## 3-4 The Crystal Structure of $(Ph_3PNPPh_3)_2[Fe_2(S_2O_3)_2(NO)_4]$

Crystals of $(Ph_3PNPPh_3)_2[Fe_2(S_2O_3)_2(NO)_4]$ suitable for X-Ray examination were grown from 1,2-dichloroethane. The structure consists of isolated ions. The thiosulphato complex was found to be dimeric and so was renamed the Thiosulphate Analogue Ester of Roussin's Red Salt. The anion lies across a centre of inversion, the $Fe_2S_2$ ring is strictly planar and the pendant $SO_3$ groups are on opposite sides of the ring, giving rise to the trans or $C_{2h}$ structure (figure 3-2). This structure is observed for the neutral Roussin Esters $Fe_2(SR)_2(NO)_4$ ($R=CH_3$[32], $C_2H_5$[33], $n\text{-}C_5H_{11}$[32] and $C_6H_4F$[18]). The dimensions obtained (table 3-2) are very similar to those observed for the neutral species; in particular the Fe-N-O angles are all found to be approximately 170°, and the Fe-Fe distances lie in the range 2.686-2.713Å. The two Fe-N-O fragments of each $Fe(NO)_2$ group are bent towards each other, (see chapt 2 ). The dimensions of the $S\text{-}SO_3$ fragment are similar to those found in the $[S(S_2O_3)_2]^{2-}$ and $[S_2(S_2O_3)_2]^{2-}$ ions[34,35],(c.f., section 3-1). The S-S-O angles found in $(Ph_3PNPPh_3)_2[Fe_2(S_2O_3)_2(NO)_4]$ are significantly less than tetrahedral, while the O-S-O angles are greater. The two independent P-N distances in the cation are 1.584(4)Å and 1.587(4)Å, and the P-N-P angle is 134.5(1)°.

The crystal structure determination clearly shows the dinuclear character of the ion, figures 3-2 and 3-3 show a perspective view of the unit cell and a view of the dianion respectively. This structural determination and the elemental analysis of the PNP salt shows that the charge associated with the ion is 2-. The near linearity of the Fe-N-O fragments indicates that the nitrosyl ligands are bound formally as $NO^+$ which in turn indicates that the irons are formally Fe(-1). As explained in chapter two these ideas of formal charge are only used as electronic book-keeping and should not be taken too literally.

| | x | y | z |
|---|---|---|---|
| Fe(1) | 4469.7(3) | 4128.6(2) | 4802.3(2) |
| S(1) | 4391.8(5) | 4246.9(4) | 6363.1(4) |
| S(2) | 4347.8(6) | 6846.9(5) | 2756.4(4) |
| N(1) | 3045(2) | 4156(2) | 4509(2) |
| N(2) | 5219(2) | 3028(2) | 4816(2) |
| O(1) | 2087(2) | 4051(2) | 4272(3) |
| O(2) | 5576(2) | 2198(2) | 4800(2) |
| O(3) | 6054(2) | 3756(2) | 7842(2) |
| O(4) | 6608(2) | 3065(2) | 6517(2) |
| O(5) | 4820(2) | 2136(2) | 7850(2) |
| P(1) | 1438.8(5) | 2786.7(4) | 10163.1(4) |
| P(2) | 188.4(5) | 1917.4(4) | 12330.7(4) |
| N(3) | 444(2) | 2701(2) | 11112(1) |
| C(1) | 2565(2) | 4026(2) | 9792(2) |
| C(2) | 2470(2) | 4739(2) | 10333(2) |
| C(3) | 3281(3) | 5740(2) | 9986(2) |
| C(4) | 4165(3) | 6028(2) | 9127(2) |
| C(5) | 4278(3) | 5313(2) | 8600(2) |
| C(6) | 3487(2) | 4311(2) | 8940(2) |
| C(7) | 2187(2) | 1519(2) | 10397(2) |
| C(8) | 3405(3) | 1467(3) | 10525(2) |
| C(9) | 3867(4) | 403(4) | 10785(3) |
| C(10) | 3129(4) | -553(3) | 10896(3) |
| C(11) | 1923(4) | -504(2) | 10771(2) |
| C(12) | 1449(3) | 534(2) | 10517(2) |
| C(13) | 690(2) | 2995(2) | 9041(2) |
| C(14) | 1219(3) | 2719(2) | 8229(2) |
| C(15) | 648(3) | 2939(3) | 7360(2) |
| C(16) | -455(3) | 3417(3) | 7295(2) |
| C(17) | -974(3) | 3683(2) | 8092(2) |
| C(18) | -411(2) | 3475(2) | 8972(2) |
| C(19) | 1532(2) | 1332(2) | 12857(2) |
| C(20) | 1683(3) | 177(2) | 13132(2) |
| C(21) | 2779(3) | -201(3) | 13447(3) |
| C(22) | 3711(3) | 541(3) | 13481(3) |
| C(23) | 3570(3) | 1688(3) | 13218(2) |
| C(24) | 2480(3) | 2082(3) | 12900(2) |
| C(25) | -1027(2) | 763(2) | 12634(2) |
| C(26) | -1619(2) | 663(2) | 11857(2) |
| C(27) | -2600(3) | -192(3) | 12099(3) |
| C(28) | -2990(3) | -927(3) | 13128(3) |
| C(29) | -2403(3) | -839(3) | 13895(3) |
| C(30) | -1428(3) | -1(2) | 13668(2) |
| C(31) | -397(2) | 2730(2) | 13037(2) |
| C(32) | -1145(3) | 3568(2) | 12578(2) |
| C(33) | -1728(3) | 4101(3) | 13167(3) |
| C(34) | -1575(3) | 3809(3) | 14185(2) |
| C(35) | -841(3) | 2985(3) | 14637(2) |
| C(36) | -246(3) | 2448(3) | 14068(2) |

**Table 3-1**

Fractional Atomic Coordinates ($x10^4$)
for $\{N(PPh_3)\}_2[Fe_2(S_2O_3)_2(NO)_4]$

## Table 3-2

Bond Lengths and Angles for the Dianion $[Fe_2(S_2O_3)_2(NO)_4]^{2-}$

(a) Bond lengths/Å

| | | | |
|---|---|---|---|
| Fe(1)-Fe(1)[a] | 2.713(4) | N(1)-O(1) | 1.156(5) |
| Fe(1)-S(1) | 2.244(3) | N(2)-O(2) | 1.161(4) |
| Fe(1)-S(1)[a] | 2.252(3) | S(1)-S(2) | 2.171(3) |
| Fe(1)-N(1) | 1.665(4) | S(2)-O(3) | 1.425(4) |
| Fe(1)-N(2) | 1.669(4) | S(2)-O(4) | 1.418(4) |
| | | S(2)-O(5) | 1.430(4) |

(b) Bond angles /°

| | | | |
|---|---|---|---|
| S(1)-Fe(1)-S(1)[a] | 105.7(2) | Fe(1)-S(1)-Fe(1)[a] | 74.3(2) |
| S(1)-Fe(1)-N(1) | 107.6(2) | Fe(1)-S(1)-S(2) | 107.5(2) |
| S(1)-Fe(1)-N(2) | 109.3(2) | Fe(1)[a]-S(1)-S(2) | 108.6(2) |
| S(1)[a]-Fe(1)-N(1) | 107.3(2) | S(1)-S(2)-O(3) | 102.3(2) |
| S(1)[a]-Fe(1)-N(2) | 107.8(2) | S(1)-S(2)-O(4) | 108.0(2) |
| N(1)-Fe(1)-N(2) | 118.3(2) | S(1)-S(2)-O(S) | 100.1(2) |
| Fe(1)-N(1)-O(1) | 170.7(3) | O(3)-S(2)-O(4) | 113.8(2) |
| Fe(1)-N(2)-O(2) | 169.9(2) | O(4)-S(2)-O(5) | 116.6(2) |
| | | O(5)-S(2)-O(3) | 113.6(2) |

Key to symmetry operation relating designated atom to reference atom at x, y, z:

[a]: 1.0-x, 1.0-y, 1.0-z.

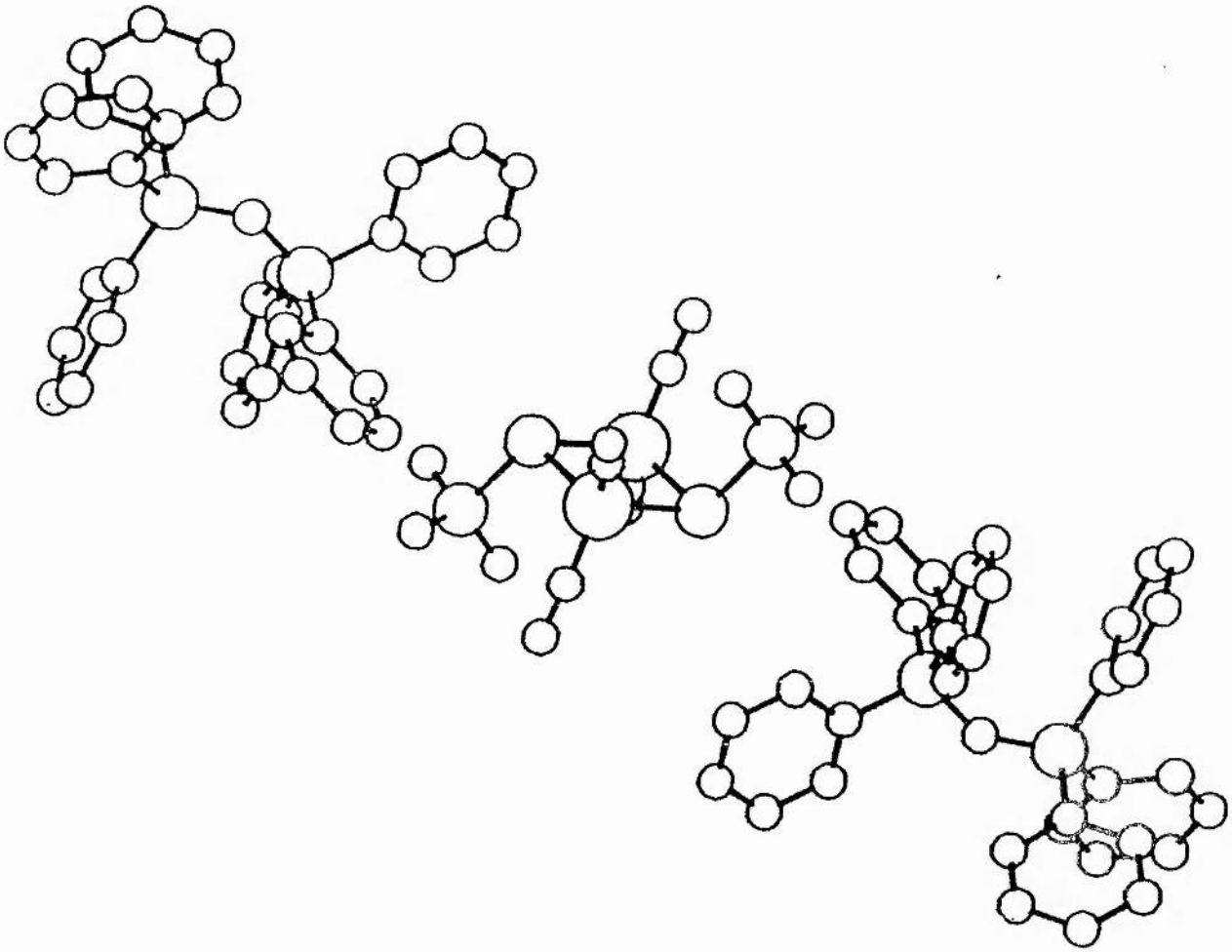

**Figure 3-2**
Perspective View of the Unit Cell of $\{N(PPh_3)\}_2[Fe_2(S_2O_3)_2(NO)_4]$

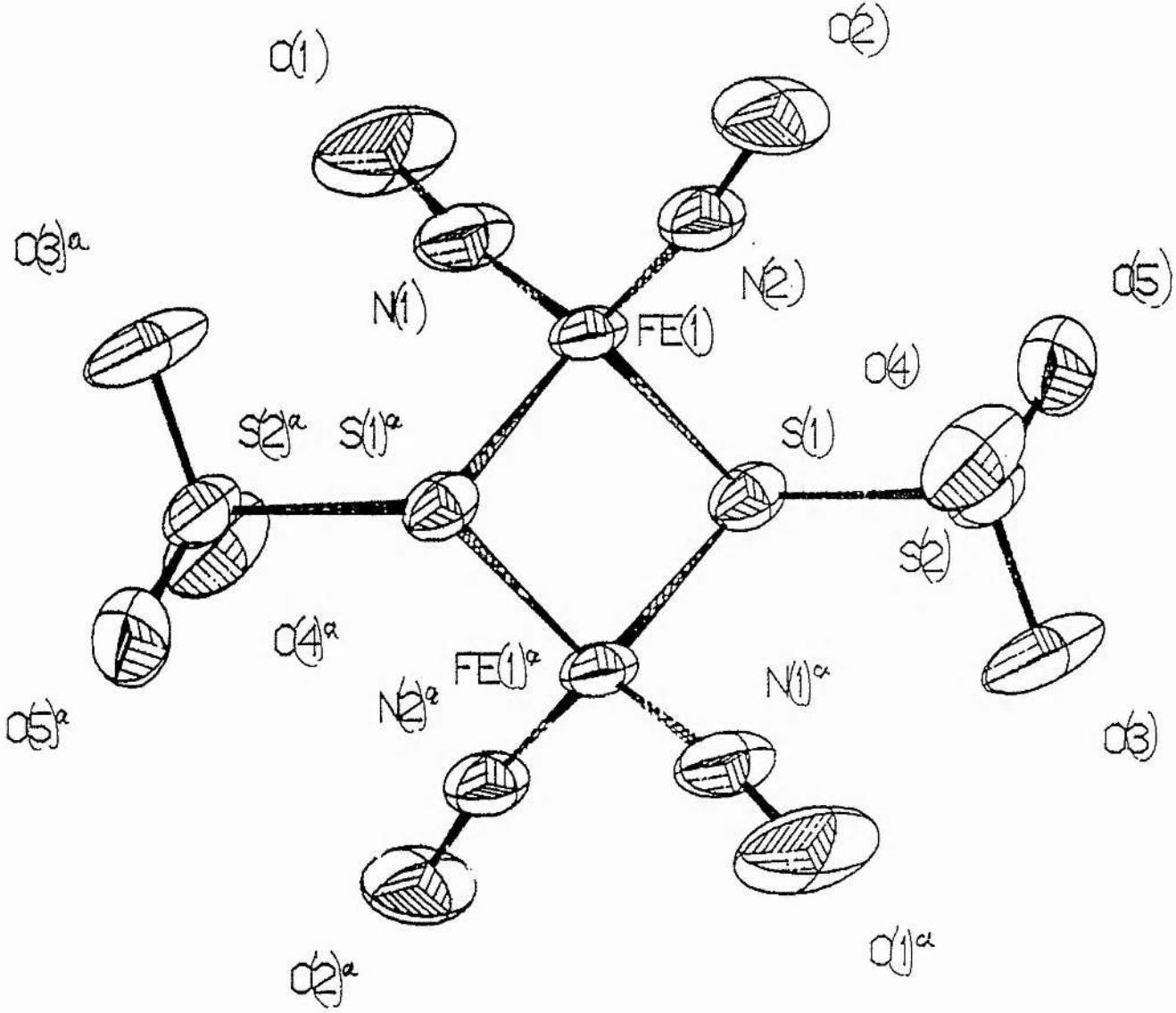


**Figure 3-3**
Perspective View of the dianion $[Fe_2(S_2O_3)_2(NO)_4]^{2-}$

3-5 The $^{15}N$ n.m.r. spectrum of $(Ph_3PNPPh_3)_2[Fe_2(S_2O_3)_2(^{15}NO)_4]$

The PNP salt of the thiosulphate analogue ester of Roussin's Red Salt was produced with all the nitrogen atoms of the nitrosyl groups labelled with $^{15}N$ at 99% enrichment. The $^{15}N$ n.m.r (figure 3-4) consists of a sharp singlet both in $CDCl_3$ and $CD_2Cl_2$. The spectrum was found to be unchanged between $+30^oC$ and $-60^oC$. This spectrum is unlike the $^{15}N$ spectra of $Fe_2(SR)_2(NO)_4$ which consist of a singlet assigned to the trans $C_{2h}$ conformer, and a pair of doublets forming an AX system, assigned to the cis $C_{2v}$ conformer [36,37], (figure 3-5). The spectrum of the $[Fe_2(S_2O_3)_2(NO)_4]^{2-}$ ion indicates therefore, that only the trans isomer is present in solution. From $^1H$ n.m.r coalescence data the barrier to inversion of the trans <==> cis interconversion for $Fe_2(SR)_2(NO)_4$ was found to be of the order of 60-80 KJ $mol^{-1}$ for R=alkyl [5]. Since on cooling the solution in $CDCl_3$ to $-60^oC$ no evidence for the existence of the cis isomer was obtained it is unlikely that the barrier in $[Fe_2(S_2O_3)_2(NO)_4]^{2-}$ is so low that the interconversion is fast on the n.m.r. timescale at this temperature.

The $^{15}N$ chemical shift obtained shows, on the basis of the criterion of a linear M-NO moiety [38,39,40], that the approximately linear Fe-N-O fragments found in the solid state are also preserved in solution, and so the formal oxidation state of the iron is also Fe(-1).

Solutions containing the $[Fe_2(S_2O_3)_2(NO)_4]^{2-}$ ion are stable for long periods of time in the absence of oxygen. Upon exposure to air the $^{15}N$ n.m.r spectrum shows the presence of $[Fe_4S_3(^{15}NO)_7]^-$ along with $[^{15}NO_3^-]$ and $[^{15}NO_2^-]$,(figure 3-6). The production of Roussin's Black Salt was found with acetone solutions of the thiosulphate ester which had been left open to the atmosphere for a period of time so this result is not too surprising. The interesting point about this observation is that the conversion requires the breakage of the $S\text{-}SO_3$ linkage, and the complete reorganisation of the core. From e.p.r. work done by myself and Johnson [41a] on an oxidised sample of $Na_2[Fe_2(S_2O_3)_2(NO)_4]$ we were able to show the existence of $[Fe(NO)_2(NO_2)_2]^-$. This species, so far observed only by e.p.r. spectroscopy, has labile $NO_2$ groups and is fluxional at room temperature [41]. Results obtained by Hyde have shown that reactions of Roussins Black Salt and of $Fe_2(SR)_2(NO)_4$

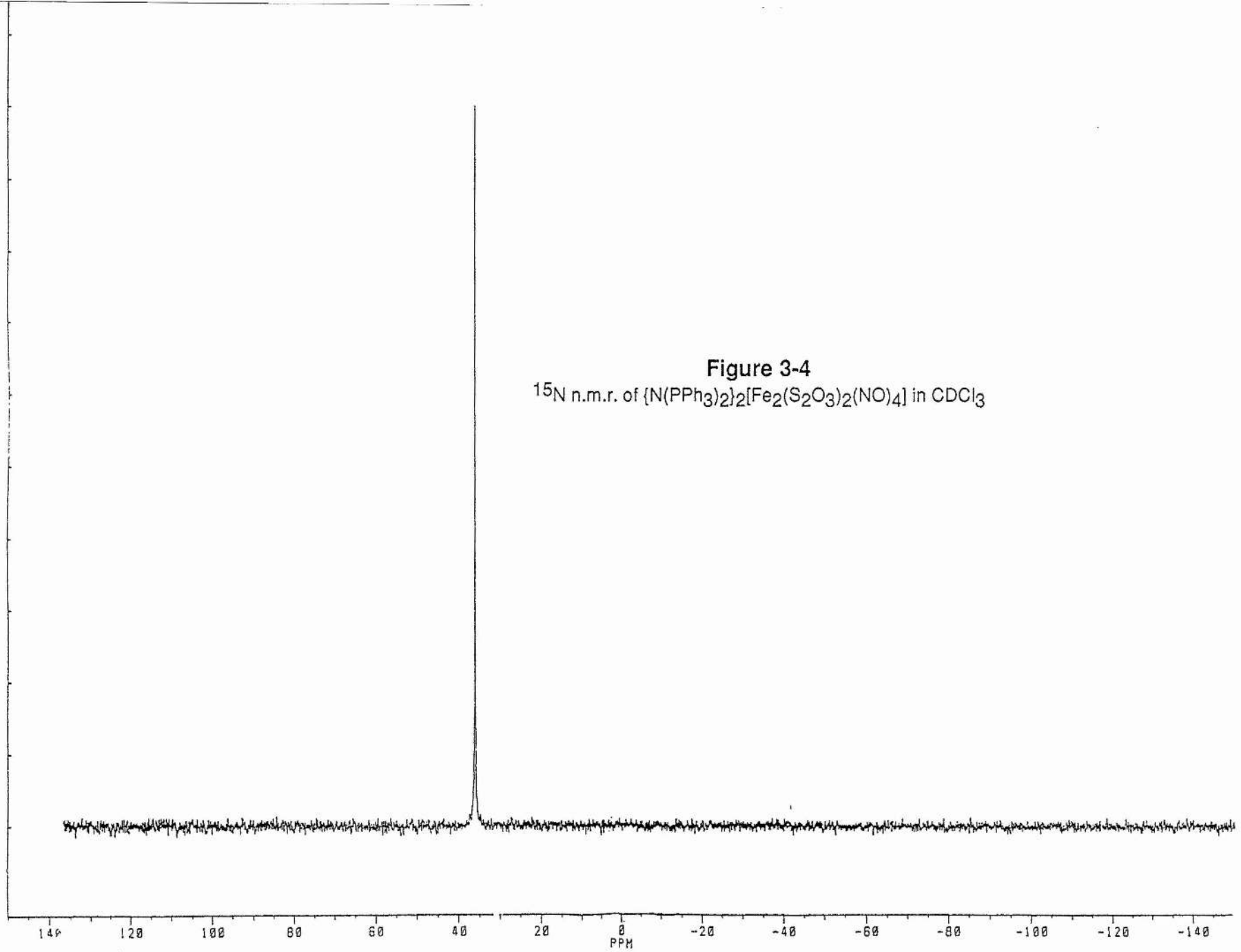


**Figure 3-4**

$^{15}N$ n.m.r. of $\{N(PPh_3)_2\}_2[Fe_2(S_2O_3)_2(NO)_4]$ in $CDCl_3$

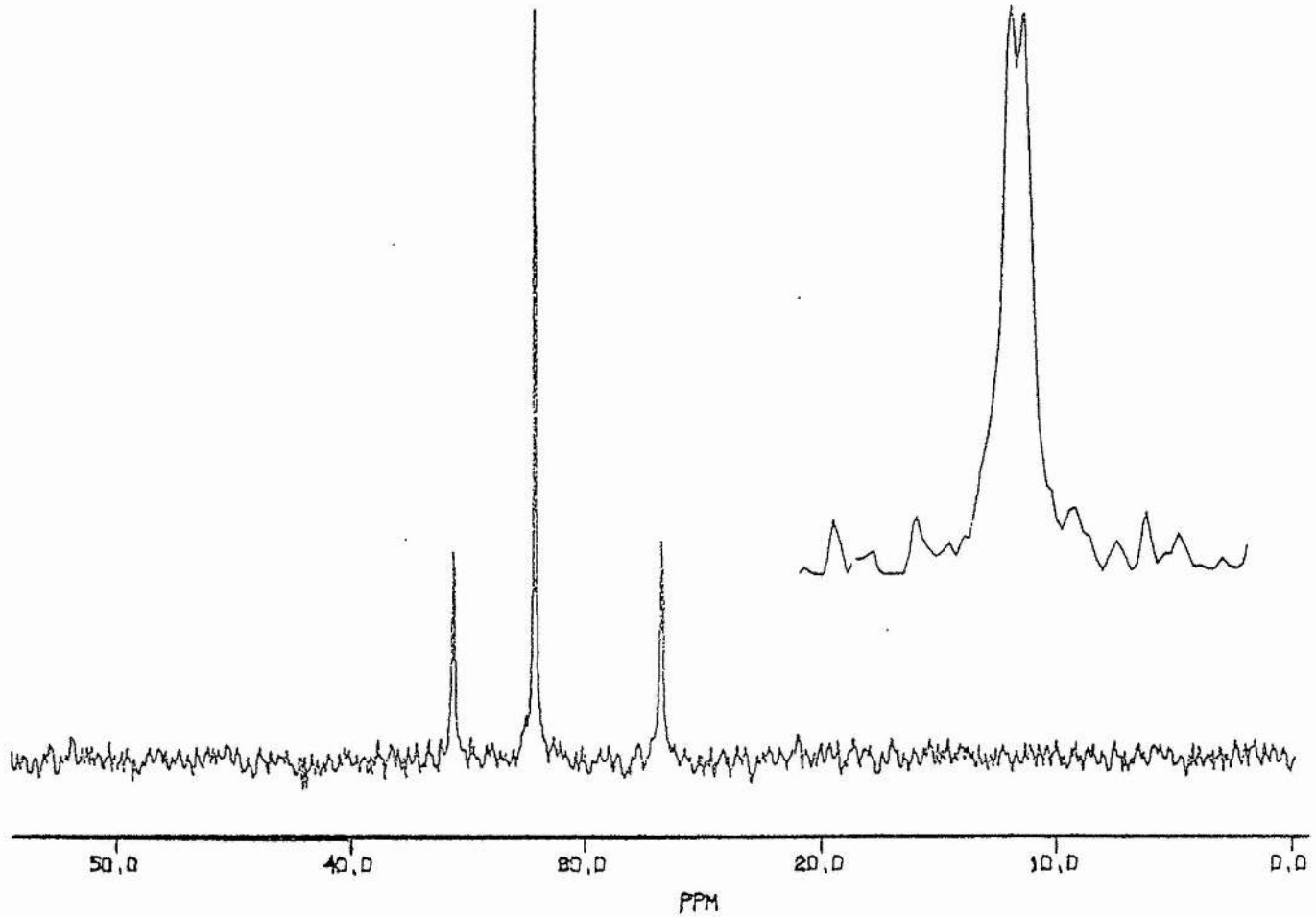


**Figure 3-5**

$^{15}N$ n.m.r. spectrum of $Fe_2(SR)_2(NO)_4$, R=alkyl, in $CDCl_3$

often proceed through the total breakup of the cluster to produce mononuclear fragments followed by reassembly at a later stage. In this case we have apparently observed the complete breakup of the dimer followed by the assembly of a larger cluster from the fragments available. From a thermodynamic point of view it suggests that the black anion sits in a deep well on the potential energy surface of these clusters.

Stirring a solution of $Na_2[Fe_2(S_2O_3)_2(NO)_4]$ in MeOH exposed to the air with added MeI resulted in the formation of a small amount of Roussins Black salt as identified by I.R. and U.V., and an amount of rust and the recovery of some of the original salt; no $Fe_2(SMe)_2(NO)_4$ was obtained. In a similar experiment replacing the MeI with pyridine a similar result was observed. Refluxing either of these two solutions resulted in complete decomposition. Refluxing under nitrogen resulted in almost complete recovery of the starting materials. If, on decomposition the thiosulphate cluster firstly lost the pendant $SO_3^-$ groups then Roussin's Red salt would result which, in the presence of MeI, would give rise to the methyl ester of Roussin's Red salt. Since the methyl ester was not observed it suggests that the loss of the $SO_3^-$ groups is not the first step in the decomposition of the cluster.

Dichloromethane solutions of $(PNP)_2[Fe_2(S_2O_3)_2(NO)_4]$ exhibit the expected two NO stretching absorptions (of $B_u$ and $A_u$ symmetry in $C_{2h}$) at 1787 and 1757$cm^{-1}$ for the unlabelled ion and at 1748 and 1718$cm^{-1}$ for the labelled $^{15}N$ ion. In THF, $Na_2[Fe_2(S_2O_3)_2(NO)_4]$ gives the absorptions at 1788 and 1750$cm^{-1}$ for the unlabelled ion. These frequencies differ somewhat from the values of 1801 and 1734$cm^{-1}$ recorded in a Nujol mull for the potassium salt described as $K_3[Fe(S_2O_3)(NO)_2].H_2O$ [31]. The infra red spectra give no evidence for the existence in solution of more than one conformer; this is also found with the alkyl esters of Roussin's Red salt which we know exist as two conformers in solution [36,37].

**Figure 3-6**

$^{15}N$ n.m.r. spectrum of the oxidised products of $\{N(PPh_3)_2\}_2[Fe_2(S_2O_3)_2(NO)_4]$

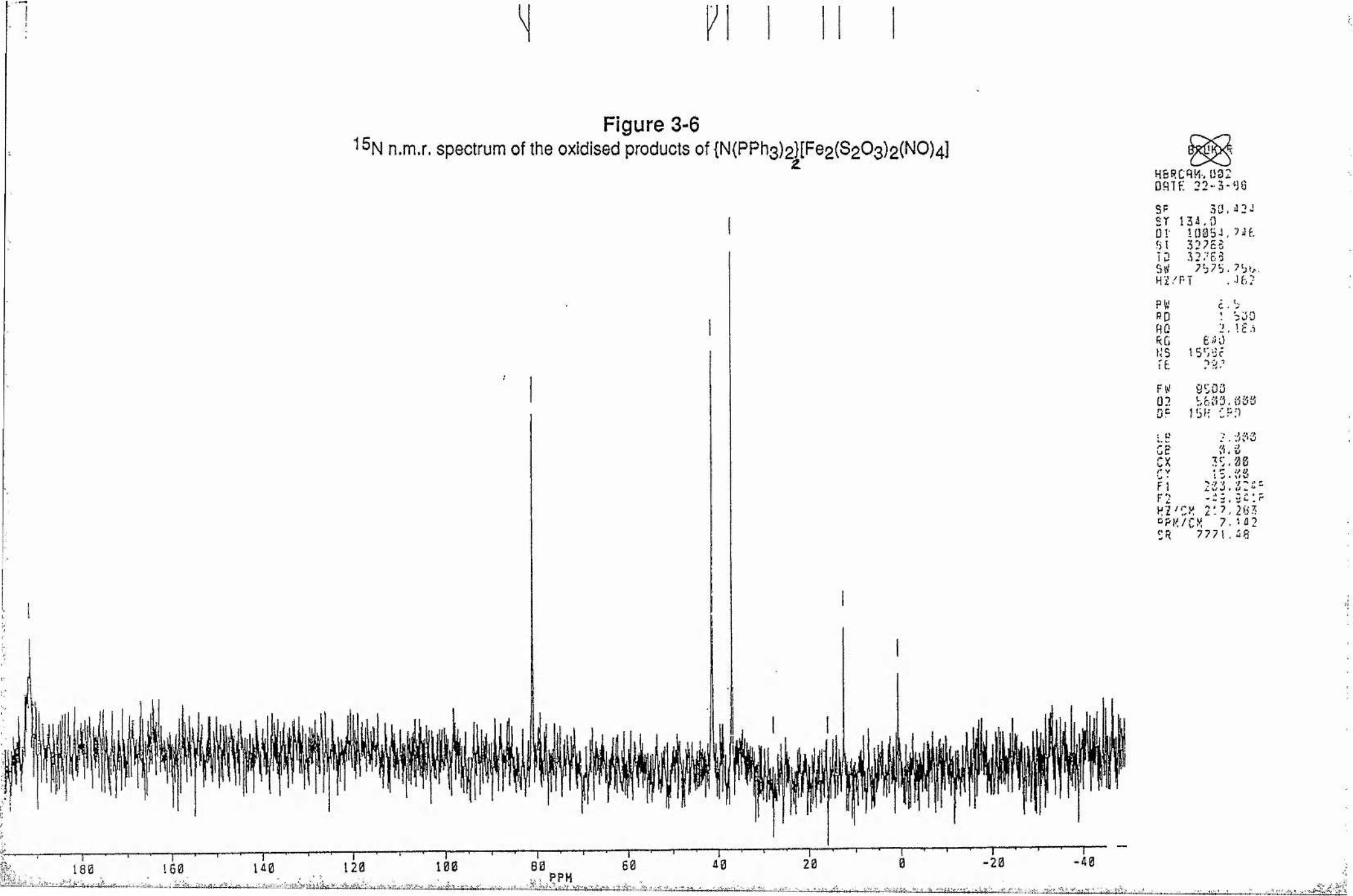

## 3-6 A Theoretical Examination of Cis <==> Trans Conversion Using EHMO Calculations

As discussed in Chapter Two, the E.H.M.O. calculations, although crude, did have some success in predicting the approximate energy barrier to the $C_{2h}$-$C_{2v}$ interconversion for $Fe_2(SMe)_2(NO)_4$. The same method of rotating one of the pendant groups $180^o$ around the plane of the ring was tried with the $[Fe_2(S_2O_3)_2(NO)_4]^{2-}$ ion. It was hoped that this would lead to an explanation for the non-existence of the cis isomer.

The results of the calculation are shown in figure 3-7 The diagram shows two minima corresponding approximately to the geometry of the $C_{2h}$ and $C_{2v}$ conformers (+/-$55^o$ relative to the plane of the $Fe_2S_2$ ring). The energy barrier to conversion is, however, calculated to be only 12 KJ $mol^{-1}$. This is *less* than that calculated for the methyl ester. Since we know the experimental result of the $^{15}N$ n.m.r. suggests that the barrier to inversion is higher than that of the alkyl esters, the calculation must be in error; in this case where a charged species is being examined the approximations inherent in the calculation method may have proven to be too approximate.

A reasonable explanation of why the $C_{2v}$ isomer does not exist at room temperature can be found by the use of molecular graphics. Examination of figure 3-8 shows that the charged oxygens of the $SO_3$ fragment, (calculated to have a charge of -0.88 each) are far apart from one another. In the case of the $C_{2v}$ conformer (figure 3-9) produced by the reflection of an $SO_3$ group through the $Fe_2S_2$ plane, clearly shows the close approach the oxygens on the two $SO_3$ to one another. This close approach would lead to a repulsion between the two groups, a factor not taken into account by the E.H.M.O. calculations. Hence this repulsion would destabilise the $C_{2v}$ conformer relative to the $C_{2h}$ and so only the latter is observed in solution.

This could possibly be confirmed by the use of a high temperature $^{15}N$ n.m.r. study, but this experiment was vetoed on the grounds of possible damage to the n.m.r. machine itself. In the absence of any other available evidence we suggest this to be a plausible reason for the non-existence of the cis conformer.

## Figure 3-7

An examination of the effect of $SO_3^-$ angle(with respect to the plane of the ring) on the stability of the cluster $[Fe_2(S_2O_3)_2(NO)_4]^{2-}$

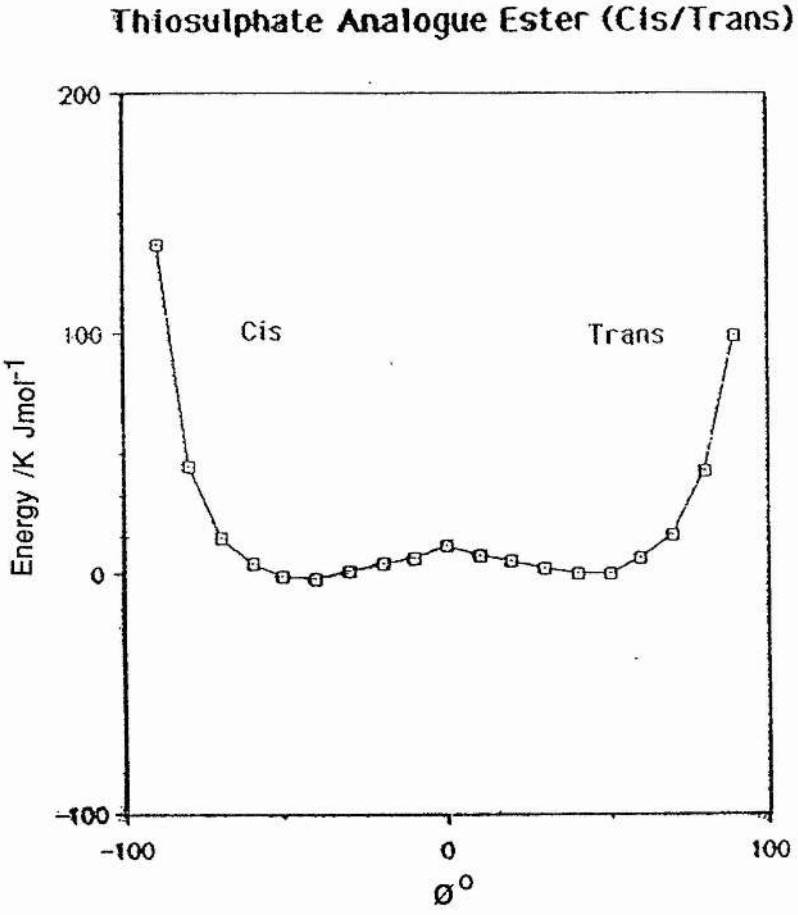


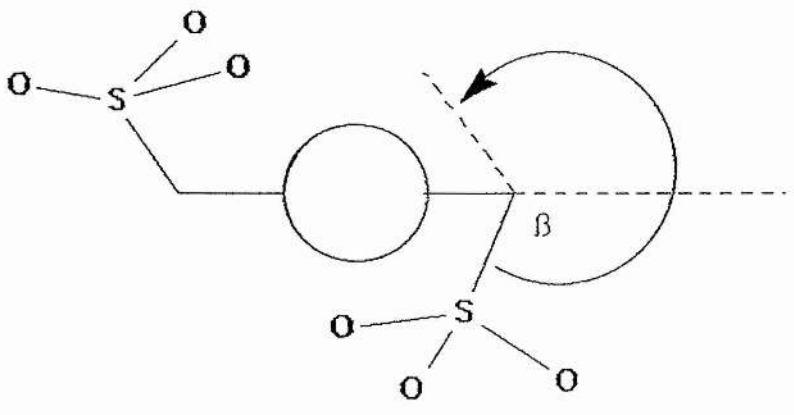

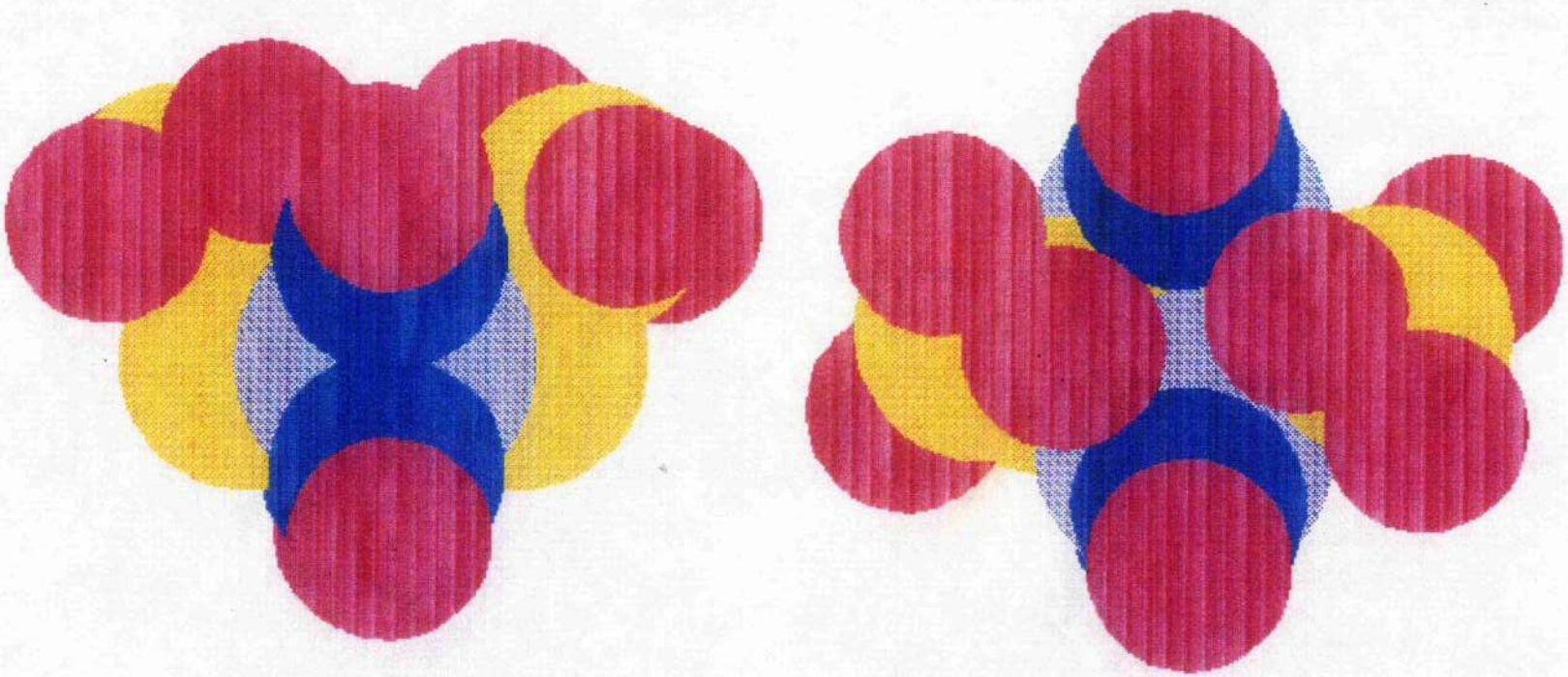

**Figure 3-9**
Two views of the Cis isomer, using the filled Van der Waals radii of the atoms

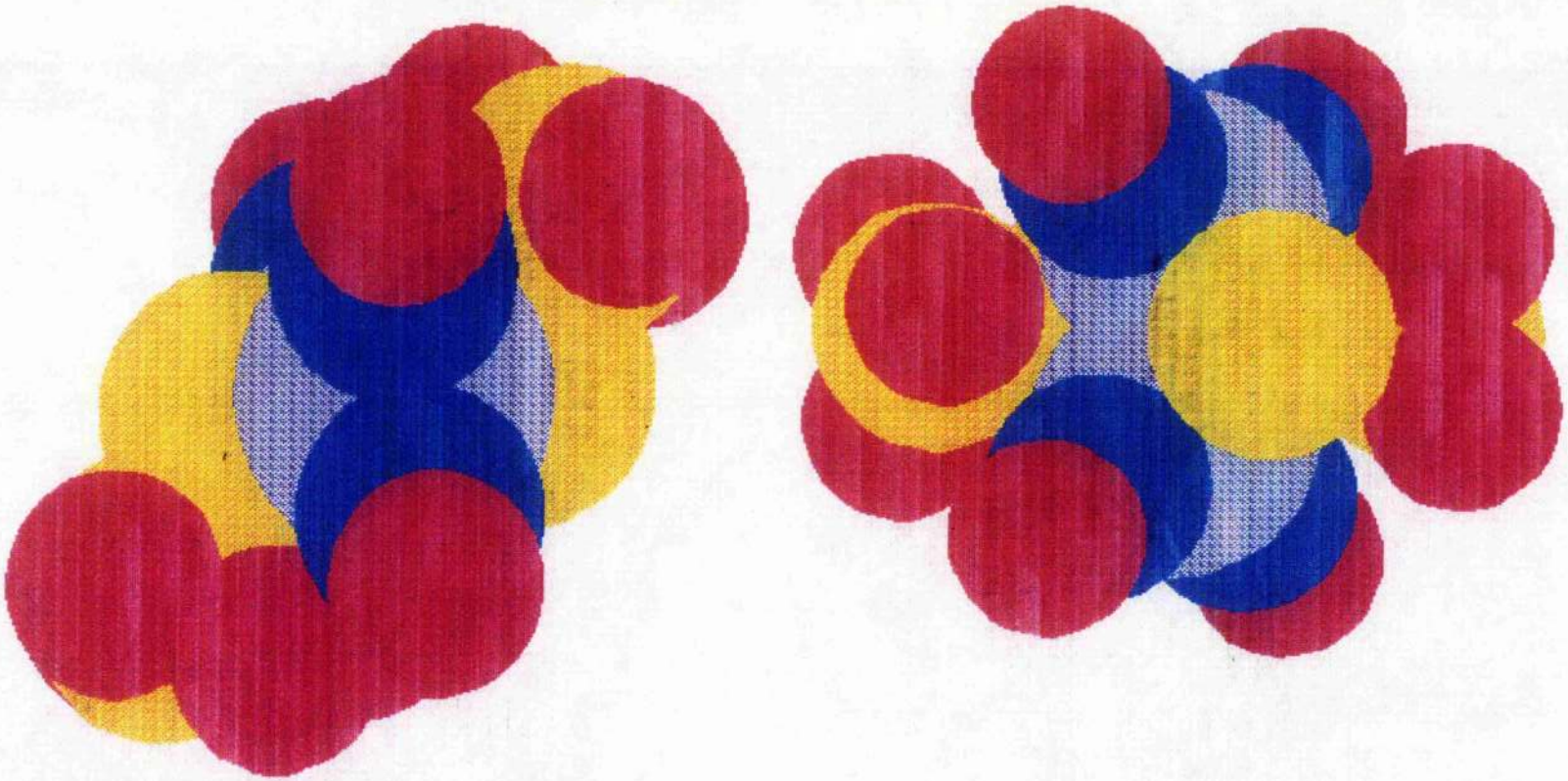

**Figure 3-8**
Two views of the Trans isomer, using the filled Van der Waals radii of the atoms

### 3-7-1 Reactions of $[Fe_2(S_2O_3)_2(NO)_4]^{2-}$

Ligand exchange reactions of $Fe_2(SR)_2(NO)_4$ have been studied extensively by Hyde who developed a method of interconverting the Roussin esters [4] based on the production of mononuclear iron nitrosyls of the type $[Fe(SR)_2(NO)_2]^-$. Originally Hyde examined the reaction of an excess of thiol with $Fe_2(SEt)_2(NO)_4$ in a variety of solvents and concluded that the exchange of an isopropyl group for ethyl was better in solvents of high polarity such as DMF or THF. An examination of the exchange in toluene by $^1H$ n.m.r. showed a very slow rate of exchange, (not reaching equilibrium after 1 year), whereas complete exchange in THF was obtained after three days. The robustness of the iron-sulphur ring in non-polar solvents was further demonstrated by attempting to produce a mixed ester of the type $Fe_2(SR)(SR')(NO)_4$. Refluxing a chloroform solution of the ethyl and methyl Roussin esters for four hours gave none of the mixed ester but reflux in DMF, however showed the presence of the mixed ester. Moreover it was shown that solutions of $Fe_2(SMe)_2(NO)_4$ in DMF examined by $^1H$ n.m.r. broadened and collapsed with time, due to the production of paramagnetic species.

Although solutions of $Fe_2(SR)_2(NO)_4$ and RSH are e.p.r. silent, addition of $RS^-$ or RSH/base causes a major enhancement in the intensity and resolution of the spectrum. The paramagnetic species present were shown [4] to be $[Fe(SR)_2(NO)_2]^-$. From this work a preparative route to $Fe_2(SR)_2(NO)_4$ based on ligand exchange with the mononuclear radical was developed, (scheme-1). The preparation of such mononuclear fragments from $Fe_2(SR)_2(NO)_4$ is often accompanied by a colour change from brown/red to green. Addition of a non-polar solvent causes the redimerisation of the iron nitrosyl fragments and the reverse colour change.

This method parallels the synthetic reaction developed by Rauchfuss and Weatherill based on the iodo complex $Fe_2I_2(NO)_4$ [12]. Examination of THF solutions of this complex in the presence of base and thiolate ion have also shown the presence of mononuclear paramagnetic fragments [13].

The work based on $Fe_2(SR)_2(NO)_4$ and $Fe_2I_2(NO)_4$ suggested that a preparative route to new iron-nitrosyl clusters could be developed from $[Fe_2(S_2O_3)_2(NO)_4]^{2-}$ which has been shown to be an analogue of the Roussin esters.

Following the procedure of Hyde $Na_2[Fe_2(S_2O_3)_2(NO)_4]$ was reacted in THF with propane-2-thiol in the presence of triethylamine as a proton acceptor. There was no obvious colour change as was reported by Hyde for his conversions. However on addition of toluene which would redimerise any paramagnetic dinitrosyl species present, $Fe_2(S^iPr)_2(NO)_4$ was obtained in 62% yield. This reaction was found to a general one for alkyl mercaptans and yields greater than 40% were recorded in all cases of R=alkyl. Reaction with $HSCH_2CO_2CH_3$ resulted in only a very low yield of $Fe_2(SCH_2CO_2CH_3)_2(NO)_4$. This was possibly due to base hydrolysis of the ester link. The similarity of this reaction method to that of Hyde's suggested a similar reaction sequence.

### 3-7-2 E.P.R. Examination of $[Fe_2(S_2O_3)_2(NO)_4]^{2-}$

DMF or THF solutions of $Fe_2(SR)_2(NO)_4$ give weak e.p.r. signals attributed to solvo complexes of mononuclear iron fragments [6]. Similarly a THF solution of $Na_2[Fe_2(S_2O_3)_2(NO)_4]$ showed the presence of a weak signal centred at g=2.03, and was assigned to THF complexes of mononuclear iron fragments. The spectrum obtained is complex and probably contains more than two paramagnetic species with overlapping spectra. In DMF, solutions of $Na_2[Fe_2(S_2O_3)_2(NO)_4]$ also show a weak e.p.r. signal centred at g=2.030. The spectrum obtained, although complex is identical to those obtained by Johnson on dissolving a Rousin Ester in DMF, and so this spectrum is also assigned to solvo complexes of mononuclear iron fragments.

Addition of $Et_3N$ to THF solutions of $Na_2[Fe_2(S_2O_3)_2(NO)_4]$ caused little change to the E.P.R. spectrum, whereas with DMF solutions the addition of $Et_3N$ produced a five line e.p.r. spectrum; g=2.03, $A^{14}N$=2.5G. The heights of the lines are in the ratio 1:2:3:2:1 and therefore the species contains two equivalent nitrogens ($^{14}N$ has a spin of 1, the use of the $(2n\mathbb{I}+1)$ rule from n.m.r. spectroscopy leads to this conclusion). The dinitrosyl species

$[Fe(SR)_2(NO)_2]^-$ which have been extensively studied have g values of between 2.027 and 2.029 and coupling constants of between 2.1 and 2.7G. These species are also produced by the addition of base to DMF solutions of Roussin's Esters, thus the dinitrosyl obtained in this work was assigned the constitution of $[Fe(S_2O_3)_2(NO)_2]^{3-}$.

The difference between the THF and DMF solutions is explained in terms of the polarity of the solvent. DMF, the more polar solvent, enhances the ring opening of the cluster in the presence of a base. This difference between DMF and THF and the effect of polar versus non-polar solvents has already been discussed.

Addition of a small aliquot of RSH, where R=$^i$Pr, to a THF solution of $Na_2[Fe_2(S_2O_3)_2(NO)_4]$ in the presence of $Et_3N$ (where a small aliquot = 1µl of thiol added to 5mg of the thiosulphato complex (giving an excess of the complex over the thiol of around 1000:1) caused a change to the spectrum of the solvo complexes already discussed. The e.p.r. spectrum showed the presence of three paramagnetic species; a five line e.p.r. signal attributed to a dinitrosyl species, g=2.028, $A^{14}N$=2.5G (2N); and two e.p.r. signals attributed to two mononitrosyl species, g=2.040, $A^{14}N$=13G (1N) and g=2.023, $A^{14}N$=3.8G (1N). The low g mononitrosyl and the dinitrosyl were the dominant features of the spectrum. Addition of a similar aliquot of $^t$BuSH to a similar solution of $Na_2[Fe_2(S_2O_3)_2(NO)_4]$ in the presence of $Et_3N$ produced two signals; a dinitrosyl, g=2.030, $A^{14}N$=2.5G(2N) and a mononitrosyl, g=2.024, $A^{14}N$=4.4G(1N) of which the mononitrosyl was the dominant feature.

During the work by Hyde a low g value mononitrosyl was observed on the addition of thiolate ion to THF solutions of $[Fe_4S_3(NO)_7]^-$. This signal was assigned the constitution of $[Fe(SR)_3NO]^-$ [4]. These paramagnetic species are characterised by a g value of 2.020 to 2.021 and a $^{14}N$ hyperfine coupling of 4.5 to 5.0G. On this basis the e.p.r. spectrum of the low g value species observed in this work was assigned the constitution of $[Fe(S_2O_3)_{3-x}(SR)_xNO]^{x-4}$ where x=1 or 2. It was not assigned to $[Fe(SR)_3NO]^-$ because of the 1000x excess of the ester over added thiol, and also because its g value was higher than those reported for $[Fe(SR)_3NO]^-$, nor was it assigned the constitution $[Fe(S_2O_3)_3NO]^{4-}$ because the g value and the $^{14}N$ hyperfine coupling show a dependence on R. Thus it was assigned an intermediate constitution.

The dinitrosyl g=2.03, $A^{14}N$=2.5G was asigned to $[Fe(S_2O_3)_2(NO)_2]^{3-}$ on the basis of previous work. The dinitrosyl g=2.028, $A^{14}N$=2.5G may be tentatively assigned to the mixed dinitrosyl $[Fe(S_2O_3)(SR)(NO)_2]^{2-}$. There was no hyperfine coupling observed to any ∝ protons of an RS group as is found in the spectrum of $[Fe(S^{i}pr)_2(NO)_2]^{-}$, (figure 3-10). This latter species has a g=2.027, $A^{14}N$=2.5G and $A^{1}H$=1.3G. The $A^{14}N$ value observed for the dinitrosyl in this work is similar as is the g value, and so an assignment to a tetrahedral dinitrosyl species is valid. In this case the $A^{1}H$ hyperfine coupling may be smaller than the line width and so the splitting due to the ∝ protons becomes a hidden feature.

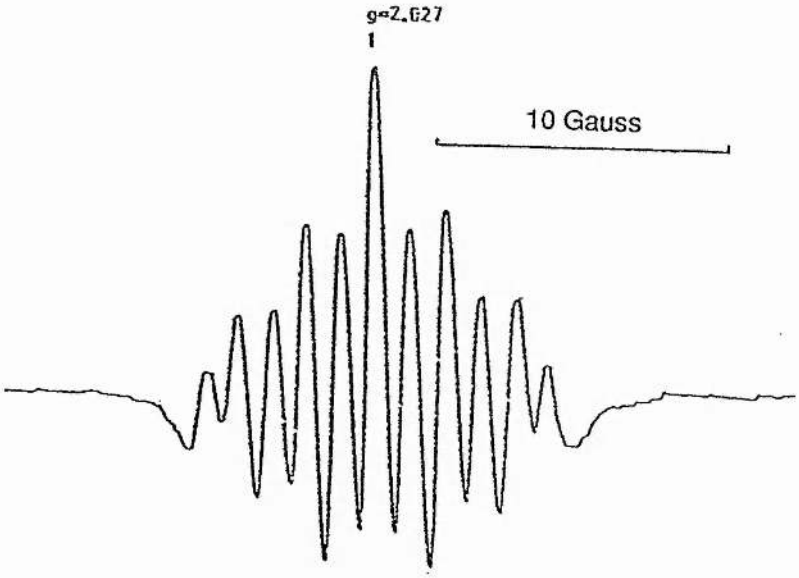


**Figure 3-10**
The e.p.r. spectrum of $[Fe(S^{i}Pr)_2(NO)_2]^{-}$

The high g value mononitrosyl observed for R=$^{i}$Pr is, on the basis of previous work, assigned the constitution of $[Fe(SR)_3NO]^{3-}$. Although in the above discussion we ruled out a constitution of $[Fe(SR)_3NO]^{-}$ for the low g value mononitrosyl because of the ratio of added thiol to thiosulphato complex, in this case the feature *was* weaker than the dinitrosyl and the low g value mononitrosyl, plus the species $[Fe(SR)_3NO]^{3-}$ have been reported in the literature. The reaction of $Fe_2I_2(NO)_4$ with $^{i}$PrSH in THF/$Et_3N$ produced a mononitrosyl species with a g=2.040, $A^{14}N$=13.5G, showing no hyperfine coupling to the ∝ protons of

the attached RS groups; similar species were also obtained with the reaction of $Fe_4S_4(NO)_4$ with $SH^-$ and $^tBuS^-$. This 13.5G species was tentatively assigned the constitution $[Fe(SR)_3NO]^{x-}$ with x>1. The similarity of the E.P.R. spectrum of these species to the one observed in this work allows the tentative assignment of the high g value mononitrosyl as $[Fe(SR)_3NO]^{3-}$.

Addition of a large excess of $^iPrSH$ to a THF/$Et_3N$ solution of $Na_2[Fe_2(S_2O_3)_2(NO)_4]$ caused an increase in the size of the g=2.040 mononitrosyl and was the sole paramagnetic species observed, (figure 3-11). This observation backs up the assignment of this species to $[Fe(SR)_3NO]^{3-}$ and not to a mixed thiosulphate/thiolate mononitrosyl. It also suggests that $RS^-$ where R=alkyl is a preferential ligating ligand relative to $R=SO_3$. If the experiment is repeated in DMF, then the same g=2.040, $A^{14}N$=13G mononitrosyl is observed along with the well characterised $[Fe(S^iPr)_2(NO)_2]^-$, (figure 3-12). Once again we observe a difference between DMF and THF. The experiment suggests that DMF helps to stabilise the dinitrosyl relative to the mononitrosyl compared to THF. From simulations, (figure 3-12a), the relative proportions of the mononitrosyl to dinitrosyl favour the mononitrosyl in a ratio of 81:19. Repeating the DMF work with $R=^tBu$ also produced a spectrum which showed the presence of the high g mononitrosyl along with the well characterised $[Fe(S^tBu)_2(NO)_2]^-$, g=2.027, $A^{14}N$=2.7G, and once again the mononitrosyl is the dominant species observed.

The high yields of the Roussin Esters obtained experimentally (40-70%) from the reaction of thiol or thiolate ion with THF/$Et_3N$ solutions of $Na_2[Fe_2(S_2O_3)_2(NO)_4]$ suggest that the high g value mononitrosyl species may be in equilibrium with the dinitrosyl species $[Fe(SR)_2(NO)_2]^-$.

$$[Fe(SR)_3NO]^{3-} \longleftrightarrow [Fe(SR)_2(NO)_2]^-$$

The corollary of this is that there must also be diamagnetic nitrosyl containing species in solution, capable of nitrosyl donation.

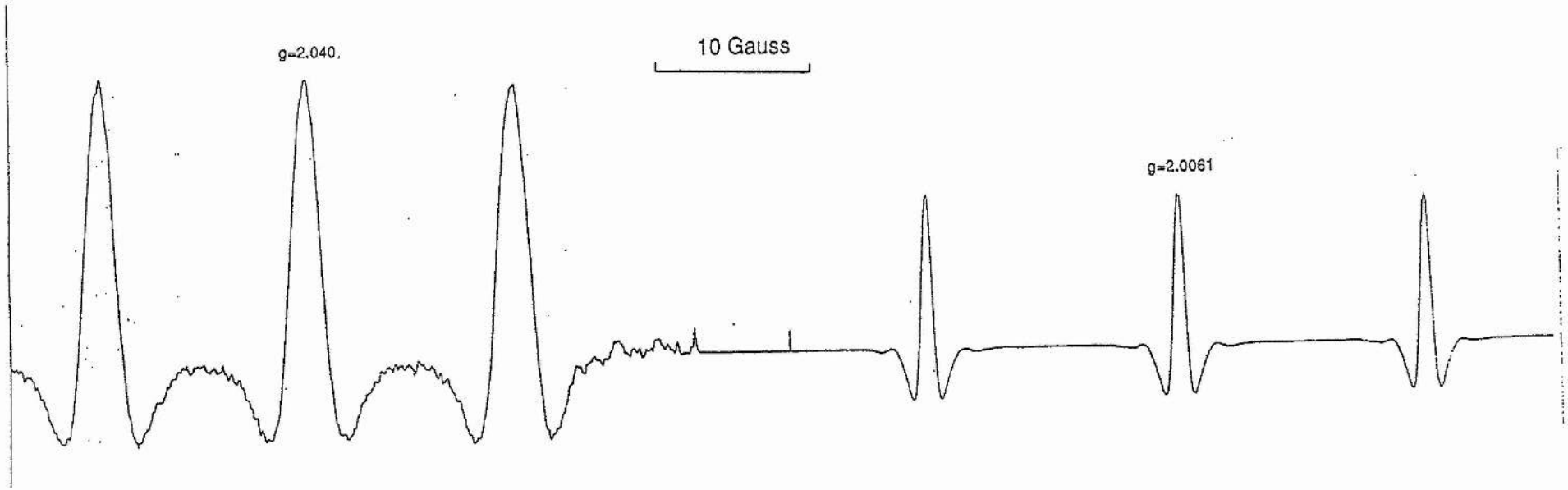


**Figure 3-11**
The e.p.r. spectrum of a THF/$Et_3N$ solution of
$Na_2[Fe_2(S_2O_3)_2(NO)_4]$ with excess $HS^iPr$

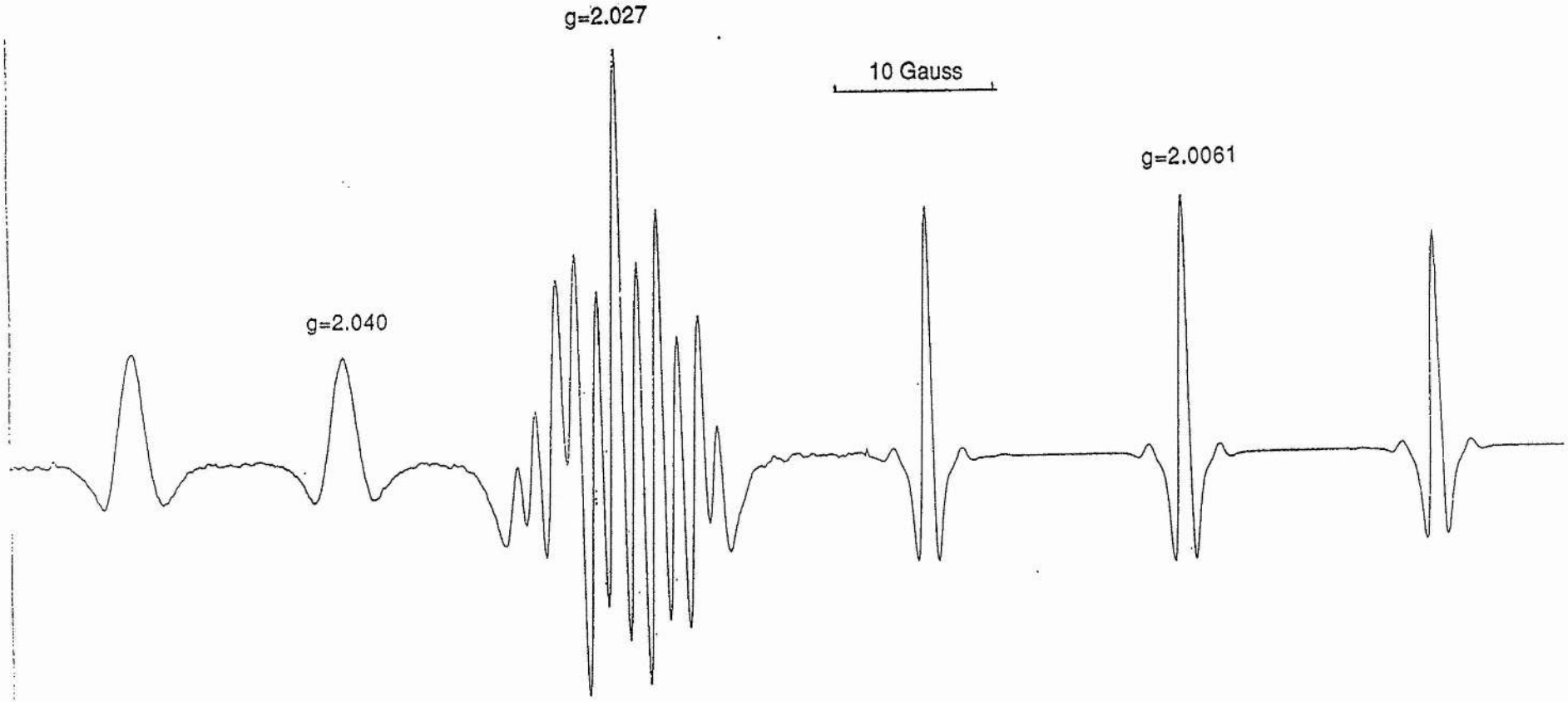


**Figure 3-12**
The e.p.r. spectrum of a DMF/$Et_3N$ solution of $Na_2[Fe_2(S_2O_3)_2(NO)_4]$ with excess $HS^iPr$

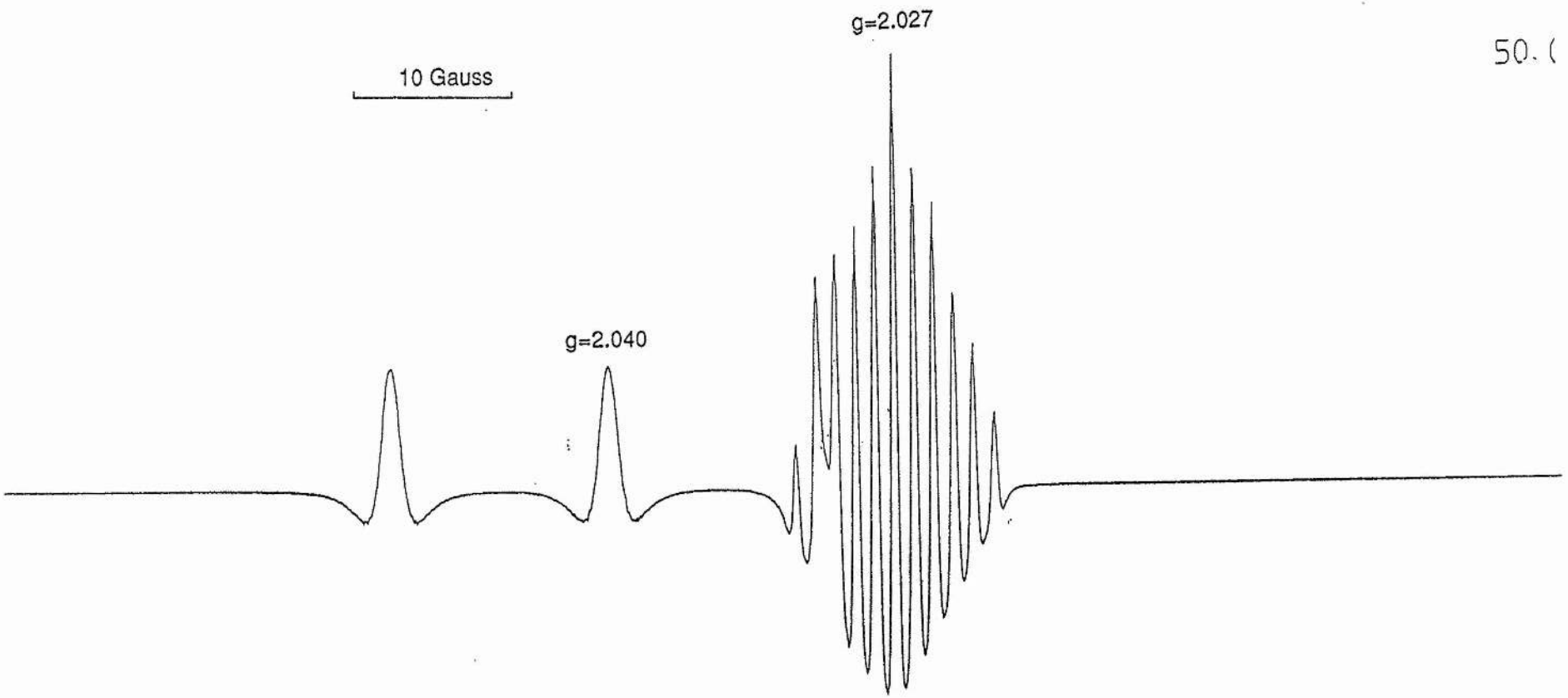


**Figure 3-12a**
A simulated e.p.r. spectrum of the above
using the parameters gained from experiment

Whether this is an accurate description of how the Roussin Esters are prepared from THF solutions of $Na_2[Fe_2(S_2O_3)_2(NO)_4]$ and thiolate ion remains open to question, however based on previous work a plausible mechanism could be;

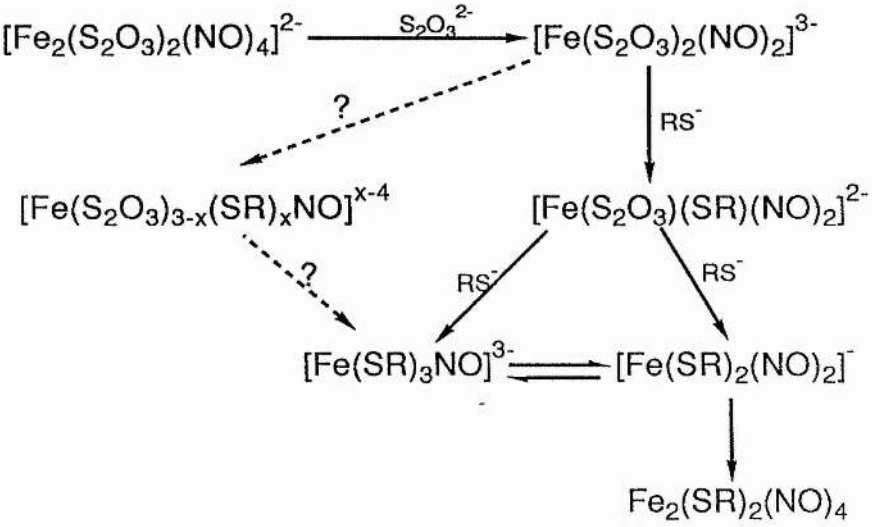


It is a possibility that the species assigned to $[Fe(S_2O_3)_{3-x}(SR)_xNO]^{x-4}$ may be an intermediate in the formation of $[Fe(SR)_3NO]^{3-}$. Such $d^7$ to $d^9$ conversions are known to occur. For instance the complex $Fe(NO)(S_2CNMe_2)_2$ can be converted into $Fe_2(SMe)_2(NO)_4$ in yields of around 24%. The apical iron nitrosyl of Roussins Black Salt whose iron is formally $d^7$ can, in the presence of $RS^-$, be converted into the $d^9$ species $[Fe(SR)_2(NO)_2]^-$. The reverse $d^9$ to $d^7$ conversion has been shown to proceed easily too. Addition of chelating ligands such as dialkydithiocarabamate salts to solutions containg $[Fe(SR)_2(NO)_2]^-$ provides a clean route to complexes of the type $Fe(NO)(S_2CNR_2)_2$. However, in this case, for $[Fe(S_2O_3)_{3-x}(SR)_xNO]^{x-4}$ to be an intermediate, an oxidation of the original iron nitrosyl species must take place, followed by a reduction to produce $[Fe(SR)_3NO]^{3-}$. Whether this actually happens is left to future investigators.

The high g value mononitrosyl shows temperature dependant g and $A^{14}N$ values, Table 3-3.

**Table 3-3**

| Added thiol | Dial Temperature | g-value | $A^{14}N$ |
|---|---|---|---|
| $^{i}PrSH$ | 220 | 2.039 | 13.60 |
| | 260 | 2.040 | 13.35 |
| | 280 | 2.041 | 13.22 |
| $^{t}BuSH$ | 210 | 2.039 | 13.47 |
| | 230 | 2.0395 | 13.50 |
| | 270 | 2.040 | 13.20 |
| | 290 | 2.042 | 12.87 |

The g value of a paramagnetic species is dependent on its electronic structure. For instance $[Fe(NO)(S_2MoS_2)_2]^{2-}$ has a g=2.024, $A^{14}N$=15G [43], and has a square pyramidal geometry. $Fe(NO)(S_2CNMe_2)_2$ also has a square pyramidal geometry but has a g=2.040, $A^{14}N$=13.5G [50]. The hyperfine interaction observed is a magnetic interaction between the magnetic moment of the unpaired electron and the magnetic nucleus. In fluid samples the dipole-dipole interaction that arises from an unpaired electron in a p-orbital is averaged to zero. An unpaired electron in an s-orbital is distributed spherically around the nucleus, and such an electron can approach the nucleus unlike an electron in a p-orbital. This gives rise to the Fermi Contact Interaction. The magnitude of the interaction can be interpreted in terms of the amount of s character of the orbital in which the unpaired electron is bound. A greater amount of s character leads to an increase Fermi Contact Interaction and hence an increase in the hyperfine coupling [42].

The temperature dependence of g and $A^{14}N$ of $[Fe(SR)_3NO]^{3-}$ suggests that as the temperature is changed the structure of the species changes slightly. The effect is reversible and so the structural change must also be reversible. One possible explanation for the observed phenomenon could be that the RS groups which are probably in a tetrahedral arrangement become more planar as the temperature is changed, figure 3-13.

**Figure 3-13**

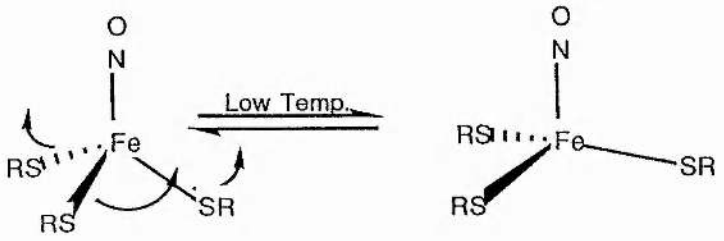

This idea could be substantiated by molecular orbital calculations by examining the amount of s character of the SOMO with the change in N-Fe-S angle. Whether the E.H.M.O. method is accurate enough to show this is questionable.

E.H.M.O. calculations have been used with this work in the past with some success. It helped to originally assign the constitutions of the two mononitrosyls $[Fe(SR)_3NO]^{3-}$ and $[Fe(SR)_3NO]^{-}$[43]. The results of similar calculations using $[FeS_3NO]^{6-}$ and $[FeS_3NO]^{4-}$, analogues of $[Fe(SR)_3NO]^{3-}$ and $[Fe(SR)_3NO]^{-}$ respectively, were carried out using the local geometry obtained from the apical iron of Roussin's Black Salt. The shape of the SUMOs obtained are given in figure 3-14. These results are in agreement with the previous calculations and help to show the basis of the assignments made. The SUMO of $[FeS_3NO]^{6-}$ has a large $\sigma$ interaction with the s-orbital of the nitrogen and so a large hyperfine coupling constant is expected, and observed. The $\pi$ character of the SUMO of $[FeS_3NO]^{4-}$ would give a dipole-dipole interaction but in a fluid this is zero, thus a small $A^{14}N$ value is expected and of course this is observed.

**Figure 3-14**

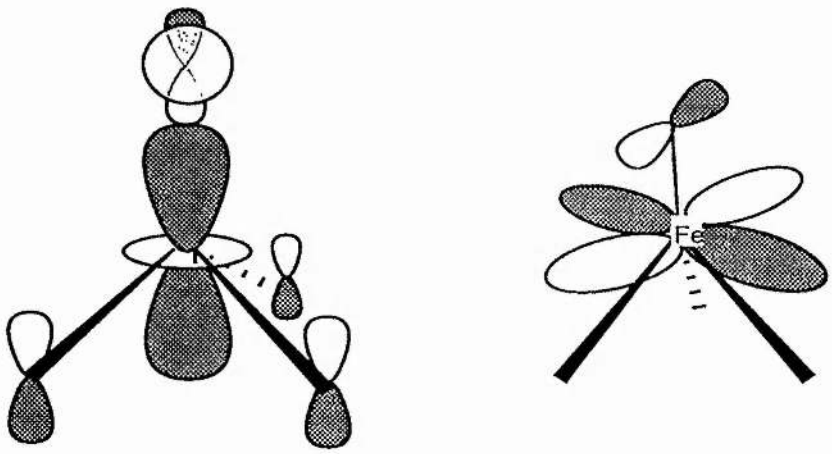


$[FeS_3NO]^{6-}$ $[FeS_3NO]^{4-}$

3-7-3 The $[Fe(NO)_2(S_2O_3)_2]^{3-}$ complex

It has been shown that in the presence of thiolate alone, Roussin's esters divide to produce paramagnetic fragments. In a similar manner, the addition of thiosulphate ion to aqueous solutions of $Na_2[Fe_2(S_2O_3)_2(NO)_4]$ causes a colour change from brown to green. A

methanolic solution of $Na_2[Fe_2(S_2O_3)_2(NO)_4]$ is E.P.R. silent, but on addition of a saturated methanolic solution of $Na_2S_2O_3$ an intense five line E.P.R. spectrum is obtained (g=2.03, $A^{14}N$=2.4G). This has been assigned to $[Fe(S_2O_3)_2(NO)_2]^{3-}$.

In the original preparation of the thiosulphate analogue ester from nitrite ion a green material was obtained in addition to the ester. A methanolic solution of this green material also reveals a five line E.P.R with the same g-value and coupling constant as that produced from $Na_2[Fe_2(S_2O_3)_2(NO)_4]$ and thiosulphate ion. The green material was therefore given the composition $Na_3[Fe(S_2O_3)_2(NO)_2]$. This result suggests that the acetone extraction procedure is in part a dimerisation of this mononuclear iron nitrosyl; also the addition of $Bu_4NBr$ to aqueous solutions of the green material, followed by extraction into an organic solvent, which leads to the preparation of $(Bu_4N)_2[Fe_2(S_2O_3)_2(NO)_4]$ supports the above suggestion. These observations are an extension of the idea that non-polar solvents close the ring while polar solvent facilitate its opening.

Examination of the UV-Vis spectrum of $Na_2[Fe_2(S_2O_3)_2(NO)_4]$ in MeOH reveals (figure 3-15) four absorptions; $\lambda$ 460nm($\epsilon$ 1417$mol^{-1}cm^{-1}$), $\lambda$ 355nm ($\epsilon$ 5909$mol^{-1}cm^{-1}$), $\lambda$ 305nm ($\epsilon$ 6329$mol^{-1}cm^{-1}$), $\lambda$ 240nm ($\epsilon$ 22088$mol^{-1}cm^{-1}$). Figure 3-15a shows a Lambert-Beer plot of the 355nm absorption.

**Figure 3-15a**

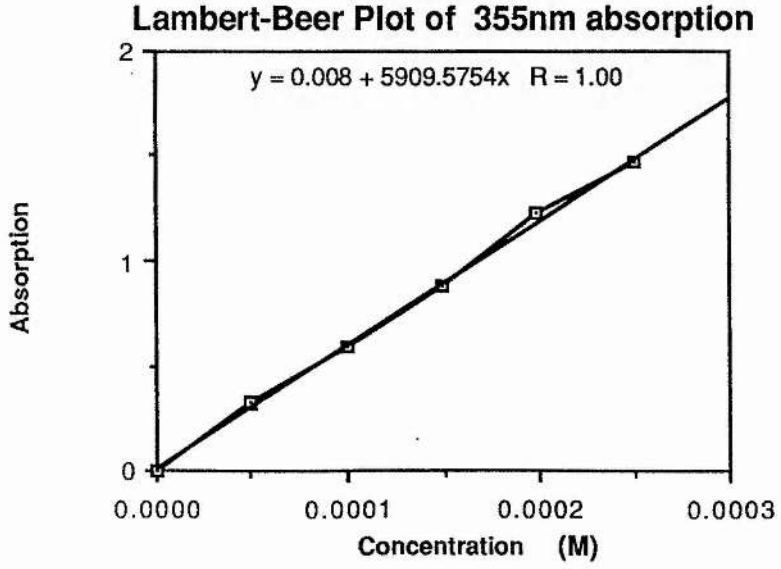

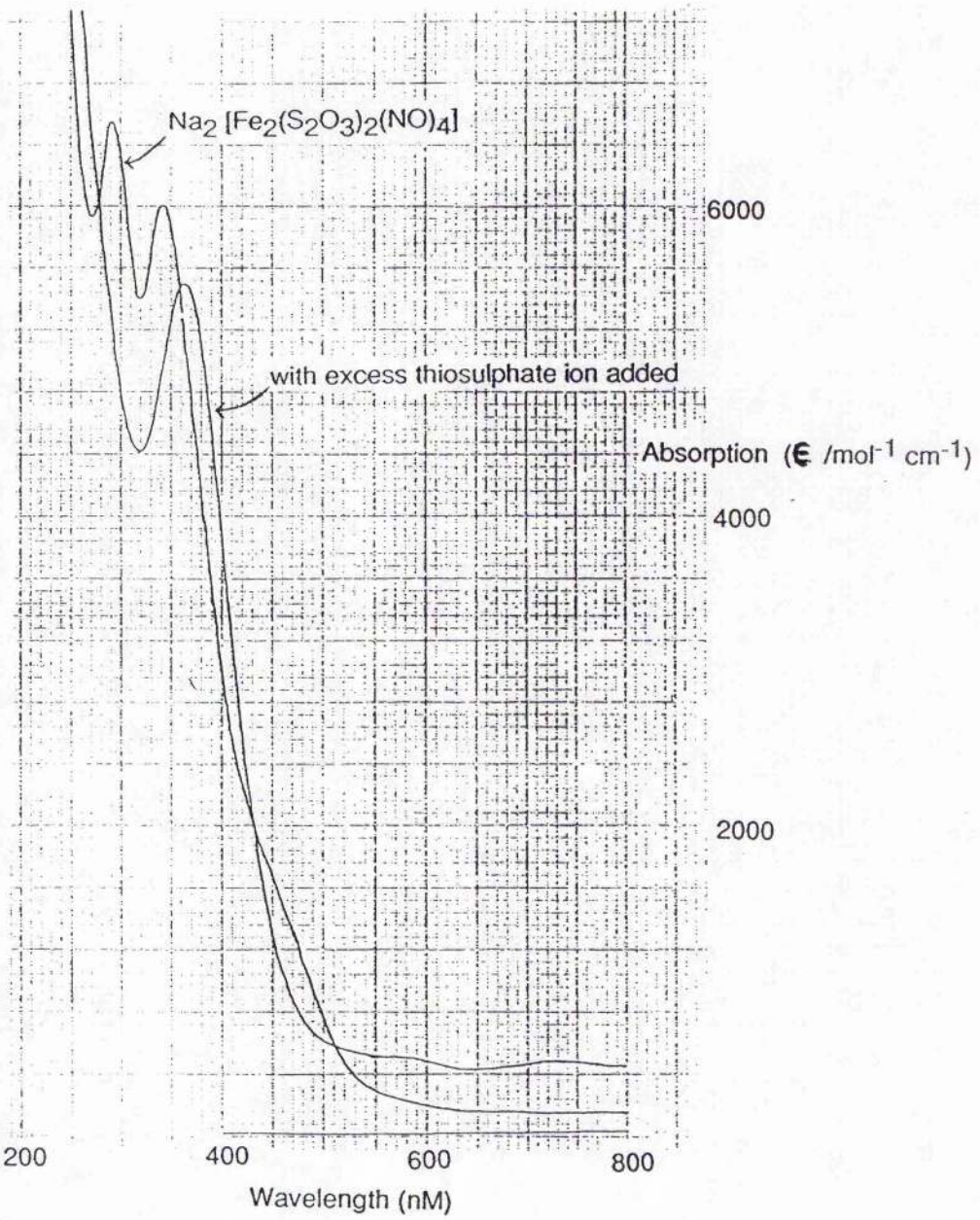


**Figure 3-15**

The UV-Vis spectrum of $Na_2$ $[Fe_2(S_2O_3)_2(NO)_4]$ in MeOH

Addition of an excess of sodium thiosulphate to a methanolic solution of $Na_2[Fe_2(S_2O_3)_2(NO)_4]$ causes a change in the UV-Vis spectrum (figure 3-14b). On the basis of the E.P.R. evidence this new spectrum is assigned to $Na_3[Fe(S_2O_3)_2(NO)_2]$. If we assume that all the dimer has been converted into the monomer then the extinction coefficients can be obtained; $\lambda$ 740nm ($\epsilon$ 197mol$^{-1}$cm$^{-1}$), $\lambda$ 585nm ($\epsilon$ 236mol$^{-1}$cm$^{-1}$), $\lambda$ 365nm ($\epsilon$ 2718mol$^{-1}$cm$^{-1}$). The two absorptions of low extinction coefficient are responsible for the green colouration of the solution.

### 3-7-4 Preparation of $Fe_2(SR)_2(NO)_4$ from Aqueous Solutions of $Na_2[Fe_2(S_2O_3)_2(NO)_4]$

The production of mono-iron dinitrosyl fragments in MeOH and in water lends itself to a new preparative method for the production of iron-sulphur nitrosyl clusters from aqueous solution.

Addition of MeSNa dissolved in sodium hydroxide solution to aqueous solutions of $Na_2[Fe_2(S_2O_3)_2(NO)_4]/Na_2S_2O_3$ (1:2) followed by immediate extraction into $CH_2Cl_2$ leads to $Fe_2(SMe)_2(NO)_4$ in high yield and purity. A small amount of ferric hydroxide was also obtained in these experiments. The use of thiolate without base or the use of thiol alone in aqueous leads to either low yields <5% or no yield of $Fe_2(SR)_2(NO)_4$. This shows that the active species is the thiolate ion, as was found in THF, scheme 3-3.

**Scheme 3-3**

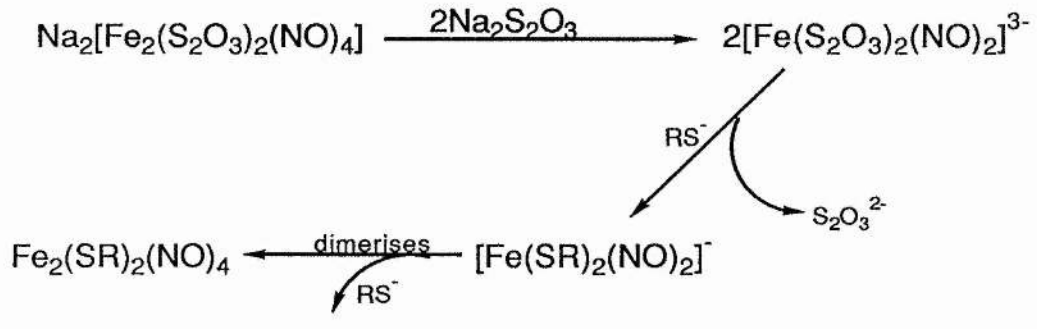


This method has proved to be successful for a wide range of alkyl mercaptans. In most

cases purification by column chromatography was unnecessary, the normal impurity in the THF method is unreacted thiol; by this method the mercaptan is present as thiolate ion and does not extract into the organic layer.

Reaction of $HSCH_2CO_2CH_3$ with the thiosulphato ion by the THF method led to low yields of the required ester possibly due to base hydrolysis of the mercaptan or the ester itself. Since by the aqueous method the reaction time is a few seconds only, repeating this reaction in water/base led to $Fe_2(SCH_2CO_2CH_3)_2(NO)_4$ in good yield and purity. At room temperature the $^1H$ n.m.r shows a broad peak centred on ∂ 3.7ppm. On cooling to -40°C the peak was split into three peaks and a shoulder. The intensity of the peaks was consistent with a 1:1 ratio of cis and trans conformers in solution. The $^{13}C$ n.m.r. confirmed this finding; using the D.E.P.T. technique the $CH_3$ and the $CH_2$ were assigned, each found as a pair in a 1:1 ratio. The relaxation of the carbonyl carbon was long and a longer pulse delay was used to observe it; no structure to the signal was observed due to its low intensity, (figure 3-16).

A $^{13}C$ and $^1H$ n.m.r study of $Fe_2(SCH_2CH_2OH)_2(NO)_4$ confirms that the solution structure of this Roussin ester is similar to that of the other alkyl or aryl Roussin esters in solution. The $^{13}C$ n.m.r shows the presence of three peaks in the ratio of 2:1:1. A DEPT study again confirmed the assignments to $CH_2$ carbons. The two smaller peaks are assigned to the carbon next to the sulphur because of the similarity of the chemical shifts with known compounds and also because of the evidence from the $^1H$ n.m.r. The ratio of 1:0.95 is seen as evidence for an approximately equal amount of cis and trans isomers in solution. The high field absorption in the $^1H$ n.m.r which is composed of two overlapping triplets helps to confirm the existence of the two isomers,(figure 3-17).

It was originally thought that hydrogen bonding may help to populate the cis isomer over the trans. However the ratio of 1:0.95 observed from the $^{13}C$ n.m.r suggests that if this effect was present then the increase in stability is not large enough compared with the energy of conversion at room temperature to be apparent. A comparison of the energy barrier to the cis == trans conversion for this compound relative to the alkyls by the aquisition of coalescence data may be fruitful.

The method has also been successful in preparing the heterocyclic ester $Fe_2(SC_4H_3N_2)_2(NO)_4$ , where $C_4H_3N_2$ is 2-pyrimidine, albeit in low yield and purity.

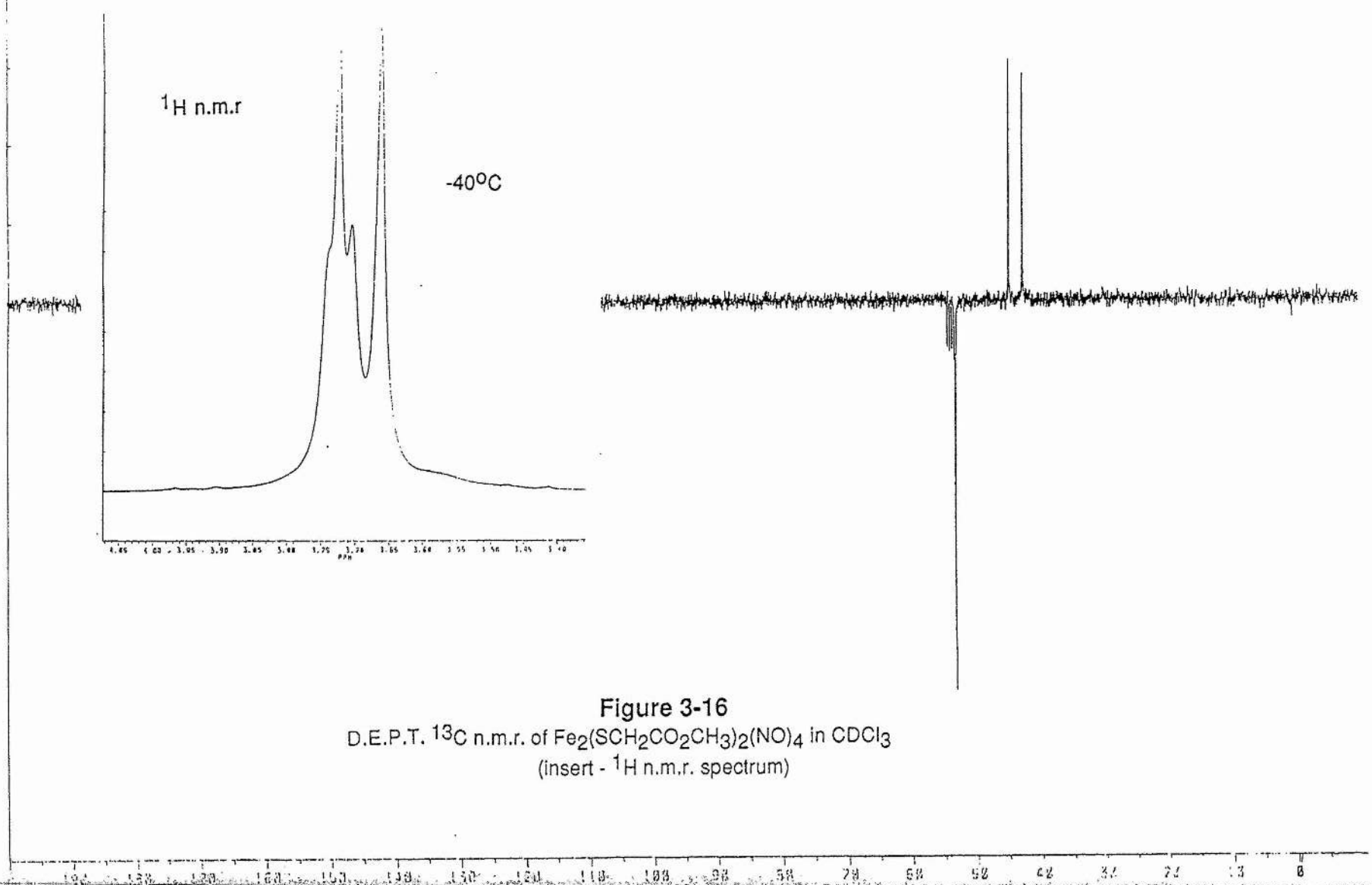


**Figure 3-16**

D.E.P.T. $^{13}$C n.m.r. of $Fe_2(SCH_2CO_2CH_3)_2(NO)_4$ in $CDCl_3$
(insert - $^1$H n.m.r. spectrum)

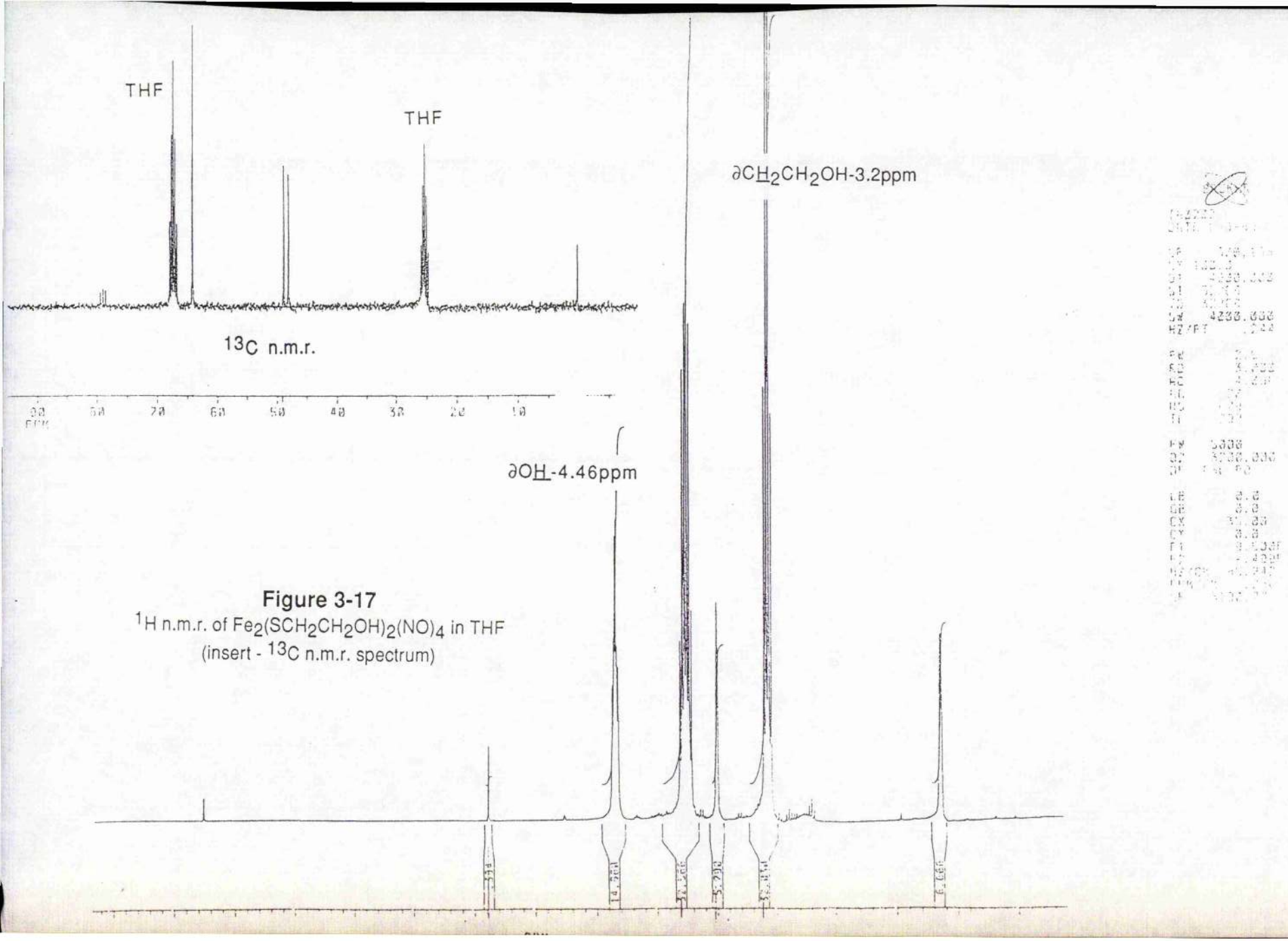


**Figure 3-17**

$^{1}H$ n.m.r. of $Fe_2(SCH_2CH_2OH)_2(NO)_4$ in THF
(insert - $^{13}C$ n.m.r. spectrum)

This method, however, has been found only to give good yields with the more non-polar mercaptans. Reaction with $HSCH_2CH_2OH$ required acidification of the aqueous solution to extract the ester into the organic layer. Attempts to prepare and purify $Fe_2(SCH_2CH_2NH_2)_2(NO)_4$ and $Fe_2(SCH_2CO_2H)_2(NO)_4$ have failed. This is in part due to their sensitivity to pH and also to their solubilities in water as well as their extreme air sensitivity.

3-8 Reaction of $Na_2[Fe_2(S_2O_3)_2(NO)_4]$ with $Na_2S.5H_2O$

Addition of sulphide ion to solutions of $Na_2[Fe_2(S_2O_3)_2(NO)_4]/Na_2S_2O_3$ produces a colour change from black/green to dark red. Such solutions were shown to contain Roussin's Red and Black Salts. From the above study of the action of the thiosulphato complex in THF or water with mercaptans, from which solutions the Roussin Esters can be isolated from paramagnetic precursors, the reaction with sulphide ion presumably produces $[Fe(SH)_2(NO)_2]^-$. This paramagnetic species will be in equilibrium with the dimeric Red Salt;

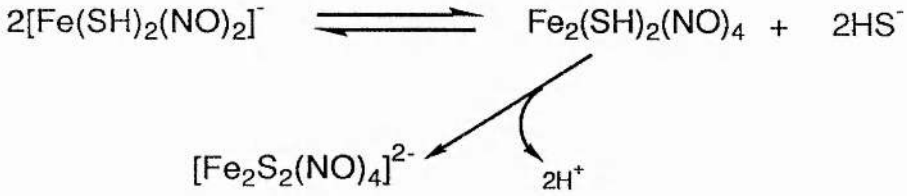


However it is also known that Roussin's Black Salt produces $[Fe(SH)_2(NO)_2]^{1-}$ when reacted with base or sulphide ion [4]. This has been shown to be a reversible reaction. Thus the isolation of the Black Salt as well as the Red is not surprising. Further it has been known for over 100 years that the Red Salt is in a pH dependent equilibrium with the Black Salt, and so the Black Salt could also be being formed as a result of this.

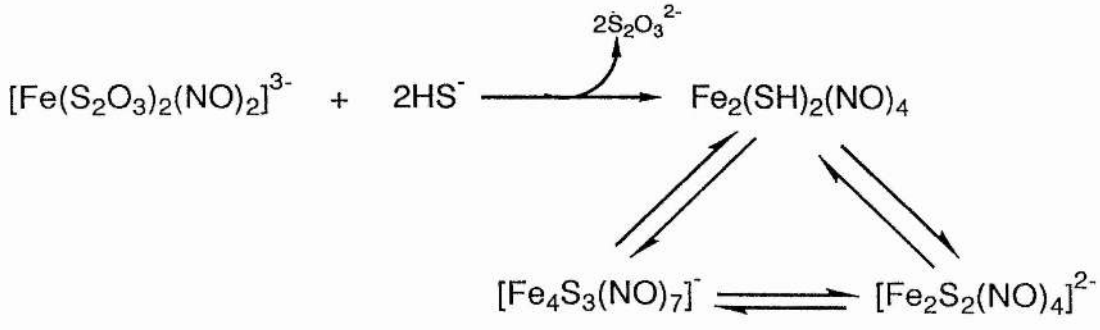

The original work of Pavel showed that the addition of alkyl halides to solutions of the Red Salt produces the Roussin Esters. Addition of methyl iodide to solutions of the thiosulphato complex/thiosulphate ion and sulphide ion produce $Fe_2(SMe)_2(NO)_4$ in low yield. Repeating the procedure with diphenylchloromethane produced $Fe_2(SCH(C_6H_5)_2)_2(NO)_4$ also in low yield. The reaction of the Red salt with alkyl halides normally leads to the alkyl esters of Roussin's Red salt in high yield [7]. The low yields found here may reflect a lower concentration of the Red salt in solution.

### 3-9 Reaction of $Na_2[Fe_2(S_2O_3)_2(NO)_4]$ with Chelating Ligands

It has been shown by Hyde [6] and more recently by Johnson [43] that the addition of chelating ligands such as dialkyldithiocarbamates produces mononitrosyl complexes such as $Fe(NO)(S_2CNR_2)_2$, while with $MoS_4^{2-}$, $[Fe(NO)(MoS_4)_2]^{2-}$ and $[Fe(NO)_2(MoS_4)]^-$ have been observed by e.p.r. spectroscopy. The production of $Fe(NO)(S_2CNR_2)_2$ involves a change in the oxidation state of the iron. The $d^7$ to $d^9$ oxidation change of the iron has been shown to proceed readily with Roussin's Black salt and the cubic tetramer $Fe_4S_4(NO)_4$, moreover addition of dialkyldithiocarbamates to solutions of $Fe_2(SR)_2(NO)_4$ also produces the mononitrosyl i.e, a $d^9$ to $d^7$ conversion.

Addition of dialkyldithiocarbamate salts to aqueous solutions of $Na_2[Fe_2(S_2O_3)_2(NO)_4]/Na_2S_2O_3$ produced $Fe(NO)(S_2CNR_2)_2$ in high yield and purity for R=Me, Et and $^n$Pro. The normal method of preparation involves the action of nitrite on solutions ferrous salts and sodium dialkyldithiocarbamates. This method also produces $Fe(S_2CNR_2)_3$ [44] and $Fe(NO)(NO_2)(S_2CNR_2)_2$ (as shown by I.R. spectroscopy). Soxhlet extraction is required to purify the mononitrosyl by this method, whereas the aqueous method using the thiosulphate ester does not produce either of these two impurities. Reaction with $[S_2CC_6H_4CS_2]^{2-}$ produced an intractable tar and may contain the polymer $[Fe(NO)(S_2CC_6H_4CS_2]_n$.

The reaction with $[MoS_4]^{2-}$ as the limiting stoichiometry, appears to have produced $[Fe(NO)_2(MoS_4)]^-$. Assignment is based on the simplicity of the I.R. spectrum and that THF

solutions of the thiosulphato complex with tetrathiomolybdate give an intense e.p.r. spectrum characteristic of a dinitrosyl species. Microanalytical results on the product of the reaction are not consistent with each other, and the identity of this material remains a mystery.

Reaction with o-xylene-dithiol produced neither a mononitrosyl nor a dinitrosyl mono-iron compound, but the bridged ester $Fe_2((SCH_2)_2C_6H_4)(NO)_4$. Although purification of this ester has not been achieved, the mass spectrum and the I.R. spectrum are consistent with the structure having a ligand bridging across the two sulphurs.

Reaction with L-cysteine is interesting beacause it results in an air sensitive purple solution which turns brown on exposure to air. The IR spectrum of the solid purple and brown materials do not show the presence of M-NO stretching. Reaction of ferrous sulphate with L-cysteine in the presence of base also produces an air sensitive purple solution. The UV/Vis of the resulting brown solution is identical to that produced from the thiosulphato complex. This suggests that on reaction with $Na_2[Fe_2(S_2O_3)_2(NO)_4]$ the NO groups are lost. However no $NO_2(g)$ was observed. In this case it is probable that complexation occurs at the carboxyl/amino end of the amino acid.

In summary we have produced a method for preparing the thiosulphato complex which is both economical in resources and time. We have proven its relationship both structurally and chemically to the Roussin esters. We have also developed its chemistry to obtain a new preparative route to the esters of Roussin's Red Salt, and have examined the possible pathways involved using e.p.r. spectroscopy. As discussed in chapter four the chemistry of $Fe(NO)_2$ groups as potential industrial catalysts has increased the awareness of the chemical community to iron-nitrosyl chemistry, and so any new "$Fe(NO)_2$" species especially with labile ligands is potentially a good industrial catalyst.

Part Two

## 3-10 Known Reactions of Roussin's Black Anion

Iron sulphur clusters found in nature are obtained in three main classes; the rubredoxins, the ferrodoxins and the high potential ferrodoxins, Rd, Fd and HiPIP respectively [45 and references therein]. Enzymes containing these prosthetic groups are called the non-haem iron proteins and are involved in a wide variety of biological processes. Since these enzymes are found in all types of life (not including the viruses) they are considered as one of the oldest types of enzymes. For example aconitase is a non-haem iron protein and contains a cubic Fe4S4 cluster, and is responsible for the conversion of citrate into isocitrate in the Krebs cycle. The main role of these ubiquitous enzymes is one of electron transfer and this is the reason for their place in the oxidative phosphorylation respiratory chain. The redox action of these clusters is discussed in chapter **1** and, in part, in chapter 4.

As discussed in chapter **1** , the incidence of oesophageal cancer in Linxian is put down to environmental factors such as the high levels of nitrite and nitrate in the local water supply and the low molybdenum concentration in the soil. The isolation of the iron sulphur nitrosyl cluster $Fe_2(SMe)_2(NO)_4$, in preserved vegetable matter was seen as a significant discovery; the material never before being detected in nature. It was thought that this cluster could be a major causal factor of the oesophageal cancer. Its *in vivo* production was uncertain. It was presumed that the non-haem iron proteins became nitrosylated and methylated to form the nitrosyl cluster.

Johnson, incubating parsley with nitrite, produced small quantities of the methyl Roussin ester [15], whereas the incubation of casein with nitrite produced Roussin's Black anion [16]. The reaction of analogues of the non-haem iron proteins with nitrite also produced Roussin's Black anion [17]. This work suggested that Roussin's Black anion was a possible intermediate on the route to the formation of $Fe_2(SMe)_2(NO)_4$ from the iron-sulphur enzymes.

Roussin's Black Salt, $Na[Fe_4S_3(NO)_7]$ was the first polymetallic nitrosyl cluster discovered. The structure of the anion is shown on page 20 and figure 3-21. The structure consists of a squashed tetrahedron of iron atoms, three faces of which are triply bridged by

sulphur. The apical iron has one nitrosyl ligand attached, and is formally Fe(1), $d^7$. The three basal irons have two terminal nitrosyl groups each in either an axial or equatorial orientation and are formally Fe(-1), $d^9$. The nitrosyl ligands are found to be approximately linear in the solid state, bending slightly towards each other. In solution the $^{15}N$ n.m.r. chemical shifts of all the nitrosyl groups fall into the linear category [38], ( $\partial^{15}NO$; +/- 50ppm for linear nitrosyls, bent nitrosyls are found in the range 360-713ppm relative to $CH_3{}^{15}NO$) c.f. figure 3-6.

The reactivity of a species is often dependent on the charges associated with a group; for instance the $\partial^+$ charge of the carbonyl carbon gives this group its particular chemistry. With Roussin's Black anion we have a unique apical iron and three basal irons with a formal charge difference of 2 between the two types. As shown in chapter 2, however the net charges associated with each iron is approximately the same ≈ +1.3. This would suggest that the differences in observed chemistry reflects more the difference between a mononitrosyl and a dinitrosyl.

If a DMF solution of $^{15}N$ labelled Roussins Black Salt, thiolate and $^{14}NO_2^-$ are mixed, the e.p.r. spectrum obtained can be attributed to a 3:1 mix of dinitrosyls of the type $[Fe(^{15}NO)_2(SR)_2]^-$ and $[Fe(^{15}NO)(^{14}NO)(SR)_2]^-$[4]. This showed that not only had nitrosyl exchange taken place, but also a change in formal oxidation state had occurred.

$$[Fe(NO)]^{2+} \text{ ---------> } [Fe(NO)_2]^+$$

$$d^7 \text{ ---------> } d^9$$

A major part of the known chemistry of Roussin's Black Salt involves the change in formal oxidation state with the change in the number of nitrosyl ligands. The initial preparation of $Na[Fe_4S_3(NO)_7]$ also involves an oxidation state change;

$$Fe(II) + NO_2^- + S^{2-} \text{ ---------> } [Fe_4S_3(NO)_7]^-$$

and involves the reduction of ferrous ion to Fe(1) and Fe(-1). The preparation of $PNP[Fe_4S_3(NO)_7]$ from $PNP[Fe(CO)_3NO]$ [4] involves the oxidation of the iron;

$$PNP[Fe(CO)_3NO] + S \text{ ---------> } PNP[Fe_4S_3(NO)_7] \ 84\%$$

Two other laboratory preparations of the Black anion which involve a $d^7$ to $d^9$ conversion are[6];

$$Fe(NO)(S_2CNMe_2)_2 + Na_2S \text{ ---------> } Na[Fe_4S_3(NO)_7] \text{ 18\%}$$

and

$$Fe_4S_4(NO)_4 \text{ ----------> } Na[Fe_4S_3(NO)_7]$$

One of the most interesting preparations of the Black anion involves the dimeric cluster $[Fe_2S_2(NO)_4]^{2-}$, which is itself produced from the black anion.

$$Na[Fe_4S_3(NO)_7] \text{ ---------> } Na_2[Fe_2S_2(NO)_4]$$

The reaction is reversible; the addition of dilute acid to a solution of $[Fe_2S_2(NO)_4]^{2-}$ causes its conversion back to the Black anion. There is also the remarkable observation that stirring $[Fe_2S_2(NO)_4]^{2-}$ salts in dichloromethane resulted in the production of the black anion [36].

As intimated above a large part of the chemistry of Roussin's Black Salt is concerned with the production of mononuclear nitrosyl fragments. Reaction with $RS^-$ causes the declustering of the tetramer to produce monomeric fragments, from which the dimeric compounds $Fe_2(SR)_2(NO)_4$ can be isolated. The production of the red dianion, $[Fe_2S_2(NO)_4]^{2-}$, involves fragmentation of the tetramer presumably through the formation of $[Fe(SH)_2(NO)_2]^-$. The formation of the cubic cluster $Fe_4S_4(NO)_4$ from the Black anion is also presumed to proceed through the production of mononuclear iron fragments.

The work reported here was based on the assumption that Roussin's Black anion may be initially formed from natural iron sulphur enzymes and subsequently converted into the dimeric iron nitrosyl, $Fe_2(SMe)_2(NO)_4$. This reaction also involves the declustering of the tetramer. From a knowledge of the known reactions of Roussin's Black Salt a possible in vivo sequence could be;

$$[FexSx] \text{ -A-> } [Fe_4S_3(NO)_7]^- \text{-B-> } [Fe_2S_2(NO)_4]^{2-} \text{ -C-> } Fe_2(SMe)_2(NO)_4$$

All of these steps involve known reactions. In the laboratory, step B involves reflux in

strong alkali and because of this the above scheme is not seen as likely in a biological matrix. In fact, the preserved vegetables are stored under water for a considerable time before consumption. Dissolved carbon dioxide gas could cause the conversion of any $[Fe_2S_2(NO)_4]^{2-}$ formed back into $[Fe_4S_3(NO)_7]^-$.

Another possible sequence could involve the fragmentation of Roussin's Black anion to give paramagnetic mononuclear fragments which in the presence of a source of $MeS^-$ would give $[Fe(NO)_2(SMe)_2]^-$. This dinitrosyl would then dimerise to give $Fe_2(SMe)_2(NO)_4$.

$[FexSx]$ --A'--> $[Fe_4S_3(NO)_7]^-$--B'--> Fragments --C'--> $[Fe(NO)_2(SMe)_2]^-$ --D'--> $Fe_2(SMe)_2(NO)_4$

The steps B' to D' are known to occur in solvents such as DMF, in the presence of a base such as $MeS^-$ which causes the tetramer to fragment. This scheme would require a source of thiolate and the requirement of basic conditions would tend to rule this scheme out. However it could be possible that a methyl group is transferred from a biological methyl donor such as tetrahydrofolate to the sulphur of a paramagnetic fragment derived from the tetramer. Although such a donation has not been experimentally verified, the possibility cannot be dismissed.

3-11 Reaction of Roussin's Black Salt with Aryl Diazonium Salts

In the above discussions, the reactivity of Roussin's Black Salt has been shown to be centred on the role of the irons and nitrosyl groups; the sulphurs, each of which carry a charge of -0.7 according to calculation (see chpt. 2) have been largely ignored. A paper by Jinhau, however, not only suggested a reaction of Roussin's Black Salt which was centred on the sulphur, but also implied the most likely reaction mechanism for the production of the dimeric Roussin Ester sought [18]. Reaction of p-fluorobenzenediazonium tetrafluoroborate in acetone with $Na[Fe_4S_3(NO)_7]$ produced the p-fluorophenyl Roussin ester, $Fe_2(SC_6H_4F)_2(NO)_4$. The material was characterised by x-ray crystallography, fig 3-1 .

Repeating this reaction in acetonitrile (aryl diazonium salts react with acetone) the desired Roussin ester was isolated in 97% yield. In solution the Roussin alkyl esters are found to exist in a 1:1 ratio of cis and trans isomers. Analysis of $Fe_2(SC_6H_4F)_2(NO)_4$ by

$^{1}H$ ,$^{13}C$ and $^{19}F$ n.m.r. was carried out to examine the solution structure of this material. The $^{19}F$ n.m.r. (figure 3-18) shows the presence of two signals. The splitting pattern observed is identical for both; the pattern is one of a triplet of triplets. The intensities of the two absorptions are approximately equal. The $^{13}C$ n.m.r. of $Fe_2(SC_6H_4F)_2(NO)_4$ is given in figure 3-18a. Peak assignments were based on the $^{13}C$ n.m.r. of known parafluoro substituted benzene rings, the use of the $^{19}F$ coupling constants being particularly useful. In all cases except Cd the peaks are split into two absorptions, of approximately equal intensity. The $^{1}H$ n.m.r. of the complex is shown in figure 3-18b. Although complex, consideration of the $^{1}H$ n.m.r. of other parafluoro substituted benzene rings shows the pattern to be a doubling of the expected spectrum, (cf the $^{1}H$ n.m.r. spectrum of p-fluoroaniline). These results confirm that in solution the complex $Fe_2(SC_6H_4F)_2(NO)_4$ exists in two isomeric forms, of approximately equal abundance.

Since this reaction of $[Fe_4S_3(NO)_7]^-$ with an aryl diazo led to a dimeric cluster in high yield it was decided to examine its reactions with other aryl diazo compounds. It had been reported, however, that the reaction of the Black anion with p-nitrobenzene diazonium terafluorborate led to a complex with the formula $Fe_4S_3(NO)_4N_2C_6H_4NO_2$ [19] A complete characterisation of this material was lacking. The diazo compounds chosen for this work all contained a para substituted benzene ring. The attached groups ranged from electron acceptors and attractors to electron repellers and donors.

Although a similar experimental procedure was used for these other diazonium compounds as used for the p-fluoro benzenediazonium, the Roussin esters produced could not be obtained in a pure crystalline form. All the compounds made were air sensitive, especialy the p-chloro, p-cyano and the p-nitrophenyl complexes. All of the complexes obtained are degraded on an alumina column. This degradation was, at first, attributed to oxygen leaking into the column packing during the purification procedure but the degradation still occurred when the column was made up and used in an inert atmosphere dry box. None of the complexes was found to be sensitive to silica packed columns.

On addition of the desired diazonium compound to a solution of $Na[Fe_4S_3(NO)_7]$ , the vigorous evolution of gas was always observed. No brown fumes of $NO_2$ were ever noticed, and the evolved gas is presumably $N_2$. Analysis of the reaction product by I.R. spectroscopy always showed a change in the IR spectrum from the three peaks of $[Fe_4S_3(NO)_7]^-$ to

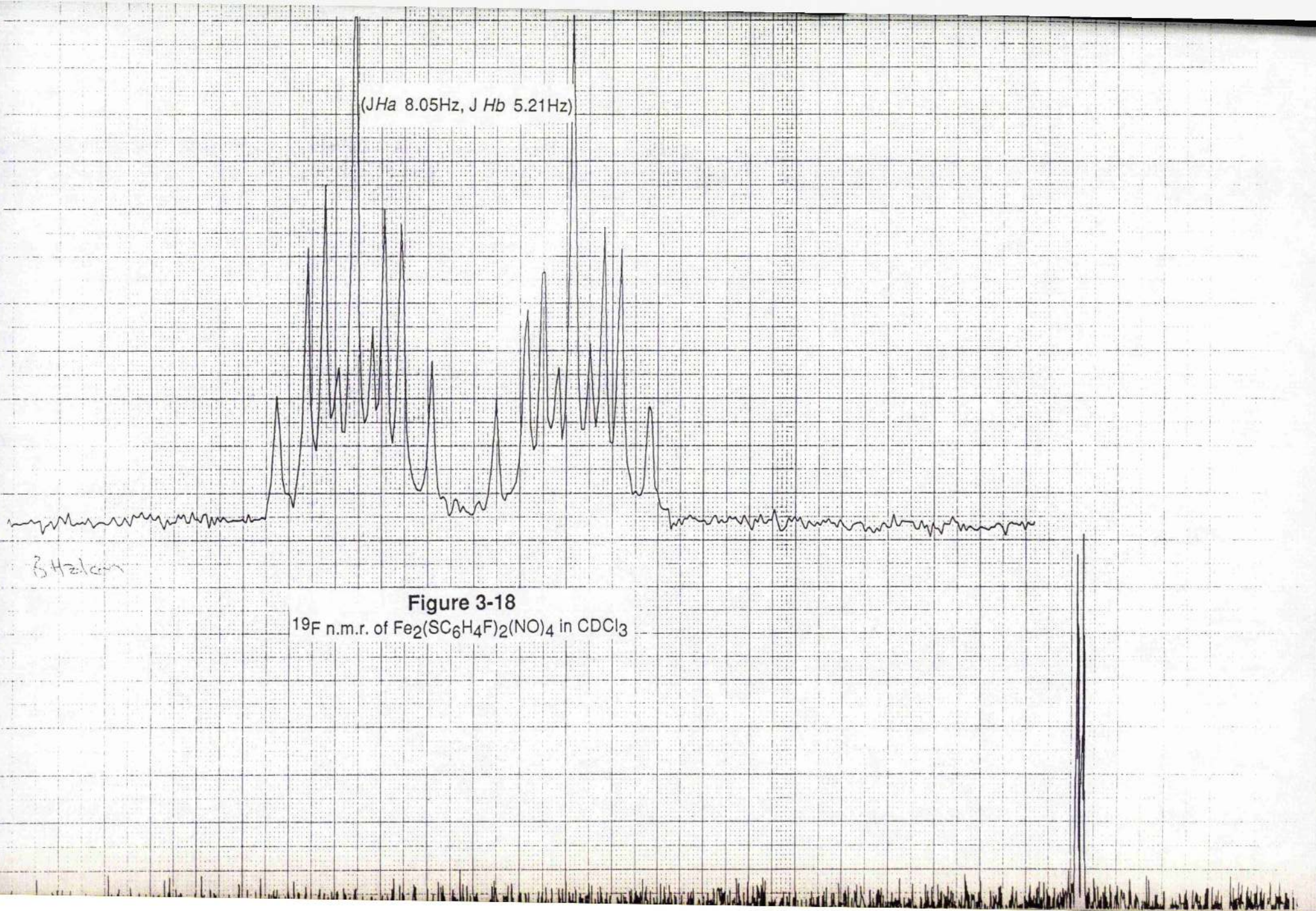


**Figure 3-18**

$^{19}F$ n.m.r. of $Fe_2(SC_6H_4F)_2(NO)_4$ in $CDCl_3$

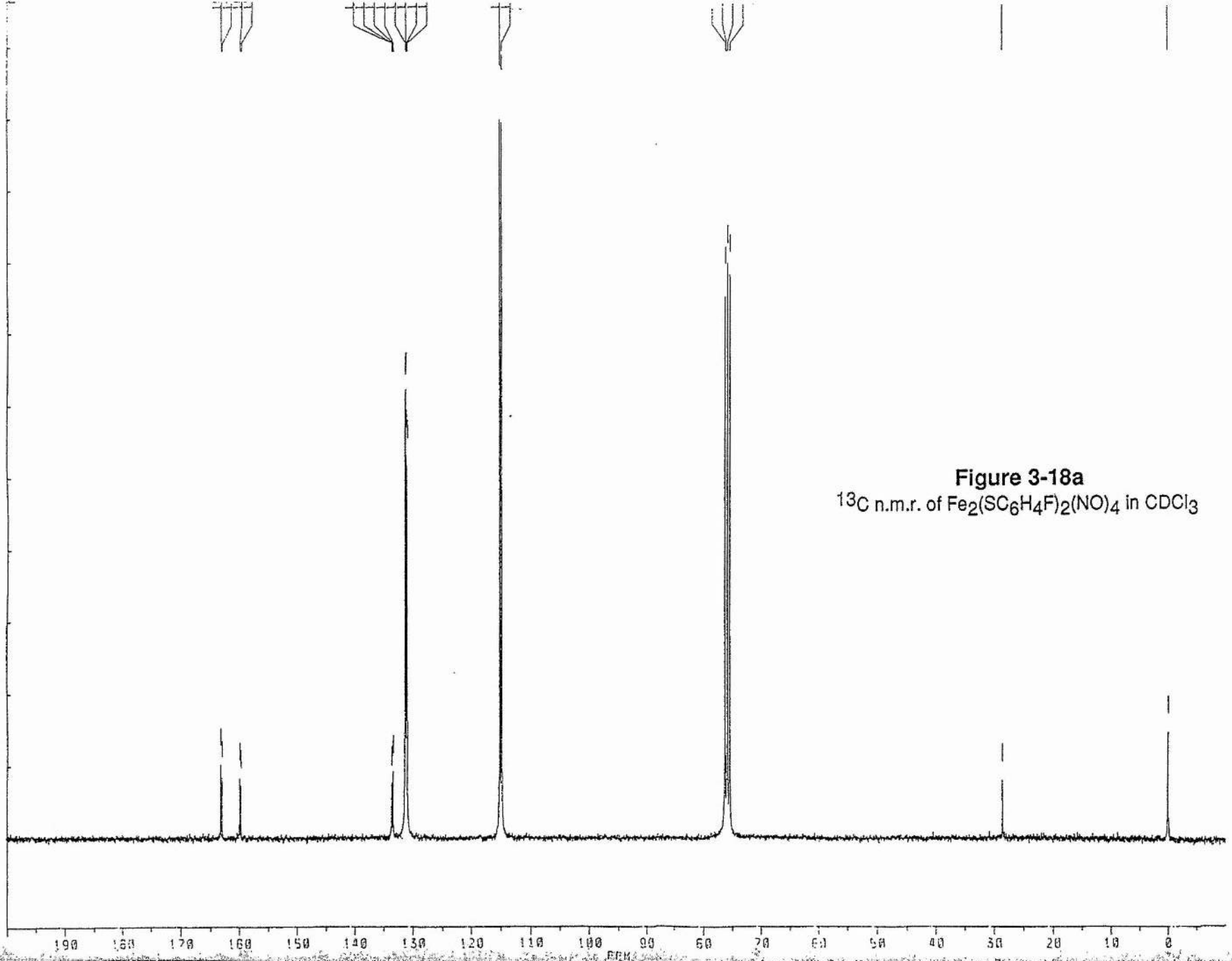


**Figure 3-18a**

$^{13}C$ n.m.r. of $Fe_2(SC_6H_4F)_2(NO)_4$ in $CDCl_3$

**Figure 3-18b**

$^1H$ n.m.r. of $Fe_2(SC_6H_4F)_2(NO)_4$ in $CDCl_3$

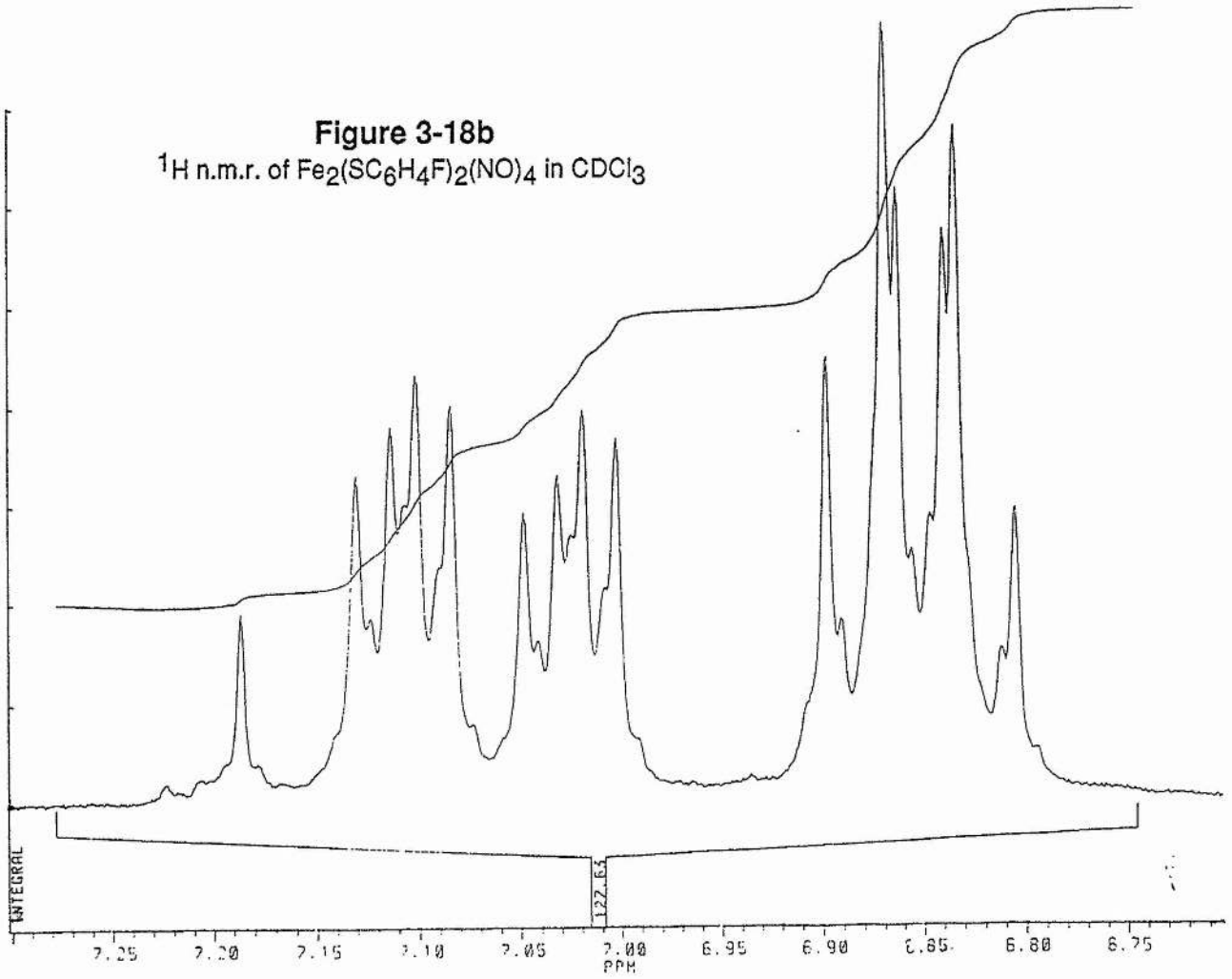

twin nitrosyl peaks of approximately of equal intensity. This immediately suggests that an iron dinitrosyl species has been produced, and with reference to the reaction of p-fluorobenzene diazonium with $[Fe_4S_3(NO)_7]^-$, this change in the IR spectrum is seen as a diagnostic test for the desired reaction.

Analysis of the materials obtained by mass-spectroscopy show the presence of the $M^+$ peaks of the required phenyl Roussin esters, and the sequential loss of four NO groups followed by the loss of the two p-substituted phenyl rings.

The results of the IR and mass-spectroscopy investigations are tabulated in table 3-4.

**Table 3-4**

| P-X- | $\nu NO_{asym}$ | $\nu NO_{sym}$ | solvent | $M^+$ peak |
|---|---|---|---|---|
| CN | 1791 | 1763 | THF | a |
| $COCH_3$ | 1792 | 1765 | DCM | 534 |
| $NO_2$ | 1790 | 1760 | DCM | a |
| F | 1789 | 1763 | CTC | 486 |
| Cl | 1787 | 1759 | BENZ | a |
| H | 1787 | 1762 | CTC | 450 |
| Me | 1795 | 1757 | CTC | 478 |
| OMe | 1784 | 1756 | DCM | 510 |

a- too air sensitive to obtain a $M^+$, only fragments observed.

Most of the $^1H$ n.m.r. spectra obtained with this work show broad features and do not allow the distinction between cis and trans isomers to be observed. The $^{13}C$ n.m.r. spectra tend to be better defined, although in many cases the spectra obtained are poor. The $^{13}C$ n.m.r. of the complex $Fe_2(SC_6H_4COCH_3)_2(NO)_4$ is given in figure 3-19. There is a strong resemblance of this spectrum to the $^{13}C$ n.m.r. of $Fe_2(SC_6H_4F)_2(NO)_4$. The splitting observed for carbons a,b and c is taken as proof for the existence of the cis and trans isomers in solution. The peak assigned to the methyl group resonance is not split and this may indicate that the further away from the ring, the less the effect of the absolute geometry on the chemical shift.

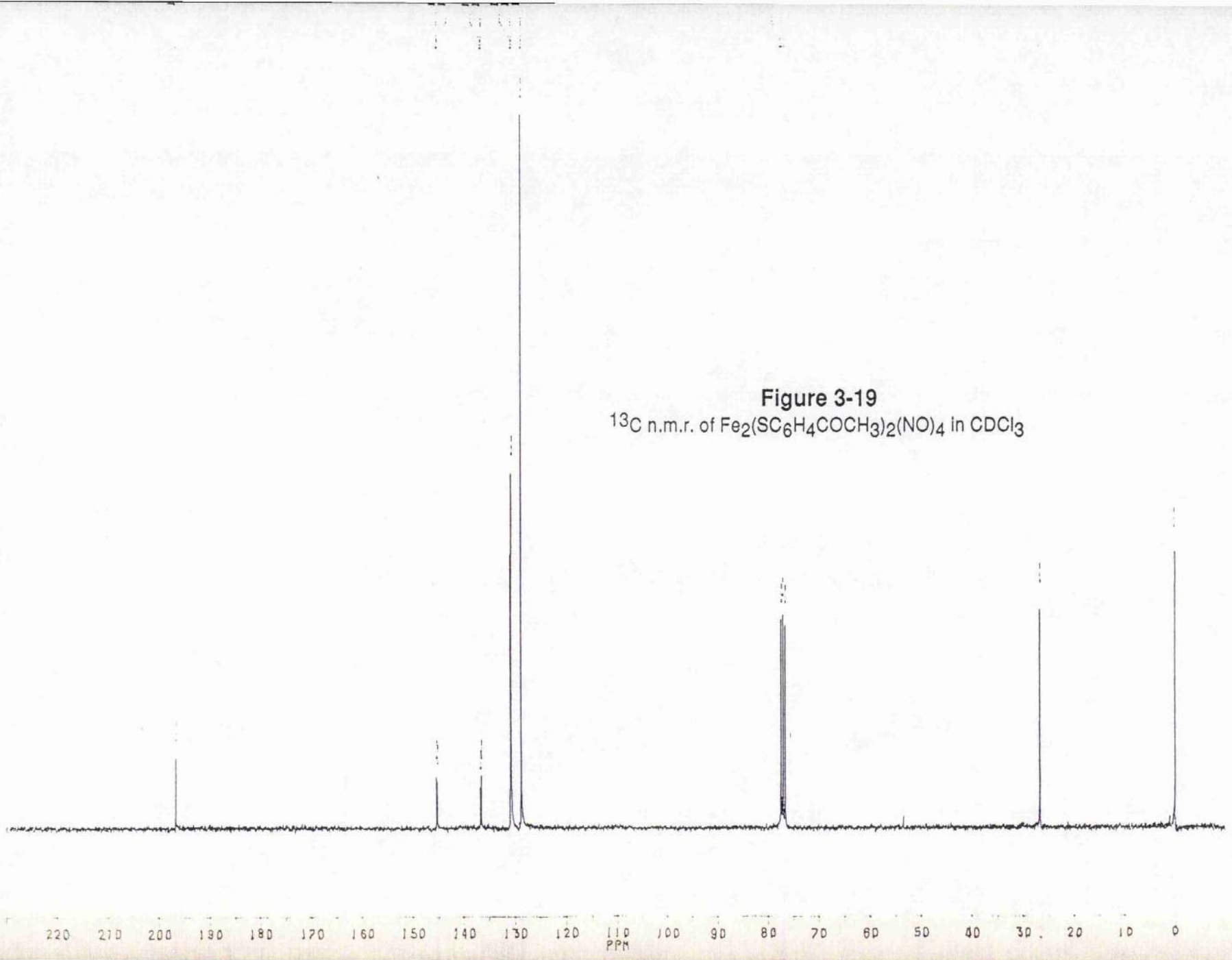


**Figure 3-19**

$^{13}C$ n.m.r. of $Fe_2(SC_6H_4COCH_3)_2(NO)_4$ in $CDCl_3$

Examination of table 3-4 shows that position of the $\nu NO_{asym}$ and $\nu NO_{sym}$ are affected somewhat by the para substituted group of the benzene ring. The trend observed moving from high to low frequency as we change from electron acceptors to electron donors, is entirely consistent with the idea of decreasing or increasing the electron density present in the iron sulphur cluster. The electron acceptors 'extract' electron density from the iron-sulphur ring thus removing a portion of the electron density used in the back bonding to the nitrosyl ligands. This has the effect of increasing the strength of the N-O bond as electron density is removed from the $\pi^*$ orbitals of N-O. The opposite effect is observed with the p-methoxy group which donates electron density into the ring.

The Japanese paper concerning the reaction of a salt of p-nitrobenzene diazonium with Roussin's Black salt gave the reaction mechanism shown on page 68 of the introduction. However, in view of the work done by the Chinese and the work described here it would appear that on reaction of Roussins Black salt with a diazonium ion the dimeric clusters $Fe_2(SR)_2(NO)_4$ are produced. Reaction of paranitrobenzenediazoniumtetrafluoroborate with Roussin's Black Salt produces a compound whose I.R. spectrum supports the formation of the dimeric cluster $Fe_2(SC_6H_4NO_2)_2(NO)_4$ as did the results of the microanalysis of the compound. This result is at odds with the result reported by the Japanese group.

The above results show that the anion $[Fe_4S_3(NO)_7]^-$ reacts with strong electrophiles such as $ArN_2^+$. The reaction mechanism may occur via attack of the sulphur, as a nucleophile, on the terminal nitrogen atom of the diazo group. The calculations carried out in chapter-2 did indeed show a large negative charge associated with the sulphur atoms of the Black anion. Examples of such a nucleophilic attack by sulphur containing compounds include the reaction of $ArN_2^+$ with arenethiolate ions, $Ar'S^-$,to give the sulphide ArSAr' [51] and with arenesulphonates to yield the diazosulphones, $ArN{=}N\text{-}SO_2Ar'$ [52]. The subsequent steps of the reaction with Roussin's Black anion involve the loss of dinitrogen and a change of nuclearity from four to two. How this is accomplished is unknown, but may go via the production of mononuclear iron fragments as discussed in part-1 of this chapter.

3-12-1 Reaction of Roussin's Black Salt with Alkylating Agents

The above work suggests that Roussin's Black salt will react with a source of electrophilic carbon. Reaction with methyl iodide nor magic methyl however do not result in

the alkylation of the Black anion with the consequent formation of $Fe_2(SMe)_2(NO)_4$. The examination of the reaction of $Na[Fe_4S_3(NO)_7]$ with various other alkyl donors was carried out.

In vivo, a major donor of methyl groups is S-adenosyl methionine. Tetrahydrofolate, shown below, is also a carrier of activated one carbon units, attached at position 5 or 10 of the pteridine ring. The transfer potential of this compound is often not sufficiently high enough for biosynthetic methylations and so S-adenosyl methionine (SAM) is used [48].

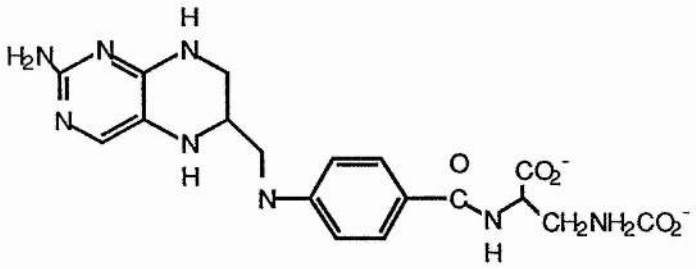

**Tetrahydrofolate**

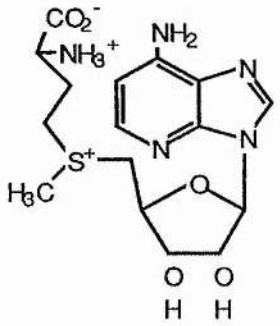

**S-Adenosylmethionine**

The positive charge associated with the sulphur atom activates the methyl group making it more reactive than tetrahydrofolate. The sequence of biosynthetic reactions involving methyl transfer are summarised below.

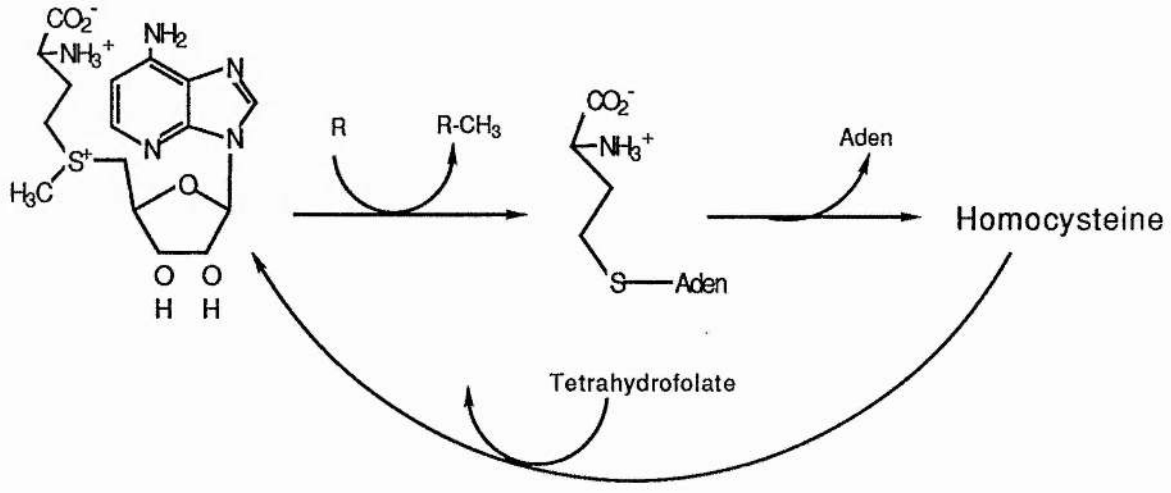


**The Activated Methyl Cycle**

A coenzyme is required to aid in the transfer of the methyl group; methylcobalamin, produced from vitamin $B_{12}$ is used to mediate this reaction. S-adenosyl methionine and its attendant enzymic complex is a very expensive chemical, because of this, laboratory analogues of this biological methylating agent were used to examine the possible reactivity of the Black anion towards such alkylating compounds.

The trimethylsulphonium ion $Me_3S^+$ is similar to the 'working end' of SAM, in that it also contains contains activated methyl groups. The reaction of the Black salt with $Me_3SI$ in water or methanol gave only the metathesis product $(Me_3S)[Fe_4S_3(NO)_7]$ as identified by IR spectroscopy and microanalysis. Refluxing the material in methanol or ethanol under $N_2$ led only to the complete recovery of the starting material. Crystals of $(Me_3S)[Fe_4S_3(NO)_7]$ were grown and were suitable for examination by X-ray crystallography. In a similar manner the reaction of a trimethylsulphoxonium salt with $Na[Fe_4S_3(NO)_7]$ led to the metathesis product $(Me_3SO)[Fe_4S_3(NO)_7]$.

Both of these materials are capable of methyl donation, and are recognised analogues of SAM. As discussed above the methyl donation of SAM is mediated by methylcobalamin. A similar catalyst for the successful reaction of $Me_3S^+$ or $Me_3SO^+$ with the Black salt may be required.

### 3-12-2 The Crystal Structure of $Me_3S[Fe_4S_3(NO)_7]$

The I.R. spectrum of the $\nu$(NO) region of $Me_3S[Fe_4S_3(NO)_7]$ in solution shows three nitrosyl absorptions identical to that of the solution IR of $Et_4N[Fe_4S_3(NO)_7]$ and identical to both the solution and solid state IR spectra of $Ph_4As[Fe_4S_3(NO)_7]$ [46]. In the solid state however the absorption pattern of $Me_3S[Fe_4S_3(NO)_7]$ was more complex, with at least five absorptions. The differences observed between the solution and the solid state suggested a possible interaction between the cation and the anion. This possible interaction was investigated by an the X-ray structural determination of $Me_3S[Fe_4S_3(NO)_7]$.

The structure consisted of isolated ions with no contacts between ions within the sums of the van der Waals' radii. Tables 3-6 and 3-7 give the fractional atomic coordinates and the

| | x | y | z | |
|---|---|---|---|---|
| Fe(1) | 253(1) | 1509(1) | 2979(1) | |
| Fe(2) | 2479(1) | 1317(1) | 1160(1) | |
| Fe(3) | -461(1) | 3468(1) | 2000(1) | |
| Fe(4) | 1777(1) | 3019(1) | 5092(1) | |
| S(1) | 213(2) | 1607(1) | 560(2) | |
| S(2) | 2451(2) | 1163(1) | 3612(2) | |
| S(3) | -469(2) | 3305(1) | 4441(2) | |
| S(4) | 3950(4) | -2158(4) | 3091(6) | |
| S(4') | 6617(13) | 2885(11) | 6623(12) | |
| N(1) | -702(5) | 456(4) | 3191(5) | |
| N(2) | 3333(6) | 2465(5) | 1116(6) | |
| N(3) | 3042(6) | -9(6) | -20(6) | |
| N(4) | 649(6) | 4412(4) | 1785(5) | |
| N(5) | -2095(6) | 3803(5) | 1567(6) | |
| N(6) | 2737(5) | 4012(5) | 4712(6) | |
| N(7) | 1766(6) | 2987(5) | 6945(6) | |
| O(1) | -1358(6) | -300(5) | 3324(6) | |
| O(2) | 4069(6) | 3157(6) | 950(7) | |
| O(3) | 3614(6) | -797(6) | -936(7) | |
| O(4) | 1217(6) | 5173(4) | 1536(6) | |
| O(5) | -3143(6) | 4250(5) | 1209(7) | |
| O(6) | 3485(6) | 4739(5) | 4746(7) | |
| O(7) | 1901(7) | 3146(5) | 8268(5) | |
| C(1) | 2090(8) | -2042(7) | 2628(10) | |
| C(2) | 4461(11) | -3657(10) | 2405(12) | |
| C(3) | 3857(10) | -2014(12) | 5192(11) | |
| S('') | 3677(29) | -1656(24) | 3889(32) | 98(8) |
| C(') | 4975(27) | -1465(23) | 2739(28) | 61(6) |

**Table 3-5**

Fractional Atomic Coordinates (x10) for $Me_3S[Fe_4S_3(NO)_7]$

## Table 3-6

Bond Lengths and Angles for $Me_3S[Fe_4S_3(NO)_7]$

| | | | |
|---|---|---|---|
| Fe(3)-Fe(1)-Fe(2) | 82.9° | Fe(4)-Fe(1)-Fe(2) | 83.3° |
| Fe(4)-Fe(1)-Fe(3) | 83.1 | S(1)-Fe(1)-Fe(2) | 53.7 |
| S(1)-Fe(1)-Fe(3) | 53.5 | S(1)-Fe(1)-Fe(4) | 118.6(2) |
| S(2)-Fe(1)-Fe(2) | 53.7 | S(2)-Fe(1)-Fe(3) | 118.2(2) |
| S(2)-Fe(1)-Fe(4) | 53.6 | S(2)-Fe(1)-S(1) | 107.4(2) |
| S(3)-Fe(1)-Fe(2) | 117.8(2) | S(3)-Fe(1)-Fe(3) | 53.4 |
| S(3)-Fe(1)-Fe(4) | 53.3 | S(3)-Fe(1)-S(1) | 106.8(2) |
| S(3)-Fe(1)-S(2) | 106.9(2) | N(1)-Fe(1)-Fe(2) | 129.4(3) |
| N(1)-Fe(1)-Fe(3) | 130.5(2) | N(1)-Fe(1)-Fe(4) | 130.0(3) |
| N(1)-Fe(1)-S(1) | 111.4(3) | N(1)-Fe(1)-S(2) | 111.3(3) |
| N(1)-Fe(1)-S(3) | 112.7(3) | Fe(3)-Fe(2)-Fe(1) | 48.6 |
| Fe(4)-Fe(2)-Fe(1) | 48.5 | Fe(4)-Fe(2)-Fe(3) | 60.1 |
| S(1)-Fe(2)-Fe(1) | 51.9 | S(1)-Fe(2)-Fe(3) | 37.5 |
| S(1)-Fe(2)-Fe(4) | 89.7 | S(2)-Fe(2)-Fe(1) | 52.2 |
| S(2)-Fe(2)-Fe(3) | 89.9 | S(2)-Fe(2)-Fe(4) | 37.5 |
| S(2)-Fe(2)-S(1) | 104.1(2) | N(2)-Fe(2)-Fe(1) | 123.1(3) |
| N(2)-Fe(2)-Fe(3) | 84.3(3) | N(2)-Fe(2)-Fe(4) | 83.6(3) |
| N(2)-Fe(2)-S(1) | 111.2(3) | N(2)-Fe(2)-S(2) | 109.6(3) |
| N(3)-Fe(2)-Fe(1) | 120.2(3) | N(3)-Fe(2)-Fe(3) | 143.1(2) |
| N(3)-Fe(2)-Fe(4) | 146.1(2) | N(3)-Fe(2)-S(1) | 105.8(3) |
| N(3)-Fe(2)-S(2) | 108.7(3) | N(3)-Fe(2)-N(2) | 116.7(4) |
| Fe(2)-Fe(3)-Fe(1) | 48.4 | Fe(4)-Fe(3)-Fe(1) | 48.4 |
| Fe(4)-Fe(3)-Fe(2) | 60.1 | S(1)-Fe(3)-Fe(1) | 51.8 |
| S(1)-Fe(3)-Fe(2) | 37.6 | S(1)-Fe(3)-Fe(4) | 89.7 |
| S(3)-Fe(3)-Fe(1) | 52.1 | S(3)-Fe(3)-Fe(2) | 89.6 |
| S(3)-Fe(3)-Fe(4) | 37.1 | S(3)-Fe(3)-S(1) | 103.9(2) |
| N(4)-Fe(3)-Fe(1) | 124.5(3) | N(4)-Fe(3)-Fe(2) | 84.4(3) |
| N(4)-Fe(3)-Fe(4) | 86.1(3) | N(4)-Fe(3)-S(1) | 110.0(3) |
| N(4)-Fe(3)-S(3) | 112.3(3) | N(5)-Fe(3)-Fe(1) | 120.6(3) |
| N(5)-Fe(3)-Fe(2) | 146.3(2) | N(5)-Fe(3)-Fe(4) | 143.1(2) |
| N(5)-Fe(3)-S(1) | 108.8(3) | N(5)-Fe(3)-S(3) | 106.2(3) |
| N(5)-Fe(3)-N(4) | 115.0(4) | Fe(2)-Fe(4)-Fe(1) | 48.2 |
| Fe(3)-Fe(4)-Fe(1) | 48.4 | Fe(3)-Fe(4)-Fe(2) | 59.8 |
| S(2)-Fe(4)-Fe(1) | 52.0 | S(2)-Fe(4)-Fe(2) | 37.4 |
| S(2)-Fe(4)-Fe(3) | 89.5 | S(3)-Fe(4)-Fe(1) | 52.1 |
| S(3)-Fe(4)-Fe(2) | 89.3 | S(3)-Fe(4)-Fe(3) | 37.1 |
| S(3)-Fe(4)-S(2) | 104.1(2) | N(6)-Fe(4)-Fe(1) | 125.2(3) |
| N(6)-Fe(4)-Fe(2) | 85.4(3) | N(6)-Fe(4)-Fe(3) | 86.4(3) |
| N(6)-Fe(4)-S(2) | 110.5(3) | N(6)-Fe(4)-S(3) | 112.1(3) |
| N(7)-Fe(4)-Fe(1) | 119.0(3) | N(7)-Fe(4)-Fe(2) | 145.5(2) |
| N(7)-Fe(4)-Fe(3) | 142.5(2) | N(7)-Fe(4)-S(2) | 108.1(3) |
| N(7)-Fe(4)-S(3) | 105.4(3) | N(7)-Fe(4)-N(6) | 115.8(4) |
| Fe(2)-S(1)-Fe(1) | 74.3(2) | Fe(3)-S(1)-Fe(1) | 74.7 |
| Fe(3)-S(1)-Fe(2) | 104.9(2) | Fe(2)-S(2)-Fe(1) | 74.2(2) |
| Fe(4)-S(2)-Fe(1) | 74.4(2) | Fe(4)-S(2)-Fe(2) | 105.2(2) |
| Fe(3)-S(3)-Fe(1) | 74.6(2) | Fe(4)-S(3)-Fe(1) | 74.6(2) |
| Fe(4)-S(3)-Fe(3) | 105.8(2) | C(1)-S(4)-S('') | 81.0(22) |
| C(2)-S(4)-S('') | 140.9(21) | C(2)-S(4)-C(1) | 104.5(6) |
| C(3)-S(4)-S('') | 41.5(20) | C(3)-S(4)-C(1) | 99.7(6) |
| C(3)-S(4)-C(2) | 100.1(7) | C(')-S(4)-S('') | 95.5(24) |
| C(')-S(4)-C(1) | 126.4(12) | C(')-S(4)-C(2) | 110.2(12) |
| C(')-S(4)-C(3) | 112.4(12) | C(1)-S('')-S(4) | 73.5(21) |
| C(3)-S('')-S(4) | 114.7(29) | C(3)-S('')-C(1) | 120.0(19) |
| C(')-S('')-S(4) | 56.0(20) | C(')-S('')-C(1) | 108.0(18) |
| C(')-S('')-C(3) | 125.9(22) | O(1)-N(1)-Fe(1) | 178.8(5) |
| O(2)-N(2)-Fe(2) | 170.3(6) | O(3)-N(3)-Fe(2) | 166.5(6) |
| O(4)-N(4)-Fe(3) | 167.7(5) | O(5)-N(5)-Fe(3) | 165.7(6) |
| O(6)-N(6)-Fe(4) | 166.6(5) | O(7)-N(7)-Fe(4) | 167.2(5) |
| S('')-C(1)-S(4) | 25.5(8) | S('')-C(3)-S(4) | 23.9(12) |
| S('')-C(')-S(4) | 28.5(10) | | |

Bond lengths (A)

| | | | |
|---|---|---|---|
| Fe(2)-Fe(1) | 2.695(4) | Fe(3)-Fe(1) | 2.703(4) |
| Fe(4)-Fe(1) | 2.704(4) | S(1)-Fe(1) | 2.203(4) |
| S(2)-Fe(1) | 2.212(4) | S(3)-Fe(1) | 2.213(4) |
| N(1)-Fe(1) | 1.657(7) | Fe(3)-Fe(2) | 3.575(5) |
| Fe(4)-Fe(2) | 3.588(5) | S(1)-Fe(2) | 2.256(4) |
| S(2)-Fe(2) | 2.257(4) | N(2)-Fe(2) | 1.647(8) |
| N(3)-Fe(2) | 1.673(8) | Fe(4)-Fe(3) | 3.587(5) |
| S(1)-Fe(3) | 2.254(4) | S(3)-Fe(3) | 2.250(4) |
| N(4)-Fe(3) | 1.657(7) | N(5)-Fe(3) | 1.653(8) |
| S(2)-Fe(4) | 2.261(4) | S(3)-Fe(4) | 2.249(4) |
| N(6)-Fe(4) | 1.661(7) | N(7)-Fe(4) | 1.673(7) |
| S('')-S(4) | 0.823(27) | C(1)-S(4) | 1.832(10) |
| C(2)-S(4) | 1.723(14) | C(3)-S(4) | 1.849(13) |
| C(')-S(4) | 1.428(27) | C(1)-S('') | 1.887(30) |
| C(3)-S('') | 1.348(27) | C(')-S('') | 1.715(39) |
| O(1)-N(1) | 1.167(7) | O(2)-N(2) | 1.166(8) |
| O(3)-N(3) | 1.161(8) | O(4)-N(4) | 1.161(7) |
| O(5)-N(5) | 1.175(8) | O(6)-N(6) | 1.157(7) |
| O(7)-N(7) | 1.154(7) | | |

**Figure 3-20**
Perspective view of the structure of $(Me_3S)[Fe_4S_3(NO)_7]$

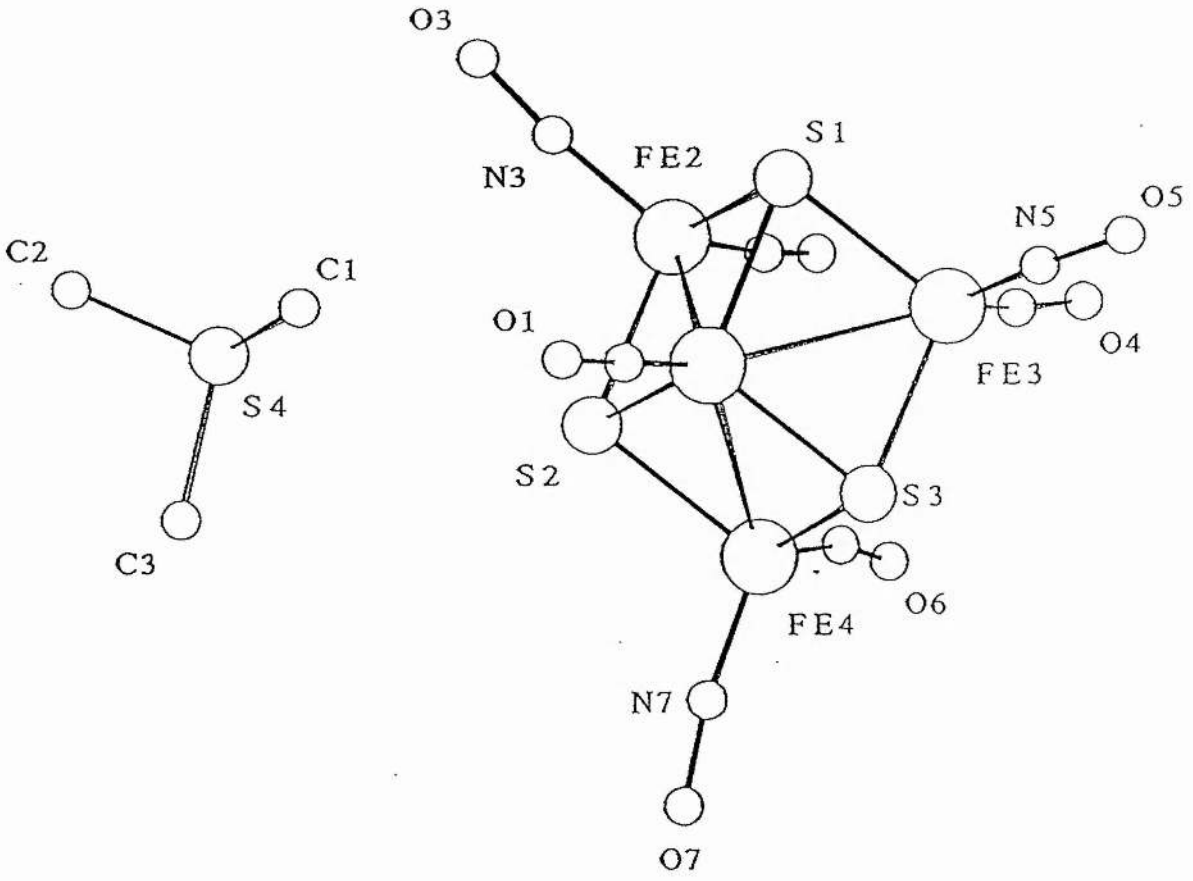


**Figure 3-21**
Perspective view of the cation in $(Me_3S)[Fe_4S_3(NO)_7]$

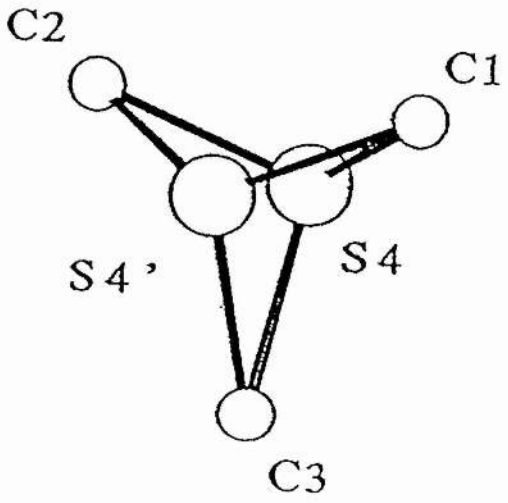

bondlengths and angles for the cluster respectively. Figure 3-20 shows a perspective view of the unit cell of the structure showing the relationship of the cation to the anion. Figure 3-21 shows the disorder observed for the cation. The structure of the anion is very similar to that found in the $Ph_4As^+$ [46]. Although mean values for given geometric parameters are almost the same in the two determinations, the anion in $Me_3S[Fe_4S_3(NO)_7]$ approximates much more closely to $C_{3v}$ symmetry than the anion in $Ph_4As[Fe_4S_3(NO)_7]$; thus the three independent iron-iron distances around the base of the tetrahedron involving Fe(2), Fe(3) and Fe(4) are 3.575, 3.587 and 3.588Å (range 0.013Å, mean 3.583Å) in the $Me_3S^+$ salt, but 3.519, 3.564 and 3.628Å (range 0.109Å , mean 3.570Å) in the $PH_4As^+$ salt. The apical iron, Fe(1) carries a single nitrosyl ligand for which the Fe-N-O angle 178.8° is close to 180°. The basal iron atoms each form $Fe(NO)_2$ fragments in which the Fe-N-O groups are bent towards one another, with a mean Fe-N-O angle of 167.3°; the structures of such $Fe(NO)_2$ fragments is discussed at length in chapter two. Within each basal $Fe(NO)_2$ the mean equatorial Fe-N distance is just significantly longer than the mean axial Fe-N distance, as also found in a recent study of $Ph_4As[Fe_4Se_3(NO)_7]$ [53]. The structure reported here for the anion $[Fe_4S_3(NO)_7]^-$ is more precise than that reported previously, as the $Ph_4As^+$ salt [46]; in the earlier work, the determination was based on 2148 observed reflections for 452 variables (ratio 4.8), while in the work presented here there are 2553 observed reflections for 244 variables (ratio 10.6). There is no indication from the structure either of a close approach between one of the sulphur atoms in the cation to the basal triangle of the anion with incipient closure of an $Fe_4S_4$ cuboid framework.

### 3-12-3 Reaction of Roussin's Black Salt with Trialkyl Oxonium Salts

In the absence of a specific catalyst to increase the potency of the methyl donor, increasing the ability of the methyl donor *itself* to donate is a likely route. Oxygen is a more electronegative element than sulphur and so replacing the trimethylsulphonium salts with trimethyloxonium salts would lead to a greater $\partial^+$ charge on the methyls, making such salts better methyl donors.

Reaction of the strong electrophile $Me_3OBF_4$ in water with $NaFe_4S_3(NO)_7]$ followed by immediate extraction into $CH_2Cl_2$, leads to the production of $Fe_2(SMe)_2(NO)_4$. Prolonged

stirring leads to decomposition, presumably due to the $HBF_4$ produced. Reaction of $Et_3OBF_4$ with the Black salt in $CH_2Cl_2$ produces $Fe_2(SEt)_2(NO)_4$. The use of $Me_3OSbCl_6$ as an analogue of SAM was detrimental to the experiment. Prolonged stirring of this methyl donor with the Black salt in dry acetonitrile caused the complete decomposition of the black salt and any methyl ester formed. Reaction in water with immediate extraction into dichloromethane gave small amounts of $Fe_2(SMe)_2(NO)_4$, but extensive decomposition was evident. Although the $SbCl_6^-$ ion is supposedly inert, it has apparently played some role in this reaction.

3-13 Reaction of Roussin's Black Salt with 2-Iodo-2-Methylpropane

Since Roussin's Black salt does not react with MeI nor magic methyl but does with trialkyloxonium salts, it suggests that the reaction may involve the production of carbonium ions. If the Black salt is refluxed in methanol with an excess of 2-iodo-2-methyl propane then a dinitrosyl species was produced. Evidence gained, however shows that it is not $Fe_2(S^tBu)_2(NO)_4$, but the iodo-bridged complex $Fe_2I_2(NO)_4$. 2-iodo-2-methyl propane dissociates in polar solvents to a small extent to give a carbonium ion and also the iodide ion. The carbonium ion will have a short life time and may not survive long enough to react with Roussin's Black anion. Work by Johnson [54] showed from an e.p.r. examination, that addition of iodide to DMF solutions of the Black anion gave rise to paramagnetic dinitrosyl iron fragments which contained coordinated iodide. The isolation of the bridged iodo complex using 2-iodo-2-methyl propane and the fact that the Black anion does not react with methyl iodide suggests that this reaction does proceed via the dissociation of the organic iodide. This method of producing the iodo complex could lead to a preparative method of labelling this complex with $^{15}N$, since the formation of the Black anion involves the use of sodium nitrite and the method of preparing the iodo complex involves NO(g). This reaction is also further evidence for the formation of dimeric nitrosyl clusters from the tetrameric Black anion.

3-14 Reaction of Roussin's Black Anion with the $Me_3S^+$ ion

As discussed above, the problem with the reaction of trialkylsulphonium salts was that they were not reactive enough to donate a methyl group to the Black salt. This problem was overcome by changing to the trialkyloxonium salts. Another method of solving this problem would be to make the Black salt a better nucleophile. An examination of the electrochemistry of Roussin's Black salt (see chapter four) revealed the presence of three reduced states;

$RBS^{-1}$--> $RBS^{-2}$--> $RBS^{-3}$--> $RBS^{-4}$. The E.H.M.O. calculations on the anion $[Fe_4S_3(NO)_7]^-$ showed that the LUMO and the LUMO+1 orbitals (of approximate equal energy) have more electron density on the sulphur atoms compared to the HOMO. If on reduction the sulphur atoms were to gain more electron density then the reduced state would perhaps act as a better nucleophile. The reduction of $[Fe_4S_3(NO)_7]^-$ with sodium benzophenone in the presence of the trimethylsulphonium ion, produced small quantities of $Fe_2(SMe)_2(NO)_4$, showing that the original premise may be correct.

3-15 Summary of the Reactions of Roussin's Black Anion

The reactions of Roussin's Black anion are summarised below;

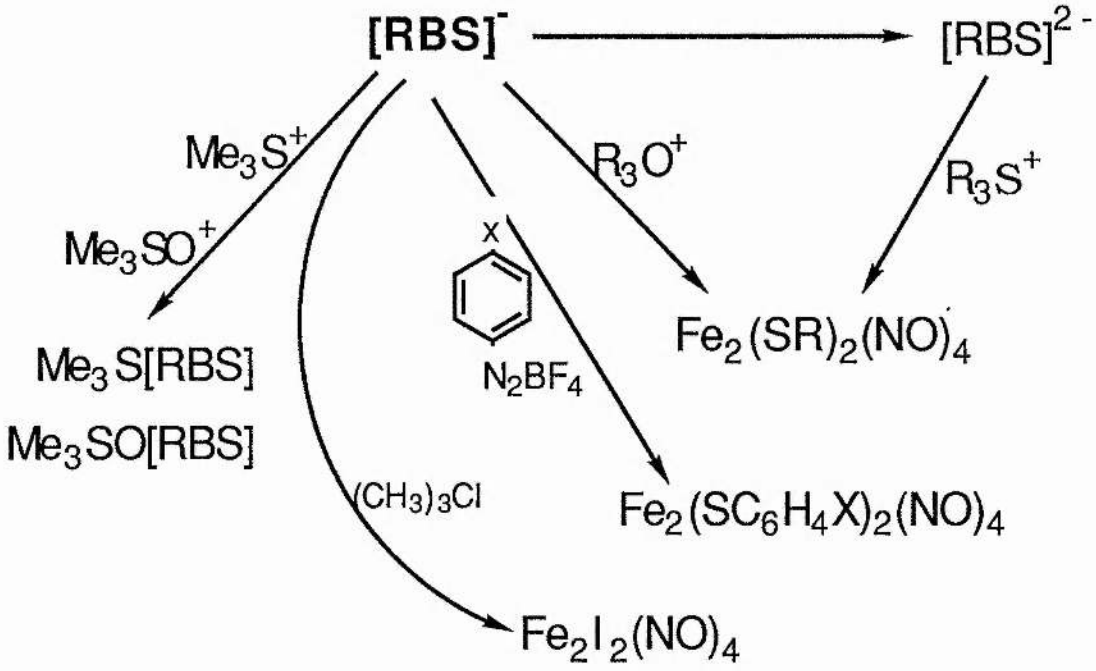


3-16 Reaction of $Fe_4S_4(NO)_4$ with p-Fluorobenzenediazonium Tetrafluoroborate

The high yield of the reaction of p-fluorobenzenediazonium salt with the Black salt suggests that the $[Fe(NO)]^{2+}$ to $[Fe(NO)_2]^+$ ( $d^7$ to $d^9$ ) conversion occurs. The iron atoms in the cubic cluster, $Fe_4S_4(NO)_4$, are all in the $d^7$ oxidation state. Reaction of this cluster with p-fluorobenzene diazonium tetrafluoroborate produced very small quantities of the p-fluorophenyl ester of Roussin's Red salt, as identified by mass-spectroscopy and I.R.

spectroscopy. This confirms that the $d^7$ to $d^9$ conversion has occurred.

In summary, Roussin's Black salt which is a possible intermediate in the possible conversion of the non-haem iron proteins into the mutagenic $Fe_2(SMe)_2(NO)_4$, can be converted into the dimeric complexes of type $Fe_2(SR)_2(NO)_4$ , where R=alkyl or aryl, by the action of electrophiles. From a biological point of view, this work suggests that the methylating agent S-adenosyl methionine in conjunction with methylcobalamin could be responsible for the in vivo methylation of $[Fe_4S_3(NO)_7]^-$ with the consequent production of $Fe_2(SMe)_2(NO)_4$.

## References


1. Roussin, F. Z., Ann. Chim. Phys., 52, 285, (1858)

2. Pavel, O., Ber.Dtsch. Chem. Ges.,15, 2600, (1882)

3. Hofmann, K. A., Wiede, O. F., Z. Anorg. Allgem. Chem., 9, 295, (1895)

4. Brauer, G.(ed), "Handbuch der Praparativen Anorganischen Chemie.", 2nd Edition Vol 2, 1526, Enke, Stuttgart, (1960)

5. Butler, A. R., Glidewell, C., Hyde, A. R., McGinnis, J., Seymour, J. E., Polyhedron, 2, 1045 (1983)

6. Butler, A. R., Glidewell, C., Hyde, A. R., Walton, J. C., Polyhedron, 4, 797, (1985)

7. Seyferth, D., Gallagher, M. K., J. Organomet. Chem., 218, C5-C10, (1981)

8. Seyferth, D., Gallagher, M. K., Cowie, M., Organometallics, 5, 539, (1986)

9. Mazany, A. M., Fackler, J.P.,Jr.,Gallagher, M. K., Seyferth, D., Inorg. Chem., 22, 2593, (1983)

10. King, R.B., J. Am. Chem. Soc., 84,2460 (1962)

11. DeBeer, J. A., Haines, R. J., J. Organomet. Chem., 24, 757, (1970)

12. Rauchfuss, T. B., Weatherill, T. D., Inorg. Chem.,21, 827 (1982)

13. Butler, A. R., Glidewell, C., Hyde, A. R., Walton, J. C., Polyhedron, 4, 303, (1985)

14. Manchot, W., Ber. Dtsch. Chem. Ges., 59, 2445, (1926)

15. Baty, J.D., Willis, R.G., Burdon, M.G., Butler, A.R., Glidewell, C., Johnson, I.L., Massey, R., Inorg. Chim. Acta 138, 15 (1987)

16. Ashworth, J., Didcock, A., Hargreaves, L. L., Jarvis, B., Walters, C. L., Larkworthy, L. F.,J. Gen. Microbiol., 84, 403, (1974)

17. Butler, A. R., Glidewell, C., Hyde, A. R., Walton, J. C., Inorg. Chim Acta 106, L7, (1985)

18. Jinhau, C., Shaoping, M., Jingling, H., Jiaxi, L., J. Struct. Chem., 2, 2263,

(1983)

19. Miwa,M., Iwasawa, K., Seikei Daigaku Kogakubu Kogaku Hokoku, 22, 1572, (1976); Chem. Abs., 86, 50094e, (1977)

20. Hieber, W.,Gruber, J., Z. Anorg. Allg. Chem., 91, 296, (1958): Anderson, E.L., Fehlner, T., Foti, A. E., Salahub, D.R., J. Am. Chem. Soc., 102,7422, (1980)

21. Perrin, D. D., Armarego, W. F., Perrin, D. R., "Purification of Laboratory Chemicals", Pergamon Press, 1st Edition (1966)

22. Herzberg, G., " Spectra of Diatomic Molecules" 2nd edition, p141, van Nostrand Reinhold, N.Y.,(1950)

23. Biochem. Biiophys. Res. Commun., 56, 654, (1974)

24. Hoffmann, R., J. Chem. Phys.,39, 1397, (1963)

25. Howell. J., Rossi. A., wallaon. D., Haruki. K., Hoffmann. R., Quantum Chemistry Exchange Program 344.

26. Albright, T. A., Hoffmann, R., Hibeault, J. C., Thorn, D. L., J. Am. Chem. Soc., 101, 3801, (1979)

27. Goldberg, K. I., Hoffmann, D. M., Hoffmann, R., Inorg. Chem. 21, 3863, (1982)

28. Hughbanks, T., Hoffmann, R., J. Am. Chem. Soc., 105, 3528, (1983)

29. Feltham, R.D., Haymore, B., Inorg. Synth. (vol.14), 81

30. Greenwood, N. N., Earnshaw, A., "Chemistry of the Elements" 1st edition, p848, Pergamon Press, Oxford, (1984)

31. Lewis, J., Irving, R. J., Wilkinson, G., J. Inorg. Nucle. Chem., 7, 32, (1958)

32. Glidewell, C., Harman, M. E.,Hursthouse, M. B., Johnson, I. L., Motevalli, M., J. Chem Research, (S) 212, (M) 1676, (1988)

33. Thomas, J. T., Robertson, J. H., Cox, E. G., Acta Cryst., 11, 599, (1982)

34. Marøy, K., Acta Chem. Scand., 25, 2580, (1971)

35. Marøy, K., Acta Chem. Scand., 27, 1684, (1973)

36. Butler, A.R., Glidewell, C., Hyde, A.R., M$^{c}$Ginnis, J., Inorg. Chem. 24, 2931, (1985)

37. Glidewell, C., Johnson, I. L., Chem. Scripta, 27, 441, (1987)

38. Bell, L. K., Mingos, D. M. P., Tew, D.G., Larkworthy L. F., Sandell, B., Povey, D. C., Mason, J., J. Chem. Soc. Chem. Commun., 125, (1983)

39. Bell, L. K., Mason, J., Mingos, D. M. P., Tew, D. G., Inorg. Chem. 22, 3497, (1983)

40. Evans, D. H., Mingos, D. M. P., Mason, J., Richards, A., J. Organomet. Chem., 249, 293,(1983)

41. Butler, A. R., Glidewell, C., Johnson, I. L., Polyhedron, 6, 2091, (1987) : a) Lambert, R.J., Johnson, I.L., unpublished work

42. Atkins, P. W., "Physical Chemistry" 2$^{nd}$ Edition, pp 634-644, Oxford University press, Oxford, (1982)

43. Butler, A. R., Glidewell, C.,Johnson, I. L., Walton, J. C., Polyhedron, 6, 2085, (1987)

44. Cambi, L., Cagnasso, A., Atti. accad. naz. Lincei, 13, 254, 809, (1931): Inorg. Synth. 16, 5.

45. Spiro, T. G.," Iron Sulphur Proteins" (1982) Wiley (Publishers); Mason, R., Zubieta, J. A., Angew. Chem. Int. Edit., 12, 390, (1973): Holm, R. H., Accs. Chem. Research, 10, 427, (1977): Lippard, S. J., Accs. Chem. Research, 6,282, (1973)

46. Chu, C, T., Dahl, L. F., Inorg. Chem., 16, 3245, (1977)

47. Chu, C. T., Lo, F. Y., Dahl, L. F., J. Am. Chem. Soc. 104, 3409, (1982)

48. Stryer, L.,"Biochemistry" 3$^{rd}$ Edition, pp 580-584, W. H. Freeman and Company, Ney York (1988)

49. Hursthouse, M. B., Jones, R. A., Malik, H. M. A., Wilkinson, G., J. Am. Chem. Soc., 101, 4128, (1979)

50. Goodman, B. A., Raynor, J. B., Symons, M. C. R., J. Chem. Soc. (A), 2572, (1969)

51. Price, C. C., Tsanawski, S., J. Org. Chem., 28, 1867, (1963)

52. Ritchie, C. D., Saltell, J. D., Lewis, E. S., J. Am. Chem. Soc, 83, 4601, (1961)

53. Lees, A., University of St. Andrews, Awaiting publication

54. Johnson, I. L., unpublished work

# Chapter Four

# Chapter Four

# The Electrochemistry of some of the Roussin Esters and the Electrochemistry of the Red and Black Roussin Salts

## Introduction

Cyclic voltammetry, C.V., has become a widely used technique for identifying the redox states available to a compound. Although it has been used in the study of organic molecules [1], it is with the rich redox chemistry found with metal complexes [2] and clusters [3] that cyclic voltammetry has become the preferred electrochemical characterisation technique.

The C.V. experiment can lead to information concerning the $E^{\emptyset}$ values of a redox couple; it can yield information concerning the stabilities of redox states reached [4] and can also lead to rate constant and formation constant evaluations [5]. This is because the technique scans a voltage across an electrochemical cell at a rate fixed by the experimentalist. The rate of scan can be varied and so the voltage scan is also a function of time.

In this chapter the electrochemistry of the Roussin esters, $Fe_2(SR)_2(NO)_4$, for a range of R is examined mainly through the use of cyclic voltammetry. Some of the chemistry of the reduced and oxidised forms of the Roussin esters is also discussed. A possible reason for the mutagenic behaviour of the Methyl Roussin ester, $Fe_2(SMe)_2(NO)_4$, is suggested on the basis of these results. Further, the electrochemistry of the tetranuclear cluster $[Fe_4E_3(NO)_7]M$, (E=S, M=Na, $Et_4N$, $Bu_4N$, $Me_3S$, and $Me_3SO$; E=Se, M=Na) are also examined.

# Experimental

Cell Design:

For the C.V. experiment a three electrode cell is used. Two electrodes carry the current, one of which, the working electrode, is solely responsible for the size of the current passed, the other is termed the counter electrode and makes up the other half of the electrochemical cell. The third electrode is a reference electrode which measures the potential at the working electrode. Fig 4-1.

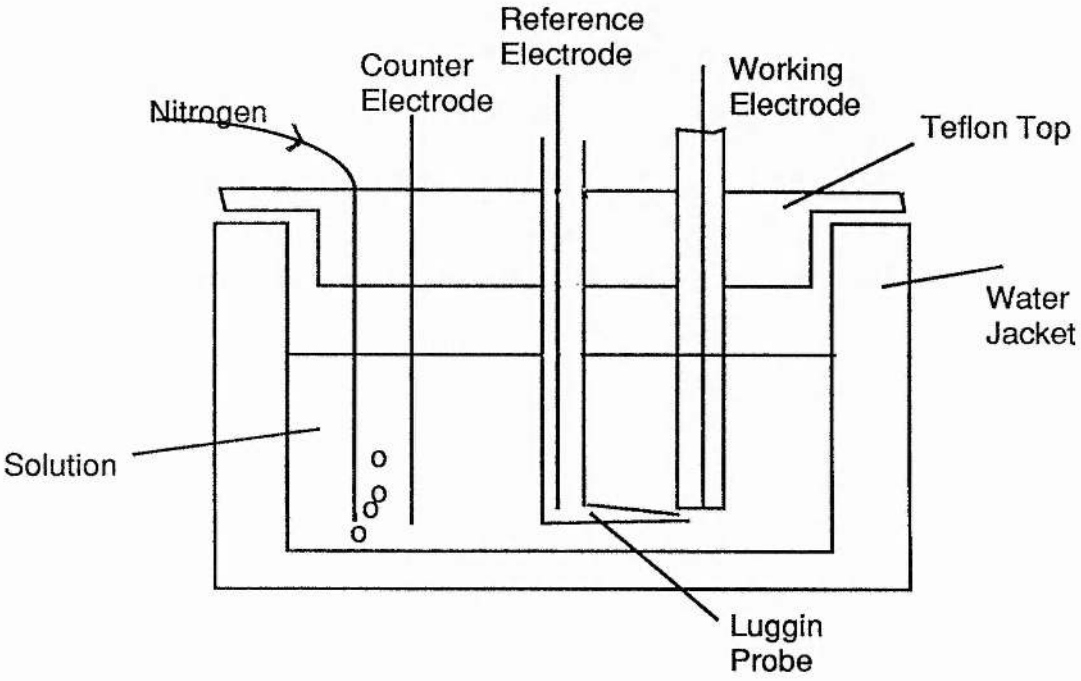


The solvent in which the experiment is taking place is thermostated to 25°C. The solution is deoxygenated by bubbling nitrogen through the solution for a period of time (5-10 minutes). The nitrogen inlet is then removed from the body of the solution and placed above it to ensure a blanket of nitrogen is always present to prevent the re-entry of oxygen into the cell. This means that evaporation of the solvent during an experiment becomes a problem, and so the nitrogen is passed through a bubbler, containing the same solvent, prior to entry into the electrochemical cell.

Electrodes:

The counter electrode used in this work was a length of platinum wire. The only requirements for a counter electrode are that the material be chemically inert and that the

area of the electrode is greater than that of the working electrode. This electrode was cleaned, prior to use, by wiping clean with acetone, and then heating to white heat in a bunsen flame.

The working electrodes used in this work were either a Pt disc electrode imbedded in either glass or kevlar or a glassy carbon electrode (G.C.E.) also imbedded in kevlar, (the kevlar imbedded electrodes were supplied by Bioanalytical systems [6]). Both types of electrodes were cleaned by rinsing in acetone and then water followed by polishing with fine alumina on a felt pad. The electrode was then rinsed with distilled water and dried with tissue prior to use. This method of cleaning always gave satisfactory C.V. background responses, Fig 4-2.

The platinum electrodes can also be cleaned by firstly wiping clean with solvent, drying and then immersing in hot aqua regia for five minutes. The aqua regia dissolves the Pt surface. The electrode is subsequently rinsed with water and polished with alumina. It is then cycled electrochemically between the positive and negative limits of a 0.5M solution of sulphuric acid. These last two steps are repeated until the voltammogram characteristic of Pt in sulphuric acid is obtained [7]. Once achieved the electrode is held at a potential of +1.3 V until the current drops to zero. The electrode is then washed with distilled water and dried with tissue prior to use.

The choice of a reference electrode is not an easy one. The saturated calomel is the reference electrode most often quoted in the literature as the reference of preference. However this reference electrode suffers from the disadvantage of being an aqueous system. Leakage of water into non-aqueous solvents is a potential problem and the calomel electrode also adds an extra potential drop (iR drop) if used in non-aqueous solutions because of the potential difference set up between the interface of the non-aqueous and aqueous solutions. The calomel electrode is also unstable in acetonitrile [7], a non-aqueous solvent of choice. The reference most often used in this work was a so-called pseudo reference or floating reference electrode [8]. This was simply a piece of silver wire. The use of this type of reference means that the zero potential measured may move slightly over the course of an experiment. This problem is alleviated by the use of an internal reference [8] such as the ferrocene/ferricinium couple as mentioned below. The standard potential of the ferrocene/ferricinium couple $E^{\emptyset}(0/1+)$ is set arbitrarily to zero and the standard potential of material undergoing investigation are quoted relative to this zero point. The use of such a reference is advantageous since it helps cut down the iR drop caused by the internal

**Figure 4-2**
Solvent Backgrounds for Acetonitrile, Dichloromethane and Tetrahydrofuran

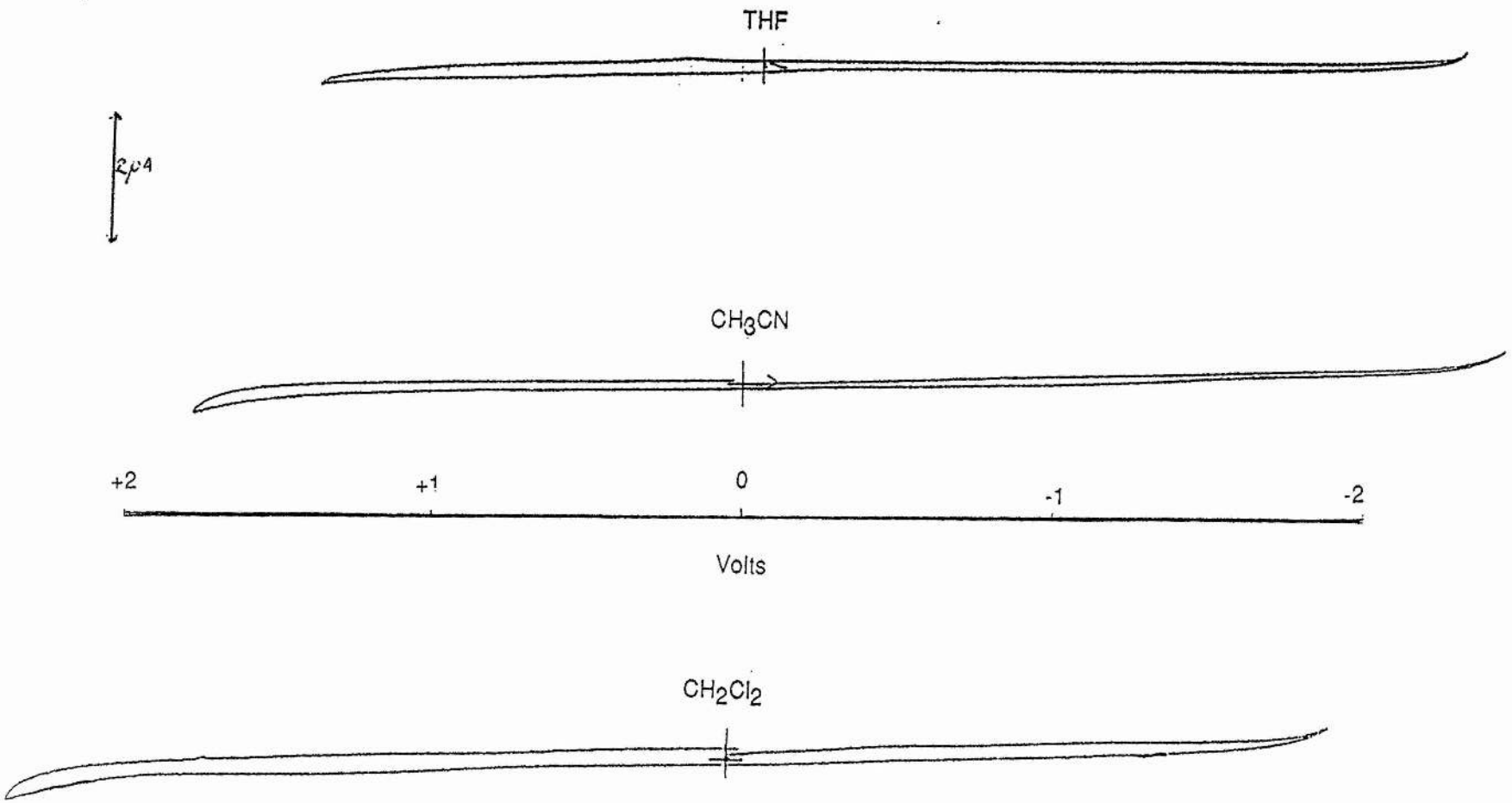

resistance of the solution since there is no extra potential barrier set up as would be the case if the calomel was used. The use of a Luggin probe [7,8], placed close to the working electrode surface, containing the reference electrode also helps to compensate for the iR drop.

Equipment:

For the C.V. experiment a potentiostat and a waveform generator are required, the former to apply the correct voltages the latter to apply these voltages in a triangular waveform to the working electrode. Two systems were used in this work. The first was a Bioanalytical Cyclic Voltammetry system which has both the potentiostat and waveform generator in the same housing. The second system was an Amel potentiostat linked up to an Amel waveform generator. The recording device was a Linseis x,y,t chart recorder. The Amel equipment and the recorder were kindly loaned by Dr. Colin Vincent for the duration of this work.

Solvents:

The main problem with solvents used for C.V. was a high water content, acetonitrile was found to be particularly hygroscopic. The following describes the preparation of the solvents used in this work.

Acetonitrile of Analar quality was dried by refluxing over $CaH_2$ for 24 hours under nitrogen. The solvent was then distilled under nitrogen onto $P_2O_5$, and refluxed for 5 hours. The solvent was then redistilled onto fresh $P_2O_5$ and this process repeated until the formation of an orange polymer in the distillation flask ceased. The solvent was then stored over $P_2O_5$ under $N_2$ and distilled prior to use.

Dichloromethane of normal laboratory quality was predried over $CaCl_2$ for 48 hours. The $CaCl_2$ was filtered off and the solvent refluxed over $CaH_2$ under $N_2$ for a minimum of 24 hours. The solvent was stored over $CaH_2$ under $N_2$ and distilled prior to use.

Tetrahyrofuran of Analar quality was dried by continually refluxing over sodium benzophenone ketyl under $N_2$, the solvent being distilled from this prior to use.

The purity of these solvents could be judged from the oxidation and reduction limits observed from the background of the C.V. experiment.

Electrolyte:

For non-aqueous work an electrochemically inert ionic material is required to carry the bulk of the charge in solution and so prevent the formation of ion gradients. The non-aqueous electrolyte of choice is $Bu_4NPF_6$. This material was prepared by a modification of the method outlined in reference [7]. Preparation was achieved by mixing aqueous solutions of $Bu_4NBr$ and $NH_4PF_6$ and filtering off the resulting product. It was found that the material was best recrystallised from the addition of ethanol to a hot aqueous slurry of the electrolyte, filtered when cool and dried at 110°C.

The C.V. experiment:

Typically, 20ml of solvent are added to the electrochemical cell containing enough electrolyte for a 0.2M solution. The solution was thermostatted to 25°C and deoxygenated with $N_2$. After bubbling for 5-10 minutes a background C.V. was taken; the background obtained not only informs as to the quality of the solvent but also gives the electrochemical limits of the experiment. From Bard [8] the electrochemical 'window' available to each solvents is, THF= +1 V, - 3.5 V; $CH_2Cl_2$ = +3.0 V, -2.0 V; and from Heinze [9], $CH_3CH_2CN$= +3.6V, -3.0V (similar to the limits for $CH_3CN$). Once a satisfactory background was obtained 3mM of ferrocene, (Fc)(purified by sublimation) was added to act as the internal standard. Since there was no real reference electrode used in this work the potential value of the ferrocene/ferricinium ($Fc^{+/o}$) couple was set to zero. 3mM of the electroactive species undergoing investigation was then added after the C.V. of the ferrocene had been recorded. The position of any oxidation or reduction waves observed for this species were referenced to the zero value given to the $E^{\emptyset}$ of the $Fc^{+/o}$ couple.

In the work reported here, all the $E^{\emptyset}$ values given are all relative to the arbitrarily assigned zero value of the ferrocene/ferricinium couple except where indicated.

During the C.V. experiment the effect of scan rate on the peak current value was examined. Scan rates ($\nu$) from 0.064 V $s^{-1}$ to 1.000 V $s^{-1}$ were normally employed. The current obtained is directly proportional to the size of the electrode area and so in some graphs the current is given as the current density, which is the current obtained divided by the electrode area in $cm^2$.

Bulk Electrolysis:

The bulk electrolysis of $Fe_2(SEt)_2(NO)_4$ (1mg,2.8μmoles) in THF under $N_2$ was carried out in a two compartment cell. Pt plate and basket electrodes of large surface areas were used as the counter and working electrode respectively. A calomel electrode was used as the reference electrode.The solution was quickly scanned to determine the position of the first reduction potential. The solution was stirred and the potential was then stepped to a position beyond the first reduction(-0.8 V) but before the second and held. The current was monitored using an integrator/potentiostat and the number of coulombs passed was recorded automatically. When the current reached background levels the electrolysis was stopped. From the number of coulombs passed, n, the number of electrons involved in the first reduction of one molecule of $Fe_2(SEt)_2(NO)_4$ was calculated to be 0.97.

Potential Step:

Using the same equipment, solution and set up used for the C.V. experiment, the potential was stepped from a region where no electrolysis was taking place to one where instantaneous electrolysis took place. The current obtained was plotted as a function of time using a Linseis x,y,t, recorder in continuous y-t mode. The results were examined using equation 10, (App 2).

Compounds:

The Roussin esters, $Fe_2(SR)_2(NO)_4$ used in this work were prepared from the nitrosylation of the analogous carbonyl clusters, $Fe_2(SR)_2(CO)_6$ [10] or from $Na_2[Fe_2(S_2O_3)_2(NO)_4]$ using the methods outlined in chapter 3. The tetrairon clusters $M[Fe_4S_3(NO)_7]$ M= $Me_3S$, $Me_3SO$ were prepared from Roussin's Black salt by metathesis as described in chapter 3. The cluster $Na[Fe_4Se_3(NO)_7]$ was kindly donated by Miss Audrey Lees.

Preparation of $(Et_4N)[Fe_4S_3(NO)_7]$

$Et_4NCl$ (0.17g, 1mmol) in water was added to $Na[Fe_4S_3(NO)_7]$(0.5g, 0.9mmol) in water. The resulting precipitate was filtered and washed with water (4x50ml). The solid was dissolved in acetone (50ml) and water (10ml) added. The acetone was removed by

rotary evaporation to obtain a black crystalline material. I.R. ($CH_3CN$ solution) $\nu$NO 1800, 1747, 1712 $cm^{-1}$. Microanalysis; calculated for $Fe_4S_3C_8H_{20}N_8O_7$; expected C 14.6, H 3.0, N 17.0%; obtained C 14.6, H 2.7, N 16.8%. Melting point 190-193 $^oC$.

Preparation of $(Bu_4N)$ $[Fe_4S_3(NO)_7]$

$(Bu_4N)$ $[Fe_4S_3(NO)_7]$ was prepared in a similar manner to the above

Preparation of $(Et_4N)_2[Fe_2S_2(NO)_4]$

The sodium salt of Roussin's Red Dianion was produced from the reflux of $Na[Fe_4S_3(NO)_7]$ in aqueous alkali. The tetraethyl ammonium salt was produced by metathesis by the addition of $Et_4NCl$ to the above solution followed by extraction into chloroform. Microanalysis; calculated for $C_{16}H_{40}Fe_2N_6O_4S_2$; expected C 34.5, H 7.5, N 15.1%; obtained C 34.1, H 7.3, N 14.9%.

Reaction of $Na_2[Fe(CN)_5NO]$ with Benzylamine using $O_2$

$Na_2[Fe(CN)_5NO]$ (25.5g,0.08mol) were dissolved in water (100ml) and added to a mixture of benzylamine (1.5g, 0.014mol) and $Na_2CO_3$ (1.5g, 0.014mol). The mix was stirred under $O_2$ for 24 hours. $K_2CO_3$ (35g) was added to the solution to salt out the organic content and the solution extracted with diethylether (4x75ml). The solution was dried over $MgSO_4$ and the solvent evaporated off to leave an orange oil (1.4g). A smell similar to that of benzaldehyde was present. The liquid was analysed by G.L.C. and G.C.M.S. to reveal the presence of benzylalcohol, benzonitrile and traces of benzaldehyde, benzoic acid and the phenylmethyl ester of benzoic acid.

Reaction of $Na_2[Fe_2(S_2O_3)_2(NO)_4]$ with benzylamine using $O_2$

$Na_2[Fe_2(S_2O_3)_2(NO)_4]$ (1.28g, 2.5mmol) in water (100ml) was added to benzylamine (0.2g,1.87mmol) and $Na_2CO_3$(0.2g, 1.87mmol). The mixture was stirred for 18 hours under an atmosphere of $O_2$. After this time the presence of iron oxides was apparent. $KCO_3$ (30g) was added to the aqueous mixture to salt out the organics, and the

mixture was extracted with diethylether (3x50ml). The organic layer was dried and subsequent evaporation of the solvent revealed an orange oil (0.11g). The oil was examined by GLC and GCMS to reveal the presence of benzylamine, benzylalcohol and surprisingly benzylidenebenzylamine, $C_6H_5CH_2NCHC_6H_5$.

Reaction of $Fe_2(SR)_2(NO)_4$ with amines using $AgNO_3$ as an oxidant.

Typically, $Fe_2(SR)_2(NO)_4$ (1mmol) and amine (5mmol) were stirred together in THF (20ml). $AgNO_3$(4mmol) was added. Reaction was complete within a few seconds; gas evolution was observed and silver was precipitated along with other insolubles. The solution was filtered and water added (300ml). The solution was extracted with diethylether, the organic layer was dried and on evaporation of the solvent a small amount of oil was obtained. The oils were analysed by GLC and GCMS. R = $^{n}$Butyl, amine = benzylamine; R = $^{s}$Butyl, amine = pyrollidine; R = $^{i}$Pr, amine = butylamine; R = $^{i}$Butyl, amine = di$^{n}$propylamine; R = $SO_3^-$, amine = cyclopentylamine.

Triphenylphosphine and trimethylphosphite were purchased from Aldrich and used as received. Tri-n-butylphosphite was kindly donated by Mr Peter Pogorzelec. All amines were purchased from Aldrich or Fisons and were dried over KOH and distilled prior to use. All thiols used were purchased from Aldrich and used as received. The e.p.r. spectra were recorded on a Bruker E.R. 200D spectrometer in 1mm quartz capillaries. All GLC examinations were made using 1µlt ether solutions (1sample:20 ether). GCMS data were obtained using an INCOS 50 GCMS system. All I.R. spectra were recorded using a Perkin Elmer 1710 FTIR. spectrometer and values given are precise to +/-2cm$^{-1}$.

# Results and Discussion

## 4-1 The Electrochemistry of $Fe_2(SR)_2(NO)_4$

The electrochemistry of $Fe_2(SEt)_2(NO)_4$ in tetrahydrofuran,(THF) by C.V was examined using a glassy carbon working electrode, (G.C.E). The voltammogram obtained is shown in figure 4-3 . Relative to the ferrocene/ferricinium couple, the formal reduction potentials are found to be -1.074 and -1.872V. These values are assigned to two formal one electron reductions of $Fe_2(SEt)_2(NO)_4$ to produce $[Fe_2(SEt)_2(NO)_4]^-$ and $[Fe_2(SEt)_2(NO)_4]^{2-}$ respectively. The result of applying the Randles-Sevcik, (R-S) equation to the current/scan rate data for the cathodic and anodic processes of both reductions are shown in figure 4-4 .

From figure 4-4 it can be observed that in all four cases the gradients are approximately the same and that all points lie on approximately the same line. This suggests that n, the number of electrons transferred for both reductions are the same and that the diffusion coefficients, $D_0$, $D_{-1}$ and $D_{-2}$ are all similar. The linearity of the plot also indicates that the reductions are electrochemically reversible for all $\nu$ examined. An examination of $i_c/i_a$ for both reductions for all $\nu$ shows that the reductions are also chemically reversible since there is no significant deviation from 0.95 and 0.995 for the first and second reductions respectively. Slight changes from this value can be correlated with the difficulties encountered when extrapolating the baseline for the estimation of the anodic current values.

An examination of $\Delta E_p$ against $\nu$ for the two reductions relative to that obtained for an equivalent amount of ferrocene shows no significant differences from the ferrocene/ferricinium data. However the $\Delta E_p$ of the second reduction was always slightly larger than that of the first reduction for a given scan rate. This may reflect a decrease in the heterogenous rate constant due to the anion being slightly more difficult to reduce than the neutral.

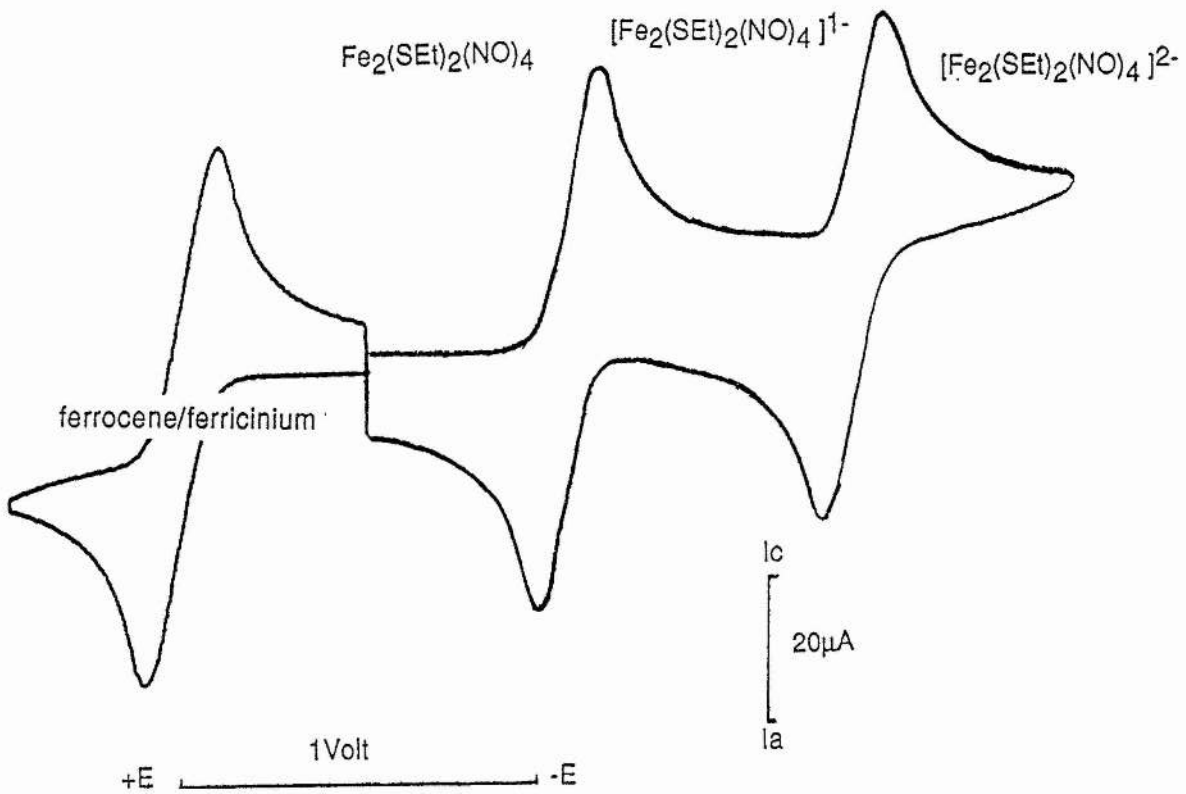


**Figure 4-3**
Cyclic Voltammogram for $Fe_2(SEt)_2(NO)_4$ in THF
at a Glassy Carbon Electrode

## Figure 4-4

Randles Sevcik Plots for the Two Reductions of $Fe_2(SEt)_2(NO)_4$ in THF

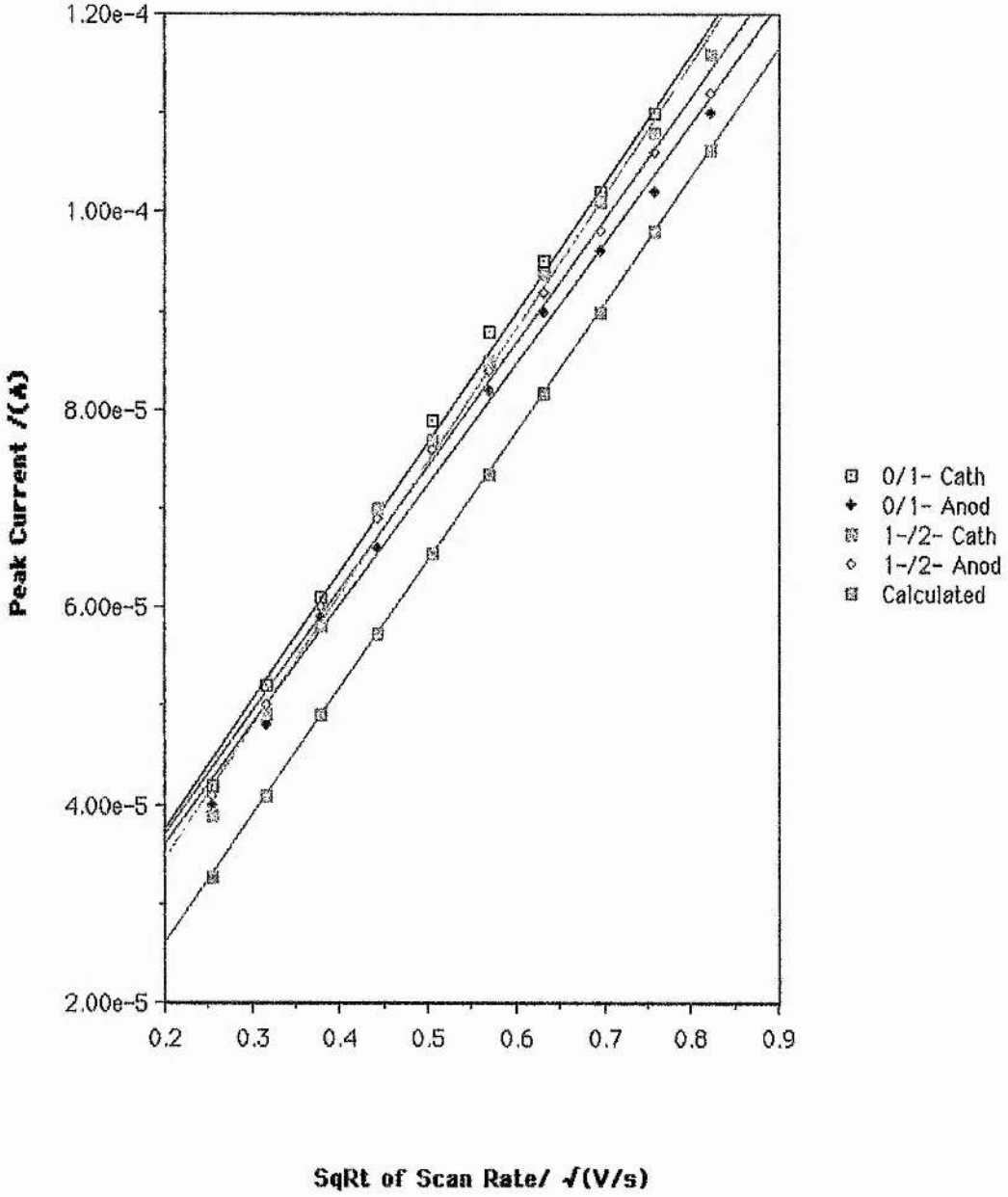

From the data obtained the value of D can be estimated. The diffusion coefficient is a measure of how fast a species moves in solution. For a metal ion in aqueous solution a diffusion coefficient of around $1x10^{-5}cm^2\ s^{-1}$ is typically found [7]. From the data $D^{0/1-}= 5.30\ x10^{-6}$, $D^{1-/0} = 4.56\ x10^{-6}$, $D^{1-/2-}= 5.53\ x10^{-6}$, $D^{2-/1-}= 4.85\ x\ 10^{-6}$ $cm^2s^{-1}$. A similar study for ferrocene gives a diffusion coefficient of $5.36\ x10^{-6}cm^2s^{-1}$. As explained earlier, the inherent difficulty in obtaining base lines for the data means that these figures are not exact. The fact that $[Fe_2(SEt)_2(NO)_4]^-$ has two differing diffusion coefficients implies this inaccuracy. An average value of $5.1x10^{-6}$ $cm^2s^{-1}$ in THF is therefore recorded. Setting $D_O = D_R$ is a normal assumption made in electrochemical measurements (eqn-9, App-2). Although it might have been expected that the reduced clusters would lower the value of D because of a greater solvation relative to the neutral complex, from the above values of D, this appears not to be the case. Therefore, because of this, in the calculation of D the assumption of $D_O=D_R$ is made throughout this work.

Figure 4-4 also shows a theoretical plot for n=1 and $D= 5.0\ x10^{-6}cm^2s^{-1}$ for 3mM of electroactive species, obtained by plugging the values into Randles-Sevcik equation (eqn-6, App-2). The similarity of the gradients further confirms the assignment of n=1 and D for $Fe_2(SEt)_2(NO)_4$.

All of the above data fit the criteria for a reversible couple given in appendix-2 and so it is possible to assign both reductions to the reversible transfer of one electron.

$$Fe_2(SEt)_2(NO)_4 \underset{-e^-}{\overset{+e^-}{\rightleftharpoons}} [Fe_2(SEt)_2(NO)_4]^- \underset{-e^-}{\overset{+e^-}{\rightleftharpoons}} [Fe_2(SEt)_2(NO)_4]^{2-}$$

An examination of $Fe_2(SR)_2(NO)_4$ for a variety of R was carried out in THF. The results are summarised in table 4-1 . If we examine the $CH_3$, $CH_2CH_3$, $CH(CH_3)_2$ and the $C(CH_3)_3$ Roussin esters we find that for each hydrogen replaced by a methyl group, the $E^{\emptyset}$ value decreases by about 23mV in each case. Examination of the straight chain alkyls, $CH_2$-R, for R= $CH_3$, $C_2H_5$, and $C_3H_7$, show a consistency of the $E^{\emptyset}$ (0/1-) value; the iso-butyl ester of Roussin's Red salt has a slightly lower $E^{\emptyset}$ value and this reflects this groups larger electron inductive effect. The sec-butyl ester of Roussin's Red salt has a higher $E^{\emptyset}$ value than the isopropyl group and suggests that the replacement of a methyl group by an ethyl lowers the inductive effect. The $E^{\emptyset}$(0/1-) value of the methylacetate ester of Roussin's Red salt has obviously been affected by the presence of the ester group.

This has had the effect of pulling electron density away from the ring towards the carboxyl group relative to the effect of the methyl group. The pyrimidine ester of Roussin's Red salt has an $E^{\emptyset}$ (0/1-) value consistent with its electron withdrawing properties relative to the methyl group. The thiosulphate analogue of Roussin's Red salt has the lowest $E^{\emptyset}$ (0/1-) value of all. The may reflect an electron rich $SO_3^-$ group, pushing a large amount of electron density into the iron sulphur ring system, however as shown later this is probably not the reason for this low $E^{\emptyset}$(0/1-) value.

**Table 4-1**

| R | $E^{\emptyset}$(0/1-) (a) | $E^{\emptyset}$(1-/2-)(a) | $D/10^{-6}cms^{-1}$ |
|---|---|---|---|
| Me | -1.050 | -1.870 | 5.2 |
| Et | -1.074 | -1.872 | 5.1 |
| n-Pro | -1.075 | -1.870 | 5.1 |
| i-Pro | -1.095 | -1.869 | 4.1 |
| n-Bu | -1.075 | -1.877 | 3.8 |
| s-Bu | -1.088 | -1.900 | 3.2 |
| i-Bu | -1.085 | -1.870 | 3.6 |
| t-Bu | -1.118 | -1.825 | 3.6 |
| $CH_2CO_2CH_3$ | -0.938 | -1.718 | 3.3 |
| Pyrimidine | -0.908 | (b) | (c) |
| $SO_3^-$(Na salt) | -1.310 | (b) | (c) |

(a) Relative to $Fc^{+/o}$ (Volts),(b) Complex, (c) Unmeasured

**Table 4-1**; the standard reduction potentials of $Fe_2(SR)_2(NO)_4$ in THF, relative to the $E^{\emptyset}$ of the ferrocene/ferricinium couple recorded at a G.C.E. at 25°C

From the data available [3] for the oxidation of the $[Fe_4S_4]^{2+}$ core in $[Fe_4S_4(SR)_4]^{2-}$, table 4-2 was constructed. From the data in table 4-2, we observe a decrease by approximately 40mV for every four $\alpha$ hydrogens replaced by four methyl groups. This would give a contribution of about 10mV per methyl group, a value which is close to that obtained per methyl group in $Fe_2(SR)_2(NO)_4$ when done in a polar solvent. The data of table 4-2 also suggests that the effect of the n-propyl group is comparable to that of the ethyl reflecting the observation found with the straight chain alkyl Roussin esters. The $E^{\emptyset}$ of $[Fe_4S_4(SR)_4]^{2-}$ for R= $CH_2C_6H_5$ is interesting, for in the absence of any data for a cluster with R=methylacetate, it shows the effect of an electron withdrawing group attached to the $\alpha$ carbon relative to the effect of the methyl group.

**Table 4-2**

| R | $E^{\emptyset}$ $(2^+/1^+)$(a) | $E^{\emptyset}(1^+/0)$(a) | Solvent |
|---|---|---|---|
| Me | -1.60 | -2.33 | DMF |
| Et | -1.64 | -2.35 | DMF |
| n-Pro | -1.65 | (b) | DMF |
| i-Pro | -1.69 | -2.41 | DMF |
| t-Bu | -1.73 | -2.47 | DMF |
| $CH_2C_6H_5$ | -1.56 | -2.27 | DMF |

(a) Relative to $Fc^{+/o}$ (Volts),(b) not given

**Table 4-2;** the reduction potentials for the core of $[Fe_4S_4(SR)_4]^{2-}$ relative to the $E^{\emptyset}$ of the ferrocene/ferricinium couple, ref.[3].

Direct evidence for the inductive effects of alkyl groups can be obtained from an examination of the data available for the acid dissociation constants of simple organic acids, table4-3.

**Table 4-3**

| Acid | Pka |
|---|---|
| HCOOH | 3.77 |
| $CH_3COOH$ | 4.80 |
| $CH_3CH_2COOH$ | 4.88 |
| $(CH_3)_3COOH$ | 5.05 |

**Table 4-3,** the pKa of some simple organic acids from ref [11].

Table 4-3 shows that the acids become weaker as we go down the table. This is due to the increasing inductive effect of the alkyl groups as the table is descended.

That the $E^{\emptyset}$ value of an iron-sulphur cluster and of other clusters is dependent on the nature of the group attached to a bridging ligand is not unusual. The effect observed can be correlated well with the electron donating/withdrawing properties of the attached group. From this study the following electrochemical series based on the electron donating ability of the attached group can be made;

Pyrim< $CH_2CO_2CH_3$< Me < Et,n-Pro,n-Bu< $CH_2CH(CH_3)_2$<i-Bu < i-Pr < t-Bu < "$SO_3^-$"

On further reducing $Fe_2(SR)_2(NO)_4$ we obtain the $E^{\emptyset}$ ($1^-/2^-$) values. Most of these values were found to lie around -1.87 V; the trend observed for the $E^{\emptyset}(0/1^-)$ is not reflected here to any extent, indeed the t-butyl ester has the highest $E^{\emptyset}$ ($1^-/2^-$) value recorded for a hydrocarbon group. The methylacetate ester does show the expected higher value in accordance with its $E^{\emptyset}(0/1\text{-})$ value. The $E^{\emptyset}(1\text{-}/2\text{-})$ of $R=SO_3^-$ and pyrimidine were not recorded due to complications arising from the second reduction. With $R=SO_3^-$, the second reduction was found to be pseudo-reversible under all conditions examined and may be due to the highly negatively charged species precipitating out of solution, the electrodes becoming electroinactive if scanned too negative. In the case of R=pyrimidine, further reduction is complex and may involve the reduction of the pyrimidine ring itself.

These results all show that the attached group makes a difference to the reduction potential of the cluster. This evidence shows that the $[Fe_2S_2]^{6-}$ core of these clusters is being reduced. The reduction or oxidation of transition metal clusters often involves the breakage of metal-metal bonds. Indeed work has shown [12]t hat in the majority of cases the HOMO is a M-M $\sigma$ bond whereas the LUMO is a M-M antibonding orbital. Thus any reduction or oxidation will weaken the structure with the possibility of fragmentation leading to clusters of lower nuclearity. The use of chelating ligands such as o-xylenedithiol [13], or capping atoms as found in the cobalt carbide clusters, $Co_3C$ [14, 15], or by the use of heteroatoms such as P, N, S [12] all help to stabilise a cluster to fragmentation. However, the fact that a change in R of an attached group, whether it is a terminal ligand or part of a bridging ligand, can affect the $E^{\emptyset}$ value of a cluster shows that the HOMO/LUMO are not entirely M-M bonding or antibonding and that the terminal/bridging groups play a role in this bonding. This is part of the reason why the use of heteroatoms as bridging groups can stabilise redox states. The reason why a change in R attached to a heteroatom in a cluster can change the $E^{\emptyset}$ value can be correlated well with the ability of the attached group to donate electron density. As the donor ability increases the amount of electron density on the core also increases. We can see from this work and that of others [3] that the reduction of an already reduced complex is often more difficult to achieve, suggesting that the more negative a cluster is the more difficult it is to add another electron to, although in some cases, particularly with the clusters of type $Fe_2(SR)_2(CO)_6$, it has been shown that it is actually easier to add the second electron [16]. Thus from the same argument, small changes in the electron density of a core will lead to small changes in the $E^{\emptyset}$ value, and these changes are found to correlate with the donating or accepting properties of R. With the t-Butyl ester of

Roussin's Red salt a large inductive effect is present giving rise to an increased amount of electron density on the core leading to a lower $E^{\emptyset}(0/1^-)$ value relative to the methyl ester of Roussin's Red salt; the methylacetate Roussin ester accepts electron density and so its $E^{\emptyset}$ $(0/1^-)$ value is higher relative to $Fe_2(SMe)_2(NO)_4$. This argument is in agreement with the results obtained for $[Fe_4S_4(SR)_4]^{2-/1-}$.

The $(0/1^-)$ and the $(1^-/2^-)$ reduction potentials for a range of R obtained in acetonitrile are given in table 4-4 .

**Table 4-4**

| R | $E^{\emptyset}(0/1^-)$(a) | $E^{\emptyset}(1^-/2^-)$(a) | Ep Ox (a) | $D/10^{-5}cm^2\ s^{-1}$ |
|---|---|---|---|---|
| Me | -0.935 | -1.595 | +1.01 | 1.7 |
| Et | -0.952 | -1.610 | +0.98 | 2.1 |
| i-Pro | -0.963 | -1.625 | +1.08 | 1.6 |
| t-Bu | -0.975 | -1.580 | +1.06 | 1.1 |

(a) relative to $E^{\emptyset}$ of $Fc^{o/+}$ (V)

**Table 4-4**; electrochemical data for $Fe_2(SR)_2(NO)_4$ in $CH_3CN$, relative to the $E^{\emptyset}$ of the ferrocene/ferricinium couple recorded at a G.C.E. at 25°C

The trend is similar to that observed in THF. The second reduction potential of the t-butyl Roussin ester is again found to be anomalous. The reason for this anomaly is unknown. The diffusion coefficients shown here are over twice those observed in THF. This shows the greater solvation of the cluster by the THF relative to $CH_3CN$; the greater the bulkiness of the ester moving through solution the slower it moves and the lower its diffusion coefficient.

The $(0/1^-)$ reduction potentials and the peak position of the oxidation wave for a range of R obtained in dichloromethane are given in table 4-5. The results obtained for the first reduction potential in DCM are in agreement with those found in THF and in $CH_3CN$. The reduction potentials of the second reduction are not given due to the quasi-reversibility of the wave observed. The differences between the unoxidised Pt and G.C.E. electrodes show up only in the second reduction of these clusters and has been found to be dependent on the preparation of the working electrode, see section 4:6 .

**Table 4-5**

| R | $E^{\emptyset}$ (0/1-)(a) | Ox (a) | D(cv)(b) | D(ps)(c) | n(d) |
|---|---|---|---|---|---|
| Me | -1.130 | +1.104 | 1.42 | 1.9 | 0.8 |
| Et | -1.161 | +1.150 | 1.49 | 1.9 | 0.8 |
| n-Pro | -1.152 | +1.171 | 1.64 | 2.2 | 0.8 |
| i-Pro | -1.176 | +1.147 | 1.51 | 1.1 | 1.3 |
| n-Bu | -1.152 | +1.170 | 1.24 | 1.6 | 0.8 |
| s-Bu | -1.161 | +1.162 | 0.86 | 1.7 | 0.5 |
| i-Bu | -1.161 | +1.142 | 0.75 | 1.1 | 0.7 |
| t-Bu | -1.191 | +1.122 | 1.46 | 1.2 | 1.2 |
| $CH_2CO_2CH_3$ | -0.994 | +1.073 | 0.99 | 1.3 | 0.7 |
| Pyrimidine | -0.896 | (e) | 1.64 | 2.0 | 0.8 |
| $SO_3^-(Bu_4N$ salt) | -1.276 | (e) | 0.47 | 1.2 | 0.4 |

(a) relative to the $E^{\emptyset}$ of $Fc^{o/+}$(V); (b) $D/10^{-5}cm^2\ s^{-1}$, from CV data;(c) $D/10^{-5}cm^2\ s^{-1}$, from potential-step data; (d) n, number of electrons transferred per molecule, from equation-11, (App-2); (e) complex, unmeasured.

**Table 4-5**; electrochemical data for $Fe_2(SR)_2(NO)_4$ obtained in DCM at an unoxidised Pt electrode, at 25°C. All potentials are given relative to the $E^{\emptyset}$ of the ferrocene/ferricinium couple.

Knowing that n=1 and C=3mM, the diffusion coefficient can, of course, be obtained from the potential step data using equation-10 (App-2), and the results of this are given table 4-5. Application of equation-11 (App-2) to the data from the C.V. and potential step experiments gives n to be between 0.7 and 1.3. This method is more crude than the bulk electrolysis which gave a value of 0.97 for n, but this method is very quick and can be done while a CV experiment is underway. The low values may reflect the fact that the potential step was often carried out at the end of the C.V. experiment; evaporation of solvent would increase the concentration of the electroactive species giving a steeper gradient than expected for the potential step experiment and thus a lower n value. The reason for the low n value obtained for $R=SO_3^-$ was due to difficulties in obtaining $i_c$ from the voltammograms.

4-2 Comparison of $E^{\emptyset}$ (0/-1) and the $\nu$(NO) Stretching Frequency

As explained in chapter 1, the nitrosyl stretching frequency of a coordinated nitrosyl ligand is dependent on a number of factors, such as the metal, the oxidation state and other ligands present. For a given structure such as $Fe_2(SR)_2(NO)_4$ changes in the nitrosyl stretching frequency will depend on changes in R. From table 4-6, section 4:4-1, it can be observed that as the electron donating ability of R increases the lower the stretching frequency becomes. Since we have already stated that the $E^{\emptyset}$(0/1-) values appear to be related to donating ability, a plot of the average value of the nitrosyl stretching frequency $\nu$(NO)asym +$\nu$(NO)sym)/2 against the observed $E^{\emptyset}$(0/1-) was constructed.

A linear relationship between $E^{\emptyset}$(0/1-) and the average $\nu$(NO) was obtained, figure 4-5a. This graph helps to prove the relationship between the donor ability of R and the $E^{\emptyset}$(0/1-)and $\nu$(NO) frequency. It also gives the series, based on donor ability;

$$Pyrim < CH_2CO_2CH_3 < Me < Et,n\text{-}Pro,CH_2CH(CH_3)_2 < i\text{-}Pr < t\text{-}Bu$$

This series complements that found from $E^{\emptyset}$(0/1-) data alone.

The graph can also be used to predict an $E^{\emptyset}$(0/1-) value. The cluster $Fe_2(SCH_2CH_2OH)_2(NO)_4$ was produced, but its cyclic voltammogram was not recorded (lack of available material). From its I.R. spectrum the average value of $\nu$(NO) was found to be 1776.5cm$^{-1}$. From the graph this was found to correspond to an $E^{\emptyset}$(0/1-)value of -1.025V in THF. This figure correlates well with its electron attracting capability relative to that of the methyl group.

An important omission from this graph was R=$SO_3^-$. Figure 4-5b shows the position of R=$SO_3^-$ relative to the other points. It can be observed at once that this is not in harmony with its expected position based on $E^{\emptyset}$ data, nor from its $\nu$(NO) stretching frequency. From its average stretching frequency of 1771cm$^{-1}$ an $E^{\emptyset}$(0/1-) value of 0.978V in THF would be expected. From its actual $E^{\emptyset}$(0/1-) value an average stretching frequency of 1739cm$^{-1}$ would have been predicted. The $E^{\emptyset}$ data implies that the $SO_3^-$ group is a strong electron repeller; the I.R. data suggest that it is in fact a moderately strong electron attracting group relative to the methyl group.

## Figure 4-5

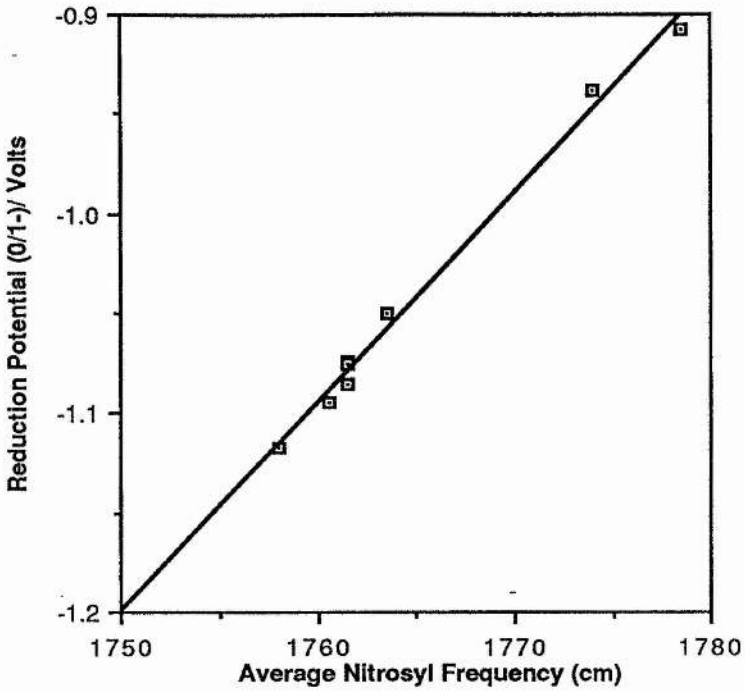


## Figure 4-5a

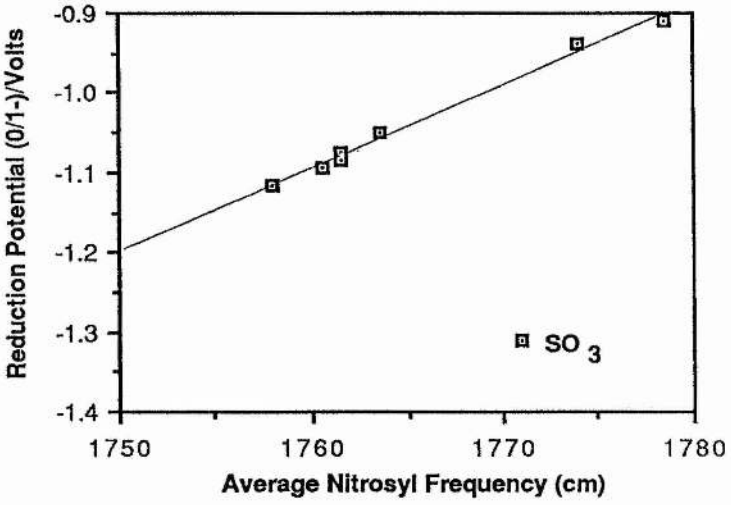

The reason for this disparity between the two results must lie with the associated negative charge of the thiosulphato complex. The X-ray structure of this complex shows that the charge associated with it is $2^-$. It has already been noted that it is more difficult to reduce a negatively charged cluster (for example the $E^{\emptyset}(0/1\text{-})$ and $E^{\emptyset}(1\text{-}/2\text{-})$ data). The low $E^{\emptyset}(2\text{-}/3\text{-})$ value of this complex is seen not as a consequence of a strong electron inductive effect of an attached group, but to the difficulty in obtaining the $3^-$ cluster. If we assume the IR criterion to be correct the effect of having a two minus charge on the cluster has added an extra -0.33V to the reduction potential. The observation that the second reduction of this cluster to produce the $4^-$ is quasi-reversible or irreversible suggests that this highly charged cluster has a short half life. Since figure 4-5a is based on the neutral Roussin esters it is therefore not surprising that a charged species does not fall onto the line obtained from these neutral clusters.

## 4-3 Calculation of the Disproportionation Constants for $Fe_2(SR)_2(NO)_4$

If we consider the following;

$$\mathbf{2Red(-1) \ <=====> \ Ox \ + \ Red(-2)}$$

Then from the equilbrium constant and the expression of the free energy in terms of potential, the constant of disproportionation can be calculated from [9];

$$\mathbf{lnK = -nF(E^{O}_{1}-E^{O}_{2})/RT}$$

The following table is a list of the calculated disproportionation constants for a variety of Roussin esters in THF or $CH_3CN$.

**Table 4-6**

| R | K, THF/$10^{-14}$ | K,$CH_3CN$/$10^{-12}$ |
|---|---|---|
| Me | 1.4 | 6.8 |
| Et | 3.1 | 7.4 |
| $^{n}Pr$ | 3.6 | (a) |
| $^{i}Pr$ | 8.1 | 6.3 |
| $^{n}Bu$ | 2.7 | (a) |
| $^{t}Bu$ | 109 | 58 |
| $CH_2CO_2CH_3$ | 6.4 | (a) |

(a) not measured

**Table 4-6**, Disproportionation constants for $[Fe_2(SR)_2(NO)_4]^-$

These figures support the view that the monoanion, $[Fe_2(SR)_2(NO)_4]^-$ is

thermodynamically stable towards disproportionation. It follows that if formed chemically, the monoanion may be stable enough to isolate. However although these figures do indicate the complex's thermodynamic stability it does not indicate its kinetic lability. The C.V. data gathered does show, however, that on the C.V. timescale the material is apparently chemically stable. Because of this data a spectroscopic examination of the monoanion was undertaken.

## 4-4 Examination of Reduced $Fe_2(SR)_2(NO)_4$

It has been reported [17] that clusters of type $Fe_2(PR_2)_2(NO)_4$ undergo two one electron reductions but the properties of these two reduced states were not investigated. A chemical and spectroscopic examination of the reduction of $Fe_2(PPh_2)_2(NO)_4$ by Wojcicki [18], showed that chemical reduction could be achieved using sodium or Super-hydride ($MBH(Et)_3$, M=Li or Na). The reduction of $Fe_2(PPh_2)_2(NO)_4$ by Na was described as the breakage of a M-M bond. The use of a good hydride donor produced the nitrosyl bridged complex, $Fe(NO)_2(\mu PPh_2)(\mu NO)Fe(NO)(PPh_2H)$. We have already shown that the first reduction of $Fe_2(SR)_2(NO)_4$ is reversible both electrochemically and chemically on the C.V. time scale, and so a spectroscopic investigation of this reduced cluster was carried out.

The reduction of $Fe_2(SMe)_2(NO)_4$ by Na wire in THF produces a deep green coloured solution, reminiscent of the colour of the radical $[Fe(SMe)_2(NO)_2]^-$. Addition of air into the solution causes the oxidation of the reduced species and the complete recovery of the methyl ester was obtained.

$$Fe_2(SMe)_2(NO)_4 \underset{O_2}{\overset{Na}{\rightleftharpoons}} [Fe_2(SMe)_2(NO)_4]^{x-}$$

A bulk electrolysis of $Fe_2(SEt)_2(NO)_4$ in THF with $Bu_4NPF_6$ as support gave as the number of electrons transferred in the first reduction as 1. The solution also turned the same green colour as found with the sodium reduction. Further evidence obtained from e.p.r. spectroscopy and I.R. spectroscopy (see later) has identified this green material as $[Fe_2(SMe)_2(NO)_4]^-$. Aerial oxidation of the electrolysed product gives back the neutral $Fe_2(SMe)_2(NO)_4$ as identified by I.R. spectroscopy and mass-spectroscopy.

### 4-4-1 I.R. Investigation of $[Fe_2(SR)_2(NO)_4]^-$

Addition of an excess of superhydride to a THF solution of $Fe_2(SMe)_2(NO)_4$ causes the solution to turn immediately bottle green, with the evolution of gas, presumably $H_2$. The I.R. spectrum of the nitrosyl stretching region for this material along with that of the neutral methyl ester is given in figure 4-6. The green solution was mixed with air and placed back in the I.R. solution cell, only the absorptions of the $\nu$(NO)asym and $\nu$(NO)sym of the neutral ester were observed. Addition of more superhydride causes the red solution to turn back to green with the loss of the $\nu$(NO)asym and $\nu$(NO)sym absorptions of the methyl ester. This shows that the following occurs;

$$Fe_2(SMe)_2(NO)_4 \underset{-1e^-}{\overset{+1e^-}{\rightleftharpoons}} [Fe_2(SMe)_2(NO)_4]^-$$

A range of Roussin esters were reduced by superhydride and their I.R. spectra obtained. The results for their $\nu$(NO) absorptions are given in table 4-7 .

**Table 4-7**

| R | Neutral (a) | Monoanion(a) |
|---|---|---|
| Me | 1776, 1751 | 1675, 1656 |
| Et | 1774, 1749 | 1674, 1655 |
| n-Pro | 1774, 1749 | 1674, 1655 |
| i-Pro | 1773, 1748 | 1673, 1653 |
| t-Bu | 1771, 1745 | 1670, 1650 |
| $CH_2CH(CH_3)_2$ | 1774, 1749 | 1674, 1655 |
| $CH_2CH_2OH$ | 1780, 1753 | 1676, 1657 |
| Pyrimidine | 1794, 1763 | 1701, 1647 |

(a) $\nu$(NO) asym, sym ($cm^{-1}$)

**Table 4-7** ; nitrosyl stretching frequencies of the neutral and reduced $Fe_2(SR)_2(NO)_4$

## Figure 4-6

The Infra-Red Spectra of the Nitrosyl Absorption Region
For $Fe_2(SR)_2(NO)_4$ and $[Fe_2(SR)_2(NO)_4]^-$ in THF (R=isopropyl)

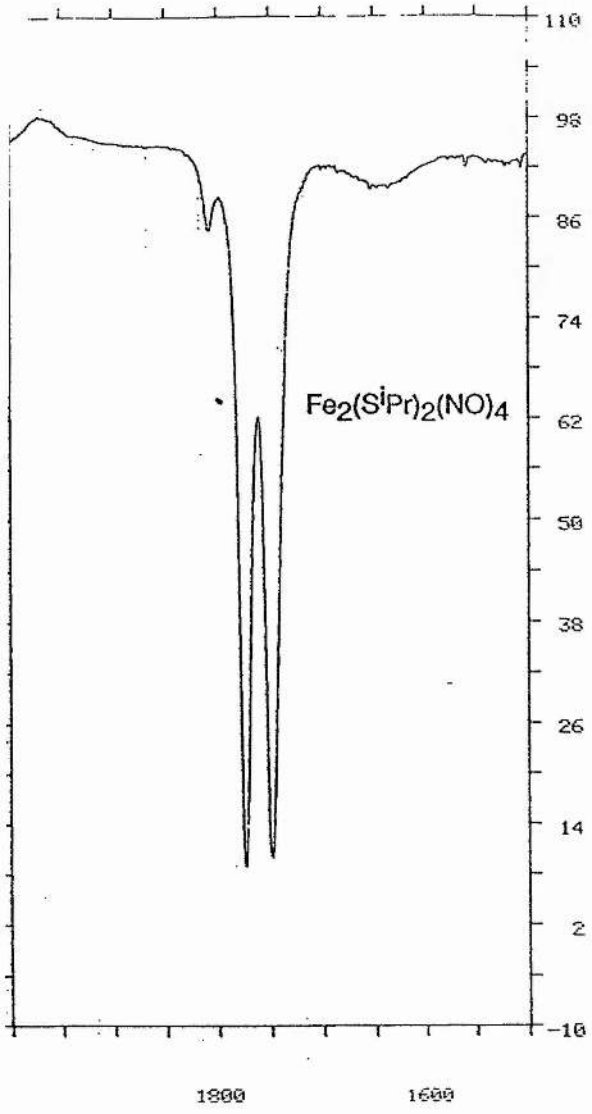


PEAK THRESHOLD = 2.40 %T

| CM-1 | %T |
|---|---|
| 1808.0 | 84.49 |
| 1773.0 | 8.89 |
| 1748.0 | 10.05 |
| 1652.0 | 89.18 |

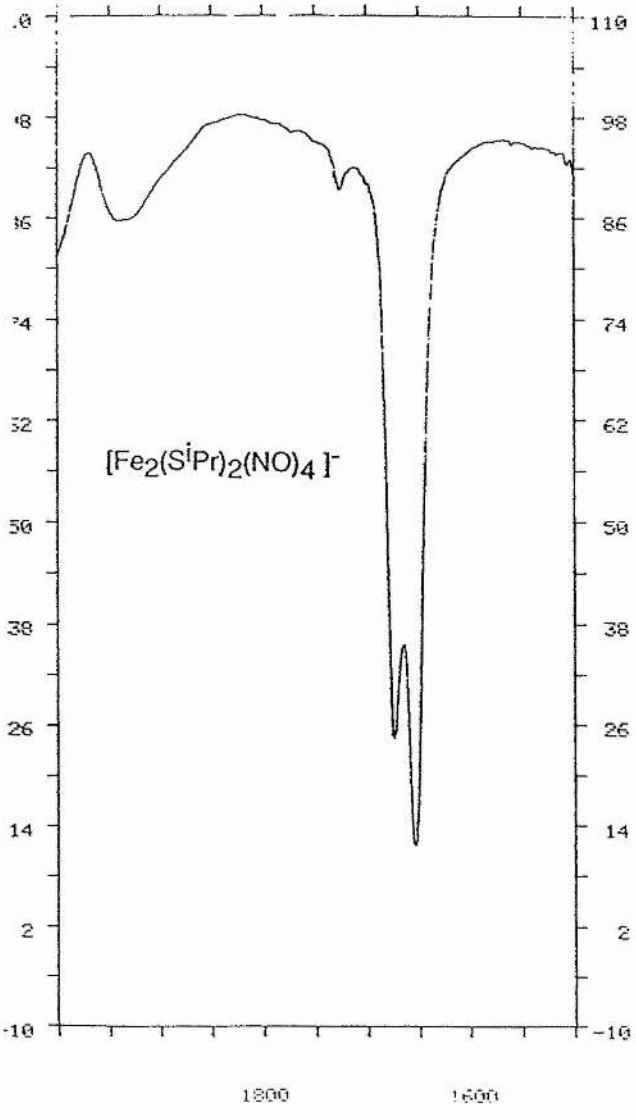


PEAK THRESHOLD = 2.40 %

| CM-1 | %T |
|---|---|
| 1939.0 | 85.56 |
| 1725.0 | 89.31 |
| 1673.0 | 24.52 |
| 1653.0 | 11.53 |

The clusters $Fe_2(SR)_2(NO)_4$ have the metals in the formal oxidation state of -1, and the nitrosyl stretching frequency is found to be around 1760cm$^{-1}$ when R=alkyl. On reduction the formal oxidation state of the metal decreases to a mean value of -1.5 and the nitrosyl absorption frequency would be expected to drop (cf, discussion in chapter-1). This is just what is observed, the frequency dropping by around 100cm$^{-1}$. This is similar to the 80cm$^{-1}$ change in frequency observed with the reduction of $Fe_2(PPh_2)_2(NO)_4$ . Since the twin dinitrosyl peaks are preserved, figure 4-6, it suggests that the structural integrity of the molecule has been kept. From table 4-7 it can be observed that in all cases but one the separation of the two peaks of the reduced state is about 20cm$^{-1}$. The values for the pyrimidine ester are not in agreement with this observation; the reason for this is unknown. In Wojcickis work, (from I.R. evidence), a bridging NO was deduced, this has not been found in this work. From the analysis of the orbitals of $Fe_2(SR)_2(NO)_4$ using Extended Hückel calculations (chp 2) it suggests that on reduction the cluster geometry becomes more open, the Fe-Fe distance increasing.

A central question at this stage was whether the added electron was delocalised over the entire cluster giving two equivalent iron atoms or whether it was localised on one iron giving a mixed valence cluster; an Fe(-1) and an Fe(-2).

### 4-4-2 E.P.R. Investigation of $[Fe_2(SR)_2(NO)_4]^-$

After electrolysis at a potential suitable for the generation of the monoanion, (-0.8 V relative to the saturated calomel electrode) a solution of $Fe_2(SMe)_2(^{14}NO)_4$ in THF showed, when placed in an e.p.r. quartz capillary, the presence of a radical with g≈1.99. No hyperfine splitting was observed. $Fe_2(SMe)_2(^{14}NO)_4$ in THF was reduced with Super-hydride and the solution placed in a quartz capillary. No e.p.r. signal other than a nine line spectrum with g=1.994, A($^{14}$N)=1.4G was observed, figure 4-7 .

The results for other Roussin esters are given in table 4-8 .

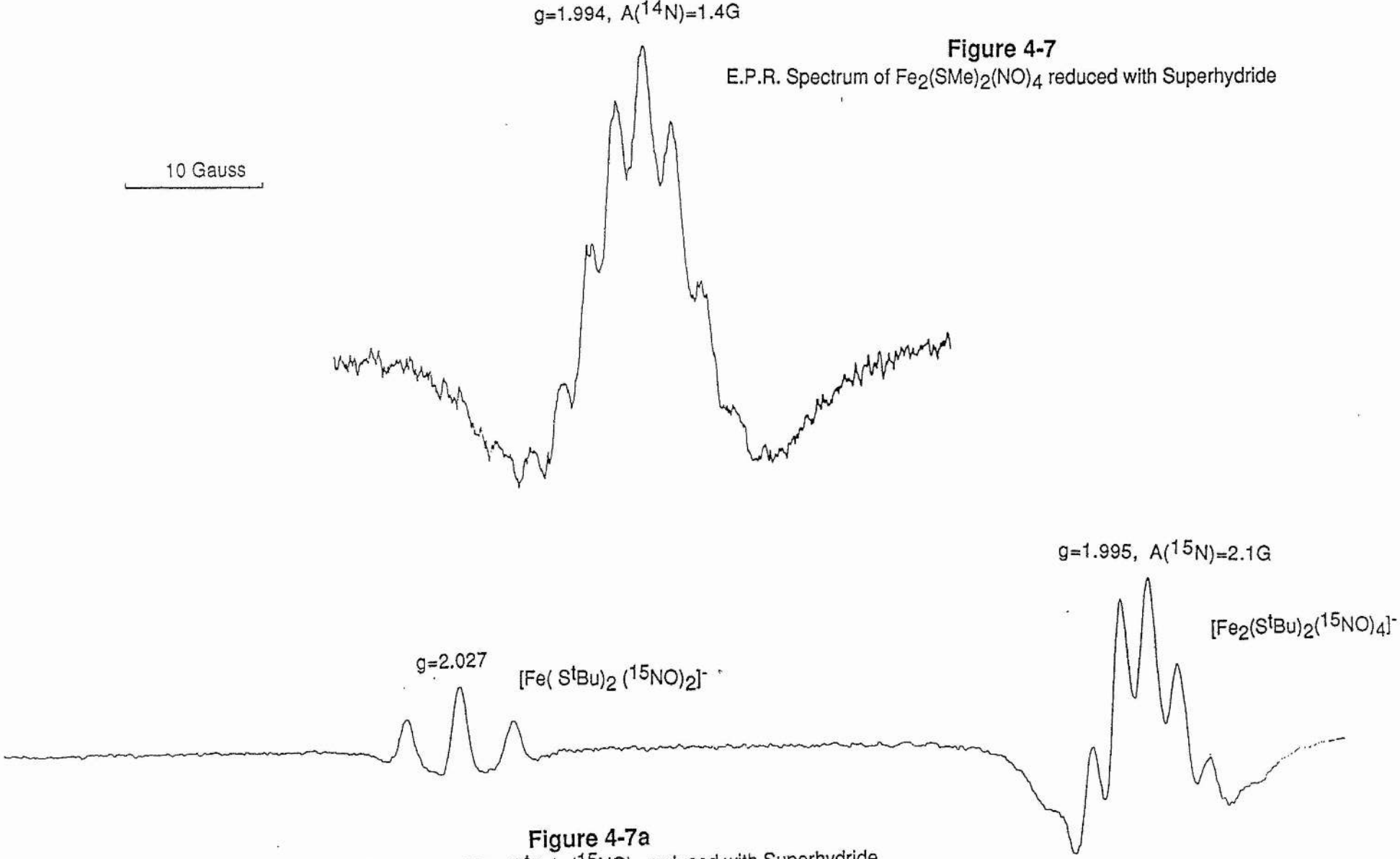


**Figure 4-7**
E.P.R. Spectrum of $Fe_2(SMe)_2(NO)_4$ reduced with Superhydride

**Figure 4-7a**
E.P.R. Spectrum of $Fe_2(S^tBu)_2(^{15}NO)_4$ reduced with Superhydride

**Table 4-8**

| R | g $[Fe_2(SR)_2(NO)_4]^-$ | A($^{14}N$)/ G |
|---|---|---|
| Me | 1.994 | 1.4 |
| Et | 1.996 | 1.3 |
| n-Pro | 1.996 | 1.0 |
| n-Bu | 1.996 | 1.5 |
| s-Bu | 1.996 | 1.5 |
| $CH_2CO_2CH_3$ | 1.995 | (a) |
| t-Bu | 1.995 | (a) |
| t-Bu ($^{15}N$) | 1.995 | 2.1 |

(a) not resolved,

**Table 4-8** ; g and A(N) values for reduced $Fe_2(SR)_2(NO)_4$ in THF

On reducing $Fe_2(S\text{-}^tBu)_2(^{14}NO)_4$ with superhydride two signals are observed, one is due to the well known $[Fe(S\text{-}^tBu)_2\ (^{14}NO)_2\ ]^-$ the other is due to the reduced ester $[Fe_2(S\text{-}^tBu)_2(^{14}NO)_4]^-$. When the $^{15}N$ labelled $Fe_2(S\text{-}^tBu)_2(NO)_4$ was used the spectrum of reduced complex gave a five line e.p.r. signal, while $[Fe(S\text{-}^tBu)_2\ (^{15}NO)_2\ ]^-$ gave the expected three line e.p.r. spectrum, figure 4-7a.

In all cases examined, an immediate colour change from red to green occurs on addition of the Super-hydride. This also occurred on addition of Super-hydride to a THF solution of $Na_2[Fe_2(S_2O_3)_2(NO)_4]$, but the green colour immediately faded and the solution turned brown and precipitates were present. This suggests that the thiosulphato complex is unstable to reduction, or else the $[Fe_2(S_2O_3)_2(NO)_4]^{3-}$ produced is unstable to disproportionation.

For a delocalised system the unpaired electron would be expected to couple equally with the four nitrogen atoms. For four equivalent $^{14}N$ atoms a 9-line e.p.r signal (2nI+1 rule) in the ratio of 1:8:28:56:70:56:28:8:1 would be expected. For a localised system one iron would be $d^{10}$ ; the other iron would be $d^9$ and the unpaired electron would be expected to couple to only two equivalent nitrogen atoms giving a five line e.p.r. spectrum. Reduction of the methyl ester gives a 9 line e.p.r. spectrum in the correct ratio expected from the 2nI+1 rule. Changing the nitrogen isotope to $^{15}N$ will sharpen the spectrum by reducing the number of lines observed and by increasing A(N) by about 40%. The $^{15}N$ labelled t-butyl

ester of Roussin's Red salt, on reduction with superhydride, gave a five line e.p.r spectrum with g=1.995, A($^{15}$N)=2.1G, figure 4-7a. All the e.p.r. evidence supports a delocalised electron in $[Fe_2(SR)_2(NO)_4]^-$.

In no case was any hyperfine coupling to the ∝ protons (where present) observed. This contrasts with the results for $[Fe(SR)_2(NO)_2]^-$, but is in accordance with the predictions of the molecular orbital calculations. In chapter-2 it was shown that the LUMO which would be populated if a geometry change to a lower energy form took place has no contribution to electron density from the groups attached to the bridging atom. The metal-nitrogen interaction of this orbital was found in chapter-2 to be formally M-NO $\pi^*$ non-bonding, but slight admixtures of nitrosyl electron density gave it about 10% nitrosyl character, because of this little s-orbital interaction was expected, which explains the low A(N) values.

From table 4-8 it can also be observed that there is no dependence of g nor A on R . This is seen as further evidence that the LUMO is core centred. Unlike the $E^{\emptyset}$(0/1-)values and the I.R. spectra which are dependent on the total structue, the e.p.r. experiment gives information primarily concerning the LUMO.

From the C.V. experiment, the addition of another electron is chemically and elecrochemically reversible. This indicates that further reduction gives two $d^{10}$ irons and a diamagnetic complex. Although molecular orbital calculations suggest that the Fe-Fe distance will increase on reducing $Fe_2(SR)_2(NO)_4$, no structural evidence is available to substantiate this prediction.

4 - 5

Estimation of the Reaction Stoichiometry Between $[Fe_2(SR)_2(NO)_4]^{2-}$ and $PR_3$(R=OMe, O$^n$Bu, Ph)

The cobalt dimers $Co_2(ER)_2(NO)_4$ (E=S,Se,Te,PR) are 36 valence electron clusters, ie, they posses two additional electrons compared to the Roussin esters which contain 34 valence electrons. These extra electrons are assumed to occupy an orbital which is mainly M-M antibonding, although there is argument about this view [12]. The use of the effective atomic number rule on these cobalt clusters and their diamagnetism [19] imply the absence of any Co-Co bond. This view is consistent with the long Co-Co distance found in

$Co_2(\mu PPh_2)_2(CO)_6$ [19]. The cobalt cluster $Co_2(SR)_2(NO)_4$ reacts rapidly with two equivalents of $PPh_3$ to give the complex $Co(NO)_2(PPh_3)(SPh)$ in approximately quantitative yield [19]. The cores of these 36 valence electron clusters are found to be kinetically labile [19] and to react quickly with two electron donors. The 34 valence electron clusters react only slowly with $PPh_3$ and require forcing conditions to convert $Fe_2(SPh)_2(NO)_4$ into the monomer $Fe(NO)_2(PPh_3)_2$ with the reductive elimination of $Ph_2S_2$ [19]. The kinetic lability of the 36 valence electron clusters relative to the 34 valence electron clusters is seen as a consequence of the absence of an M-M bond.

Reaction of $Fe_2(PPh_2)_2(NO)_4$ with sodium affords the dianion $[Fe_2(PPh_2)_2(NO)_4]^{2-}$ [18]. Reaction with $MB(Et)_3H$ (M=Li,Na) gives a hydride transfer from this hydride donor to the bridging phosphorus. This reaction leads to a change in the bridging ligands and a rearrangement to give the mixed bridge cluster $[(NO)_2Fe(\mu PPh_2)(\mu NO)Fe(NO)(PPh_2H)]^-$ occurs. Deprotonation of this complex with butyl lithium removes this added hydrogen atom as a proton to give the analogous dianion. This mixed bridge dianion rearranges to give the phosphido bridged cluster $[Fe_2(PPh_2)_2(NO)_4]^{2-}$ as found previously. This dianion reacts with electrophiles such as $H^+$ and $R^+$ to give a mixed bridged anionic complex similar to that above. The monanion itself reacts with electrophiles but fragmentation of the cluster occurs although some of the original neutral $Fe_2(PPh_2)_2(NO)_4$ is obtained suggesting its thermodynamic stability. The rearrangement reactions of the monoanion and dianion suggest cleavage of the bridge and the absence of a strong M-M bond, since this would stop the bridging ligand becoming a terminal ligand due to the prevention of free rotation by such an M-M bond. These reactions also show an electron-induced change of reactivity; the neutral complex reacts with nucleophiles, the dianion with electrophiles.

In a recent review by Lemoine [12], electron-induced *nucleophilic* substitution on *reduced* complexes was discussed. In this review the replacement of ligated CO by phosphines in reduced clusters was examined. For instance an electrochemical examination of the complex $[YCCo(CO)_9]$ (Y=Ph, Cl) showed that in the presence of phosphines or phosphites [20] the first reduction wave of this complex drops nearly to zero. This was taken as evidence for the electron-induced nucleophilic substitution of this complex to give $YCCo(CO)_8L$ (L=phosphine or phosphite).

Since nucleophiles, such as phosphines and phosphites have been shown to react with 36 valence electron clusters [19] it was decided to use C.V. as a probe in the reactions of these nucleophiles with the electrochemically generated 36 valence electron cluster $[Fe_2(SR)_2(NO)_4]^{2-}$. The method employed was simple; if phosphines or phosphites react with this doubly reduced cluster then the return wave for the $[Fe_2(SR)_2(NO)_4]^{1-/2-}$ couple should be suppressed. By titrating into the electrochemical cell a known amount of phosphine or phosphite and examining the ratio of ia to ic for this couple, then a reaction stoichiometry should be realised.

The reaction of $[Fe_2(SR)_2(NO)_4]^{2-}$ with $PR'_3$ (R=Me, R'=OMe, Ph; R=Et, R'=OMe; R=$^{i}$Pro, R'=O$^{n}$Bu) was examined by C.V. The effect of added $PR'_3$ on the ratio ia/ic was recorded. For example the plot of added $P(O^{n}Bu)_3$ against ia/ic for the iso-propyl ester of Roussin's Red salt is given in figure 4-8. An initial straight line plot is observed. The tailing off of the slope at ia/ic=0.4 is due to the current from the reduction of the monoanion to the dianion. The straight line is extrapolated to ia/ic=0. From figure 4-8, ia/ic=0= 38.5µlt of phosphite added. From the density of this phosphite this is equivalent to 35.6mg. Since in the experiment 20ml of a 3mM solution of $Fe_2(S^{i}Pro)_2(NO)_4$ was used, the amount of phosphite added was equal to 7.1 mM. This gives a reaction stoichiometry of Roussin ester to phosphite of 1: 2.4. The results of the other experiments are given in table 4-9.

**Table 4-9**

| $Fe_2(SR)_2(NO)_4$ | Concentration | $PR_3'$ | Amount added | moles |
|---|---|---|---|---|
| R | mM | R' | (mg) | equivalent |
| Me | 3 | OMe | 11.7 | 1.6 |
| Me | 6 | OMe | 27.4 | 1.8 |
| Et | 3 | OMe | 11.7 | 1.6 |
| $^{i}$Pro | 3 | O$^{n}$Bu | 35.6 | 2.4 |
| Me | 3 | Ph | 73.8 | 4.7 |

**Table 4-9** ; titration of electrochemically generated $[Fe_2(SR)_2(NO)_4]^{2-}$ with $PR'_3$.

A similar experiment with 3mM of $Fe_2(SMe)_2(NO)_4$ with $P(OMe)_3$ gave a result corresponding to the addition of 1.6 mole equivalents of phosphite. Doubling the quantity of $Fe_2(SMe)_2(NO)_4$ required double the quantity of phosphite to give ia/ic=0. The results of a similar study with $Fe_2(SEt)_2(NO)_4$ gave a result in agreement with those found for $Fe_2(SMe)_2(NO)_4$.

**Figure 4-8**

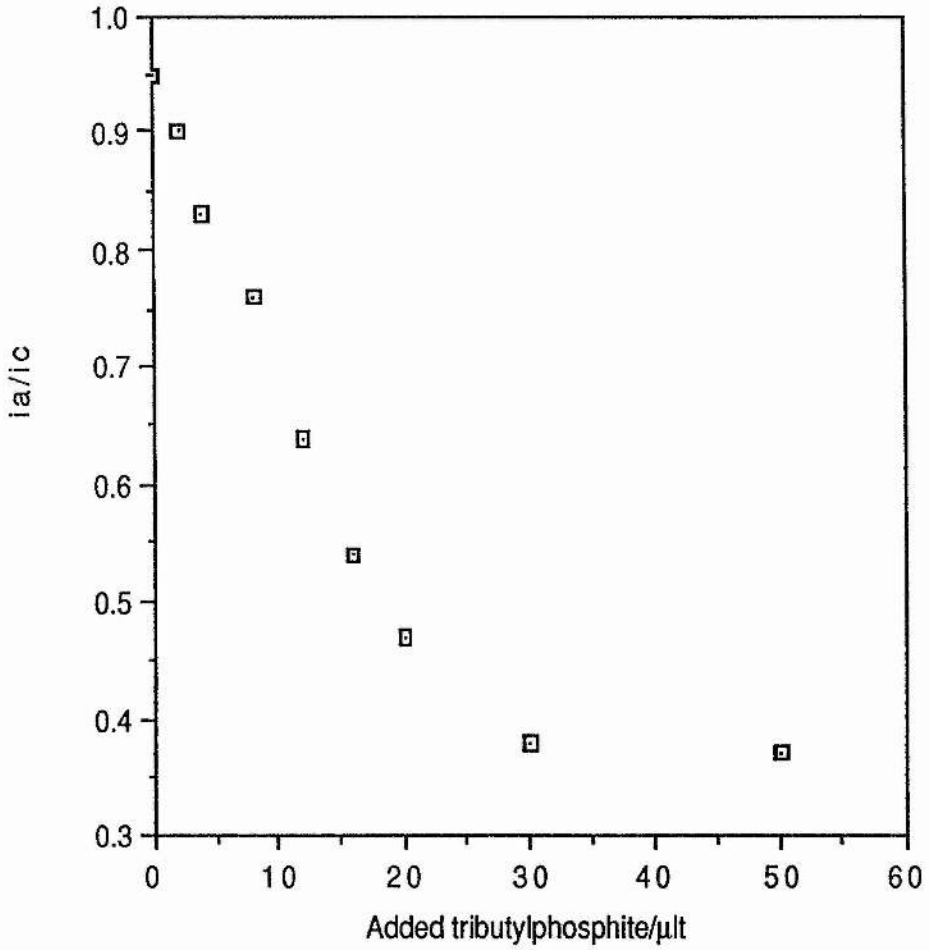

These results suggest a linear relationship between added phosphite, the amount of ester and the ratio of ia/ic. The similarity of the results for these four experiments suggest that this could be a valid method for the estimation of reaction stoichiometries between the Roussin esters and phosphites. From the results the following is suggested;

$$1[Fe_2(SR)_2(NO)_4]^{2-} + 2P(OR)_3 \longrightarrow \text{products}$$

In a similar experiment with $PPh_3$ and $Fe_2(SMe)_2(NO)_4$ a titrant of 4.7 moles equivalent was recorded, figure 4-8a.

**Figure 4-8a**

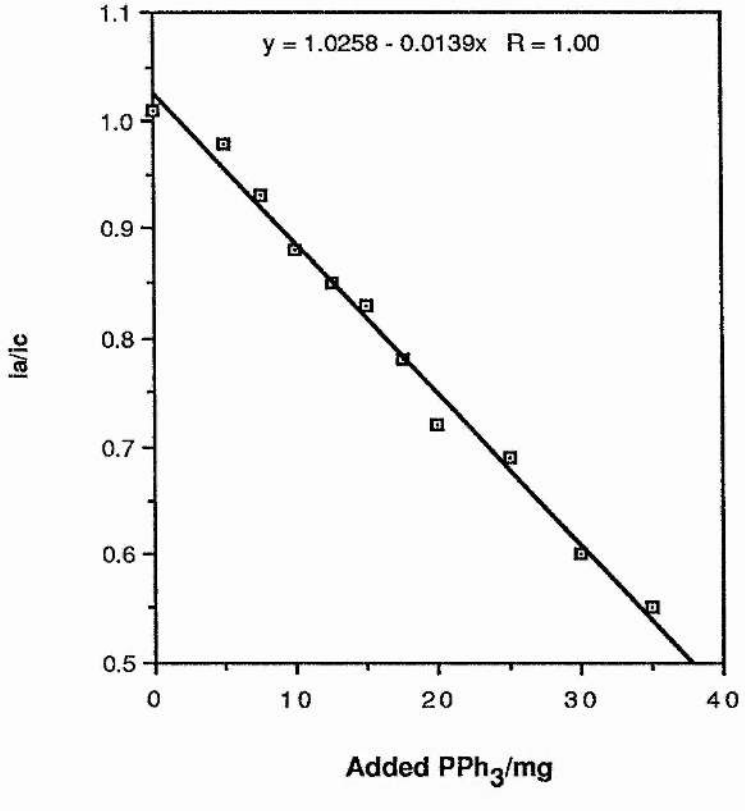


This result is significantly higher than those previously found and suggests;

$$1[Fe_2(SR)_2(NO)_4]^{2-} + 4 \text{ or } 5\ PPh_3 \longrightarrow \text{products}$$

It has already been found that the cobalt clusters $Co_2(SR)_2(NO)_4$ react rapidly with 2 moles equvalent of $PPh_3$. It is assumed that a similar reaction may be occurring with the

addition of phosphite to a solution of $Fe_2(SR)_2(NO)_4$; the reduction of the Roussin ester inducing the reaction. It is possible that an electron-induced nucleophilic substitution is occurring, in this case an NO group being ejected rather than the CO discussed at length by Lemoine [12]. However, since the reaction of the cobalt nitrosyls or the reaction of the neutral Roussin esters with $PPh_3$ lead to fragmentation of the cluster with the formation of mononuclear fragment of the type $M(NO)_2LY$ it is unlikely that a loss of NO occurs on reaction of a doubly reduced Roussin ester with phosphites or phosphines. Attack of $PR_3$ to give bridge cleavage would on the basis of Weatherills [19] and Wojcickis [18] work seem the most probable, giving perhaps the species $[Fe(NO)_2(P(OR)_3)SR]^-$ with phosphites and $[Fe(NO)_2(PPH_3)_2]^-$ with $PPh_3$. However until a full synthetic investigation of these reactions is carried out these proposals of possible products must remain speculative.

## 4-6 Differences Between Pt and G.C. Electrodes

During the course of the electrochemical work it was observed that the second reduction of $Fe_2(SR)_2(NO)_4$, (R=alkyl), was not reversible, but pseudo-reversible in all solvents when a non-oxidised platinum working electrode was used. For instance at a scan rate of $200mvs^{-1}$ in acetonitrile the first reduction of $Fe_2(SMe)_2(NO)_4$ was found to have, for a particular experiment, a peak separation, $\Delta Ep$, of 60mv, whereas the second reduction had a separation of 260mv; in dichloromethane, $Fe_2(S^tBu)_2(NO)_4$ was found to have a peak separation of 120mv for the first reduction but a value of 380mv was recorded for the second. Figure 4-9 shows the voltammogram obtained for $Fe_2(SMe)_2(NO)_4$ in DCM at a non-oxidised Pt (non-oxPt)working electrode.

Examination of table 4-10 gives the data obtained from an examination of a solution of 3 and 6mM of $Fe_2(SMe)_2(NO)_4$ in DCM at a non-oxPt working electrode. R-S plots for the first reduction gave straight line relationships and the current densities are as those obtained from an examination of similar amounts of ferrocene. An examination of $ip_a/ip_c$ for the second reduction by the normal baseline method proved difficult, and so the empirical Nicholson method was employed (eqn-7, App-2). Using this equation a value of

**Figure 4-9**
The Reductions of $Fe_2(SMe)_2(NO)_4$ in $CH_2Cl_2$
at a Non-Oxidised Platinum Working Electrode

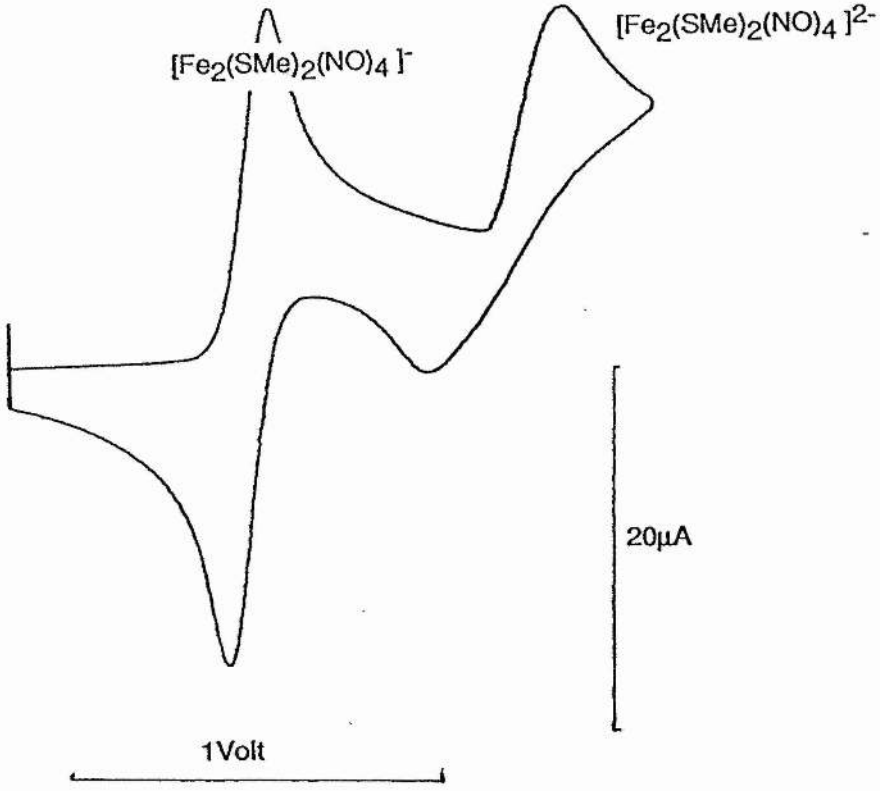

approximately 1 was obtained for all $\nu$ examined. This sets the value of $\alpha$, the transfer coefficient to 0.5 for the range examined. The change in $\Delta$Ep with scan rate for $Fe_2(SMe)_2(NO)_4$ was the same observed for the ferrocene/ferricinium reversible couple. The change of $\Delta$Ep with increasing scan rate for the first reduction is therefore solely due to the iR drop effect.

**Table 4-10**

**3mM $Fe_2(SMe)_2(NO)_4$**

| $\nu$ (a) | $\Delta$Ep(1-)(b) | $\Delta$Ep(2-)(b) | ipc(c) | ipa(c) | ia/ic (d) |
|---|---|---|---|---|---|
| 0.064 | 100 | 280 | 11 | 9 | 1.09 |
| 0.100 | 111.5 | 290 | 14 | 9 | 0.93 |
| 0.196 | 130 | 380 | 18 | 9 | 1.08 |
| 0.324 | 140 | 440 | 22.5 | 9 | 1.08 |
| 0.400 | 160 | 470 | 25.5 | 7 | 1.10 |
| 0.484 | 170 | 475 | 26 | 6 | 1.23 |
| 0.576 | 180 | 510 | 30 | 5 | 1.15 |
| 0.676 | 190 | 520 | 31.5 | 3 | 1.14 |

**6mM $Fe_2(SMe)_2(NO)_4$**

| $\nu$ (a) | $\Delta$Ep(1-)(b) | $\Delta$Ep(2-)(b) | ipc (c) | ipa (c) | ia/ic (e) |
|---|---|---|---|---|---|
| 0.064 | 80 | 260 | 22 | 15 | 0.96 |
| 0.100 | 85 | 330 | 25 | 17 | 1.03 |
| 0.196 | 95 | 360 | 33 | 14 | 1.13 |
| 0.324 | 110 | 420 | 41 | 8 | 1.15 |
| 0.400 | 120 | 450 | 46 | 2 | 1.19 |
| 0.484 | 120 | 465 | 50 | 4 | 1.17 |
| 0.576 | 120 | 480 | 54 | (d) | 1.18 |
| 0.676 | 130 | 495 | 54 | (d) | 1.23 |

(a) Scan rate (V $s^{-1}$); (b) peak separation of cathodic and anodic peaks (mV); (c) peak current obtained by extrapolating the baseline ($\mu$A); (d)baseline method of obtaining the anodic current is invalid in this case; (e) ratio of anodic to cathodic peak currents as calculated by the Nicholson-Shane empirical method (eqn 7 , App-2).

**Table 4-10** ; the effect of scan rate on the peak spearation of the voltammograms obtained for the first and second reductions of $Fe_2(SR)_2(NO)_4$, at a non-oxidised Pt electrode in DCM at 25$^{o}$C.

The internal resistance, R, of the solution is, to all intents and purposes, constant over the potential range examined; the changes in peak separation are due to changes in the current. These changes in current alter the potential applied to the working electrode and so an extra term is placed into the basic equations of C.V., because of this ΔEp is not simply a function of the current. For the second reduction we have already shown that it is as reversible as the first reduction and that the diffusion coefficients are equal when a glassy carbon or oxidised Pt electrode are used. Thus it follows that the effect of iR drop for the second reduction will closely mimick that observed for the first. This was indeed found to be the case when a glassy carbon or oxidised platinum working electrode was used. In this case, where a non-ox Pt electrode was used, the peak separation of the second reduction was far greater than the first and so cannot be purely due to iR drop. When the non-oxPt electrode is used there is an effect due to iR drop but there is also an effect due to a slow electron transfer.

Since the first reduction wave was a proven reversible system ΔEp should not change with $\nu$. From figure 4-10 it can be seen that a linear relationship exists between ΔEp and $\nu^{1/2}$. In his paper on slow electron transfer kinetics [21], Nicholson based the examination of these kinetics on a dimensionless parameter, $\psi$. He also found that the effect of iR drop was similar to that of slow electron transfer and could also be described by $\psi$. Thus the relationship between between ΔEp and iR drop is a complex one. This does not however, explain the apparent linear relationships observed.

Examination of equation-9, (App-2) shows that $\psi$ is dependent on $1/\nu^{1/2}$. From tables of $\psi$ and ΔEp [9,21] (figure 4-10a shows a plot of $\psi$ against ΔEp) it is obvious that some sort of reciprocal relationship exists between $\psi$ and ΔEp. A plot of ΔEp against $1/\psi$ gives an approximate straight line between 60 and 210mV peak separations, figure 4-10b. For ΔEp; $60 \leq \Delta Ep \leq 90$ mV a linear relationship exists with an intercept of 60mV. For ΔEp; $90 \leq \Delta Ep \leq 210$ mV a linear relationship is found with an intercept of 77mV; for ΔEp; $140 \leq \Delta Ep \leq 210$ an intercept of 94mV for the best line is found. This tells us that for ΔEp; $60 \leq \Delta Ep \leq 150$mV an approximately linear relationship exists between ΔEp and $1/\psi$, and as ΔEp becomes larger the intercept increases above its 59mV theoretical value. Since $\psi$ is proportional to $1/\nu^{1/2}$, $1/\psi$ is proportional to $\nu^{1/2}$. Thus for small values of ΔEp a linear relationship will exist between ΔEp and $\nu^{1/2}$, with a theoretical intercept of 59mV. This linearity will be present whether a peak separation is due to slow electron transfer or

**Figure 4-10**

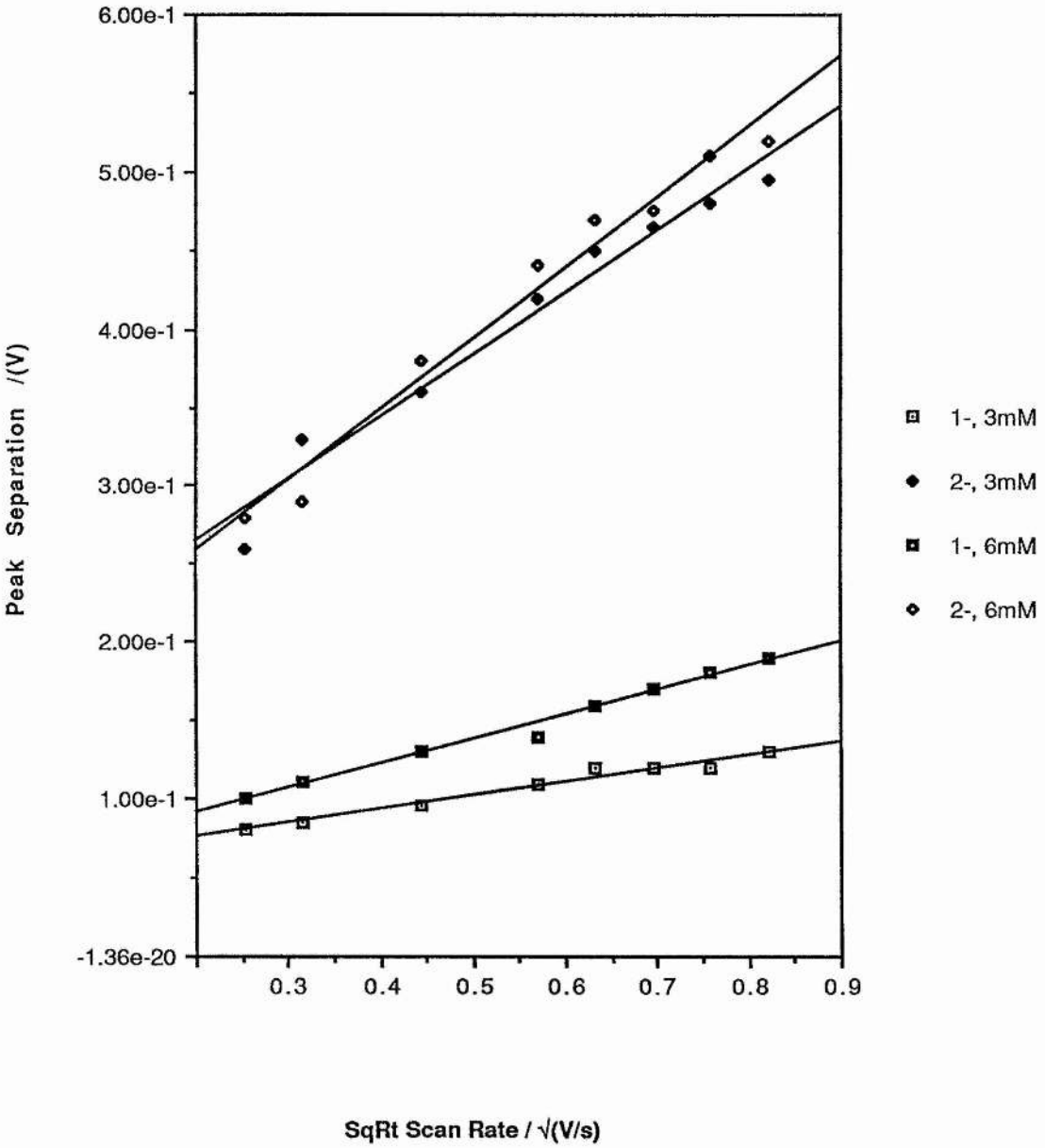
6.00e-1
5.00e-1
4.00e-1
3.00e-1
2.00e-1
1.00e-1
-1.36e-20
Peak Separation /(V)
0.3
0.4
0.5
0.6
0.7
0.8
0.9
SqRt Scan Rate / √(V/s)
1-, 3mM
2-, 3mM
1-, 6mM
2-, 6mM

Figure 4-10a
Dependence of Peak Separation on $\psi$

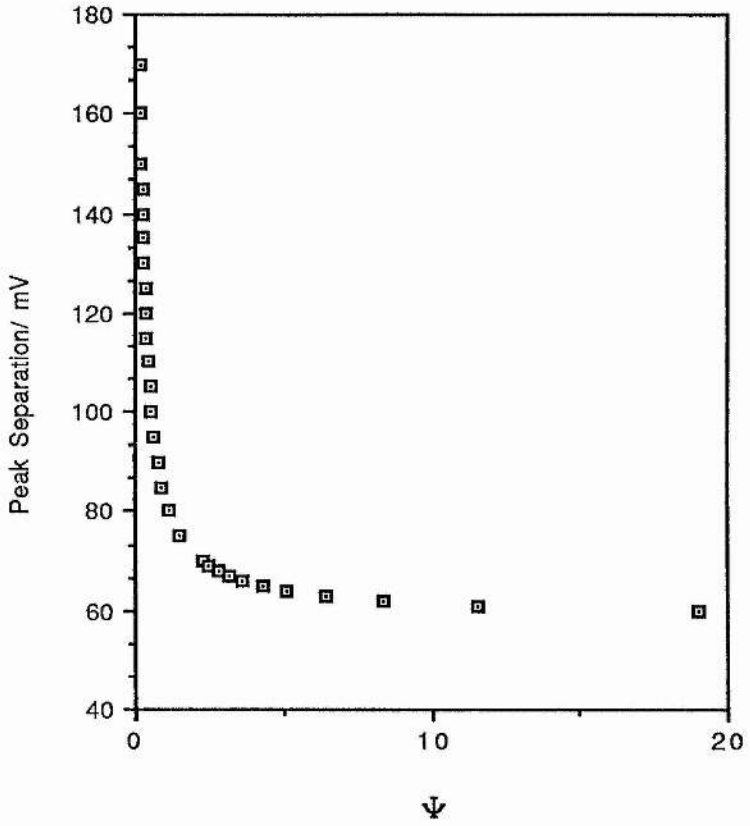


Figure 4-10b
Dependence of Peak Separation on $1/\psi$

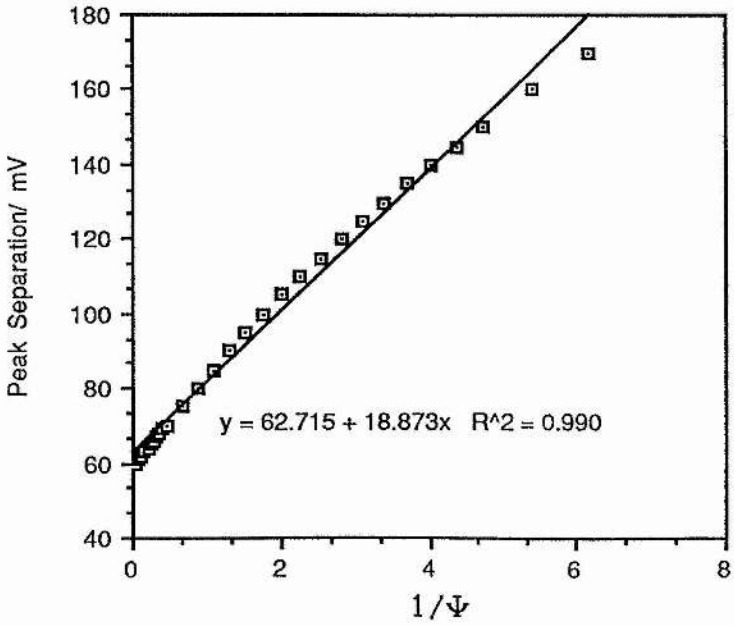

due to iR drop.

An examination of Nicholson's own work [21] shows that a plot of $\Delta Ep$ against $\nu^{1/2}$ gives a linear relationship with an intercept of 57 mV. The values of $\Delta Ep$ were betwen 94 and 115 mV. From the data given in the Bioanalytical handbook [6] a plot of $\Delta Ep$ against $\nu^{1/2}$ gives a linear relationship with an intercept of 59 mV. The values of $\Delta Ep$ were betwen 72 and 106 mV. From figure 4-10a for the first reduction a linear relationship between $\Delta Ep$ and $\nu^{1/2}$ is obtained with an intercept of 62mV. The linearity of the plot and its intercept are in agreement with the foregoing discussion. The gradient observed is due solely to the ohmic drop effect.

For the 1-/2- couple, the $\Delta Ep$ obtained are in a range outwith Nicholson's $\psi$ parameters and also outside the working area for a linear $\Delta Ep/\ \nu^{1/2}$ for a 59mV intercept. This explains the large intercept value obtained in figure 4-10a. Due to the above the rate transfer constant cannot be worked out using Nicholson's method, moreover the actual gradient observed will be a mix of the term due to the iR drop and the term due to the slow electron transfer, ie;

$$\Delta Ep = f(\psi)_k\ ;\ f(\psi)_{iR}$$

Since iR drop affects the potential this will in turn affect the slow electron transfer thus $f(\psi)_k$ will also be a function of iR drop and a very complex expression will occur. Removal of the iR effect from the observed change in $\Delta Ep$ with scan rate would not be possible. Thus if there is an appreciable amount of iR drop present in an experiment, the slow electron transfer rate constant cannot be evaluated. If the iR effect is very small then this term will be negligible and a rate constant could be found.

If we replace the non-oxidised platinum working electrode with a glassy carbon one, then both reductions are observed to be equally reversible. An examination of the early work done using a platinum working electrode, however, reveals that the first and second reductions of the Roussin esters were equally reversible. The only difference between the work presented here and earlier work was in the preparation of the Pt electrode before commencement of the experiment. In the original work the platinum electrode has an oxide layer placed on it whereas in the latest work the electrode has a bare platinum surface.

It is proposed that a possible mechanism involves a weak coordination of the ring of the

Roussin ester to the bare platinum surface. The fact that reversible waves are observed for a glassy carbon and an oxidised platinum electrode and not with the bare platinum suggests some sort of surface interaction. However, the shape of the wave for the second reduction does not suggest a surface adsorption, and the characteristics of a normal pseudo reversible wave are observed. The surfaces of the glassy carbon electrode have hydroxyl groups attached [22] and fast electron transfer occurs from this surface and from the oxidised platinum surface probably via such oxides. Platinum catalysts are known to be poisoned by sulphur or sulphur containing groups [23]. The electrochemistry of the anion $[MoS_4]^{2-}$ showed irreversible features when examined using a platinum working electrode, but reversible behaviour when a glassy carbon electrode was used [24]. What is proposed here to account for the slow electron transfer is a weak interaction between the platinum and the sulphur of the Roussin esters. It is also known that 36 electron clusters are labile to ring opening, since the doubly reduced Roussin ester is such a 36 electron species it is possible that the platinum metal enhances this ring opening. These ideas are summarised in the following diagrams;

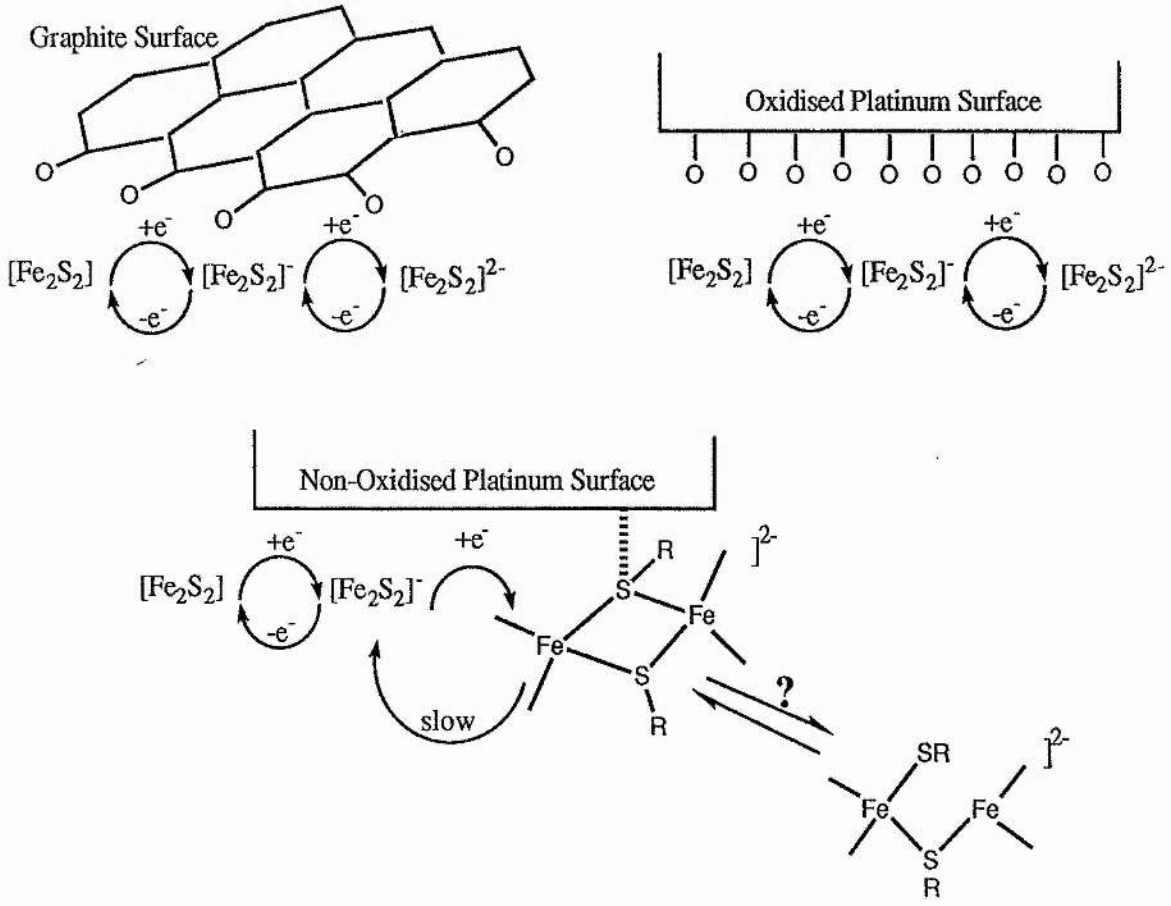

## 4-7 Oxidation of $Fe_2(SR)_2(NO)_4$

The oxidation of $Fe_2(SR)_2(NO)_4$ cannot be examined in THF because this solvent breaks down at a lower positive potential than that at which the Roussin esters are oxidised. In $CH_3CN$ and DCM the oxidation of $Fe_2(SR)_2(NO)_4$ is irreversible in nature. Although in both of these solvents the oxidation is irreversible, in $CH_3CN$ a normal diffusion wave is observed, in DCM however a wave indicative of a surface effect is produced, figs 4-11 and 4-11a. Furthermore this surface effect leads to the deactivation of the working electrode (whether a Pt or G.C.E.) due to the deposition of an inert film on its surface. The second scan of fig 4-11a shows this effect.

There are two reasons for the appearance of an irreversible wave. One is due to a very slow heterogeneous electron transfer from the electrode to the material in solution ie, electrochemical irreversibility and the second involves a chemical step which leads to the fragmentation of the cluster ie, chemical irreversibility. In this case the latter is occurring. With a chemically irreversible step the peak position will not change with scan rate (iR effects compensated for), whereas if it were an electrochemically irreversible step then a change in peak position with scan rate would occur. The former is observed with this work in $CH_3CN$.

The estimation of how many electrons are involved in the oxidation in $CH_3CN$ can be quite easily estimated from R-S plots. Figure 4-12 shows R-S plots for the first reduction and the oxidation of $Fe_2(SMe)_2(NO)_4$. Dividing the two gradients leads directly to a value of n for the oxidation. This value is calculated to be 3.1; similar results are obtained for the Et, i-Pro and t-Bu Roussin esters. Thus the initial oxidation of $Fe_2(SR)_2(NO)_4$ involves the transfer of three electrons to the electrode, followed by the decomposition/fragmentation of the cluster. The decomposed cluster does not plate out onto the electrode in $CH_3CN$ since further scans do not show any changes from the voltammogram obtained in the first scan. From table 4-4, the position of Ep(ox) does not appear to vary much with R.

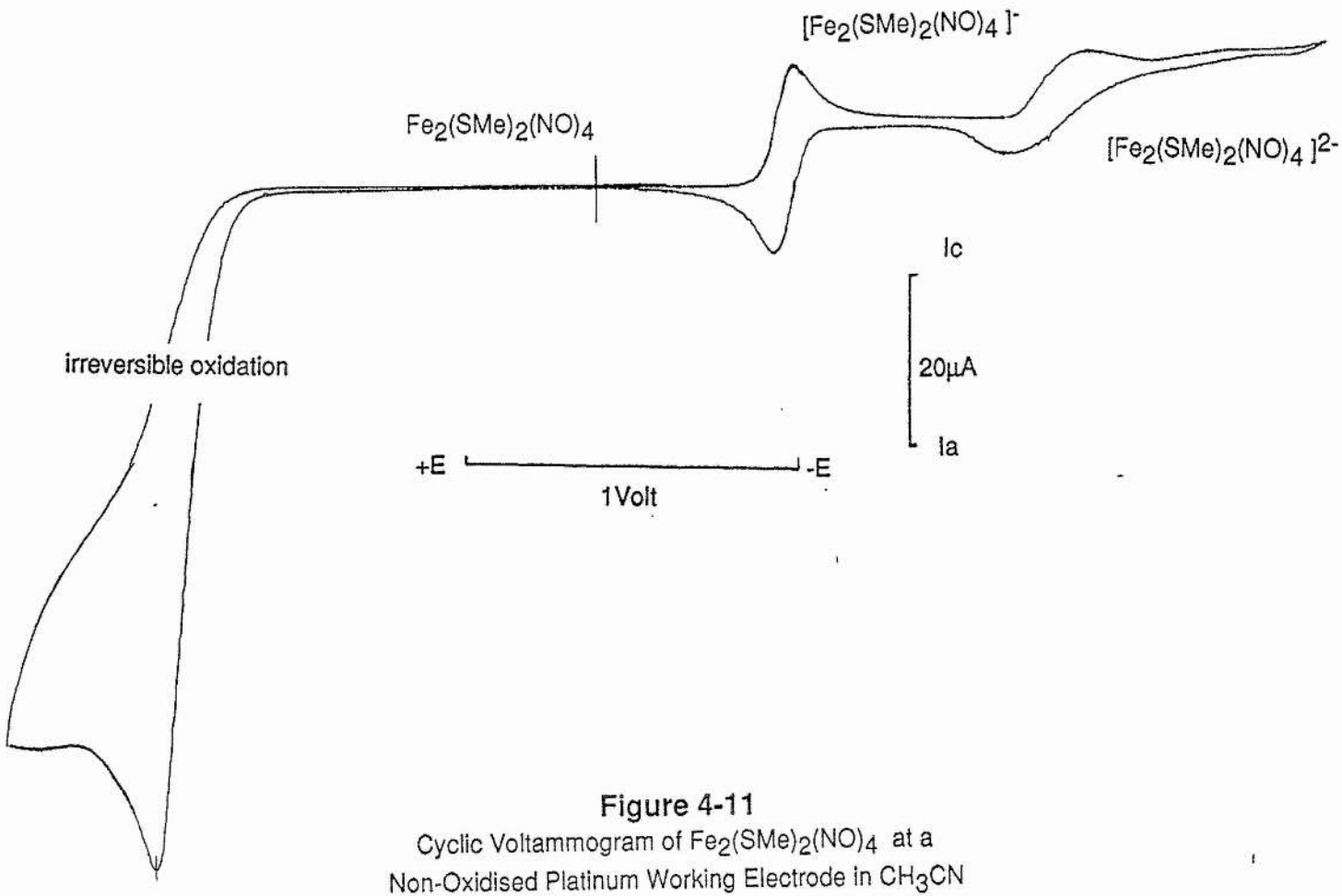


**Figure 4-11**

Cyclic Voltammogram of $Fe_2(SMe)_2(NO)_4$ at a Non-Oxidised Platinum Working Electrode in $CH_3CN$

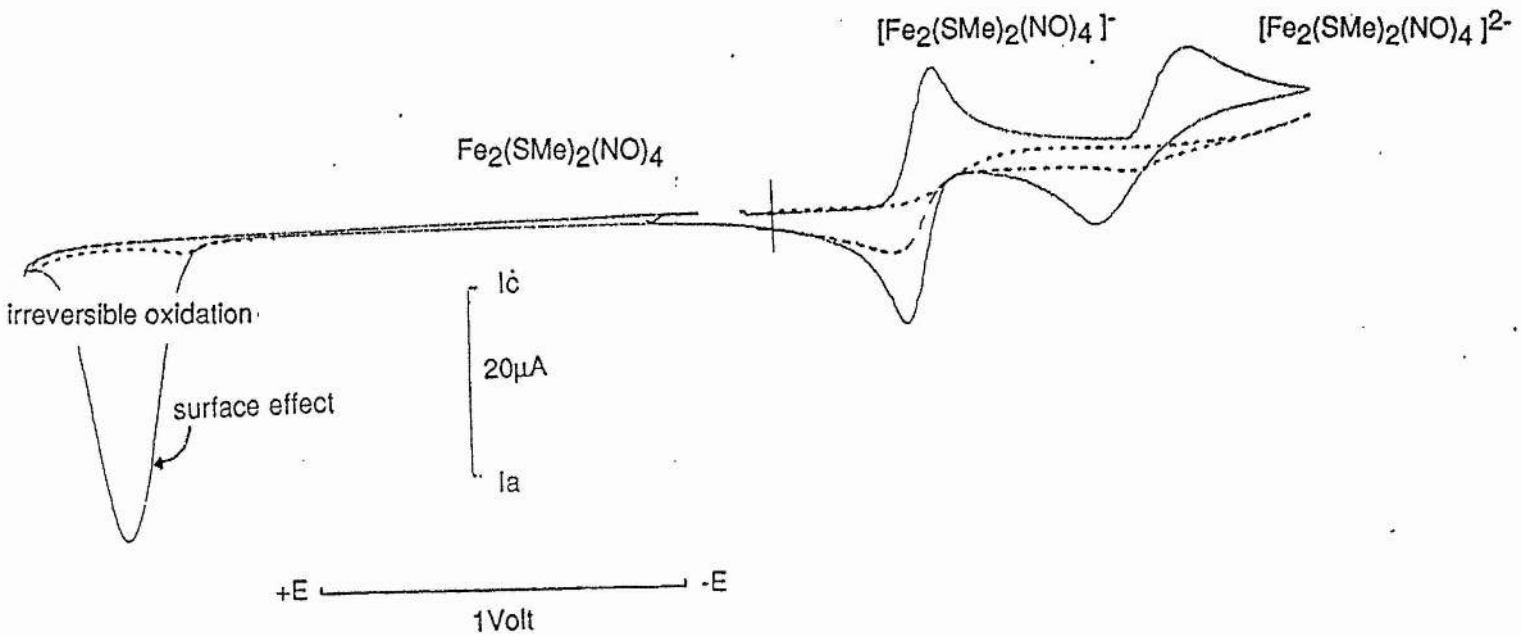


**Figure 4-11a.**
Cyclic Voltammogram of $Fe_2(SMe)_2(NO)_4$ at a
Non-Oxidised Platinum Working Electrode in $CH_2Cl_2$

## Figure 4-12

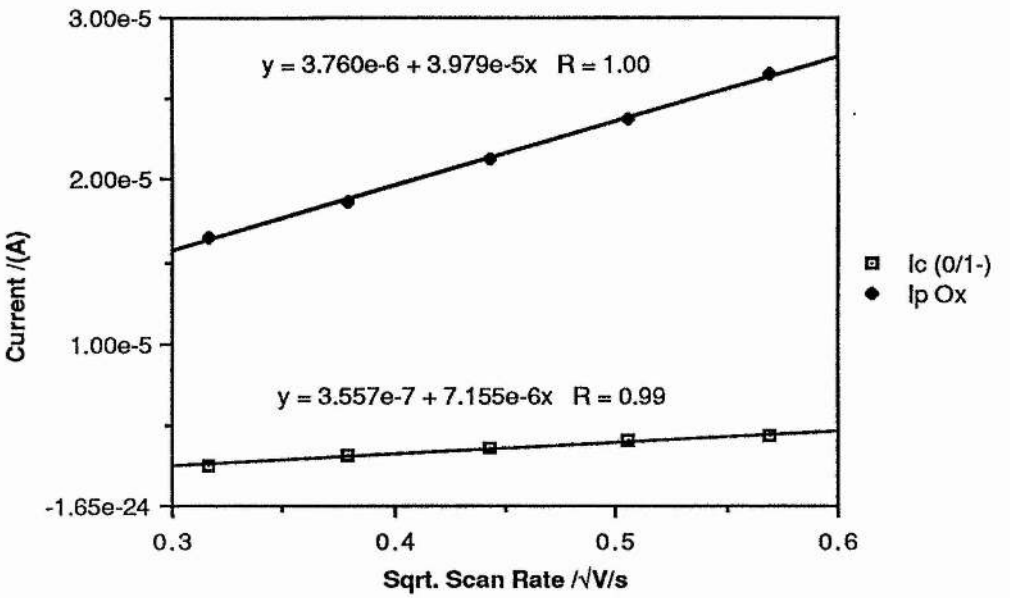


In DCM the position of Ep, relative to $Fc^{+/o}$, correlates well with those found in $CH_3CN$ and centres on +1.15v. The wide range observed +1.07-1.17v, may reflect the difficulty in obtaining an accurate estimation of the peak position, since in DCM, because of the surface effect, the peak is flatter than those found for $CH_3CN$. For the reduction or oxidation of an adsorbed species the limiting current is proportional to the scan rate [7]. In this case plots of $I_{lim}$ are found to be proportional to the square root of the scan rate, ie a normal diffusion limited current, figure 4-12a. This shows that the electroactive species diffuses to the electrode where it is oxidised and then becomes irreversibly attached to the electrode. Since this process is diffusion limited, n can be obtained in a similar manner to that obtained in acetonitrile solutions. A value of n=2.8 is found. The potential-step/C.V. method of working out n will not work in this case since on stepping the potential, as the material is oxidised and plates onto the electrode, the electrode area decreases.

If the electrode, after oxidation in DCM, is taken out of solution and placed in a fresh solution of DCM containing electrolyte only, no electrochemical activity is recorded on scanning the potential. If the electrode is wiped with tissue and placed back in the original solution then a normal C.V. is obtained. If the electrode, after oxidation, is held at a low negative potential eg, -2v, close to or past the position of solvent breakdown for a few seconds and then scanned as normal, the reductions of the Roussin ester are observed again. This suggests that the electrode cleans itself by pushing off the adsorbed material at low

potentials.

**Figure 4-12a**

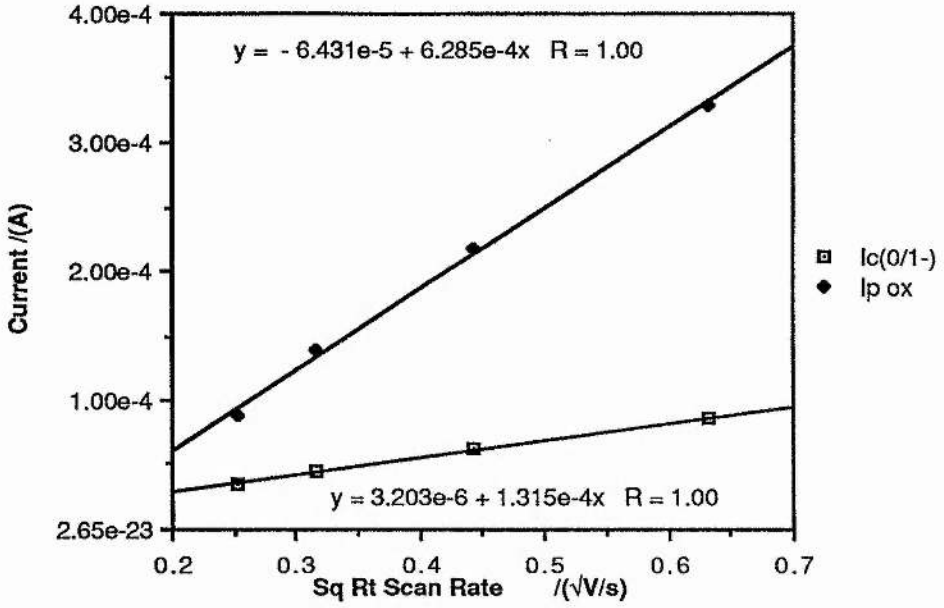


4-8 The Electrochemistry of $(Bu_4N)_2[Fe_2S_2(NO)_4]$

A sample of $(Bu_4N)_2[Fe_2S_2(NO)_4]$ was produced from the reflux of $Na[Fe_4S_3(NO)_7]$ in aqueous sodium hydroxide solution. The material was identified from its I.R. spectrum. Since dichloromethane solutions of Roussin's Red salt produce almost quantitatively Roussin's Black salt [25],and since THF solutions of the Red salt are also unstable [26] the C.V. of this material was carried out in acetonitrile. After a period of time the initial red solution turned black and so it appears that the Red salt is also unstable in acetonitrile. However the C.V. of the material was obtained. Two reversible one electron reductions were observed. Relative to the $E^{\emptyset}$ of the ferrocence/ferricinium couple the reduction potentials of $[Fe_2S_2(NO)_4]^{2-/3-}$ and $[Fe_2S_2(NO)_4]^{3-/4-}$ were found to be -1.08 and -1.68V respectively.

With reference to the electrochemistry of $Fe_2(SR)_2(NO)_4$ and the Extended Hückel calculations performed on an idealised geometry of $[Fe_2S_2(NO)_4]^{2-}$ and $Fe_2(SR)_2(NO)_4$,

the electrochemistry of the 'parent' cluster, $M_2[Fe_2S_2(NO)_4]$ ($M=Bu_4N$) was expected to show a similar electrochemistry to the neutral esters of Roussin's Red salt. The actual similarity found suggests that this complex has a similar structure to the alkyl esters of Roussin's Red salt, and of course this has been confirmed by X-ray structure to be the case [27].

## 4-9 The Electrochemistry of the Tetranuclear Roussinate Anions, $[Fe_4E_3(NO)_7]^-$, E=S, Se

The electrochemistry of $M[Fe_4S_3(NO)_7]$, (M= Na, $Et_4N$, $Bu_4N$, $Me_3S$ and $Me_3SO$) and $Na[Fe_4Se_3(NO)_7]$ were examined by cyclic voltammetry. The C.V. of salts of $[Fe_4S_3(NO)_7]^-$ were reported to show an irreversible oxidation [28] and the ammonium salt of $[Fe_4Se_3(NO)_7]^-$ was been reported to show two reversible one electron reductions [29]. No further investigations of these reductions or oxidation have been carried out since to our knowledge.

### 4-9-1 The Electrochemistry of Roussin's Black Anion, $[Fe_4S_3(NO)_7]^-$

The production of a variety of salts of Roussin's Black anion were available from the examination of the reactions of Roussin's Black salts discussed in chapter three. An examination of THF solutions of $M[Fe_4S_3(NO)_7]$ ($M=Et_4N$, $Bu_4N$, $Me_3S$ and $Me_3SO$) was carried out. Figure 4-13 gives the voltammogram obtained from the reduction of $(Me_3S)[Fe_4S_3(NO)_7]$. In <u>all</u> cases examined the same reductive electrochemistry was found and the potentials obtained for a particular reductive process differed by only +/- 5mV between the salts. This showed that the counterions played no part in the electrochemistry of this cluster on the C.V. timescale. Three reductions were observed and the reduction potentials of these processes relative to the $E^{\emptyset}$ of the ferrocene/ferricinium couple occur at -1.31, -1.91 and -2.41V.

R-S plots for the first and second reduction waves were found to be linear, figure 4-14 gives the R-S plots for the first reduction wave of $Me_3S[Fe_4S_3(NO)_7]$. Figure 4-14a compares the gradient of a theoretical R-S plot,with n=1 and $D=1x10^{-5}$ $cm^2$ $s^{-1}$ for 3mM

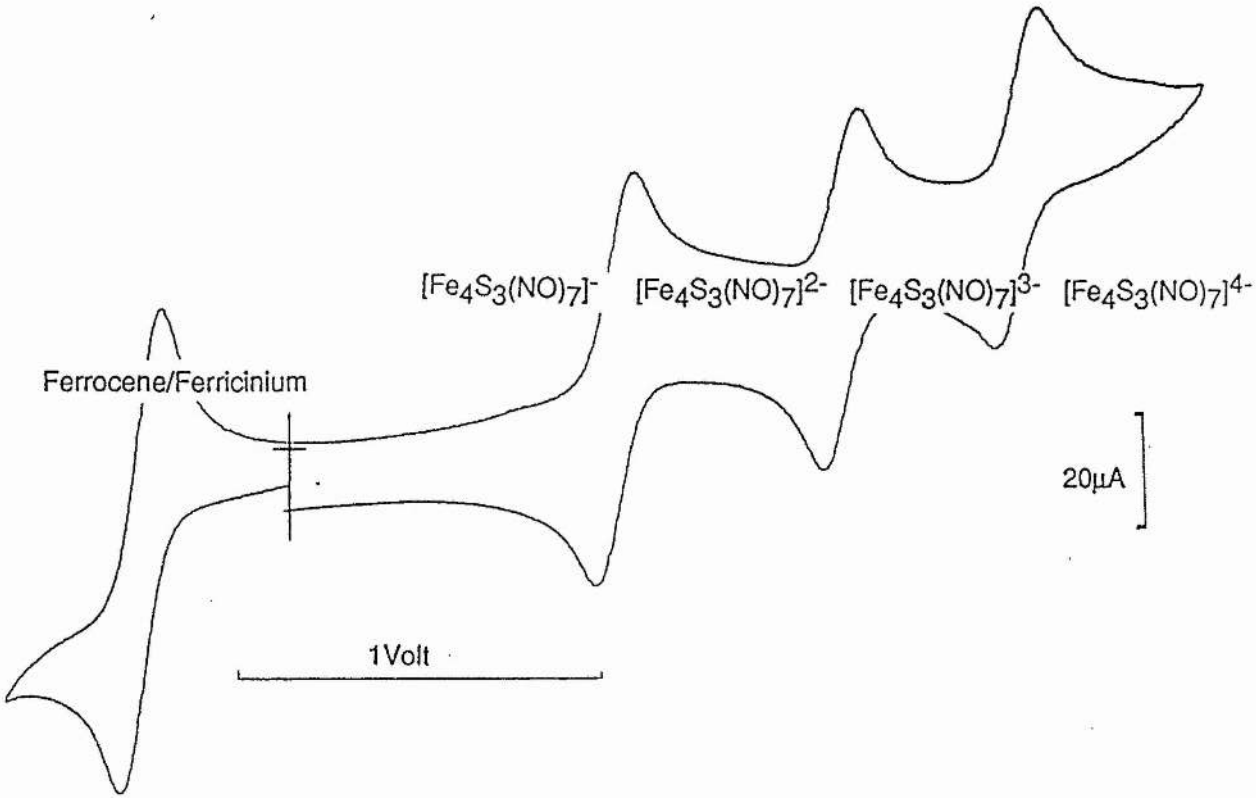


**Figure 4-13**

Cyclic Voltammogram of the Three Reductions of $Me_3S[Fe_4S_3(NO)_7]$ in THF at a Glassy Carbon Working Electrode

of electroactive material, to the gradient of the cathodic current of the first reduction of this cluster. This evidence and that an equal amount of ferrocene gives an identical limiting current, show that the reductions are indicative of three reversible one-electron reductions of $[Fe_4S_3(NO)_7]^-$, ie;

$$[Fe_4S_3]^- \overset{-1.31V}{====} [Fe_4S_3]^{2-} \overset{-1.91V}{====} [Fe_4S_3]^{3-} \overset{-2.41V}{====} [Fe_4S_3]^{4-}$$

**Figure 4-14**

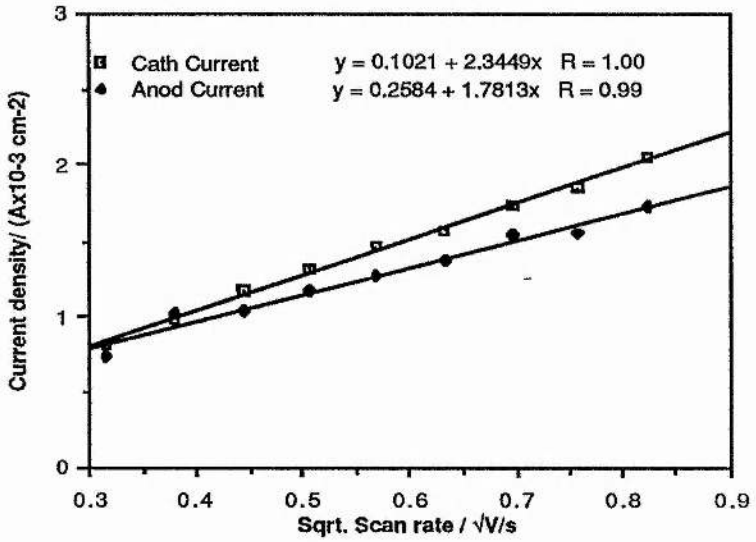


**Figure 4-15**

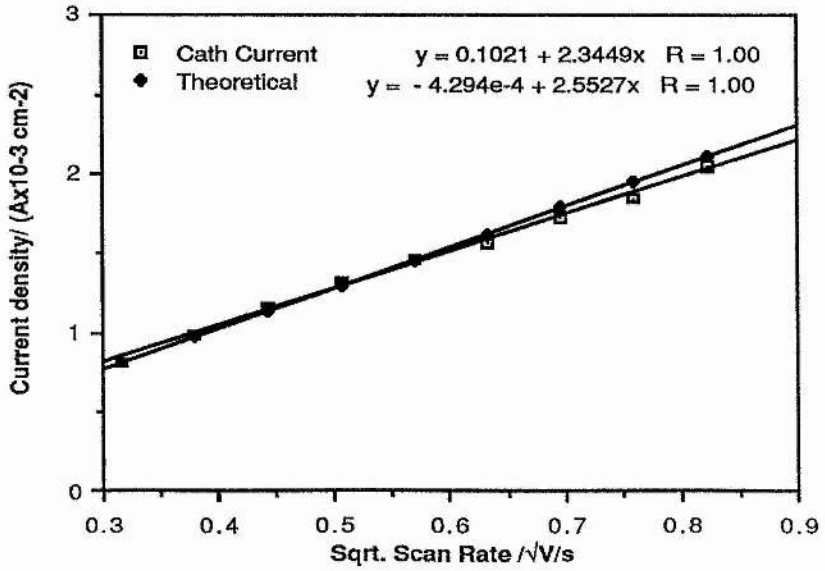

An examination of the ratio ia/ic for a range of scan rate (0.064- 0.9 V $s^{-1}$) gives for all three reductions and for all salts examined in THF a value of approximately 1. The $\Delta Ep$ value of an equivalent amount of ferrocene was measured at 100mV, for the $Me_3S$ salt of Roussin's Black anion values of 100, 100 and 120 mV were recorded for the first, second and third reduction waves respectively. All this data fits with the criteria for reversible couples.

In DCM, the electrochemistry of $(Et_4N)$ $[Fe_4S_3(NO)_7]$ was examined. Two reversible one-electron reductions were observed, the third reduction was partly obscured by the negative limit of the solvent and accurate current values could not be obtained. Relative to the Ag/AgCl electrode the reduction potentials were;

$$[Fe_4S_3]^- \rightleftharpoons [Fe_4S_3]^{2-} \rightleftharpoons [Fe_4S_3]^{3-} \rightleftharpoons [Fe_4S_3]^{4-}$$
$$-0.675V \qquad -1.195V \qquad -1.655V$$

It had been suggested that the first wave may be the one electron oxidation of the cluster giving the neutral $Fe_4S_3(NO)_7$. If the working electrode was switched on a slight anodic current was obtained due to a background current. If the potential was held at -0.8 V and the electrode turned on, then a large cathodic current was observed. If the potential was held at -1.3V and the working electrode switched on, a cathodic current twice as large was obtained. Thus the first wave obtained is the reduction of the monoanion to the dianion.

In addition to the three reductions, a complex oxidation was also observed; on cycling a waveform indicative of the reduction of an adsorbed species was evident. The oxidation of the Black anion was first performed on the sodium salt in aqueous solution at pH=9.2. On scanning to positive potentials first, an irreversible oxidation was observed and on cycling back an adsorption peak was present. This was determined from the shape of the peak and the linear dependence of the peak current on the scan rate and not on the square root of the scan rate as is found for species in solution. Thus the oxidation of the Black anion in water and DCM gives a material adsorbed onto the electrode which is capable of undergoing reduction.

The electrochemistry of $(Me_3S)$ $[Fe_4S_3(NO)_7]$ in acetonitrile was also examined. The two reductions $[Fe_4S_3]^{1-/2-}$ and $[Fe_4S_3]^{2-/3-}$ were found to be equally reversible, the $[Fe_4S_3]^{3-/4-}$ reduction was found to be quasi-reversible, figure 4-16. On scanning positive there are two one-electron irreversible oxidations, judging from the relative

**Figure 4-16**

Cyclic Voltammogram of $Me_3S[Fe_4S_3(NO)_7]$ in $CH_3CN$
at a Glassy Carbon Working Electrode

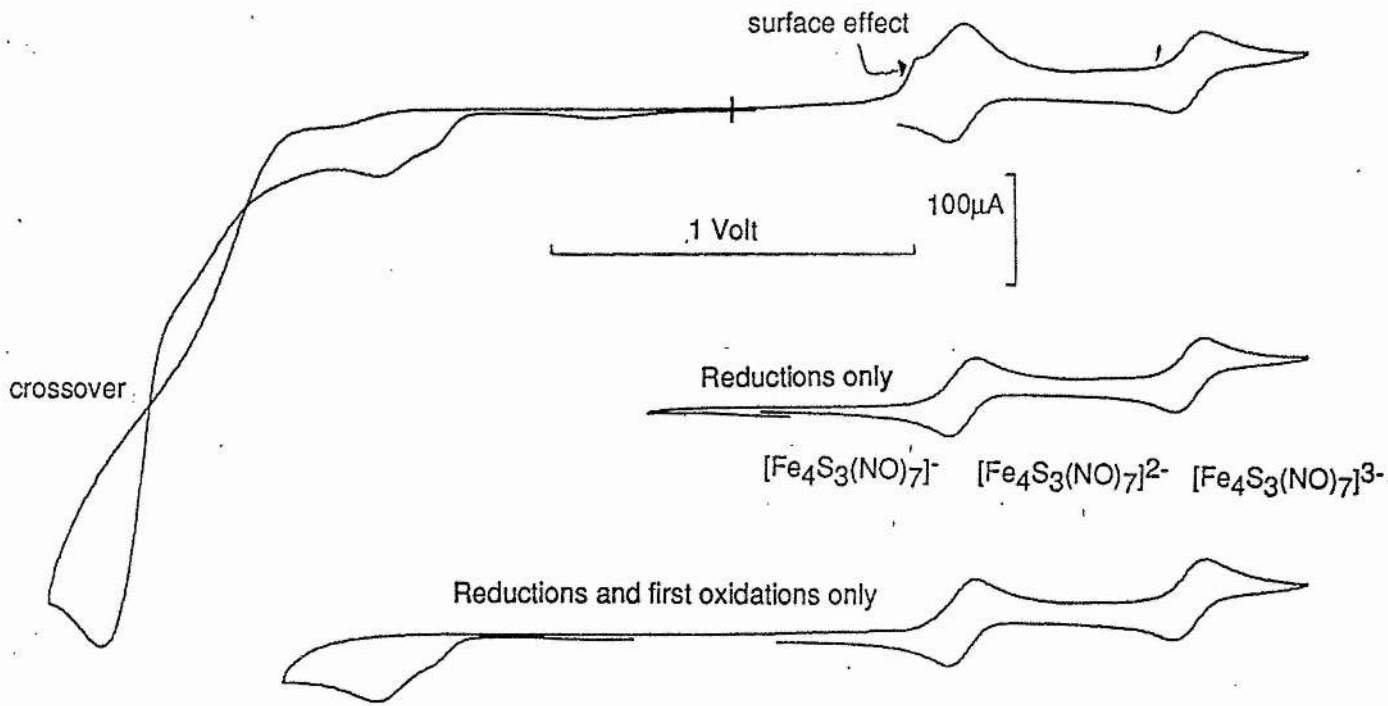

heights of the peak current values relative to that of the $[Fe_4S_3]^{1-/2-}$ couple. If the scan is moved more positive then a complex, multielectron oxidation takes place. From the height of the peak current relative to the $[Fe_4S_3]^{1-/2-}$ couple a transfer of 6 electrons is indicated. The figure also shows the presence of a cross-over, as the returning cathodic current crosses over the forward anodic current. This implies that there is more material being reduced than there was being oxidised. This usually occurs for metallation, disproportionation or when gas release is present. On returning to the potential of the first reduction a new cathodic peak is observed. If the electrode is scanned negative and then forward again the electrode becomes clean again. Chemical oxidation of salts of the Black anion with $AgNO_3$ and other oxidising agents first reported by Roussin [30], give rise to the evolution of NO(g).

The chemical reduction of $Na[Fe_4S_3(NO)_7]$ was attempted using sodiumbenzophenone ketyl as a reductant. An examination of the material obtained by e.p.r. spectroscopy showed only the presence of $[Fe(SH)_2(NO)_2]^-$. The disproportionation constant for the Black anion was calculated to be $1.6x10^{-9}$. The reason for the non-isolation of the dianion may be a kinetic factor.

4-9-2 The Electrochemistry of Na $[Fe_4Se_3(NO)_7]$

The structure of $Na[Fe_4Se_3(NO)_7]$ has recently been determined [31]. The structure of the anion is very similar to that of $[Fe_4S_3(NO)_7]^-$ as had been deduced from $^{15}N$ and $^{77}Se$ n.m.r. spectroscopy [10]. An examination of the molecular orbitals of this anion by the Extended Hückel approach shows strong similarity to that calculated for the sulphur analogue. Thus it was not surprising to find that the electrochemistry of the selenium anion paralleled that of the sulphur anion.

In acetonitrile solution $Na[Fe_4Se_3(NO)_7]$ shows the presence of three reductions, figure 4-17. The first two both meet the requirements of reversible couples, the third is quasi-reversible as observed for the sulphur analogue in acetonitrile. The reduction potentials occur at -1.06, -1.67 and approximately -2.41V for the first, second and third reductions respectively, relative to the $E^{\emptyset}$ of the ferrocene/ferricinium couple.

$$[Fe_4Se_3]^- \overset{-1.06V}{====} [Fe_4Se_3]^{2-} \overset{-1.67V}{====} [Fe_4Se_3]^{3-} \overset{-2.41V}{====} [Fe_4Se_3]^{4-}$$

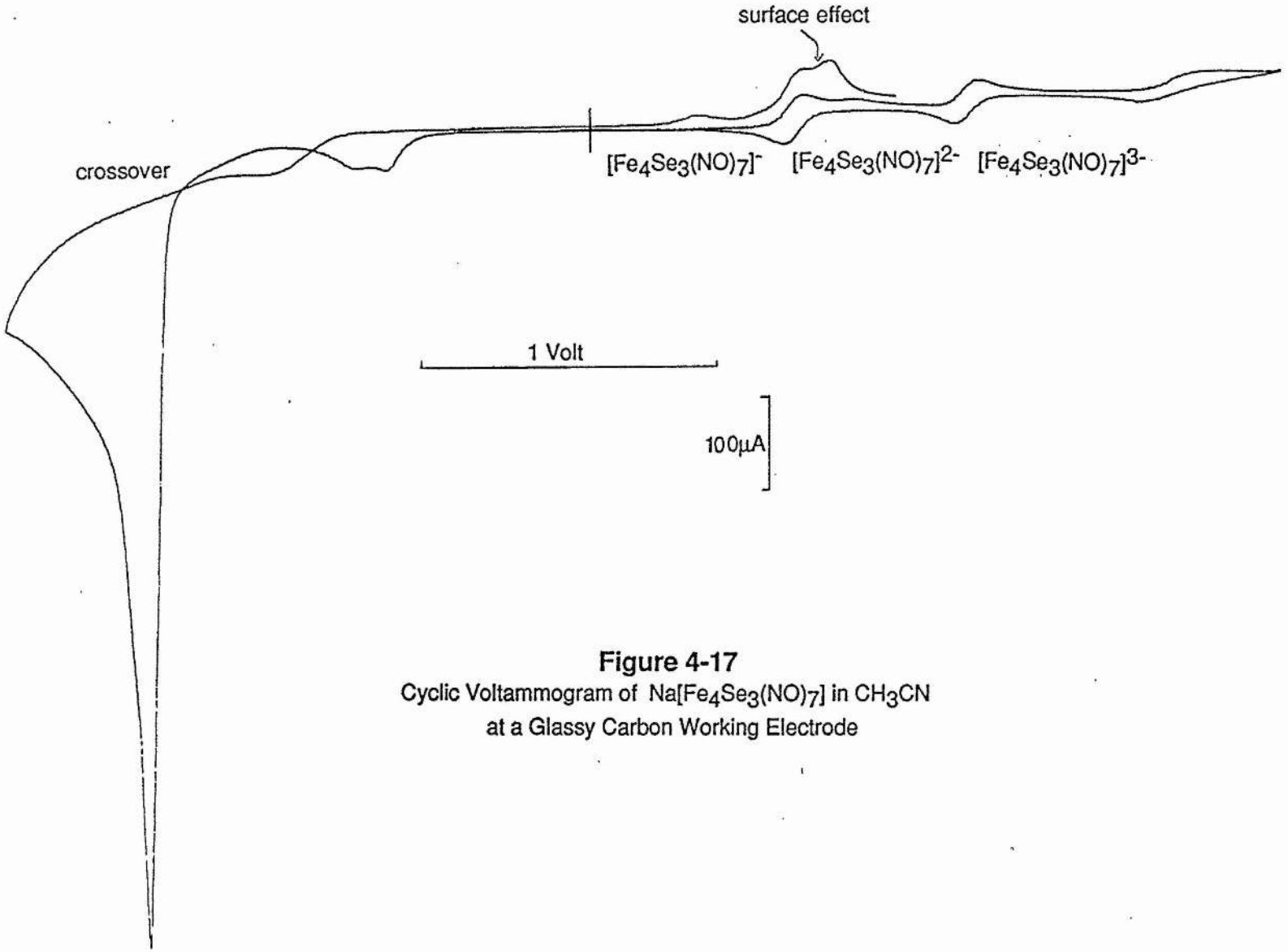


**Figure 4-17**
Cyclic Voltammogram of $Na[Fe_4Se_3(NO)_7]$ in $CH_3CN$
at a Glassy Carbon Working Electrode

The oxidation of the selenium anion also shows an initial one electron, irreversible oxidation. On scanning the potential more positive a large multielectron oxidation was observed, figure 4-17. From the relative height of the peak current to that of the $[Fe_4Se_3]^{1-/2-}$ couple, an electron transfer of 9 electrons for this oxidation was calculated. The cross-over present in the sulphur analogue was also observed for the selenium cluster.

## 4-10 The Oxidation of Amines and Alcohols via Nitrosyl Complexes

The oxidation of alcohols and amines using nitroxides have been widely reported [32,33,34]. Semmelhack and co-workers have shown that 2,2,6,6, tetramethylpiperidine nitrosonium cation catalyses these oxidations [33];

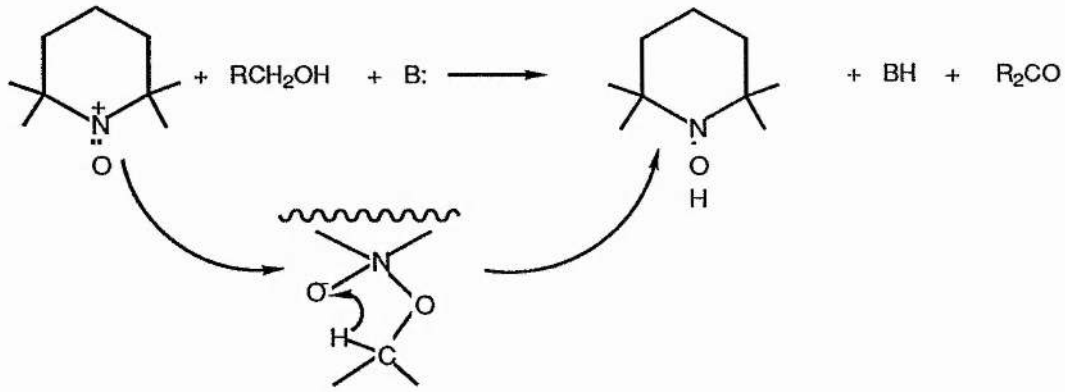


Using cuprous chloride, oxygen and the above nitroxide, Semmelhack developed a catalytic system to oxidise alcohols,(see below). Using such a reaction scheme benzylalcohol can be converted to benzaldehyde in 95% yield [35].

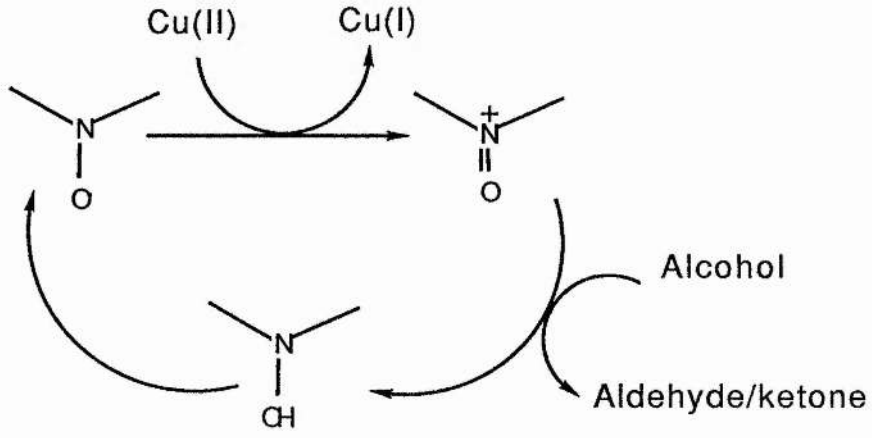


$$4Cu(I) + 4H^+ + O_2 \longrightarrow 4Cu(II) + 2H_2O$$

Miyazawo and co-workers have shown that it is the nitrosonium part of the structure that is responsible for the observed activity [32]. Metal nitrosyls such as the nitroprusside ion, $[Fe(CN)_5NO]^{2-}$ and the Roussin esters, $Fe_2(SR)_2(NO)_4$, have nitrosyl ligands which are formally $=N^+=O$, thus complexes containing such ligands might be expected to show a type of chemistry towards alcohols and amines similar to the above organic nitrosyl.

In a review of the reactivity of coordinated nitrosyls, M$^c$Cleverty suggests that the bending of the M-NO angle may be an essential precursor to the activity observed [36]. Bottomley [37] has shown that, in general, if $\nu$(NO) > 1886cm$^{-1}$ then the complex is susceptible to attack on the nitrogen by nucleophiles such as $RO^-$, $OH^-$, $RS^-$ and $NH_3$. The corollary of this being that a complex with a low $\nu$NO will be susceptible to electrophilic attack. For instance the reaction of $PhCH_2CH_2NH_2$ with $[Co(NO)X_2]_n$ in acetonitrile leads to the formation of a mix of compounds consisting mainly of $PhCH_2CHX_2$, but also containing $PhCH_2CH_2OH$ and $PhCH_2CN$ [36]. It has been reasoned that the reaction with the complex leads to the production of a diazo species, ie $RCH_2N_2^+$, although this would not explain the presence of the nitrile.

In a paper by Maltz [38], the reaction of sodium nitroprusside with benzylamine in aqueous alkali in the presence of oxygen was described. Benzylalcohol, benzonitrile and a trace of benzaldehyde were obtained. Again a diazo compound was proposed as an intermediate. The formation of the aldehyde may be via a nitrosyl, the alcohol being further oxidised by a nitrosyl, in a similar manner to the scheme outlined by Semmelhack. The presence of the nitrile does suggest more than one mechanism operating.

Recently Postel reported the formation of $Fe(NO)_2Cl(HMPA)$ complexes, which on oxidation give nitrato species, such as $Fe(NO_3)_2ClHMPA$ and $Fe(NO_3)Cl_2HMPA$ [39]. The latter complex was capable of oxygen transfer to phosphines, regenerating the Fe(NO) moiety. These nitrato complexes have proven capable catalysts in the autoxidation of cyclohexene.

4-10-1 The Effect of Amines on the Electrochemical Behaviour of $Fe_2(SR)_2(NO)_4$

Addition of a small quantity of benzylamine into a dichloromethane solution of $Fe_2(SR)_2(NO)_4$ (R=Me, Et, $^iPr$, $^tBu$) which was undergoing examination by cyclic voltammetry resulted in the production of a large anodic current, coincident with the oxidation peak of these Roussin esters. Addition of benzylamine to a solution of $Et_4N[Fe_4S_3(NO)_7]$ also led to a large anodic current coincident with the first oxidation peak of this cluster. The effect of added amine to the electrochemical behaviour of the Roussin esters was further examined.

Addition of small aliquots of benzylamine to a solution of $Fe_2(SMe)_2(NO)_4$ and the effect of the amine on the voltammogram observed; a complex picture was apparent. The oxidation of the amine by itself was found to be an irreversible affair with an ill-defined voltammogram; it was apparently a slow electron transfer with an oxidation around the edge of the positive solvent breakdown limit. The Roussin esters however show a well defined oxidation coupled to a surface effect as described earlier. As amine is added the oxidation peak shifts slightly to a more positive value. As addition continues two peaks are observed; one coincident with the oxidation of the Roussin esters the other slightly more positive. This former peak becomes the dominant feature as addition continues. The current of this peak was found to be linearly dependent on the amount of amine added. This behaviour has also been observed on the addition of n-butylamine to solutions of these Roussin esters.

Although the complexity of what occurs does mean that an exact mechanism cannot be given, a possible mechanism could be the following;

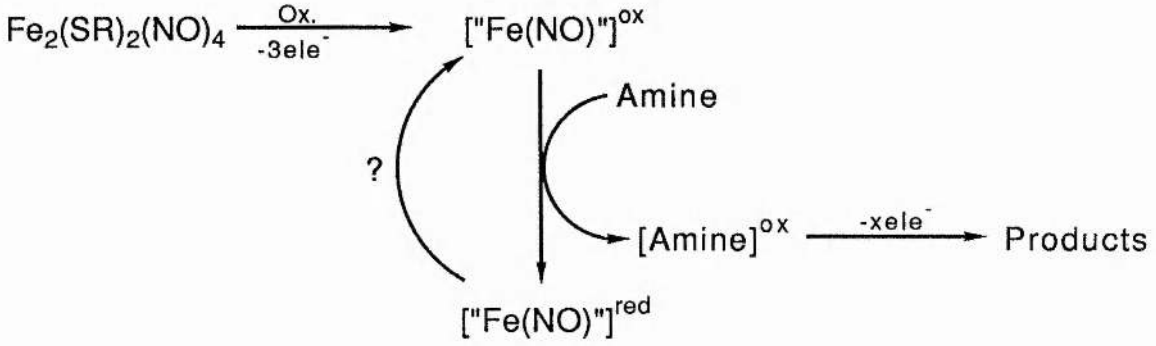


The Roussin ester is first of all oxidised to a species capable of reacting with amines, either sacrificially by producing a diazonum ion or catalytically by oxidising the amine by a method similar to Semmelhack's. The current obtained would be dependent on the concentration of the amine as was experimentally observed. The increase in anodic current

may be due to the product of the oxidised amine further oxidising at the breakdown potential of the cluster.

What is worthy of comment here is that the addition of amines does not affect the current values nor the shape of the voltammograms for the two reduced states of the cluster, ie only the oxidised ester is affected. This observation is in accord with Bottomley's observation [37]. Since reduction reduces the $\nu$NO observed, oxidation might be expected to increase the value such that it reaches the criterion for reaction with nucleophiles. This may be what is occurring, but the production of an oxidised form of $Fe_2(SR)_2(NO)_4$ has not been realised. Since this electrochemical work suggested a possible reaction between an oxidised ester and amines, the chemical reaction of a variety of amines with a variety of Roussin esters under oxidising conditions were carried out.

The autoxidation of the clusters $Na_2[Fe_2(S_2O_3)_2(NO)_4]$ and $Fe_2(SMe)_2(NO)_4$ have been shown to produce the complex $[Fe(NO)_2(NO_2)_2]^-$. This species has labile nitrosyl as well as nitrite groups; the material shows fluxionality at room temperature [40]. The electrochemical oxidation of these clusters may also be producing a similar complex.

4-10-2 Reaction of $Na_2[Fe(CN)_5NO]$ with Benzylamine using $O_2$

Reacting $Na_2[Fe(CN)_5NO]$ with benzylamine in aqueous alkali under oxygen for 24 hours, in an identical manner to Maltz [38], resulted in the production of an orange oil. According to Maltz three products were obtained; benzaldehyde, benzonitrile and benzylalcohol. An examination of the orange oil obtained from this work also revealed these three components. However, when subjected to an examination by G.C.M.S., two further products were observed,( <0.05% of oil). Using the library search facilities of the G.C.M.S. system, which compares the observed mass-spectrum to the mass-spectra of known compounds, these two products were found to be benzoic acid (probably from the aerial oxidation of the aldehyde) and surprisingly the phenylmethylester of benzoic acid. A possible reaction scheme is given on the next page.

The formation of the nitrile does not fit with the proposed mechanism of a diazo intermediate. A possible route to the nitrile involves the loss of two electrons to produce RCH=NH, with the further loss of two electrons to produce the nitrile. It is possible that these electrons are transferred to the $Fe\text{-}NO^+$ moiety producing NO(g).

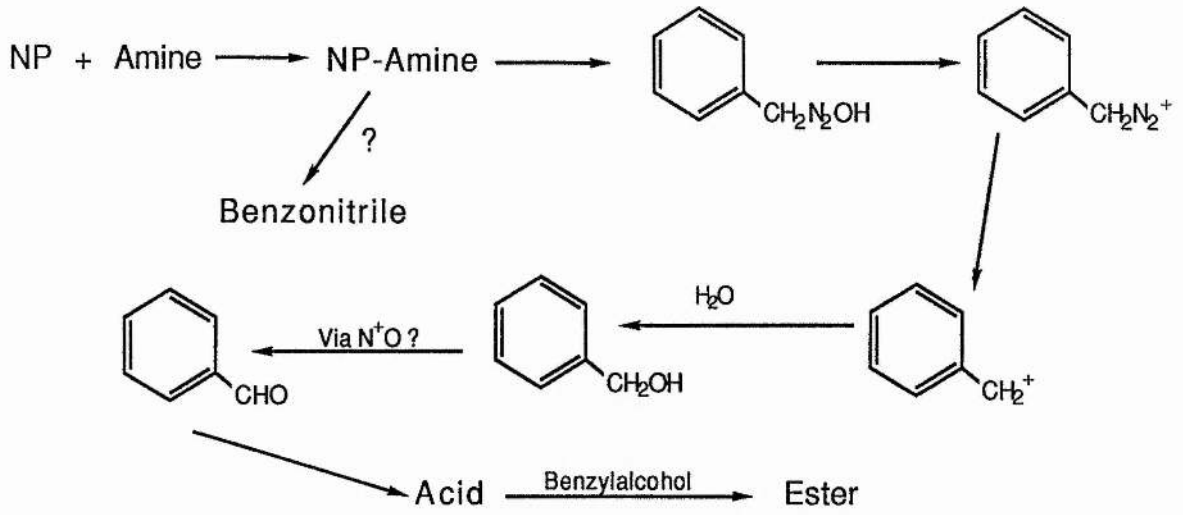


4-10-3 Reaction of $Na_2[Fe_2(S_2O_3)_2(NO)_4]$ with Benzylamine using $O_2$

In a similar reaction to the above, the oil obtained was subjected to an examination by G.L.C. and G.C.M.S. From the G.L.C. trace two peaks were obtained and from the retention times corresponded to benzylamine and benzylalcohol, in the proportions 3:2 respectively. On examination by G.C.M.S. a further peak with a long retention time was observed. From the library search facility of the G.C.M.S. the asignments of the peaks to the amine and alcohol were confirmed. The third product corresponded to benzylidenebenzylamine, $PhCH_2NCHPh$. Neither the aldehyde, nitrile nor acid were observed. From this result a diazonium intermediate can also be formulated. Although the formation of the imine could, theoretically, be accomplished by the direct attack of an amine on the carbocation, this is highly unlikely and a more plausable method involves the attack of the amine on the aldehyde. No aldehyde was actually observed, but the formation of this imine is highly suggestive of its transient appearance. It should also be noted that the imine was not observed with the reaction of nitroprusside with amine.

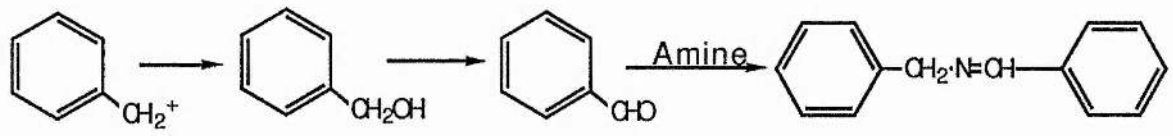


The reason for the presence of benzylamine in the oil obtained may be due to unreacted amine or due to the hydrolysis of this imine, however it would be impossible to distinguish between the two possibilities.

What is clear from this work is that the aerial oxidation of the thiosulphato complex in the presence of benzylamine causes the conversion of the amine presumably via a diazonium intermediate to the corresponding alcohol.

4-10-4 Reaction of $Fe_2(SR)_2(NO)_4$ with amines using $AgNO_3$

Silver nitrate was used as an oxidising agent instead of oxygen as had been done with the above. The reason was speed of reaction and control of oxidising stoichiometry. Controls were set up to ensure that the silver nitrate did not, by itself, oxidise the amines. N-methylaniline was found to be oxidised rapidly by silver nitrate and so was not used in this work. The secondary amines used with this work were oxidised only slowly by silver nitrate, >2-8 hours. Since reaction times in this work were measured in seconds, this slow oxidation was not seen as a problem. The primary amines however were not affected by the silver nitrate.

On addition of $AgNO_3$ to a THF solution of Roussin ester and amine, decomposition of the iron sulphur cluster occurred and bubbles presumably NO --> $NO_2$ were observed, (the air above the reaction vessel turned slightly brown, indicating the presence of $NO_2$).

For R= n-butyl and amine = benzylamine, the G.L.C. showed the presence of benzaldehyde, benzonitrile and benzylalcohol, in the relative proportions 16 : 1.5 : 83. $^{n}$Butyl thiol was also observed as was the disulphide and a variety of iron-sulphur fragments, which have so far eluded identification. In the work up any remaining amine would have remained in the aqueous layer. It has been observed that $AgNO_3$ will oxidise benzylalcohol. This oxidation is slower than the reaction with the ester, but is significant. The presence of the aldehyde could be due to this oxidation, however this is unclear at the moment and further work is being done.

Reaction of di$^{n}$proylamine and pyrollidine with the isobutyl and secbutyl esters of Roussin's Red salt respectively in the presence of $AgNO_3$ resulted in the decomposition of the Roussin esters and the evolution of brown fumes. An analysis by GLC of the reaction products for both these experiments indicated a variety of products. Analysis by GCMS was inconclusive, the peak with the largest retention time did, however, correspond to

Butyl-S-Butyl in both cases. There was no evidence for the production of N-nitrosamines with this work.

Analysis of the products of the reaction between the thiosulphato complex and cyclopentylamine and the isopropyl ester of Roussin's Red salt with butylamine did not give any observable product by GLC. A peak originally assigned to butyraldehyde from the latter experiment was found from the GCMS library search to be THF. With these latter two experiments if a diazonium ion was produced then butylamine would give but-ene, and cyclopentylamine would yield cyclopentene and neither would of course be observed by the methodology used in working up the reactions.

Although these latter experiments are inconclusive, the former experiments with benzylamine do strongly suggest that the oxidation of $Fe_2(SR)_2(NO)_4$ in the presence of an amine results in the oxidation of that amine. If this is so then the production of N-nitrosamines from secondary amines should be possible. Further work in this area is being caried out by Miss Audrey Lees at the University of St. Andrews.

## References


1. For instance, Bartak, D. E., Houser, K. J., Rudy, B. C., Hawly, M. D., J. Am. Chem. Soc., 94, 7526, (1972)

2. For instance, Geiger, W. E., Prog. Inorg. Chem., 33, 275

3. Zanello, P., Coord. Chem. Rev, 83, 199, (1988)

4. Kissinger, P. T., Heinemann, W. R., J. Chem. Ed., 60, 702, (1983)

5. Mabbot, G. A., J. Chem. Ed., 60, 697, (1983)

6. Bioanalytical Systems Inc, West Lafayette, Indiana, 47906

7. Southhampton Electrochemistry Group, " Instrumental Methods in Electrochemistry", (1985), Ellis and Horwood, (Publishers)

8. Bard, A. J., Faulkner, L. R., "Electrochemical methods, Fundamentals and Applications", (1980), John Wiley and Sons

9. Heinze, J., Angew. Chem. Int. Ed., 23, 831, (1984)

10. Butler, A. R., Glidewell, C., Hyde, A. R., M$^{c}$Ginnis, J., Inorg. Chem., 24, 2931, (1985)

11. Ege, S., "Organic Chemistry", 2$^{nd}$ Edition, (1989), Heath (Publishers) Lexington

12. Lemoine, P., Coord. Chem. Rev., 83, 199, (1988)

13. Holm, R. H., Accs. Chem. Res.,10, 427, (1977)

14. Peake, B. M., Robinson, B. H., Simpson, J., Watson, D. J., Inorg. Chem, 16, 405, (1977)

15. Bond, A. M., Peake, B. M., Robinson, B. H., Simpson, J., Watson, D. J., ibib 16, 410, (1977)

16. Darchen, A., Mousser, H., Patin, H., J.C.S. Chem. Comm., 968, (1988)

17. Dessey, R. C., Kornmann, R., Smith, C., Haytor, R., J. Am. Chem. Soc., 90, 2001, (1968)

18. Yu, Y-F., Chau, C-N., Wojcicki, A., Inorg. Chem., 25, 4098, (1986)

19. Weatherill, T. D., PhD Thesis, University of Illinois Urbana-Champaign, (1985)

20. Bezems, G. J., Rieger, P. H., Visco, S., J. C. S., Chem. Comm., 265, (1981)

21. Nicholson, R. S., Shain, I., Anal. Chem., 36, 706, (1964): ibid, 37, 178, (1965)

22. Abruna, H. D., Coord. Chem. Rev., 86, 135, (1988)

23. Bond G. C., "Heterogeneous Catalysis", Clarendon Press, (1987)

24. Pratt, D. E., Laurie, S. H., Dahm, R. H., Inorg. Chim. Acta., L21, 135, (1987)

25. Butler, A. R., Glidewell, C., Li, M-H., Adv. Inorg. Chem., 32, 335, (1988)

26. On dissolving a solution of $Na[Fe_2S_2(NO)_4]$ in THF and allowing it to sit for an hour the twin dinitrosyl peaks observed in the infra-red spectrum of this material are replaced by the three peaks characteristic of Roussin's Black anion.

27. Lin Xianti, Zheng An, Lin Shunhao, Huang Jingling, Lu Jiaxi, J. Struct. Chem. (Wuhan), 1, 79, (1982)

28. Chu, C. T-W., PhD Thesis, University of Wisconsin-Madison, (1977)

29. Nelson,L. L., PhD Thesis, University of Wisconsin-Madison, (1981)

30. Roussin, Z. F., Ann. Chem. Phys., 52, 283, (1856)

31. Lees, A. University of St. Andrews, Awaiting publication.

32. Miyazawa, T., Endo, T., Shiihashi, S., Okanawa, M., J. Org. Chem., 50, 1332, (1985)

33. Semmelhack, M. F., Schmid, C. R., J. Am. Chem. Soc., 105, 6732, (1983)

34. Rozantsev, E. G., Sholle, V. D., Synth., 401, (1971)

35. Semmelhack, M. F., Schmid, C. R., Cortés, D. A., Chou, C. S., J. Am. Chem. Soc., 106, 3374, (1984)

36. M$^{C}$Cleverty, J., Chem. Rev., 79, 53, (1979)

37. Bottomley, F., Brookes, W. V. F., Clarkson, S. G., Tong, S-B, J. C. S., Chem. Comm, 919, (1973)

38. Maltz, H., Grant, M. A., Navaroli, M. C., J. Org. Chem., 36, 363, (1971)

39. Wah, H. L., Postel, M., Tomi, F., Inorg. Chem., 28, 233, (1989)

40. Butler, A. R., Glidewell, C., Johnson, I. L., Polyhedron, 6, 2091, (1987)

# Chapter Five

# Chapter Five

## An Electrochemical Examination of Some Mononitrosyl Dialkyldithiocarbamate Complexes of Iron, and Related Compounds

### Introduction

Sulphur ligands have often been used to stabilise transition metal complexes. In biochemistry we observe their use, for instance, in the stabilisation of iron-sulphur enzymes where the use of inorganic or 'labile' sulphur ($S^{2-}$) as well as organo-sulphur (S-cysteinyl) is present [1]. The iron-sulphur nitrosyl cluster $Fe_2(SMe)_2(NO)_4$, recently implicated in the occurrence of oesophageal cancer [2], shows the use of a bridging organo-sulphur ligand. Holm and co-workers, in their elegant work on models of the active sites of iron-sulphur enzymes, brought into use a bichelating organo-sulphur ligand o-xylene $\alpha,\alpha'$ dithiol [1]. The use of organo-sulphur ligands in the chelate effect, which is known to increase the stability of complexes, has been widely used. The dialkyldithiocarbamate complexes of transition metals have been extensively studied; the iron complexes are the classic spin cross-over compounds [3]. Apart from iron, the Mn, V, Zn, Co, Ni, Cu and Au complexes are known [5,6] and a wide range of metal diselenocarbamates have also been characterised [6].

The dialkyldithiocarbamates ($R_2DTC$) help stabilise metals in high oxidation states [6]. For instance halogens oxidise $R_2DTC$ complexes by oxidative addition [6].

$$Au^{I}(R_2DTC) + X_2 \text{ -----> } Au^{III}(R_2DTC)X_2 \quad [8]$$

$$Cu^{I}(^{n}Bu_2DTC)_x + Br_2 \text{ -----> } Cu^{III}(^{n}Bu_2DTC)Br_2 \quad [9]$$

$$Ni^{II}(Et_2DTC)_2 + Br_2 \text{ -----> } Ni^{IV}(Et_2DTC)_2Br_2 \quad [10]$$

Oxidation of $Fe(R_2DTC)_3$ with iodine produces the iron (IV) complex $Fe(R_2DTC)_3I_3$, whereas oxidation by $Br_2$ or $Cl_2$ causes the oxidation of $R_2DTC$ to the corresponding thiuramdisulphide , TDS [6]. Reaction of $Fe(R_2DTC)_3$ or $Fe(R_2DTC)_2X$ (X=hal) with $Cl_2$ or $Br_2$ also produces the $FeX_4^-$ anion. A similar complex is also found for the Sb, Cu(I) and

Co(III) dialkyldithiocarbamato compounds on oxidation with these halogens [6].

The reaction of $Fe(acac)_3$ or similar complexes with $NO_2$ produces $Fe(NO_3)_3$ [5]. Reaction of $NO_2$ with $Fe(R_2DTC)_3$ gives an intense E.P.R. spectrum, continued use of $NO_2$ however leads also to $Fe(NO_3)_3$. A similar reaction is found with the Mn and Cr $R_2DTC$ compounds [5]. With $Fe(R_2DTC)_3$ however the complex $Fe(NO)(R_2DTC)_2$ ( $Fe=d^7$) was also found. The following scheme was developed to account for these observations.

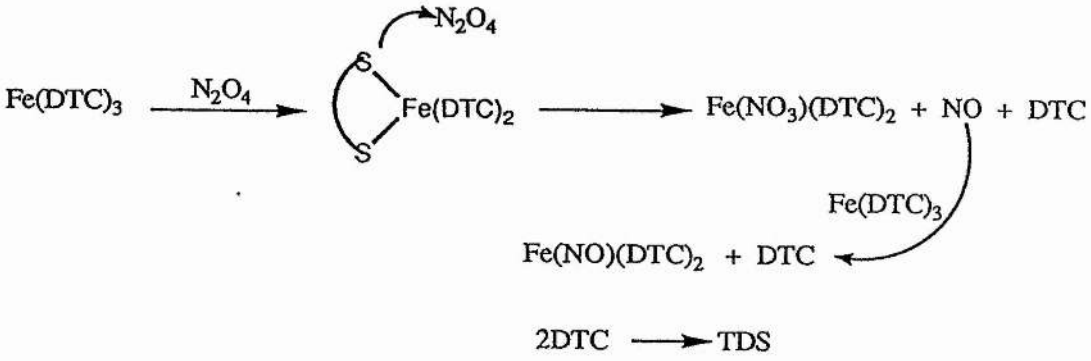


Thus continued oxidation produces the diamagnetic $Fe(NO_2)(NO)(R_2DTC)_2$. This mononitrosyl has been much studied. The highest occupied orbital of the complex contains a single electron residing mainly in the $dz^2$ orbital of the iron [11,12]. The Fe-N-O fragment is approximately linear whereas the cobalt complex which contains one more electron has a bent Co-N-O fragment [13].

The effect of R on the electron density of the iron is well documented [14,15] The effect on the complex can be seen by an examination of the following two hybrids.

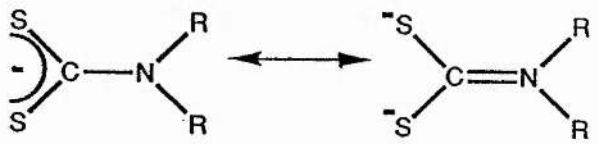


(a) (b)

Increasing the amount of (b) increases the electron density on the iron, thus leading to more elecron density being available to enter the $\pi^*$ orbitals of the NO ligand; a stronger M-N bond is formed but a weaker N-O is observed.

Previous preparations of the complexes $Fe(NO)(R_2DTC)_2$ have involved the use of

NO(g). However $Fe(R_2DTC)_3$ and $Fe(NO)(NO_2)(R_2DTC)_2$ are often found contaminating the sample. Preparations from preformed iron nitrosyl groups involving the use of $[Fe_4S_3(NO)_7]^-$ and $Fe_4S_4(NO)_4$ have been described [16], and reactions of $[Fe_2(S_2O_3)_2(NO)_4]^{2-}$ with $R_2DTC$ salts produce the mononitrosyl complexes in good yield and purity [see Chpt-3]

Reaction of $Fe(NO)(R_2DTC)_2$ with oxidising agents leads to the oxidative addition complex with the attached group in the cis configuration [4a,17]. Reaction with $NO_2$ at -60°C produces the trans isomer which converts to the cis on heating. There appears to be no reaction with NO(g), but if $^{15}NO$ is used an exchange with M-$^{14}NO$ is observed; thus a dinitrosyl intermediate may be present [17]. It is noteworthy that in the preparation from $[Fe_2(S_2O_3)_2(NO)_4]^{2-}$ , the dinitrosyl $Fe(NO)_2(R_2DTC)_2$ is not obtained even although a cis-dinitrosyl was the starting material; this perhaps shows the lability of such a dinitrosyl.

Reduction of $Fe_2(SR)_2(NO)_4$ shows a decrease in the $\nu$(NO) stretching frequencies. This is due to an increase in the back-bonding of the metal to the $\pi^*$ orbitals of the nitrosyls. As discussed in chapter four this is in agreement with Pauling's electroneutrality principle. Reduction of $Fe(NO)(R_2DTC)_2$ would place an electron in the $dz^2$ SOMO, assuming that no major restructuring took place, to produce a diamagnetic compound. This compound would be isoelectronic with $Co(NO)(R_2DTC)_2$, and perhaps isostructural with a bent Fe-N-O fragment. It should also be obvious that $[Co(NO)(R_2DTC)_2]^+$ would be isoelectronic and perhaps also isostructural with $Fe(NO)(R_2DTC)_2$.

This chapter examines the electrochemistry of some dialkyldithiocarbamate complexes and also some related complexes with $R_2DTC$ ligands.

## Experimental

Preparation of tris(diethyldithiocarbamato)iron(III), $Fe(S_2CNEt_2)_3$

To an aqueous solution of $FeCl_3$ (5.0g, 0.03moles) was added $NaS_2CNEt_2.3H_2O$ (20.5 g, 0.09 moles). The black/brown mixture was extracted with $CH_2Cl_2$. The organic layer was dried over $MgSO_4$ and on subsequent removal of the solvent, black prisms of $Fe(S_2CNEt_2)_3$ were obtained.

Microanalysis, calculated for $C_{15}H_{30}N_3FeS_6$; expected C 36.0, H 6.0, N 8.4%, obtained, C 35.7, H 6.0, N 8.3%. Mass-Spectrum; $M^+$ = 500, $M^+$-$S_2CNEt_2$= 352, $M^+$-$2S_2CNEt_2$= 204.

Preparation of $Fe(CO)_2(S_2CNEt_2)_2$ (modified from ref.[18])

To a stirred solution of $Fe_2(SEt)_2(CO)_6$ ( 2.01g, 5mmol) in methanol(50ml) was added, under nitrogen, $NaS_2CNEt_2.3H_2O$ (4.5g, 20mmol). The solution was stirred for 2 hours after which time the nitrogen inlet was removed and the solution left to stir for a further 2 days. The resulting mixture was filtered and washed with methanol to remove unreacted carbonyl. The solid was extracted with $CH_2Cl_2$ (3x150ml). The solvent was removed by evaporation and the resulting solid recrystallised from $CH_2Cl_2$ and MeOH. Yield of $Fe(CO)_2(S_2CNEt_2)_2$ = 19%.

Microanalysis, calculated for $C_{12}H_{20}N_2S_4FeO_2$ ; expected C 35.3, H 4.9, N 6.9%, obtained, C 34.9, H 5.3, N 6.5%. I.R.,($CH_2Cl_2$ solution) $\nu$(CO)asym=2010cm$^{-1}$, $\nu$(CO)sym=1958cm$^{-1}$, (consistent with a cis-dicarbonyl structure). Mass-Spectrum, $M^+$= 408, $M^+$-CO =380, $M^+$-2CO = 352, $M^+$-2CO,$S_2CNEt_2$=205.

Preparation of $Fe(NO)(S_2CNR)_2$ R=Me, Et, $^nPr$

These compounds were prepared from aqueous solutions of $Na_2[Fe_2(S_2O_3)_2(NO)_4]$ as described in chapter three, page 76. The materials were analysed by I.R. and mass spectroscopy (only shows the $M^+$-NO peak as the highest) and by microanalysis.

Preparation of $Co(NO)(S_2CNMe_2)_2$

The method of preparation followed that given by Feltham [19]. This involved the preparation of $[Co(NO)(H_2NC_2H_4NH_2)_2](ClO_4)_2$ and its subsequent conversion to the bis-dithiocarbamato compound.

Microanalysis of $[Co(NO)(H_2NC_2H_4N_2H)_2](ClO_4)_2$, calculated for $C_4H_{10}N_5CoCl_2O_9$; expected, C 11.8, H 4.0, N 17.2%, obtained, C 11.8, H 4.0, N 17.3%. Microanalysis of $Co(NO)(S_2CNMe_2)_2$, calculated for $C_6H_{12}CoN_3S_4O$; C 21.9, H 3.7, N 12.8%, obtained, C 21.8, H 3.5, N 12.6%. Mass-spectrum, $M^+$=329, $M^+$-NO = 299.

Oxidation of $Co(NO)(S_2CNMe_2)_2$

A solution of $Co(NO)(S_2CNMe_2)_2$ (1g, 3mmol) in $CH_2Cl_2$ was stirred for three days in air. During this period the solution changed colour from brown to green. The solvent was removed and the material recrystallised from acetone and water.

The I.R. spectrum of the material shows the loss of the $\nu$(NO) absorption at 1644cm$^{-1}$. A weak absorption at 1688cm$^{-1}$ was present (NB, $Fe(NO)(S_2CNR_2)_2$, $\nu$(NO)≈ 1689cm$^{-1}$). Mass-spectrum shows the presence of $Co(S_2CNMe_2)_3$ and a peak due to $[Co(S_2CNMe_2)_2]^+$. Microanalysis calculated for $Co(S_2CNMe_2)_3$ , C 25.8, H 4.3, N 10.0%, obtained C 25.9, H 4.3, N 9.4%.

Reduction of $Fe(NO)(S_2CNEt_2)_2$

To a stirred solution of $Fe(NO)(S_2CNEt_2)_2$ (1.0g, 3mmol, THF(30ml)) was added an excess of $LiBH(Et)_3$ (Super-Hydride) under nitrogen. Gas evolution was observed and the solution turned brown within a few minutes. The solvent was removed under vacuum leaving a sticky brown solid. Examination by I.R. spectroscopy revealed the loss of the $\nu$(NO) absorption: the absorptions of the dithiocarbamate ligands were still present. $^1$H n.m.r. of the material in $CDCl_3$ gave broad features with two resonances centred at 1.3 and 2.6ppm in the ratio 3:2. The material gave no e.p.r. signal.

Electrochemistry; Electrochemical measurements on $Fe(NO)(S_2CNR_2)_2$ (R=Me, Et, $^n$Pr), $Co(NO)(S_2CNMe_2)_2$ , $Fe(CO)_2(S_2CNEt_2)_2$ and $Fe(S_2CNEt_2)_3$ were carried out as outlined in chapter four.

## Results and Discussion

### 5-1 Electrochemistry of $Fe(S_2CNEt_2)_3$

In Chapter two the molecular orbitals of the dimer $[Fe_2S_2(NO)_4]^{2-}$ and its associated complexes $Fe_2(SR)_2(NO)_4$ and $[Fe_2(S_2O_3)_2(NO)_4]^{2-}$ were examined. The tetranuclear anion $[Fe_4S_3(NO)_7]^-$ was also subject to a similar examination. In chapter four the electrochemistry of these clusters was examined. With reference to Enemark and Feltham [23] the bonding of metal nitrosyl complexes was considered to be a predominantly M-NO interaction perturbed by the other ligands attached to the metal. To examine further the electrochemistry of the Fe-NO moiety the dithiocarbamato complexes $Fe(NO)(S_2CNR_2)_2$ R=Me, Et, $^nPr$ were examined by cyclic-voltammetry. The associated complexes $Co(NO)(S_2CNMe_2)_2$ and $Fe(CO)_2(S_2CNEt_2)_2$ were also examined by cyclic-voltammetry.

Firstly, the electrochemistry of the complex $Fe(S_2CNEt_2)_3$ was determined. Although the electrochemistry of this material has been documented [20a] the electrochemical examination by C.V. was repeated here to obtain a direct comparison of the electrochemistry of this complex to that of $Fe(NO)(S_2CNR_2)_2$. An excellent review of the electrochemistry of metal dithiocarbamato compounds is available [20].

The C.V. of $Fe(S_2CNEt_2)_3$ is shown in figure 5-1. With reference to the Ag/AgCl reference electrode, a reversible one electron reduction and a reversible one electron oxidation are observed with reduction potentials of -0.40 V and +0.44 V respectively. The oxidation of the compound was found to be chemically reversible for all scan rates examined ( $i_a/i_c \approx 1$ ). The reduction however also shows a chemical step interfering with the return wave, ie an EC mechanism [21] ( $i_a/i_c$ decreases as the scan rate decreases but approaches 1 as the scan rate > 0.9 V $s^{-1}$). On scanning positive after the reduction, the oxidation of the breakdown products can be observed. At more negative potentials a second reduction was observed, but this shows slow electron transfer kinetics.

Figure 5-1
Cyclic Voltammogram of $Fe(S_2CNEt_2)_3$
in $CH_2Cl_2$ at a Platinum Working Electrode

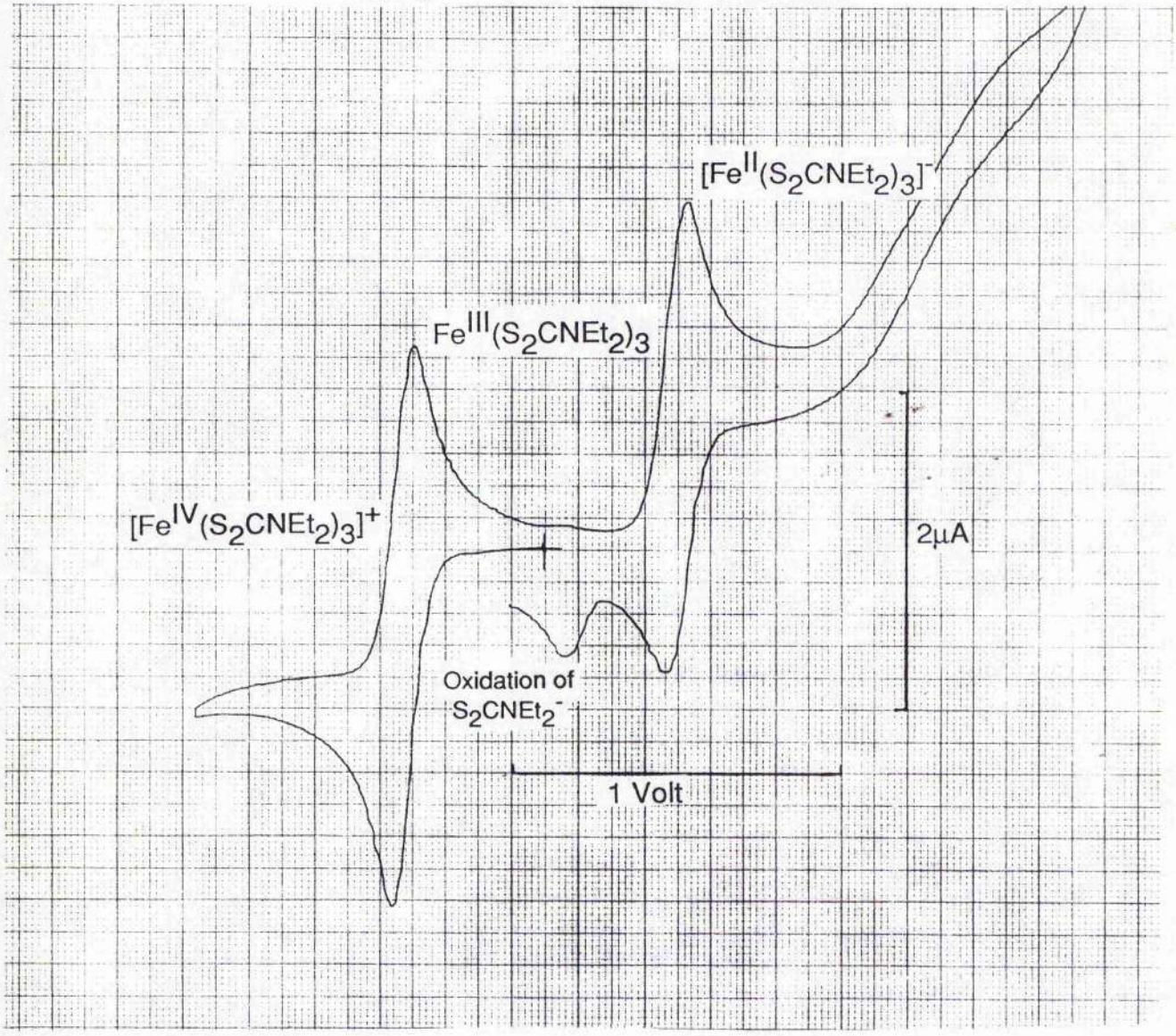

This electrochemical behaviour fits well with what is known both chemically and electrochemically about this type of complex [20, 20a]; the dialkyldithiocarbamate ligand stabilises higher oxidation states, and that on reduction there is a rearrangement of the reduced species as is shown below.

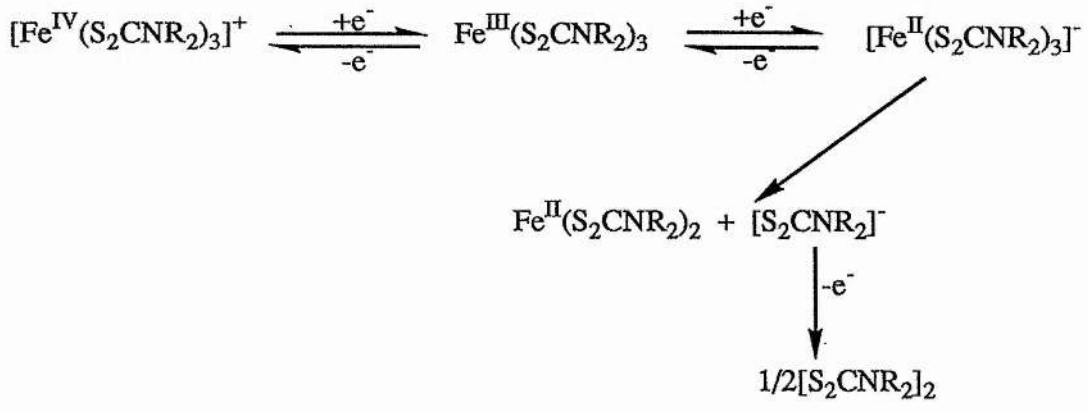


5-2 Redox Chemistry of $M(NO)(S_2CNR_2)_2$ M=Co, Fe , R= alkyl

In THF, $Fe(NO)(S_2CNR_2)_2$, for R=Me, Et, $^nPr$ all exhibit the same type of of electrochemical response at a Pt (oxidised or non-oxidised) or glassy carbon working electrode. A reversible one electron reduction and a one electron irreversible oxidation are observed; both processes involve the production of oxidisable or reducible byproducts respectively, (figure 5-2). In $CH_2Cl_2$ similar behaviour was observed. Table 5-1 gives the reduction potentials for these compounds relative to the ferrocene/ferricinium couple.

**Table 5-1**

| Compound | $E^{\emptyset}$(0/1-)(a) | E(ox)(b) |
|---|---|---|
| $Fe(NO)(S_2CNMe_2)_2$ | -1.340 | +0.29 |
| $Fe(NO)(S_2CNEt_2)_2$ | -1.385 | +0.30 |
| $Fe(NO)(S_2CN^nPr_2)_2$ | -1.380 | +0.36 |
| $Co(NO)(S_2CNMe_2)_2$ | -1.330 | +0.29 |

(a) reduction potential of the 0/1- couple relative to $Fc^{+/o}$, (b) position of the peak relative to $Fc^{+/o}$.

**Table 5-1**, electrochemical data for the $M(NO)(S_2CNR_2)_2$ complexes examined

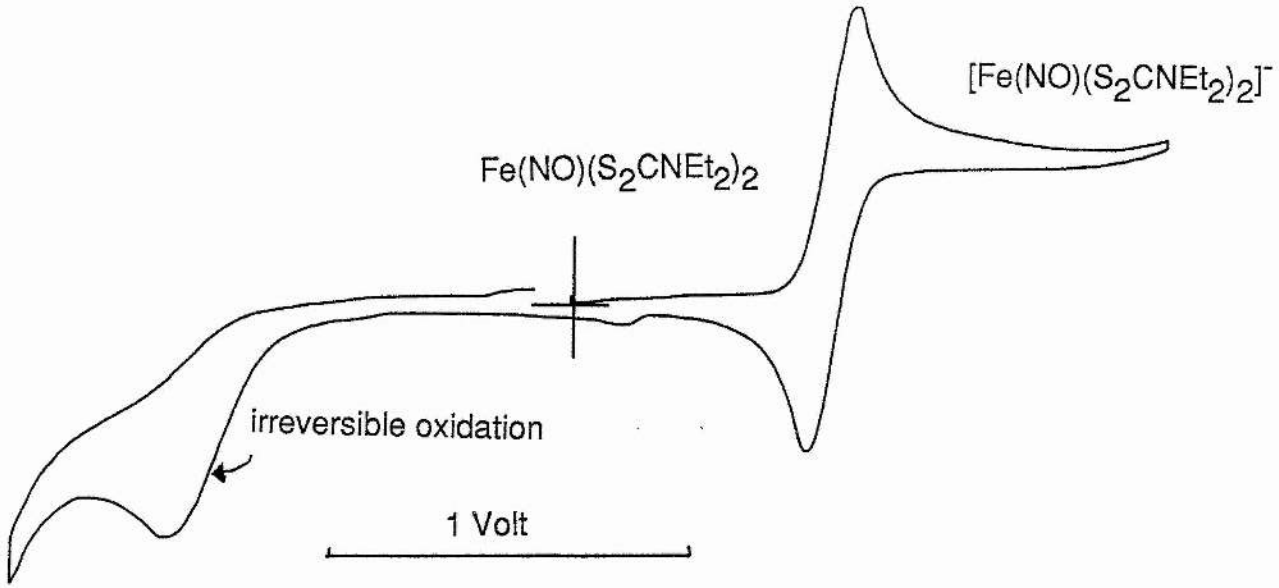


Figure 5-2
Cyclic Voltammogram of $Fe(NO)(S_2CNR_2)_2$, R=Et
in $CH_2Cl_2$ at a Platinum Working Electrode

The result shown in table 5-1 for the effect of R=Me relative to that for R=Et and $^{n}Pr$ is similar to that observed for $Fe_2(SR)_2(NO)_4$ ; the greater the electron donor the lower the reduction potential. Such a result was expected considering the differences observed by other workers concerned with the effect of R on the $\nu$(NO) stretching frequency [14].

An interesting observation with this work followed form the addition of ferrocene to the solutions undergoing electrochemical examination. At potentials greater than 0.4 V relative to $Fc^{+/o}$ no return wave was observed for the conversion of $Fc^{+}$ to Fc, ie ic/ia =0, suggesting that $Fc^{+}$ was reacting with an oxidation product of $Fe(NO)(S_2CNR_2)_2$.

Examination of ia/ic for the 0/1- reduction of these complexes revealed that at low scan rate the ratio was low but that it increased towards 1 as the scan rate increased. If the electrochemistry of these iron complexes was examined in acetonitrile then the reduction was found to be chemically irreversible. However as the scan rate was increased then the return wave for the reduction became apparent, (figure 5-3). It was also observed that current for the oxidation of the breakdown products had increased relative to that in $CH_2Cl_2$. These results indicate a chemical step taking place.

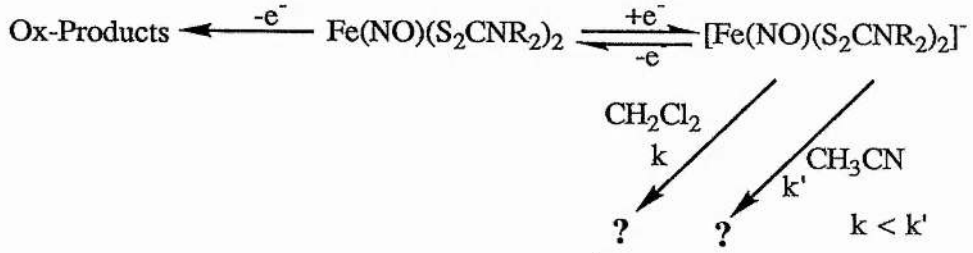


Further evidence for this chemical step was obtained from the addition of small amounts of acetonitrile into a $CH_2Cl_2$ solution of the complex and examining the effect on the ratio ia/ic; the more acetonitrile added the smaller the ratio becomes, and the peak for the breakdown product appears. The loss of the return wave was also achieved by the addition of primary amines into $CH_2Cl_2$ solutions of the complex. Addition of di-$^{n}$propyldithiocarbamate to a $CH_2Cl_2$ solution of $Fe(NO)(S_2CNR_2)_2$ containing a little $CH_3CN$ caused an increase in the anodic current of the reduction ie ia/ic increased. This suggests an equilibrium exists between the primary breakdown product and the reduced iron nitrosyl complex.

Figure 5-3

(i) Reduction of $Fe(NO)(S_2CNEt)_2$ in $CH_3CN$ at a Platinum Working Electrode

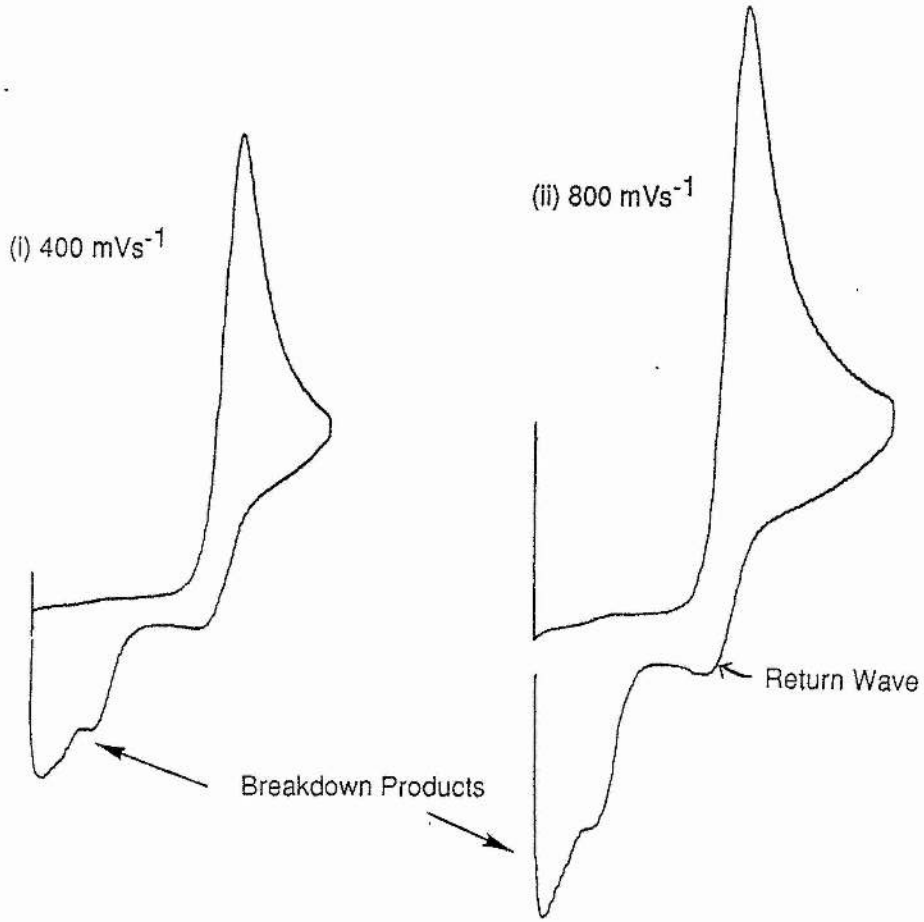


(iii) Reduction of $Fe(NO)(S_2CNEt)_2$ in $CH_2Cl_2$ with a small amount of $CH_3CN$ added.

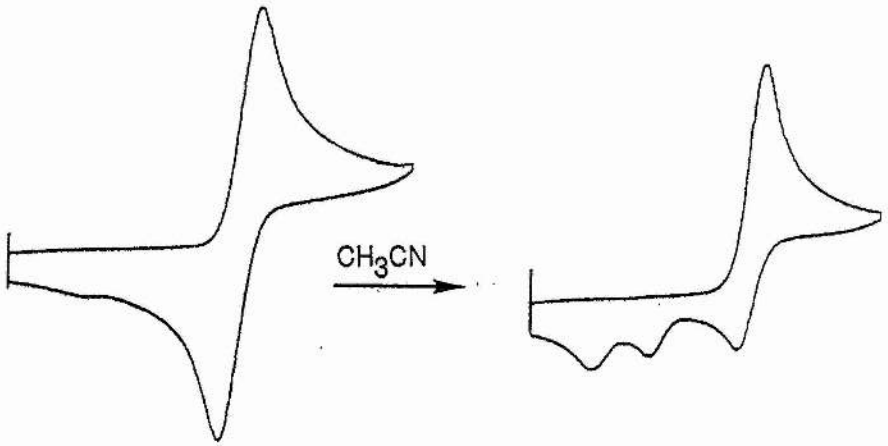


(iv) The effect of added $NaS_2CNEt_2$ on the reduction observed in (iii)

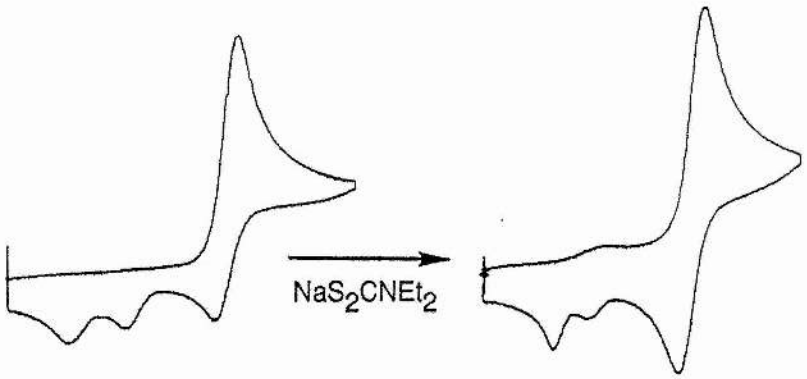

This phenomenon would appear at first glance to resemble the 'nucleophilic induced substitution' described by Lemoine [22] in that the reduced complex is being attacked by nucleophiles. Whether this actually involves an attack of the amine or $CH_3CN$ on the reduced species leading to substitution is unknown.

A solution of $Fe(NO)(S_2CNR_2)_2$, R=Me and Et in THF was examined by e.p.r. spectroscopy. A very prominent three line spectrum was obtained for each ( g=2.038, $A^{14}N$≈13.2G). The addition of Super-Hydride to these solutions resulted in gas evolution and the loss of the e.p.r. signal. This suggested that a diamagnetic material was produced, or that there had been a loss of NO, although no signal attributable to NO was observed.

Addition of an electron to $Fe(NO)(S_2CNR_2)_2$ which contains a linear Fe-NO group [24] would produce a complex isoelectronic with the diamagnetic cobalt complex $Co(NO)(S_2CNR_2)_2$. This cobalt complex has a bent M-NO bond [13]. It is proposed that the chemical reduction of $Fe(NO)(S_2CNR_2)_2$ to $[Fe(NO)(S_2CNR_2)_2]^-$ may have produced an isostructural complex to the cobalt one.

Chemical reduction of the iron nitrosyl complex was achieved using either sodium or by Super-Hydride, $LiB(Et)_3H$. In both cases there was a colour change from green to brown. The $^1H$ n.m.r. of the brown material in $CDCl_3$ showed the presence of the dithiocarbamate ligands, showing that the material was indeed diamagnetic. However the I.R. spectrum of the material gave no indication of coordinated NO either bound in a linear or a bent fashion. The I.R. spectrum however was consistent with the presence of $Fe\text{-}S_2CNR_2$ ligands.

Because of the isoelectronic nature of $[Fe(NO)(S_2CNR_2)_2]^-$ and $Co(NO)(S_2CNR_2)_2$, the cobalt complex with R=Me was prepared and examined by cyclic voltammetry in $CH_2Cl_2$. The electrochemical behaviour is summarised in table 5-1. The electrochemistry is very similar to that of the iron complexes although this complex has one more electron. The 0/1-reduction was found to be both electrochemically and chemically reversible for all scan rates examined.

On aerial oxidation of cobalt complex in $CH_2Cl_2$, the solution changes colour from brown to green, ie the reverse colour change for the reduction of $Fe(NO)(S_2CNR_2)_2$. The I.R.

spectrum of the isolated material did show a weak absorption at 1682cm$^{-1}$ ($\nu$(NO) $Fe(NO)(S_2CNR_2)_2$ ≈1689cm$^{-1}$). Microanalysis of the material suggests the formulation $Co(S_2CNMe_2)_3$; a C:H:N ratio of $C_{3.2}H_{6.2}N$ was found. The mass-spectrum revealed the presence of the tris complex as the $M^+$ peak. The following scheme summarises these observations;

$$[Co^{II}(NO)(S_2CNR_2)_2]^+ \xleftarrow{-e^-} Co^{I}(NO)(S_2CNR_2)_2 \underset{-e^-}{\overset{+e^-}{\rightleftharpoons}} [Co^{0}(NO)(S_2CNR_2)_2]^-$$

$$[Co^{II}(NO)(S_2CNR_2)_2]^+ \xrightarrow{-e^-} Co^{III}(S_2CNR_2)_3$$

These results suggest that (i) the reduction of $Fe(NO)(S_2CNR_2)_2$ leads to the loss of NO and that (ii) the oxidation of $Co(NO)(S_2CNR_2)_2$ also leads to the loss of NO. It is suggested that the reduction of $Fe(NO)(S_2CNR_2)_2$ produces a material which is isostructural to the isoelectronic cobalt complex. This is unstable and loses the NO ligand, a step which is catalysed by the presence of acetonitrile or amines.

## 5-3 Electrochemistry of $Fe(CO)_2(S_2CNEt_2)_2$

The complex $Fe(CO)_2(S_2CNEt_2)_2$ was examined by cyclic voltammetry in $CH_2Cl_2$. Although this complex is six coordinate and contains the iron in the +2 oxidation state it is similar to both the cobalt and iron mononitrosyl complexes discussed above. The voltammogram obtained for this complex is shown in figure 5-4. The potentials are relative to the Ag/AgCl reference electrode. A reversible reduction and a reversible oxidation are observed; both are chemically reversible. On scanning further positive or further negaitive an irreversible oxidation and and reduction are observed respectively. The electrochemical behaviour of this complex is summarised below.

$$[Fe^{III}(CO)_2(S_2CNEt_2)_2]^+ \underset{-e^-}{\overset{+e^-}{\rightleftharpoons}} Fe^{II}(CO)_2(S_2CNEt_2)_2 \underset{-e^-}{\overset{+e^-}{\rightleftharpoons}} [Fe^{I}(CO)_2(S_2CNEt_2)_2]^-$$

+0.48 V

-0.39 V

+1.03 V $\xrightarrow{-e^-}$ Products

-1.46 V $\xrightarrow{+e^-}$ Products

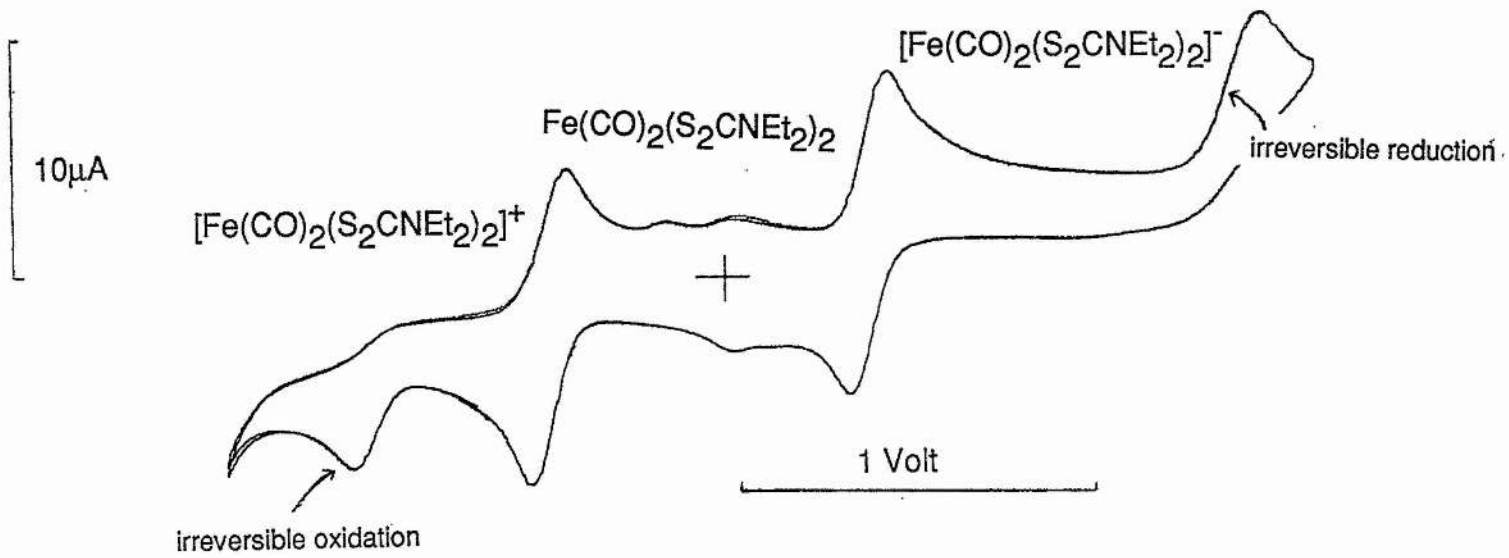


Figure 5-4
Cyclic Voltammogram of $Fe(CO)_2(S_2CNEt_2)$ in $CH_2Cl_2$ at a Platinum Working Electrode Relative to the Ag/AgCl Electrode

The electrochemistry of this complex is unlike that of the metal nitrosyls discussed above. However there are similarities with that of $Fe(S_2CNEt_2)_3$. This may suggest that the electrochemistry of this latter complex and the carbonyl complex may be iron centred whereas the electrochemistry of the metal nitrosyls does appear to be concerned with the M-NO bond.

## References

1. Holm, R. H., Accs. Chem. Res., 10, 427, (1977) : Spiro, T. G., "Iron-Sulphur Proteins" (1982) Wiley (Publishers)

2. Wang, G. H., Zhang, W. X., Chai, W. G., Acta Chim. Sin., 38, 95, (1980)

3. Cambi, L., Cagnasso, R., Atti. Accad. Naz. Lincei., 13, 809, (1931) : Martin, R. L.,. White, A. H., Trans. Met. Chem., 15, 113, (1965) : Butcher, R. J., Ferraro, J. R., Sinn, E., Inorg. Chem.,15, 2077, (1976)

4. Epstein, L. M., Straub, D. K., Inorg. Chem., 8, 784, (1969), 4a) Ileperuma, O. A., Feltham, R. D., ibid, 10, 1876, (1977)

5. Yordanov, N. D., Shopov, I. D., Jezieski, A., Jezowska-Trzebiatowska, B., Inorg. Chim. Acta, 60, 9, (1982)

6. Pasek, E. A., Straub, D. K., ibid, 21, 23, (1977)

7. Jensen, K. A., Krishnan, V., Acta. Chem. Scand., 21, 2909, (1967) : Jensen, K. A., Krishnan, V. Jørgensen, C. K., ibid, 24, 743, (1970)

8. Blaauw, H. J. A., Nivard, B. J. F., van der Kerk, J. M., J. Organomet. Chem., 2, 236, (1964)

9. Buerskens, P. T., Cras, J. A., Steggerdi, J. J., Inorg. Chem., 7, 808, (1968)

10. Nigo, Y., Masuda, I., Shinra, K., Chem. Comm., 476, (1970)

11. Gyzy, C. M., Raynor, J. B., Symons, M. C. R., J. Chem. Soc. (A), 2987, (1969)

12. Iliev, V. I., Shopov, D., Polyhedron, 6 1497, (1987)

13. Enemark, J. H., Feltham, R. D., J. C. S. dalton Trans., 718, (1972)

14. Sarte, B., Stanford, J., LaPrice, W. J., Uhrich, D. L., Lockhart, J. E., Gelerinter, E., Duffy, N. V., Inorg. Chem, 17, 3361, (1978)

15. Fitzsimmons, B., Hume, A. R., J. C. S. Dalton Trans., 1549, (1979)

16. Butler, A. R., Glidewell, C., Hyde, A. R., Walton, J. C., Polyhedron, 4, 797, (1985)

17. Ileperuma, O. A., PhD Thesis, University of Arizona, (1976)

18. Zimmerman, J. B., Starinshak, T. W., Uhrich, D. C., Duffy, N. V., Inorg. Chem., 16, 3107, (1977)

19. Ileperuma, O. A., Feltham, R. D., Inorg. Synth.,16, 7

20. Bond, A. M., Martin, R. L., Coord. Chem. Rev., 54, 23, (1984); 20a) Couquis, G., Lachenal, D., Inorg. Nucl. Lett., 9, 1095, (1973)

21. Bard, A. J., Faulkner, L. R., "Electrochemical Methods, Fundamentals and Applications", (1980), John Wiley (Publishers)

22. Lemione, P., Coord. Chem. Rev, 83, 199, (1988)

23. Enemark, J. H., Feltham, R. D., Coord. Chem. Rev., 13, 339, (1974)

# Epilogue

This thesis has been concerned with the advancement of the chemistry associated with iron-sulphur-nitrosyl complexes. The underlying reason for this piece of research was the natural occurrence of the methyl ester of Roussin's Red salt, $Fe_2(SMe)_2(NO)_4$ , and its possible link with the high incidence of oesophageal cancer in a particular area of China. It is presently thought that natural iron-sulphur enzymes become nitrosylated by nitrite to produce firstly Roussin's Black anion, $[Fe_4S_3(NO)_7]^-$, which is subsequently methylated to produce $Fe_2(SMe)_2(NO)_4$. The work outlined in the latter half of chapter three strongly suggests this to be the most plausable route to the biological formation of the methyl ester. The methylation probably occurring through the involvement of the S-adenosyl methionine enzyme complex. Vitamin B12, cobalamin is used as a catalyst for biological methylations and it would be of interest to see the effect of cobalamin with the enzyme analogues used in chapter three on the Black anion.

Once produced, $Fe_2(SMe)_2(NO)_4$ enters the body as a contaminant in the food eaten by the local people. Once ingested it is thought that most of the complex becomes destroyed in the stomach because of the low pH. N-nitrosamines are not produced as a consequence of this low pH. However since $Fe_2(SMe)_2(NO)_4$ is lipid soluble it is possible that the complex enters into the body via the cell lining of the oesophagus. Inside a cell the complex will be subject to the oxidising/reducing capabilities of the cell's own biochemistry. The electrochemical study of the Roussin esters described in chapter four shows that these complexes are chemically irreversible to oxidation, and that this oxidation appears to aid the oxidation of amines. It is possible that once inside the cell, $Fe_2(SMe)_2(NO)_4$ becomes oxidised by an oxygenase such as the cytochrome P450 complex, to produce a species capable of facile nitrosyl donation, ie capable of interacting with amines to produce N-nitrosamines. Cells of the oesophagus are constantly being replaced, ie have a high turnover rate, thus DNA damage to the cells caused by N-nitrosamines would have a more pronounced effect with these cells than with a cell with a low turnover. However in the absence of any specific evidence as to the nature of the oxidised methyl ester and its effect on secondary amines this scheme is only speculative.

The synthetic chemistry associated with the dianion, $[Fe_2(S_2O_3)_2(NO)_4]^{2-}$ described in chapter three has been very fruitful. This complex has been found to be a better starting material for the production of the neutral Roussin esters than any other currently available.

This complex has also been found to be a useful source of the $\{Fe(NO)\}^{2+}$ and $\{Fe(NO)_2\}^{+}$ moieties and the chemistry of these fragments is currently being exploited in association with thiomolybdate chemistry.

The electrochemistry of the neutral Roussin esters, $Fe_2(SR)_2(NO)_4$ revealed the presence of two reduced states, the monoanion of which was bottle green in colour. The change in colour associated with electrolysis could possibly be exploited in the production of a red-green electrochromic material. Attempts to produce a polymeric form of Roussin's Red salt by attachment to an organic polymer have so far failed to produce such a material.

The photochemical behaviour of the Roussin esters was also investigated during the course of this research. It was shown that in the presence of $[Fe(SR)_2(NO)_2]^-$ ions, the illumination of a solution of $Fe_2(SR)_2(NO)_4$ produced the green anion $[Fe_2(SR)_2(NO)_4]^-$. However much of this work was difficult to reproduce and so has not been discussed in this thesis, more work in this fascinating area of metal nitrosyl chemistry is needed.

# Appendices

# Appendix-1

## Orbital Symmetry Terms

| | | | |
|---|---|---|---|
| A, B | | singlet | |
| E | | doubly degenerate representation | |
| T | | triply degenerate representation | |
| A | | symmetric | with respect to rotation through $180^{o}$ about |
| B | | antisymmetric | principle axis |
| Superscripts | ' | symmetric | reflection in $\sigma h$ |
| | " | antisymmetric | |
| Subscripts | g | symmetric (gerade) | inversion in a centre |
| | u | antisymmetric (ungerade) | of symmetry |
| | 1 | symmetric | reflection in $\sigma v$ |
| | 2 | antisymmetric | |

# Appendix-2

This appendix describes some of the theory behind the electrochemical experiments performed in chapter four.

In the C.V. experiment a triangular waveform is applied linearly to a working electrode. The voltage is scanned between limits set by the operator. As the voltage is linearly scanned across the electrode as the potential applied approaches the standard reduction potential, $E^{\emptyset}$, of a redox couple, the current increases as we gain or lose electrons from the electrode as we reduce or oxidise the material present respectively. The current obtained is plotted as a function of the voltage. As the voltage is scanned, the current obtained increases until it reaches a peak and then decays, a typical voltammogram for a reversible couple can be found reference 2. If we consider the following reduction of an oxidised species O, as the potential applied to a working electrode is scanned to a reduced species R, by the addition of an integral number of electrons per molecule, $ne^-$,ie;

$$O + ne^- = R$$

If the electron transfer from the electrode to the substance in solution is fast, a change in potential will change 'instantaneously' the relative amounts of O and R, producing a current as the amounts adjust to the new overpotential.The relative amounts of O and R can be obtained from the Nernst Equation;

$$[O]/[R] = \exp\{(nF/RT)(E - E^{\emptyset})\} \quad \textbf{(eqn-1)}$$

[O]/[R] = Relative concentrations of the oxidised and reduced species,
n= integral number of electrons transferred per molecule,
F= Faradays constant,
R=Universal Gas constant,
$E-E^{\emptyset}$ = overpotential,(V).

On changing the value of $E-E^{\emptyset}$, the current obtained is dependent not only on the magnitude of the potential change but also on the concentration of redox active materials at the electrode as well as on the electrode kinetics. If there is not enough reducible material at the electrode surface then the transportation of new material to the electrode will dominate the size of the current. For instance when $E-E^{\emptyset}$ is <0.4 then, from the equation-1, the relative proportions of O and R at the electrode are $1: 5.8 \times 10^6$. From Ficks laws of diffusion we obtain the following;

$$i_t = nFAD_O (\partial C_O/\partial x)_{x=0,t} \quad \textbf{(eqn-2)}$$

$i_t$ = the current with respect to time (Amps)

A = area of the electrode ($cm^2$)

$D_O$= Diffusion coefficient for the oxidised species,( $cm\ s^{-1}$)

$(\partial C_O/\partial x)_{x=0,t}$ change in the concentration of the oxidised species at the electrode surface with respect to time.

n and F have the definitions as given in eqn-1.

The electron transfer to or from the electrode is described by the electron transfer rate constant, given by;

$$k_f = k^O \exp((-\alpha nF/RT)(E-E^{\emptyset})) \quad \textbf{(eqn-3)}$$

kf= electron transfer rate coefficient,($cm\ s^{-1}$)

$k^O$= standard heterogeneous rate constant, dependent on electrode surface and compound under examination, ($cm\ s^{-1}$)

$\alpha$ = transfer coefficient, it normally has the value 0.5,

T= absolute temperature,

n, F, R and $E-E^{\emptyset}$ have their normal meanings.

The exponential dependence of $k_f$ on E signifies a steep rise in the current. Since the experiment is done in an unstirred or 'quiet' solution, diffusion is the main method by which material arrives at the electrode. As the amount of O is depleted through electrolysis, the value of $(\partial C_O/\partial x)_{x=0,t}$ decreases. The current reaches a peak value and beyond this the current is totally under the control of diffusion, and the current which is now independent of the applied voltage falls off with $t^{-1/2}$.

The shape of the voltammogram is dependent on two factors; the heterogeneous rate constant, $k^{\emptyset}$ , and the diffusion mass transport. The former is expressed by the Butler-Volmer equation, the latter from Fick's second law of diffusion. When $k^{\emptyset} > 10^{-1} cms^{-1}$ then the electron transfer is fast enough to maintain the dynamic equilibrium ratio of the concentrations of the oxidised and reduced species as given by the Nernst equation, and the process is only mass-transfer controlled. This is called a reversible or Nernstian couple. If $k^{\emptyset} < 10^{-5}$ then the charge transfer is the controlling step and a return wave may not even be detected. For intermediate cases where $10^{-5} < k^{\emptyset} < 10^{-1} cms^{-1}$ then

both processes determine the shape of the voltammogram.

The formal redox potential of a reversible couple can be found from the potentials of the peak positions;

$$E^{\emptyset} = (E_{pa} + E_{pc})/2 \quad \textbf{(eqn-4)}$$

and for a reversible system the peak separation is given by

$$\Delta E_p = 0.059/n \text{ V} \quad \textbf{(eqn-5)}$$

This figure is rarely obtained without specialised equipment mainly because of the uncompensated resistance of the solution, the so called iR drop effect. However carefull design of the cell, the electrodes and choice of solvent help to limit the effect of the potential drop.

For a reversible system, the peak current observed is described by the Randles-Sevcik equation;

$$i_p = (2.69 \times 10^5)\, n^{3/2} A D^{1/2} C \nu^{1/2} \quad \textbf{(eqn- 6)}$$

$i_p$= peak current (A),

C = bulk concentration of the material undergoing investigation (mol $cm^{-3}$),

$\nu$ = scan rate (V $s^{-1}$)

n, A, D have their normal definitions.

Diagnostic tests for reversibility are obtaining a straight line plot obtained by plotting $i_p$ against $\nu^{1/2}$ , showing that $i_{pa}/i_{pc} = 1$ for all $\nu$ , and showing that the position of the formal reduction potential does not change with scan rate. Although finding that $\Delta E_p$ = 0.059/n V would be a good test for a reversible couple, as noted earlier this is rarely found without specialised equipment and other methods are used to obtain data from the peak separation. From a knowledge of the value of n, the diffusion coefficient can be evaluated.

Estimation of the peak currents is often difficult, especially when a base line cannot be accurately gauged. An empirical method developed by Nicholson and Shane [1] can be used in such cases to obtain the value of $i_{pa}/i_{pc}$;

$$i_{pa}/i_{pc} = (i_{pa})_o/i_{pc} + 0.485(i\lambda)_o/i_{pc} + 0.086 \quad \textbf{(eqn-7)}$$

If $k^o < 1x10^{-5}\nu^{1/2}$cm $s^{-1}$ , however then a system is *electrochemically* irreversible in nature. The values of $\Delta E_p$ and $i_{pa}/i_{pc}$ cannot be applied nor does the Randles-Sevcik equation apply since in most cases a return wave will not be observed. For *chemically* irreversible systems the equation does hold and plots of $i_p/\nu^{1/2}$ normally give straight line relationships. This is because a normal electron transfer is occurring prior to some chemical rearrangement or reaction. For a quasi-reversible system the evaluation of constants from the current/ scan rate data is complex. For such a system the current is given by;

$$i = n\,F\,A\,C\,D^{1/2}\,(nF/RT)\,\Psi(E)\,\nu^{1/2} \quad \textbf{(eqn-8)}$$

$\Psi(E)$ = a dimensionless kinetic parameter defined by Nicholson [1] see eqn-9

Thus the current is not only dependent on $\nu^{1/2}$ but also on a term which is a function of the applied potential. We find that $\Delta E_p$ > 59mv, and plots of $i/\nu^{1/2}$ are not linear.

$\Delta$Ep can be used as a measure of the reversibility of the charge transfer step. For quasi-reversible systems, for a given $k^{\varnothing}$ the $\Delta$Ep increases as $\nu$ is increased. $\Delta$Ep can be correlated with $k^{\varnothing}$ and measurement of $\Delta$Ep with $\nu$ can lead to an estimation of the rate constant.

Nicholson introduced a dimensionless parameter from which the value of $k^{\varnothing}$ can be obtained;

$$\Psi = (D_o^{\alpha/2}/D_r^{\alpha/2})\,k^{\varnothing}/(D_o \pi\, a\, \nu)^{1/2}$$

a= nF/RT

For $D_o = D_r$ ( this is normally the case) this equation reduces to

$$\Psi = k^{\varnothing}/(D\pi\, a\, \nu)^{1/2} \quad \textbf{(eqn-9)}$$

$\Delta$Ep is a function of $\psi$. From published tables of $\psi$ [1,2] , the value of $\psi$ can be obtained for a given $\Delta$Ep, hence $k^{\varnothing}$ can be obtained if D is known. For a reversible couple or

for a pseudo-reversible couple with $\alpha$ =0.5 then $ip_a = ip_c$.

Since the current obtained is proportional to the scan rate of the experiment, as the scan rate increases so too does the iR drop. This has the effect of increasing the peak separation, $\Delta E_p$. This effect is particularly pronounced in non-aqueous solvents. Since in the case of a quasi-reversible system changes in $\Delta E_p$ with scan rate are a good diagnostic test for a quasi-reversible system, erroneous results can be obtained if the effect of iR drop is not taken into consideration. One method used to alleviate this problem is by the use of feedback; the electronics are *tuned* in such a way to compensate for the iR drop. Of course this method cannot be used if the electronics does not contain such a feedback circuit and another way is used to compensate. A compound whose electrochemistry is understood and has been shown to be a Nernstian system is used as an internal standard. Such internal standards include benzophenone and ferrocene. These systems can also be used as an internal reference system alleviating the use of aqueous reference electrodes such as the saturated calomel or the silver/silver chloride system. Examination of the effect of scan rate on $\Delta E_p$ for the internal standard relative to that of the system undergoing investigation can determine whether the observed changes in peak separation are due to iR drop or due to slow electron transfer. These quasi-reversible or pseudo-reversible systems as they are known are often quoted simply as irreversible systems.

As an example of the effect of iR drop on a Nernstian system the ferrocene/ferricinium couple was examined in THF. From plots made using equation-6, the diffusion coefficients $DFc^{o} = 6.24 \times 10^{-6}$ $cm^2s^{-1}$, $DFc^{+1} = 5.36 \times 10^{-6}$ $cm^2s^{-1}$ were obtained. The plot of $i_p^c/\nu^{1/2}$ gave the same gradient as a plot obtained theoretically (eqn-6) by calculating for 3mM of an electroactive species with n = 1 and $D = 5.4 \times 10^{-6}$ $cm^2s^{-1}$.

The ferrocene/ferricinium couple is known to be both an electrochemically and chemically one electron reversible system. In THF, however, peak widths are greater than the theoretical value of 59mV, and the separation increases with the scan rate. The peak separation increases linearly with the current and with the square root of the scan rate, fig 2. Since we know that the system under examination is a reversible couple the observed peak separation must be a direct consequence of the iR drop.

Although n, the number of electrons transferred per molecule can be obtained from an examination of the peak currents obtained from C.V. data or better from a bulk electrolysis

of the electroactive material under investigation, it is possible to obtain n directly from the C.V. data if combined with the data obtained from a potential step experiment [3]. If we perform a potential step to the material undergoing examination, that is we instantaneously move the potential from a region where no electrolysis is taking place to one where instant electrolysis takes place, then the current obtained is given by;

$$I_{ps} = nFD^{1/2}CA\pi^{-1/2}t^{-1/2} \quad \textbf{(eqn-10)}$$

Ips = current obtained (A),

t = time after the initiation of the potential step (s)

A plot of $I_{ps}/t^{-1/2}$ will give a gradient equal to $nFD^{1/2}CA\pi^{-1/2}$. If we divide this gradient by the one obtained from plots of $i_p/\nu^{1/2}$ given by equation-6 then we obtain an expression for n;

$$n = (0.20236\, m^{cv}/m^{ps})^2 \quad \textbf{(eqn-11)}$$

$m^{cv}$= gradient obtained from plots of $i/\nu^{1/2}$

$m^{ps}$= gradient obtained from plots of $i/t^{-1/2}$

References

General Reading; Southhampton Electrochemistry Group,"Instrumental Methods in Electrochemistry", (1985), Ellis and Horwood (Publishers) : Bard, A. J., Faulkner, L. R., "Electrochemical Methods, Fundamentals and Applications", (1980) John Wiley (Publishers)

1. Nicholson, R. S., Shain, I., Anal. Chem., 36, 706, (1964); ibid, 37, 178, (1965)
2. Heinze, J., Ange. Chem. Int. Ed., 23, 831, (1984)
3. Alan J Bard, Private Communication.